https://doi.org/10.35662/unine-thesis-2914

University of Neuchâtel

Faculty of Science

Laboratory of Technologies for Heritage Materials

Chemometrics application for the preservation of waterlogged archaeological wood

Dissertation submitted to the University of Neuchâtel for the degree of

Doctor ès Sciences

Presented by

Mathilde Monachon

Thesis supervisor: Prof. Edith Joseph, University of Neuchâtel

Jury members:

Prof Edith Joseph, University of Neuchâtel, Switzerland

Prof. Stephan von Reuss, University of Neuchâtel, Switzerland

Dr. Elodie Guilminot, Arc'Antique, France

Defended on March 2021

Faculté des Sciences
Secrétariat-décanat de Faculté
Rue Emile-Argand 11
2000 Neuchâtel – Suisse
Tél : + 41 (0)32 718 21 00
E-mail : secretariat.sciences@unine.ch

IMPRIMATUR POUR THESE DE DOCTORAT

La Faculté des sciences de l'Université de Neuchâtel autorise l'impression de la présente thèse soutenue par

Madame Mathilde MONACHON

Titre:

"Chemometrics application for the preservation of waterlogged archaeological wood"

sur le rapport des membres du jury composé comme suit:

- Prof. ass. Edith Joseph, directrice de thèse, Université de Neuchâtel, Suisse
- Prof. Stephan von Reuss, Université de Neuchâtel, Suisse
- Dr Elodie Guilminot, Arc'Antique, Nantes. France

Neuchâtel, le 19 avril 2021

Le Doyen, Prof. A. Bangerter

Abstract

Waterlogged archaeological wood (WAW) artefacts present severe degradation issues once recovered from their burial environment. Indeed, in anoxic environment, microorganisms enhanced carbohydrates degradation of the wood materials as well as formation and accumulation of iron sulfide FeS*x* compounds. FeS*x* are harmless in the burial environment but undergo an oxidation after recovery, and thus to irreversible physical and chemical damages. Consolidation of WAW artefacts did not prevent the degradation, even with application of extraction and/or neutralization treatments. Nowadays, new trends are based on eco-friendly methods. Among these new trends, utilization of microorganisms has proven its efficiency toward the conservation of different heritage materials, such as bio passivation of copper patina, or bio stabilization of harmful iron corrosion products. In addition, studies have demonstrated the potential of the bacterium strain *Thiobacillus denitrificans* to oxidize and dissolved FeS*x* compounds. An innovative bio-extraction method was then developed based on the properties of *T. denitrificans* combined with natural iron chelators called siderophores and compared to common chemical extraction for the preservation of WAW artefacts. The aims of this thesis are i) to define an artificial protocol to degrade and contaminate fresh wood to form WAW mock-ups, ii) and to evaluate the innovative bio-based extraction method on the analogues and real WAW samples. To empathize the results, chemometric approach was performed.

In the first part, preparation of analogues samples was studied through artificial degradation and contamination protocols on fresh hard- and softwood samples. Two main criteria were evaluated: carbohydrates degradation and formation of FeS*x*. Water-immersion under vacuum was identified as the most promising protocol when applied on both hard- and softwood samples. On surface, the degradation induce was similar to the degradation observed on real WAW artefacts. In addition, the samples appearance was altered, validating the degradation of carbohydrates content. The artificial contamination with equimolar solutions of $FeCl_2 \cdot 4H_2O$ and $Na_2S \cdot 9H_2O$ 0.5M showed the formation of FeS*x* only for softwood while hardwood only presented elemental sulfur. Yet, these results were encouraging, and these samples were then employed to evaluate the efficiency of the bio-based extraction method in the second part of the thesis. Chemometric revealed that this innovative method was as effective as chemical extraction, as no degradation was induced during the extraction and with iron and sulfur extraction rates in the same range or more elevated rates than chemically treated samples. Furthermore, wood samples treated with bio-based method conserved their appearance contrary to chemically treated samples. Though, application of common conservation procedures (*i.e.* consolidation follow by freeze-drying) showed that an oxidation occurred for bio-treated samples, suggesting that the extraction was not complete. Yet, the results obtained were encouraging to preserve WAW artefacts with microorganisms and further investigations should be performed to optimize the innovative and bio-based extraction method.

Keywords: waterlogged archaeological wood; artificial degradation; artificial contamination; chemometric approach; iron sulfide; bio-based extraction

Résumé

Les bois archéologiques gorgés d'eau présentent de graves problèmes après excavation de leur environnement d'enfouissement. En effet, lors de cette période, les microorganismes induisent une dégradation du bois ainsi que la formation et l'accumulation de composés ferreux soufrés FeS*x*. Ces composés sont inoffensifs dans ces conditions d'enfouissement mais présentent une oxydation lors de l'excavation des objets, et mènent donc à des dommages physiques et chimiques irréversibles. La consolidation des bois archéologiques gorgés d'eau ne peut empêcher une telle dégradation, même lorsque des traitements d'extraction et de neutralisation sont appliqués sur les objets. De nos jours, les nouvelles tendances sont tournées vers des méthodes plus écologiques. Parmi ces tendances, l'utilisation de microorganismes a prouvé son efficacité quant à la conservation du patrimoine culturel avec par exemple la bio passivation des patines de cuivre ou encore la bio stabilisation des produits de corrosion du fer nocifs pour les objets. De plus, des études ont montré le potentiel de la souche bactérienne *Thiobacillus denitrificans* pour l'oxydation et dissolution des composés FeS*x*. De ce fait, un traitement d'extraction biologique basé sur les propriétés de *T. denitrificans* combinées avec des chélateurs naturels, appelés sidérophores, a été développé et comparé avec un traitement d'extraction chimique pour la préservation des bois archéologiques gorgés d'eau. Les objectifs de cette thèse sont i) de définir un protocole artificiel de dégradation et de contamination pour former des échantillons analogues ainsi que ii) l'évaluation de l'innovative bio-extraction sur ces analogues et véritables échantillons. Pour appuyer les résultats, une approche statistique fut appliquée.

Concernant la première tâche, la préparation d'échantillons analogues par des protocoles artificiels a été menée sur des différentes espèces de bois. Les deux critères évalués étaient la dégradation des carbohydrates et la formation de FeS*x*. L'immersion des échantillons dans de l'eau avec le vide tiré a présenté des résultats prometteurs pour les différents bois. A la surface, la dégradation induite fut similaire à celle observée sur les objets réels. De plus, l'apparence des échantillons s'altéra, validant la dégradation des carbohydrates. La contamination artificielle par une solution équimolaire de $FeCl_2 \cdot 4H_2O$ and $Na_2S \cdot 9H_2O$ 0.5M montra la formation de FeS*x* seulement pour les conifères, les bois tendres n'étant contaminés que par du soufre. Néanmoins, ces résultats sont encourageant et les échantillons furent utilisés pour évaluer la performance de l'extraction biologique. Les statistiques révélèrent que cette méthode innovative fut aussi efficace que l'extraction chimique. Aucune dégradation ne fut observée et les taux d'extraction pour le fer et le soufre étaient dans les mêmes gammes que celles du traitement chimique, voire parfois supérieurs. De plus, les échantillons traités par bio-extraction conservèrent leur apparence et non les échantillons traités chimiquement. Néanmoins, l'application d'un traitement de conservation (*i.e.* consolidation suivie de lyophilisation) montrèrent qu'une oxydation se produisit pour les échantillons traités biologiquement et donc que l'extraction ne fut pas complète. Tout de même, ces résultats sont très encourageants concernant la préservation des bois archéologiques gorgés d'eau à l'aide de microorganismes. De futures recherches seront menées pour optimiser ce traitement biologique innovatif.

Mots-clés : bois archéologiques gorgés d'eau ; dégradation artificielle ; contamination artificielle ; approche statistique ; composés ferreux soufrés ; extraction biologique

Abbreviations

ADB	Archaeological Service of Bern Canton
ANOVA	Analysis of Variance
ATR-FTIR	Attenuated Total Reflectance Fourier Transformed Infrared
CC	Cellulose content
DFO	Desferoxamine siderophore
DTPA	Diethylenetriaminepentaacetic acid
EB	Erosion bacteira
EDMA	Ethylenediiminobis (2-hydroxy-4-methyl-phenyl) acetic acid
EDTA	Ethylenediaminetetraacetic acid
HC	Holocellulose content
ICP-OES	Inductively Coupled Plasma - Optical Emission Spectroscopy
IP	Impregnation protocol
L	Lepidocrocite
LC	Lignin content
MICMAC	MICrobes for Archaeological wood Conservation
MWC	Maximum Water Content
PCA	Principal Component Analysis
PEG	Polyethylene glycol
POM	Partially Oxidized Mackinawite
R1	ATR-FTIR ratio I(1158)/I(1506)
R2	ATR-FTIR ratio I(1374)/I(1506)
R3	ATR-FTIR ratio I(1034)/I(1506)
Rd	Radial plane section
S	Elemental sulfur
SEM-EDS	Scanning Electron Microscopy - Emission X-ray Dispersive Spectroscopy
SNM	Swiss National Museum
SRB	Sulfate-reducing bacteria
Tg	Tangential plane section
Tv	Transversal plane section
WAW	Waterlogged Archaeological Wood

Table of contents

Chapter 1: Introduction

1 – Wood chemistry

Domestication of fire was a key factor for humankind's evolution. Indeed, with the utilization of fire it was possible for human to cook some foods as well as warming their primary accommodations [1]. This discovery permits humankind to live in hostile environments and develop our actual civilizations. And this development was only possible due to wood material. Historically, wood was employed in countless ways to build many artifacts. These artifacts were representative of their time [2]–[4]. For instance, houses were made of wood, then several everyday life items (buckets, chest, plates) and agricultural tools (cart, fork) were produced. Its use was extended to the fabrication of weapons, such as bow, or means of transport, such as boats [5], [6]. But wood also provided a source of food in the form of fruits, berries or preys as a source of fuel. Wood-fueled fires permitted turning inedible grains into food and the human diet evolved into a variated dietary regime [7]. Even though other materials got more important with the years, wood remained a raw material with its demand still increasing [5].

Wood trees can be classified into two categories: gymnosperms and angiosperms. Gymnosperms (naked seeds) are mainly conifers such as pine (*Pinus*), spruce (*Picea*), and fir (*Abies*). They possess needle leaves and are called softwood [3]. Angiosperms (flower plants) refer to the tree with leaves such as maple (*Acer*), birch (*Betula*), and oak (*Quercus*) [3], [8]. They are defined as hardwood. Generally, hardwood species lose leaves when autumn arrives while softwood species conserve their leaves, offering an evergreen appearance [8]. These two wood families are then different based on their foliage (macroscopic level). Yet, other differences allow to classify wood as hard- or softwood at microscopic and molecular levels. Besides, similarities also exist at these three different levels such as the components forming wood and its cells. Such differences and similarities are described in the following sections.

1.1 – Wood layers

Wood material presents three main plane sections: transversal (Tv), tangential (Tg), and radial (Rd) (Wood trunk with characteristic wood layers and parts (adapted from Merriam-Webster, Inc. 2006)Figure 1). Both Tg and Rd plane sections are longitudinal sections, *i.e.* parallel to the wood trunk, while Tv (also referred to as cross-section) is perpendicular to Tg and Rd [9]. These three sections give different information about wood.

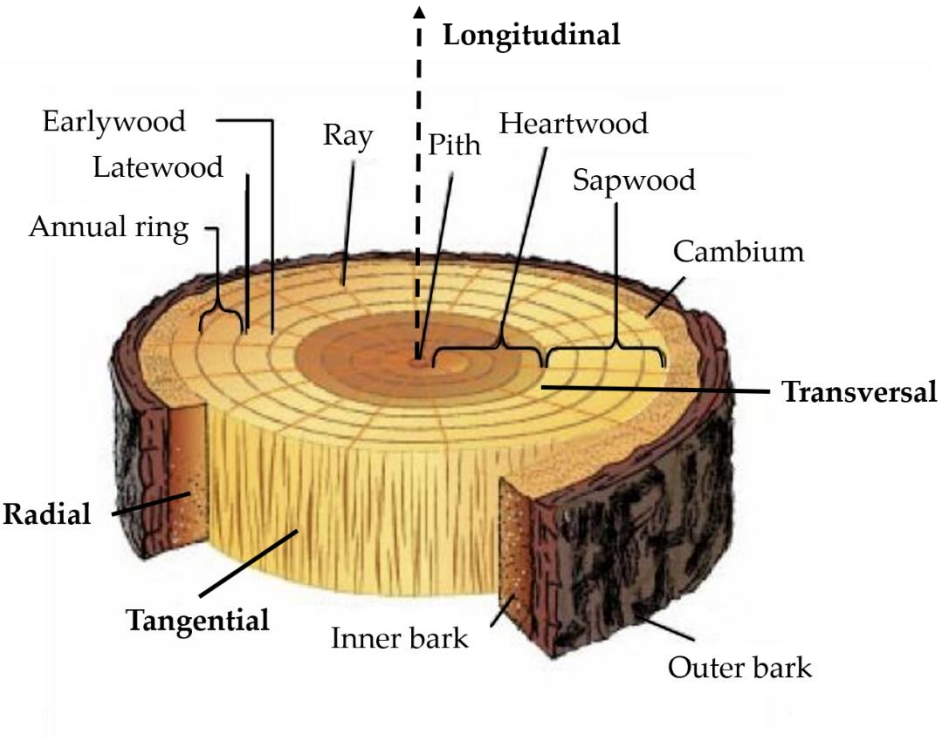

Figure 1: Wood trunk with characteristic wood layers and parts (adapted from Merriam-Webster, Inc. 2006)

The different wood layers are visible on the Tv plane section (Figure 1). The first layer is the bark, divided into outer and inner bark. The former provides mechanical protection to the inner bark and the later allows the sugar to translocate from wood leaves to the roots [1], [8]. The following parts are sapwood and heartwood. Roughly, sapwood refers to the light-colored band adjacent to the wood's bark while the heartwood is the darker zone surrounded by the sapwood [1]. Water and mineral transport is provided through sapwood while heartwood's main function is to store chemicals [8]. At the center of the trunk is the pith composed of juvenile wood cells. Within sap-and heartwood, one can observe early-and latewood. Earlywood is the wood produced in the early growing season while latewood is produced during the late season. Earlywood is softer and more porous than latewood. Changes can be gradual or abrupt between earlywood and latewood and produced annual rings. The pattern of the annual rings depends on the wood species [10].

1.2 – Wood cells

1.2.1 – Vessels, tracheids, and parenchyma cells

Among the different wood cells forming the layers previously described, vessels and tracheids are the unique cells separating hard from softwood species [1].

Hardwood possesses vessels that are specialized conducting cells [1], [8], [11]. The cells are piled on top of each other, forming tubes with entirely perforate ends. On Tv section, vessels appear as holes on the wood. Hardwood can then be referred to as "porous woods" [8]. Concerning softwood, their characteristic cells are imperforate elements called tracheids. Tracheids are longer cells than vessels. Contrary to vessels, tracheids present a square appearance on the transverse section, and softwood can be designed as "non-porous woods"

[8]. If both cells have conduction properties, vessels are more efficient than tracheids for this purpose [1]. They are most visible on the annual ring.

While vessels and tracheids die when they reach maturity, wood species all present living cells named parenchyma and present in sapwood [8]. Parenchyma cells provide a storage function for wood species, allowing maintaining their physiological activity [12]. Parenchyma cell's role is important in wood longevity as they transport and store the essential elements required by the wood to grow [1], [8]. In addition, parenchyma cells have an active role regarding the regulation of the pressure inside the vessels and tracheids [8].

1.2.2 – Cell wall structure

Several cells compose the different layers. All the cells present a similar wall structure. Wood cell walls can be divided into three main layers: middle lamella, primary wall, and secondary wall. The distribution of these layers is illustrated in Figure 2.

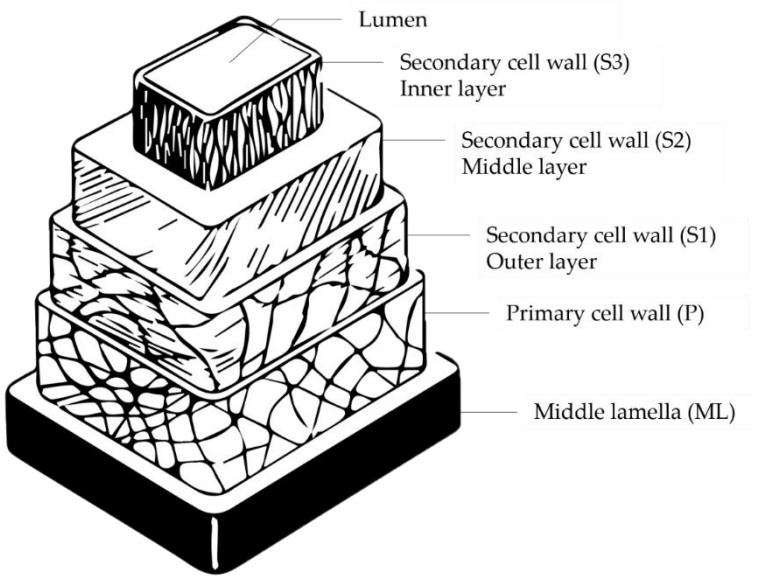

Figure 2: Wood fiber cell wall structure (adapted from the Handbook of Wood Chemistry and Wood Composites, 2005)

Wood cells by themselves do not exist in nature. All the cells are adjacent and their association forms the different wood organs [1]. Each cell must adhere to the other cells as a uniform and coherent structure. Such adhesion is provided by the first layer of the wood cell wall, the middle lamellae (ML). Every cell possesses ML as the outermost layer. The following layer is the primary cell wall (P). P is also a very thin layer and it is then complicated to dissociate ML from P layers, even with Transmission Electron Microscopy, as both ML and P are very lignified [1]. The last cell wall is the secondary cell wall (S). S consists of subsequent three layers known as thin outer S1, thick middle S2, and thin inner S3, as observed in Figure 2. These three layers are distinguishable by their cellulose orientation which provides different optical properties [13] as well as physical properties [8]. S3 layer is poor in lignin. This is in direct correlation with tree physiology. For water to rise in the plant through the lumen (a phenomenon called transpiration), water molecules should adhere to the cell wall of S3. Lignin being a hydrophobic molecule, its concentration must be low for the transpiration phenomenon to occur.

1.3 – Wood composition

At a molecular level, wood possesses many constituents but three of them composed the main part of wood structure. These three constituents are cellulose, hemicellulose, and lignin. The rest of the wood composition is made of extractives (organic parts) and ash (inorganic parts) [1], [8], [14], [15]. Their proportion differs for hard-and softwood, as summarized in Table 1:

Table 1: Wood components percentages in hard-and softwood

	Cellulose	**Hemicellulose**	**Lignin**	**Extractives**	**Ash**
Hardwood	40-45%	25-30%	15-35%	14.2	1.2
Softwood	40-50%	17-35%	20-30%	11.4	1.2

1.3.1 – Holocellulose

Holocellulose represents a major part of the carbohydrates wood components. It is a combination of cellulose (40-50%) and hemicellulose (17-35%) of the wood as well as lesser amounts of other sugars [14]. Cellulose and hemicellulose are polymers, composed of sugars such as D-glucose, D-mannose, D-galactose, or D-fructose. They possess hydroxyl groups -OH responsible for the sorption of moisture on the wood through hydrogen bond.

1.3.1.1 – Cellulose

Cellulose represents the most important part of wood composition [13], with a mean content of 45.4% ± 3.5 for hardwood and 43.7% ± 2.6 for softwood [14]. It is surrounded and encrusted by the two other main wood components (*i.e.*, hemicellulose and lignin) [3]. The main building block of cellulose is called cellobiose, a two-sugar unit repeating indefinitely [14]. The sugar repeated in cellobiose is glucose, of chemical formula $C_6H_{12}O_6$ (Figure 3) [3], [13]. This pattern is referred to as cellobiose residue. Its structure is defined as linear but theoretical calculations specified that the chain formed is an extended helix where each cellobiose residue rotates 180° compare to the previous residue.

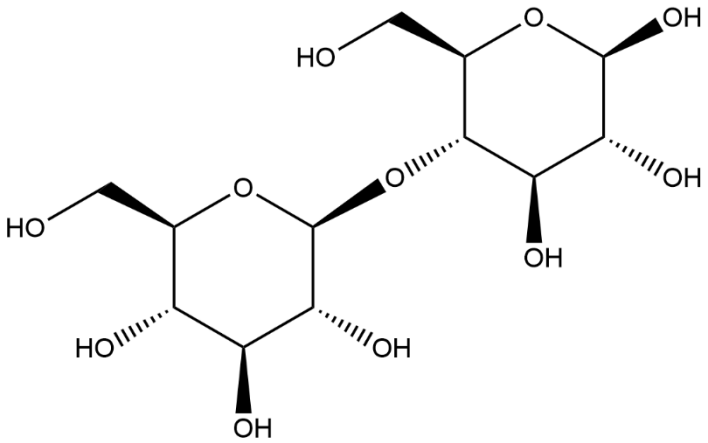

Figure 3: Structure of cellobiose molecule, main block unit of cellulose

The number of glucose units within the cellulosic molecules allows calculating the degree of polymerization (DP) of the wood [14]. DP represents the number of sugar units making a polymer, cellobiose residue in the case of cellulose [16]. An average DP of cellulose compound

is 9 000-15 000, referring to cellulose as a high polymer molecule and one of the longest polysaccharides identified [8], [13]. In general, a mean DP value of 10 000 implies a 5 μm cellulose chain in the wood.

The hydroxyl groups within the cellulose molecules allow two hydrogen bonding which depends on their position in the sugar units. Cellulose chains made of glucose molecules bundle to form layers held by van der Waal's bonds (intermolecular hydrogen bonds) [16]. Within the layers, intramolecular hydrogen bonds held the adjacent atoms of glucose in the same cellulose molecule [16], [17]. The whole structure is referred to as native cellulose, or cellulose I. The formation of these inter- and intramolecular bonds leads to a random orientation of the cellulose molecules. The strong covalent bonds (intramolecular) within the cellulose chains are referred to as primary bonding while the van der Walls bonds (intermolecular) are called secondary bonding [3]. Secondary bonding is weakened by water as well as the wood stiffness while primary bonding gives strength to wood fibers [3].

Bundles of cellulose chains are referred to as microfibrils that can present different stages of crystallinity [3]. Generally, wood-derived cellulose presents a higher proportion of crystalline cellulose, up to 65% in some regions. The other proportion presents a lower density and is referred to as amorphous cellulose [14]. The surface of crystalline cellulose is accessible, meaning that it could adsorb water, interact with microorganisms, or be chemically modified [14]. The remaining part of cellulose is considered as inaccessible as it is covered by the other wood compounds (*i.e.,* hemicellulose and lignin).

1.3.1.2 – Hemicellulose

Hemicellulose is the second main component of holocellulose. Its name assumed that this polymer is a precursor of cellulose and hydrolyzes more easily than cellulose [8], [18]. Contrary to cellulose, hemicellulose is a polymer composed of diverse sugars, such as D-xylopyranose and D-glucopyranose [13], [14]. It is then a heteropolysaccharide. The numerous sugar units contained in the hemicellulose polymer affects the complexity as well as the nonuniformity of the wood matrix [13]. In addition, the DP of hemicellulose is lower than the one of cellulose, with an average value of 100-200 [8], [14] such as a lower crystallinity is observed for hemicellulose than cellulose [3]. The amorphous structure of hemicellulose is more accessible than cellulose and more reactive to hydrolysis [3].

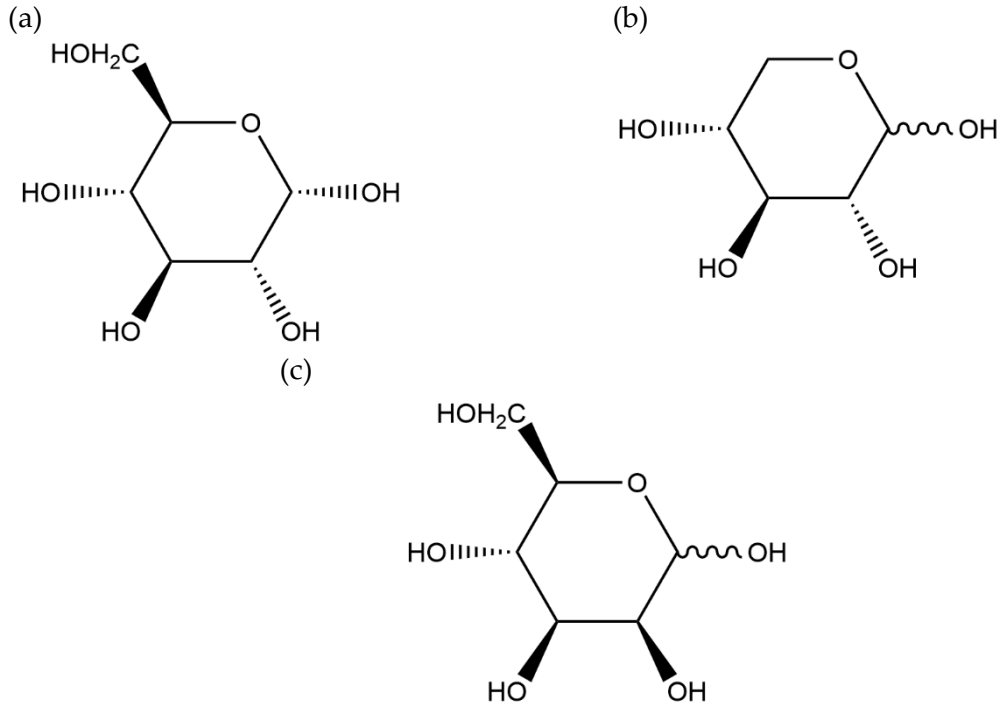

Figure 4: Structure of the main hemicellulose units (a) glucose, (b) xylose, and (c) mannose

Xylan and galactoglucomannan are two main components of hemicellulose. Xylan is mainly found in hardwood while galactoglucomannan, simplified as glucomannan, in softwood [13], [14], [17]. Xylan content is higher in earlywood while glucomannan content is higher in latewood. Xylan is a homopolymer of xylose units while glucomannan possesses a heteropolymer structure consisting of glucose and mannose units (Figure 4). The ratio glucose:mannose is generally 1:3 with a random distribution of these units within the molecule with other sugar units. Indeed, xylan and glucomannan are the main hemicellulose constituents but other units are present in the hemicellulose chains, in a lower concentration. Hardwood xylan presents a laced structure while softwood glucomannan structure depends on the wood species. For instance, red pine possesses a branching blackbone while scots pine a linear chain [17].

Hemicellulose content is more important in the S3 layer while cellulose content is superior in S1 and S2 layers.

1.3.2 – Lignin

Lignin is the second main constituent of wood [13]. It is a large and complex polymer mainly composed of phenylpropane units, with a content of 20-35% for hardwood and 15-35% for softwood [13], [14], [18]. Lignin acts as a glue between wood materials, maintaining the cellulosic microfibrils together through ML where its proportion is high, and giving rigidity to the cell wall [3]. Due to its heterogeneous and complex structure, the DP of lignin is complicated to calculate.

Lignin is composed of a large group of aromatic polymers named monolignols. These polymers derived from the polymerization of hydroxycinnamyl alcohols: p-coumaryl, sinapyl, and coniferyl alcohols [19]. They are represented in Figure 5. These three monolignols are connected by three different ether bonds (C-O-C) and four carbon-carbon bonds (C-C) [3]. Yet,

when incorporated into the polymeric structure of lignin, the monolignols give new lignin units: p-hydroxyphenyl, syringyl, and guaiacyl.

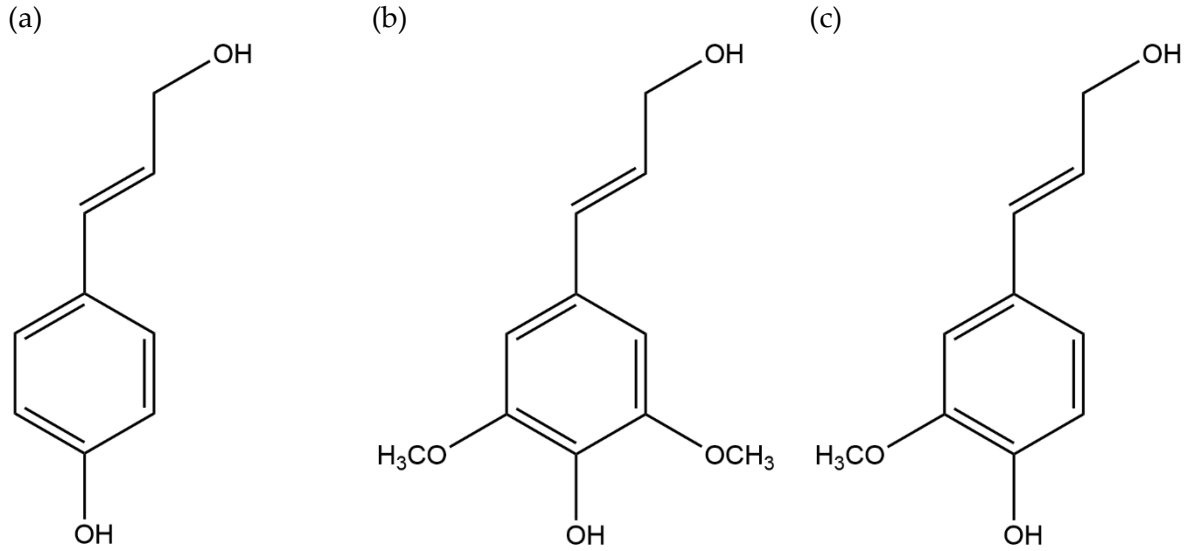

Figure 5: Structure of the main lignin units (a) p-coumaryl, (b) sinapyl, and (c) coniferyl alcohols

The three units are found for both hard- and softwood lignin but in different proportions. Regarding softwood, lignin consists exclusively of guaiacyl, obtaining the name of guaiacyl lignin. p-hydroxyphenyl molecules are also present in smaller amounts while syringyl molecules are absent or only detected as traces [3], [8], [16]. Hardwood lignin contains guaiacyl and syringyl molecules in approximately equal proportions with small amounts of p-hydroxyphenyl. Hardwood lignin is also mentioned as syringyl-guaiacyl lignin. Due to the high content of syringyl within their lignin, hardwood has less condensed structures than softwood and more ether bonds. From a structural scale, hardwood is more linear and less branched while softwood lignin is more crosslinked [3]. The three-dimensional web structure of lignin only consists of these three monomers. The aromatic rings and hydroxyl groups of lignin allow forming van der Waals and hydrogen bonds with the holocellulose content. [3], [8]. Lignin content gives its hydrophobic properties to cell walls and inhibits the swelling of the structure [3].

In general, cellulose polymer structures the wood material while lignin and other polysaccharides form the encrusting substances of the wood [13], [20].

1.3.3 – Extractives

Extractives represent the organic parts of the wood composition. As suggested by their names, extractives refer to chemicals that can easily be extracted using solvents [14]. More than a hundred extractives have been isolated and identified as well as their role in the wood understood. For instance, some extractives could respond to wounds inflicted on the plant or as a mechanical defense against fungi or insects [8], [14]. Extractives are mainly located in heartwood and bark, giving their dark appearance to these parts. Main extractives components can be divided into three groups: aliphatic compounds, terpenes, and phenolic compounds [8]. Extractives composition varies between hard-and softwood. In general, softwood species contain higher extractives than hardwood species. Phenolic compounds, such as tannins or

flavonoids, are more water-soluble than the two other groups. The different extractives present in the wood influence wood color, smell but also its durability [8], [10], [14].

1.3.4 – Ash

Finally, ash represents the inorganic parts of the wood composition. It is an approximation measurement of the salts and inorganic matter present in the wood fibers. As described in Table 1, ash content within the wood is very low. Up to 80% of ash are made of Ca, Mg, and K elements probably under the form of oxalates, carbonates, and sulfates [14]. These inorganics may be essential for the growth of the plants. They penetrate through the roots of the plants and then are distributed in different parts of the trees. As for extractives, the concentration of ash varies from one wood species to another [21]. These differences are based on the environment surrounding the trees. In addition, ash content seems to affect the pH of wood species. The higher the inorganic content, the lower the pH value [14].

2 – Waterlogged archaeological wood

2.1 – Definition

Archaeological wood artifacts are defined as objects carrying traces of cultural activities and giving information about civilizations [3], [22]. Wood was used by humans for a long time and everyday items recovered are most often made of wood [3]. In special conditions, the artifacts are very well preserved. This is the case for waterlogged archaeological wood [22].

Waterlogged archaeological wood (WAW) artifacts are excavated from anoxic environments that can be aquatic, such as marine or freshwater, or terrestrial [3], [22], [23]. The state of degradation of marine, freshwater, and soil WAW artifacts vary, depending on the environmental conditions of burial. For instance, in marine environments, crustaceans are as responsible for wood decay as microorganisms while in freshwater environments, mainly bacteria and fungi are responsible of such degradation [11]. Moreover, a non-uniform degradation of the artifacts occurs depending on the environmental conditions but also on the wood species or on the duration of burial [3]. In general, the inner parts of the artifacts are more preserved than the outer ones. Outer parts also present high water content, inorganic inclusions, and biopolymer decay [3]. In particular, the cellulose content decreases with the increase of water content. This is due to microbial degradation. Oxygen content, salinity, or sediments present in the environment are the key factors of microbial decay [24].

(a)

(b)

(c)

Figure 6: Pictures of (a) the Vasa warship (Vasa museum ©), (b) the Mary Rose (The Mary Rose Trust ©) and (c) some objects from the Oseberg collection (Oseberg collection ©)

Vasa and *Mary Rose* warships are two famous marine WAW artifacts (Figure 6a and Figure 6b). *Vasa* wrecked in 1628 in the harbor of Stockholm and remained in the seabed for 333 years [22]. A low salinity and a low oxygen content, explain the good preservation state of this warship [24], [25]. On the contrary, *Mary Rose* wrecked in 1545 in the Channel sea (https://maryrose.org/recovering-the-mary-rose/). In such saline water, parts embedded in seabed are protected from worms and bacteria degradation. Even if bacteria are present in seabed, the degradation process is slowed down by sediments establishing a protective environment [26]. *Mary Rose* was partially embedded in sediments, preserving this part from the marine microbial activity [26], [27]. WAW artifacts can also be found in freshwater sites. Freshwater WAW artifacts were recovered around the world, as for boats discovered in lake George, New York, the United-States, or in different parts of Europe, such as lake Bolsena in Italy or wreck of Lyon Saint-Georges in France [28]–[30]. Some freshwater artifacts were also discovered in Switzerland, as it is the case in lake Neuchâtel [31]. One of the most known freshwater sites is the Palafittes registered at the UNESCO patrimony (https://whc.unesco.org/en/list/1363/). This site is settled in and around the Alps. The Latenium, Neuchâtel, Switzerland, is part of the Palafittes site. Lacustrine construction parts and everyday items were recovered and after conservation interventions, some artifacts displayed at the Latenium park and Museum of Archaeology, Hauterive-Neuchâtel. Recent studies showed that the degradation of lake wood occurred when the water level dropped [32]. The Oseberg collection is an example of terrestrial waterlogged wood artifacts (Figure 6c) [22], [33]. The artifacts were recovered from waterlogged clay at a land site in Norway in 1902 [22]. The collection is composed of a Viking ship with its equipment as some furniture and textiles.

If WAW artifacts seem to present a well-preserved structure at a first glance, deeper investigations reveal that they present a spongy texture and a significant alteration occurred within the wood cells and tissues during the burial time [24].

2.2 – Biological degradation process

In oxic environment, wood is mainly degraded by fungi, bacteria, and insects [22]. They degrade cellulose and hemicellulose contents in a fast process. Lignin acts as a defense against microbial activities and degradation, preventing the microorganisms to penetrate the cell wall. If specific fungi and bacteria can degrade some parts, the complex and heterogeneous structure of lignin, however, slows down the process. The higher the lignin content, the higher the wood resists to microbial decay [3], [34]. However, in anoxic environments, the oxygen content is low or null and then wood degradation agents differ. The known degrading agents are hence shipworms and bacteria and their degradation process is quite slow [22], [24], [35]. It has been established that the two main bacteria degrading wood in anoxic environments are erosion bacteria and sulfate-reducing bacteria [9], [22].

2.2.1 – Erosion bacteria

Erosion bacteria (EB) are the primary wood degraders in near-anoxic or anoxic environments [22], [24], [26], [36], [37]. They are rod-shaped bacteria of 2-8 μm length and 0.5-0.9 μm diameter [22]. Their small size allows them to enter within wood cells such as vessels or tracheids.

EB start their degradation process at the surface and proceed inwards the wood, breaking down the lignocellulose structure of the cell walls, for both hard- and softwood [9], [24], [35], [38]. They reach the inner parts through rays and piths [22]. Once there, EB enter the cell lumen of the wood. The cell wall is attacked and erodes then EB align along the microfibrils [22]. Erosion troughs are formed during the degradation process [26]. In the secondary cell wall, rich in holocellulose, cellulose is converted into an amorphous substance [9], [26], [39] while the middle lamella, rich in lignin, remains intact [22]. The erosion process is the most visible in Tv plane section, with the amorphous cellulosic substance presenting a granular material, specific of EB degradation process, inside the lumen part of cell wall [26]. Some S3 layer may remain after the cellulose decay. WAW artifacts conserve their form and integrity under wet conditions due to EB's inability to degrade lignin-rich parts of wood cell wall. Water only fills the degraded cell wall inside the three layers of secondary wall. Even if ML is not decayed by EB, this layer is weakened. When filled with water, all the mechanical strength to maintain the wood structure relies on ML [22]. However, after recovery, wood will dry, and all water be removed from wood cells. The water capillary forces being strong, wood fibers disintegration will lead to a collapse of the structure with water evaporation.

The degradation enhanced by EB continues until all cellulose parts of the wood are decayed. For instance, some WAW artifacts still present active cellulosic degradation after recovery and storage [22]. The degradation rate of EB does not depend only on the burial duration. The wood species and environmental conditions also influence EB wood degradation [22], [26].

2.2.2 – Sulfate reducing bacteria

If present, in anoxic sulfate-rich environment such as seabed, sulfate-reducing bacteria (SRB) can act as secondary wood degraders [9], [40]. Sulfates are abundant in water, and thus the microbial sulfur cycle is active in coastal marine sediments, freshwater, or wetland ecological systems [9]. SRB use wood as a carbon and energy source. SRB cells are in the range 0.5-1.3x0.8-5 μm and 0.5-2x2-9 μm [41].

SRB enter the area previously degraded by EB and reduce the sulfate ions SO_4^{2-} provided by the environment with the carbohydrates formed as EB degradation products [9], [40], [42]. Sulfates act as electron acceptor and carbohydrates as electron donor And sulfur hydrogen H_2S is produced, according to equation (1) [3]:

$$2(CH_2O) + SO_4^{2-} + 2H^+ \rightarrow H_2S + 2H_2O + 2CO_2 \quad (1)$$

The formed H_2S accumulates within the degraded tracheids and vessels of wood. H_2S interacts then with the lignin content of cell walls to form organosulfur products and/or elemental sulfur [3]. Other compounds can also serve as electron donors for SRB such as inorganic compounds, amino acids, sugars, and aromatic compounds [3]. Lignin being classified as an aromatic compound can thus be used as electron donor as well. However, even if SRB interact with lignin, the aromatic core of the lignin molecule remains unaffected [43]–[45].

2.3 – Iron sulfide accumulation

Iron sulfides may form within the wood tracheids and vessels by reaction with H_2S [46]. Iron is provided from the surrounding environment or the wooden artifacts themselves, for example the bolts of the *Vasa* and *Mary Rose* warships [47], [48]. Under the influence of microorganisms, the iron pieces corrode and generate Fe^{2+} ions [3], [35], [40], [46]. These ions interact then with the formed H_2S and produce iron sulfides [46], [49]. Equation (2) shows the chemical reaction occurring between Fe^{2+} and H_2S and forming mackinawite.

$$Fe^{2+} + H_2S \rightarrow FeS + 2H^+ \quad (2)$$

Mackinawite, of chemical formula FeS, is one of the main iron sulfides formed [46]. Three main iron sulfides compounds are represented in Figure 7. Their main properties are discussed in the following paragraphs.

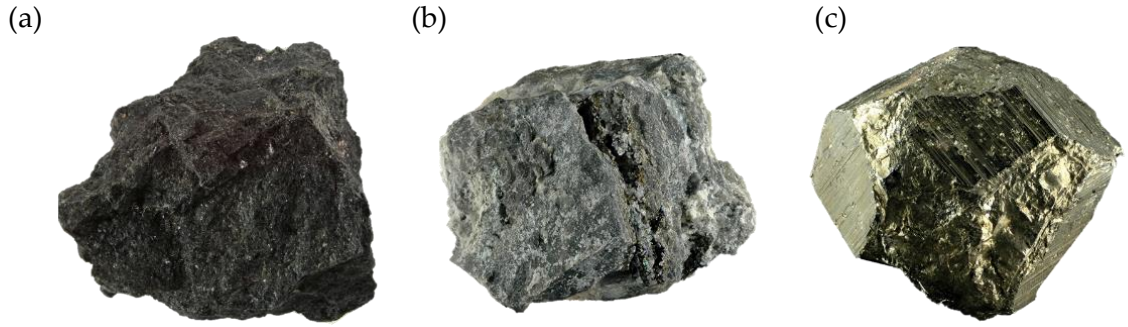

Figure 7: Pictures of (a) mackinawite FeS, (b) greigite Fe_3S_4, and (c) pyrite FeS_2 minerals (RRUFF ©).

Mackinawite presents a black hue (Figure 7a) and can stay for a long period in anoxic environment [50]. It is a widespread iron sulfide mineral in low-temperature and aqueous

environments [49]. FeS crystallizes in a tetragonal structure, with sheets of Fe atoms in a square planar coordination. Fe atoms are linked in a tetrahedral coordination, to four equidistant sulfur atoms. Mackinawite is classified as an acid-soluble and unstable mineral [51], [52]. Indeed, FeS formed previously during the burial period starts to oxidize once exposed to O_2. An unstable intermediary phase forms as partially oxidized mackinawite $Fe_{1-x}S$. This phase is not found in nature and directly converts into greigite Fe_3S_4 [50], [53], [54].

Greigite (Figure 7b) presents a greyish appearance and crystallizes in a reverse spinel structure, with general formula AB_2X_4. A represents the atoms in tetrahedral sites and B the ones in octagonal sites. Fe atoms occupy the A and B sites. However, A sites are only occupied by Fe^{2+} ions while B sites consist of a mix of Fe^{2+} and Fe^{3+} ions. S atoms occupy all the X sites and are surrounded by Fe atoms [49]. Fe_3S_4 mineral is a more stable phase than FeS and is generally associated with freshwater environments. Just like FeS, Fe_3S_4 is an acid-soluble mineral, with one mole of sulfur S^0 produced every mole of Fe_3S_4 digested. Exposed to atmospheric temperature and humidity, Fe_3S_4 oxidizes and forms sulfur α-S_8 and/or iron oxyhydroxides $Fe(OH)_3$ [46]. But in anoxic environment, greigite is converted into pyrite FeS_2 [46], [49].

Pyrite FeS_2 (Figure 7c) is the most common iron sulfide found in WAW. It is also the most prevalent and abundant iron disulfide on Earth [49]. Pyrite is commonly named *fool's gold* due to its characteristic gold color and metallic luster. This mineral crystallizes in face-centered cubic crystal structure, the same structure as NaCl, with S atoms at the center of the cube and midpoints of the cube edges and Fe atoms localized at the corners and face centers of the cubes. FeS_2 is acid-insoluble with a stable structure in pH range 2-10 and in oxic environment [51], [52], [55]. However, the stability of pyrite is under discussion as some oxidation issues were encountered in museum collections [56]. Several parameters could be responsible for such oxidation to occur: FeS_2 surface area, water amount, oxygen concentration, temperature, pH, and presence of bacteria, especially *Thiobacillus* species [57].

It was noticed that the occurrence of iron sulfides was correlated with the burial duration of the WAW items. FeS was mainly identified for WAW artifacts recovered after a short burial period while FeS_2 was more important on more ancient artifacts, as observed by Rémazeilles et al where FeS_2 and Fe_3S_4 were the main phases observed in Gallo-Roman boats [30]. The presence of the compounds could allow to better estimate the period of the archeological site and the degradation state of WAW present.

In addition to the formation of iron sulfides, iron ions can act as a catalyst for the degradation of cellulose, through the Fenton reaction [9], [48], [58], [59]:

$$Fe^{2+} + H_2O_2 \rightarrow HO^{\cdot} + HO^{-} \quad (3)$$

The reaction initiates and catalyzes the oxidation processes of cellulose [60]. A partial degradation occurs then during the burial of WAW artifacts.

While stable in anoxic environments, formed iron sulfides oxidized once exposed to different relative humidity and oxygen concentration. They are converted into iron oxyhydroxides such

as goethite α-FeOOH, iron sulfates such as melanterite $FeSO_4 \cdot 7H_2O$, elemental sulfur α-S_8 and/or sulfuric acid H_2SO_4 [41], [47], [54] (Figure 8).

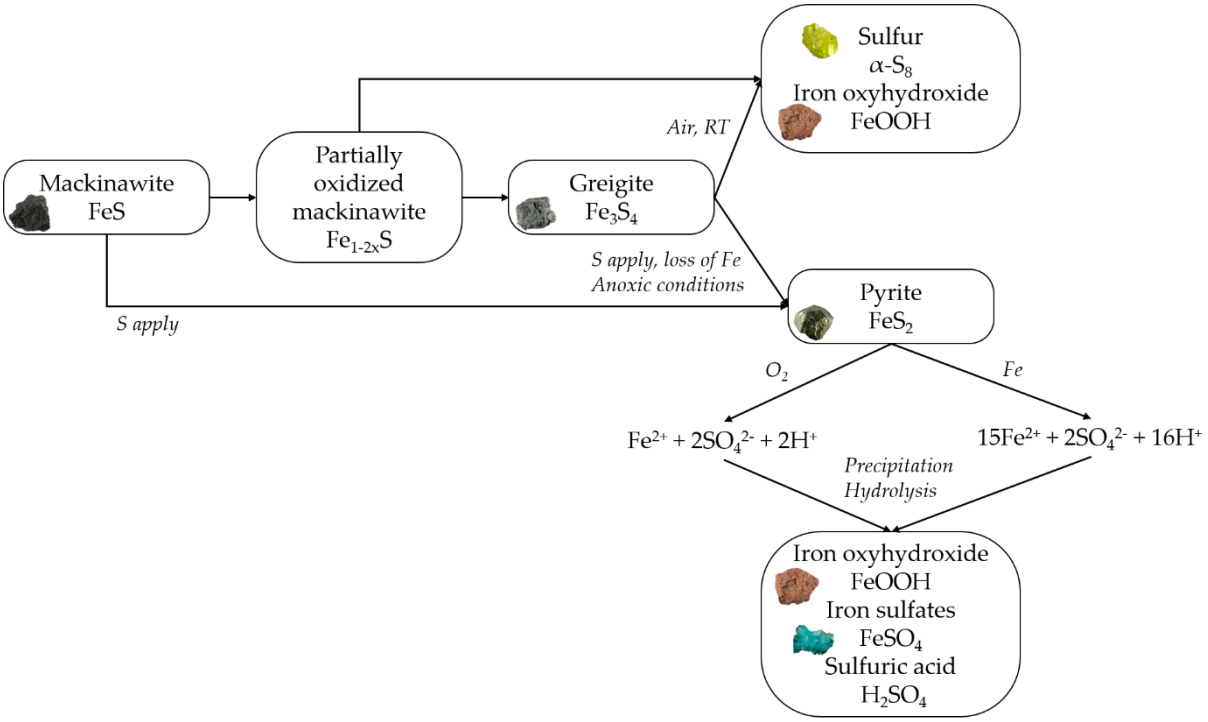

Figure 8: Structural evolution and oxidation process of mackinawite FeS depending on the environmental conditions (adapted from Rémazeilles et al, 2013)

These conversions induce irreversible physical and chemical damages on the wooden artifacts. Equations (4), (5) and (6) are representative oxidation reactions occurring for mackinawite FeS and pyrite FeS_2 [56], [61]:

$$FeS + 2O_2 \rightarrow Fe^{2+} + SO_4^{2-} \quad (4)$$

$$FeS_2 + H_2O + 3O_2 \rightarrow Fe^{2+} + SO_4^{2-} + H_2 + SO_2 \quad (5)$$

$$Fe^{2+} + 0.25O_2 + 2.5H_2O \rightarrow Fe(OH)_3 + 2H^+ \quad (6)$$

Precipitated iron oxides and/or iron sulfates expand in volume compared to the initial iron sulfides present. They then fill the wood vessels/tracheids and induce cracks of the structure [9], [58], [62], [63]. Related problems can be observed when water evaporates from wood timbers. Water-soluble minerals are transported with water and washed out from the artifacts. Yet, some minerals are not water-soluble, such as natrojarosite $NaFe_3(OH)_6(SO_4)_2$, and their expansion continues with water evaporation. In parallel, the acid produced interacts with the organic matter and hydrolyzes wood cellulose and hemicellulose components [58]. These phenomena result in structural damages: loss of strength, reduction of mechanical stability, and shrinkage of the structure [9], [58], [63].

Conservation interventions were then developed to prevent the collapse of the whole structure. Since the middle of the XIXth century, conservators report that WAW artifacts have to be handled with care but also kept immersed [22], [23]. If the artifacts are maintained in waterlogged conditions, the dimensions and integrity of the artifacts remain stable [23]. In the

past decades, WAW conservation investigated the use of different chemicals to slow down or inhibit the degradation processes induced by iron and sulfur contamination. Not only stabilization protocols were applied, but extraction methods were also proposed to remediate the harmful Fe/S species.

2.4 – Current preservation methods

2.4.1 – Stabilization

Several conservation methods have been proposed to avoid the degradation of WAW objects after their excavation. Among others, polyethylene glycol (PEG) is the most common consolidation agent employed [40], [58], [64], [65]. PEG is a polymer with a rigid structure at room temperature but soluble in water if heated. When *Vasa* was recovered, different conservation procedures were applied to stabilize the artifact. Yet, the methods employed at that time were not satisfactory regarding the conservation of large WAW items, such as the alum treatment mainly employed for the Oseberg collection [33]. PEG was then first applied on the large marine *Vasa* warship [3], [66]. The hull of *Vasa* was sprayed for 9 years with PEG solution, whose concentration was increased gradually, from 10% initially to a final concentration of 45% [3]. The PEG solution diffused inside the wood and gradually replaced the water in wood vessels. This prevents degraded wood cells to collapse while drying, avoiding shrinkage and loss of mechanical stability [58], [64], [65], [67]–[69]. This procedure was then applied to most of the large WAW artifacts recovered, such as *Mary Rose* warship or *Bremen Cog*, and is nowadays commonly employed with freeze-drying [3], [70]. Freeze-drying is the most employed method since the mid-XXth century to dry WAW, allowing to prevent structural collapse [71]. One advantage of using freeze-drying is to maintain PEG under a crystalline form that avoids further wood decay [72].

However, this stabilization method presents some disadvantages. PEG application results in an important gain of weight, an unnatural dark color, and a "waxy" surface of the treated objects [65], [73]. Moreover, its application does not prevent degradation when iron and sulfur species are present in the wood cells. Salts precipitation and acidification still occur, compromising the long-term preservation of the objects. Indeed, the presence of iron catalyzes cellulose depolymerization and reduced sulfur compounds oxidation, through Fenton reaction, as shown in equation (3) [48]. Moreover, studies also demonstrated that Fe^{3+} ions catalyze PEG oxidation, but also that iron metal corrodes to Fe^{2+} ions in contact with moist PEG [59]. A circular reaction occurs then, as Fe^{2+} ions will form Fe^{3+} ions through Fenton reaction which will then continue to oxidize the PEG consolidating agent and so on. Investigation on *Vasa* and *Mary Rose* have estimated a total sulfur content of 2–3 tons for both shipwrecks [9], [59], [64] and around 5 tons of iron for *Vasa* [74]. To prevent cellulose depolymerization as well as PEG oxidation, extraction methods are hence required and are detailed below. Concerning freeze-drying, generally small objects can be dried due to the reduced chamber dimensions. For larger objects, a dismantlement is then required, resulting in long processes [30]. In addition, a discoloration has been observed when WAW artifacts are dried with this method [75]. Wood depolymerization and discoloration of stabilized WAW artifacts go against the ethical criteria of cultural heritage as conservation treatments should not affect the integrity of the items [34].

2.4.2 – Remediation for Fe and S species

Curative extraction methods are generally applied once the WAW artifacts have been stabilized. As described in equations (4)-(6), iron sulfides convert into iron oxides and/or sulfates, but also sulfuric acid H_2SO_4 and in some cases some elemental sulfur α-S_8 crystals were observed [3]. Depending on the harmful species to be extracted, different strategies are adopted.

Concerning iron, strong chelating or complexings agents are generally employed. The most commonly used in heritage conservation is ethylenediaminetetraacetic acid (EDTA). It was first employed for paper and textile and then extended to wood [76], [77]. Indeed, EDTA forms strong complex with Fe^{2+} and Fe^{3+} ions that present a stability constant of log Kf = 14.30 and log Kf = 25.10, respectively [78]. Stronger chelators and derivatives of EDTA have also been investigated, such as ethylenediiminobis (2-hydroxy-4-methyl-phenyl) acetic acid (EDMA) or diethylethylenetriamine pentaacetic acid (DTPA) [74]. EDMA forms complex with Fe^{3+} ions that has a stability constant log Kf = 38 [74], and DTPA-Fe^{3+} complexes have a stability constant log Kf = 28 [78]. Utilization of these three chelating agents leads to stable and water-soluble complexes [79]. Their solubility depends on pH, with EDTA being more soluble in pH range 4-6.3 [80], [81]. In combination with sodium dithionite, a reducing agent, EDTA has been reported as the most efficient method for iron extraction [82], [83]. However, sodium dithionite is potentially harmful to conservators as well as very flammable, limiting its utilization [84]. The utilization of the other chelating agents cited above is also very controversial. For instance, EDMA and DTPA colored in red the artifacts and a prolonged application time is required for complete extraction of iron [74], [85]. In addition, the application of EDMA and DTPA dissolves PEG and thus the stabilization step should be then renewed. Regarding sulfur species, until recently, sulfur mitigation and acid neutralization were treated with alkaline baths or ammonia gas [3]. However, alkaline baths led to an increase of pH and so a decay to the cellulosic content as well as the removal of PEG applied previously. The artifacts present then a dried surface, accompanied with a fragilized structure, and altered appearance. Also, this method showed to be inefficient regarding sulfuric acid neutralization, even after an extension of the application duration. Concerning ammonia gas treatment, the application was easier, and pH remained stable, preventing an important degradation of carbohydrates. Under ammoniac atmosphere, the sulfur salts converted into ammonium salts, such as ammonium jarosite $(NH_4)Fe_3(OH)_6(SO_4)_2$. No volume extension neither cracks were reported, meaning the mechanical structure was not endangered, and PEG impregnation was not affected neither. Some disadvantages were highlighted thus, such as a loss in cellulose crystallinity inducing a decrease of WAW artifacts stability [3]. In the case of the Oseberg collection, the objects were treated with hot (90 °C) concentrated potassium aluminum solutions $KAl(SO_4)_2{\cdot}12H_2O$ for 36 hours, in order to prevent shrinkage. The method was performed at the beginning of the XX^{th} century (1905-1913) and is referred to as the alum method [33]. However, unexpected ammonium compounds formed [86]. It was observed that the structure of the treated wooden artifacts was compromised and weakened after treatment, with the formation of sulfuric acid leading to wood degradation and very low pH values.

2.5 – Latest advancements

As the current methods are not completely satisfactory, new research are ongoing regarding stabilization and extraction. A new tendency toward green chemistry applied to conservation emerges in the last decade. While designing novel conservation methods, some criteria have to be fulfilled. One of these criteria is to respect the integrity of the artifacts [34]. This ethic criterium implies that the aesthetic of the WAW object should not be altered by the treatment applied but also that the treatment should be innocuous for the artifact. If listed as one of the conservation criteria, the aesthetic of the treated samples may be subjective. The appearance of the recovered artifacts is usually first observed. Yet, some interventions that modified the appearance can lead to some discussion among the conservation community [87]. In this case, the preservation of the material takes priority over the aesthetical aspect. In addition, Brandi suggested that historical traces of the artifacts could remain visible after conservation [87]. Thus, the conservation of cultural materials should respect the historical modifications occurring on the artifacts as they are considered as part of the artifacts by the conservators, scientists, and public. Other important criteria have to be considered. If the treatment should be inoffensive for the artifacts, the same is true for the users and the environment. In addition, the new methods proposed should be reversible, or at least re-treatable [88]. Finally, a last criterium is the stability and durability of the treatment applied [34].

2.5.1 – Novel stabilization methods

Alternatives to PEG consolidation are currently investigated with ecofriendly approaches based on the utilization of carbohydrates. For instance, trehalose, in its amorphous state, can absorb moisture and once reaching its crystalline form, converts into a glassy and rigid structure. The high transparency and rigidity of crystallized trehalose permits maintaining the appearance of the recovered objects as well as their texture when touched [89]. Long-term monitoring after trehalose treatment showed that wood elasticity increases, as well as the resistance to loads (stress at failure) and no corrosion, occurs [68]. In addition, objects treated with trehalose showed stability facing high temperature and relative humidity [90]. Another recent alternative method is the employment of D-mannitol, a small sugar molecule with a higher eutectic temperature compared to PEG (-2 °C versus -22 °C). The impregnation and freeze-drying time with D-mannitol is then decreased by 3-4 times. Monitoring showed that a 5% w/w aqueous D-mannitol solution is not corrosive towards metals (if present) and avoids cracks and collapse of wooden artifacts [91]. Also, chitosan and aminocellulose, having a similar structure to cellulose, can form hydrogen bonds with the degraded polymeric content of WAW. These methods strengthen WAW structure, avoiding collapse [92].

A recent master thesis was released by the University of Oslo dealing with alternatives to freeze-drying [93]. Even if the study focused mainly on waterlogged oak, it resulted that air-drying could be a less aggressive method to conserve WAW artifacts, with either uncontrolled or controlled parameters. In fact, relative humidity (RH) and temperature could be monitored to stimulate evaporation from wood [94]. Even if these methods lasted longer than common freeze-drying procedures, the results obtained in terms of shrinkage, weight, and visual appearance were encouraging.

2.5.2 – Preventive extraction methods

The current curative methods are not completely efficient. Therefore, preventive approaches gain attention compared to traditional curative strategies for the conservation of heritage materials [95]. For example, the HeritageCare project, an international project involving partners from Portugal, Spain, and France, aims to develop preventive conservation methods for cultural heritage. This method could then be applied by any conservator based on defined protocols [95]. If not clearly defined in the HeritageCare project, application of preventive method for the preservation of WAW artifacts could be also considered. As for curative method, application of preventive methods should remediate to iron and sulfur contamination present on WAW.

Nowadays, recovered waterlogged wooden artifacts are not directly consolidated. The artifacts are placed in sealed containers, filled either with water from the burial site or with tap or deionized water. This prevents from the oxidation of reduced sulfur species present within the wood [96]. The storage methodology allows preserving the waterlogged wooden artifacts integrity before any further intervention is conducted. This is that is defined as preventive methods.

The aim of preventive methods is to remove the iron sulfide phases prior to the stabilization of the artifacts while artifacts are still wet. Extracting harmful iron and sulfur species before consolidation would prevent the oxidation and thus the precipitation of salts and acidification of the wood structure. Thereby, cracks and loss of strength should not appear, and the artifacts integrity conserved. Other advantages of preventive methods would be the compatibility with consolidation procedure. Indeed, some curatives methods described in section 2.4.2 degraded the PEG molecules. Renew of consolidation was thus necessary. With preventive methods, only one consolidation step would be foreseen.

Therefore, preventive methods could be promising extraction methods to preserve WAW artifacts. Their actions and properties may be different from the curative extraction methods presented above.

Dissolution of iron sulfides with chelators is widely studied especially in waste, ore, and gas industry [97], [98]. For example, Ramanathan et al [99] have studied the employment of EDTA, DTPA, and HDTPA (N-(2-hydroxyethyl)ethylenediamine-N,N',N'-triacetic acid) solutions at different concentrations and pH. Their research showed similar results when these agents are employed in preventive methods on iron sulfide powders, with important Fe extraction rates. Though, the extraction was pH-dependent with higher rates obtained in the acidic range. Furthermore, the extraction was carried out at an elevated temperature (≈ 65 °C). Based on the encouraging results obtained, chelating agents such as EDTA, were investigated on WAW contaminated with iron sulfides. To prevent wood degradation, parameters were modified, such as pH and temperature. In particular, EDTA was examined when combined with a pre-treatment in sodium persulfate $Na_2S_2O_8$ [100]. Sodium persulfate is an oxidant that possesses the ability to oxidize pyrite into sulfates [100]. This oxidant has a higher redox potential (E^0 = 2.6 V) compared to common oxidizing agents ($E^0(H_2O_2)$ = 1.78 V, $E^0(KMnO_4)$ 0 1.7 V, $E^0(O_3)$ = 2.07 V) [101]. In general, iron (II) compounds may be electron donor for persulfate reduction

even if the reaction mechanisms are not fully understood. In addition to the conversion into soluble sulfates, the iron entity of iron sulfides could also be transformed into more soluble iron phases. In the case of an incomplete solubilization of iron species, further extraction with EDTA as current and common treatment should extract the remained traces iron species present. Employment of sodium persulfate was then suggested to increase the extraction rates of both iron and sulfur species. The results obtained showed that pre-immersion in $Na_2S_2O_8$ improved iron dissolution during treatment with EDTA: 30% of iron was extracted in 24 hours when using sodium persulfate/EDTA while 60% of iron was extracted in 72 hours using only EDTA solution. In addition, the wood treated with sodium persulfate and EDTA solutions presented a brown appearance. However, this study only focused on iron extraction and further investigation regarding sulfur mitigation should be performed. An alternative to chelating agents is dissolution with hydrochloric acid HCl [102]. As discussed in paragraph 2.3, some iron sulfide minerals are acid-soluble, such as mackinawite FeS and greigite Fe_3S_4 and could be solubilized with HCl, leading however to the production of toxic H_2S gas (equation (7)):

$$FeS + 2HCl \rightarrow Fe^{2+} + 2Cl^{-} + H_2S \quad (7)$$

HCl treatment may be also problematic for the wooden artifacts with metal parts as chlorides are released. If metal parts are present in the object, Cl^- ions present may lead to further corrosion processes [103]. In addition, the application of HCl on wood may degrade wood components [104]. When immersed in strong acidic solutions, the cellulose content of the wood material gets hydrolyzed. The acidic pH may endanger the wood structure and lead to more decay. This is that is currently observed on consolidated and exposed artifacts with the production of sulfuric acid [62]. Thus, the application of HCl on WAW may be avoided in order to conserve WAW structure as preventing the formation of harmful Cl^- and H_2S. Therefore, eco-friendly, and less aggressive treatment was investigated by Gamal et al that proposed a biodegradable acid derived from HCl to dissolve iron sulfide minerals [102]. The first results obtained showed that the high solubility of iron sulfides was enough to result in their dissolution in a shorter reaction time than with pure HCl without reporting which species were released at this end of the experiment (Fe^{2+}, Fe^{3+}, S^{2-}, SO_4^{2-}). Even if this green solution could be a promising alternative for acidic dissolution of iron sulfides, no study about its employment on WAW is reported yet and application of acid solution may decay the wood material. Regarding the neutralization of produced H_2SO_4, investigations of nanoparticles of earth alkaline hydroxides were proposed by Taglieri et al [105]. Magnesium nanoparticles produced in water were investigated as preventive deacidification method. Treated artifacts presented neutral pH but also maintained their appearance after recovery. Another method under study is the application of strontium carbonate $SrCO_3$ nanoparticles embedded in cellulose patches [106]. The first results showed that iron was leached from the surface layers and strontium sulfate salts $SrSO_4$ were formed. Regarding sulfur species, the local application of the cellulose patches mentioned above also reduces the production of sulfuric acid. The use of $SrCO_3$ nanoparticles could then be a promising extraction method for both iron and sulfur species.

2.5.3 – Biotechnologies

Alternatively, biological methods are currently being proposed. Indeed, bio-based methods have proven to be sustainable solutions for the preservation of cultural artifacts [88]. Microbial processes can be used for consolidation, cleaning, or even mitigation of reactive corrosion products while reducing the potential risks associated with traditionally used methods [89]. Concerning stone conservation, the application of bacterial carbonatogenesis promotes the consolidation of porous stone with the production of calcite $CaCO_3$ through the biomineralization process [102], [107]. The strain *Pseudomonas stutzeri*, applied with an agar carrier, showed to be a promising alternative to clean animal glue of indoor wall painting and in a short time (2 h) [108]. For metal conservation, a strain of *Beauvaria bassiana* produces oxalic acid in presence of toxic metals such as copper. Reactive copper salts are then converted into copper oxalates. Applied on bronze sculptures, this method allows forming a protective and stable system preventing further corrosion and leaching [90]. Microorganisms can also be employed to stabilize corroded layers of archaeological iron artifacts. Akaganeite β-FeOOH, a chlorine-containing iron oxyhydroxide, can hence be converted into chemically stable vivianite $Fe_3(PO_4)_2{\cdot}8H_2O$, siderite $FeCO_3$ or magnetite Fe_3O_4 [91]–[93].

In addition, microorganisms can be employed as consolidation agents or as extraction agents for waterlogged wood preservation. In fact, *Acetobacter xylinum* strain was employed to grow bacterial cellulose, allowing the consolidation of wood degraded parts [109]. The experiments were performed at room temperature in a liquid medium with fructose as a carbon source. Even when competing bacteria already present in WAW, bacterial cellulose was formed in the degraded parts of wood, preventing the collapse of the structure. Also, specific bacteria proved their ability regarding the removal of mackinawite FeS and pyrite FeS_2, the main iron sulfides detected in such artifacts [110]. Studies of ore metal recovery showed that acidophilic iron-oxidizing and sulfur-oxidizing bacteria such as *Acidothiobacillus ferrooxidans* and *Thiobacillus denitrificans* were able to solubilize the targeted minerals [111], [112]. Both these strains are facultative anaerobes but *A. ferrooxidans* grows in acidic range while *T. denitrificans* in neutral range, making this bacterium more adequate regarding a potential application in WAW conservation. Thus, *T. denitrificans* was suggested to develop a bio-based extraction method for WAW artifacts [110]. A preliminary master thesis of the University of Neuchâtel (Switzerland) was conducted on the topic in 2015-2016 [113]. The results obtained demonstrated the ability of *T. denitrificans* to convert reduced sulfur phases into soluble sulfates. Furthermore, no wood degradation was observed. Based on the encouraging results, it was decided to develop a preventive bio-based extraction method, employing the unique properties of microorganisms such as *T. denitrificans*.

3 – MICrobes for Archaeological wood Conservation

The MICMAC project (MICrobes for Archaeological wood Conservation) aims to develop a microbial extraction of iron and sulfur species present in waterlogged archaeological wood when this latter is still soaked by water and before any consolidation. It stands as a preventive approach, using the unique properties of selected microorganisms to oxidize iron sulfides.

Previous studies reported that specific bacteria, such as *Thiobacillus denitrificans,* could oxidize iron sulfides and be used in WAW conservation [110]. This chemolithotrophic bacteria is known to employ nitrates as electron donors to oxidize iron sulfides. Even if anaerobic oxidation has been reported, its mechanism remains unclear. Bosch and Meckenstock [51] have observed during their experiments that, for a direct oxidation by *T. denitrificans*, iron sulfide minerals, like pyrite FeS_2 should be at nanometric size. Of interest, the microenvironment created at the mineral-bacteria interface is at neutral pH. The most probably occurring mechanisms of oxidation of mackinawite and pyrite are thus given in equations (8) and (9):

$$5FeS + 8NO_3^- + 8H^+ \rightarrow 5Fe^{2+} + 5SO_4^{2-} + 4N_2 + 4H_2O \quad (8)$$

$$5FeS_2 + 14NO_3^- + 4H^+ \rightarrow 5Fe^{2+} + 10SO_4^{2-} + 7N_2 + 2H_2O \quad (9)$$

Soluble sulfate SO_4^{2-} ions are produced as well as soluble ferrous Fe^{2+} ions. Under these forms, their extraction from WAW artifacts would be facilitated. Nitrogen N_2 and nitrites NO_2^- can both be end products, but nitrites are only formed if the reduction from nitrates is incomplete, as shown in equation (10):

$$FeS_2 + 7.5NO_3^- + 3.5H_2O \rightarrow Fe(OH)_3 + 2SO_4^{2-} + 7.5NO_2^- + 4H^+ \quad (10)$$

This mechanism also suggests the formation of iron (oxy)hydroxides $Fe(OH)_3$ as end products. However, the formation of iron oxyhydroxides was always suggested but never confirmed [114], [115]. In addition, if the oxidation is incomplete and iron (oxy)hydroxides precipitated within WAW, their extraction could be more problematic due to the low solubility of these minerals at circumneutral pH [116]. A biological approach to complex and dissolve ferric minerals is the use of naturally occurring iron-chelating agents. These chelating agents are known as siderophores. Produced in iron depletion conditions, siderophores present the highest binding affinities for iron as the capacity to solubilize several iron minerals [117]-[119]. Employment of *T. denitrificans* and siderophores was thus investigated in the MICMAC project to solubilize iron and sulfur and to facilitate their extraction from WAW.

With the financial support of the Swiss National Science Foundation (Professorship Grant PP00P2_163653/1,2016-2020), the microbial oxidation processes of iron sulfides were investigated. Degradation and contamination protocols to replicate WAW artifacts were also defined and allowed to compare the efficiency of different preventive extraction methods.

The MICMAC project is divided into three main work packages (WP) described in Figure 9:

- *WP1: Study of a relevant chemical processes in microorganisms*
  Selection of adapted microorganisms able to dissolve and/or chelate iron sulfides
- *WP2: Definition of an application protocol on model samples*
  Preparation of model samples through degradation of carbohydrates and Fe/S contamination, and definition of a specific analytical protocol
- *WP3: Evaluation of proposed preventive extraction treatments*
  Application of optimized biological and chemical extraction treatments on WAW samples with monitoring allowing to assess performances, limits, and long-term behavior.

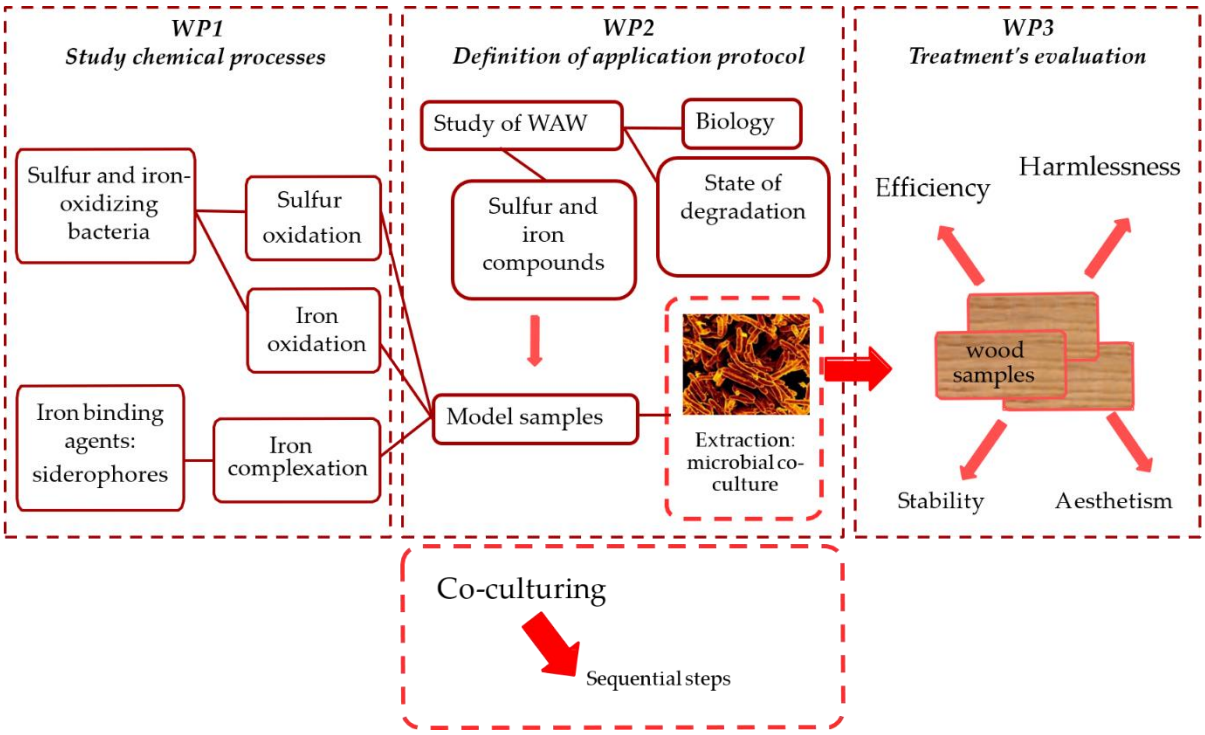

Figure 9: Schematic representation of the MICMAC work packages (WP) and main goals foreseen (Unine ©)

This PhD project was mostly involved with WP2 and WP3. The objectives of the thesis were i) to define degradation and contamination protocols to replicate WAW by preparing model samples either from fresh or freshwater WAW wood, ii) to propose a specific analytical protocol, and iii) to evaluate preventive biological and chemical extraction methods under study. The samples selection, protocols and conservation methods designed as well as the analytical techniques employed are described in Chapter 2. Chapter 3 presents the different protocols applied to degrade and contaminate either fresh or to contaminate naturally degraded wood model samples. WAW wood samples were used as reference to validate modeling. In Chapter 4, biological and chemical extraction methods were tested on model samples defined in Chapter 3 and on WAW samples. Their efficiency was evaluated in terms of visual appearance, innocuousness for the wood substrate, and Fe/S extraction rates. To go further in the validation of the treatments, a traditionally used conservation procedure was applied on treated models and WAW samples to evaluate compatibility. If not foreseen, chemometrics was successfully applied, allowing to validate the observations and to ascertain the protocols studied in Chapters 3 and 4.

References

[1] A. C. Wiedenhoeft and R. B. Miller, "2. Structure and Function of Wood," *Handb. Wood Chem. Wood Compos.*, 2005.

[2] J. Radkau and I. Schäfer, *Holz: wie ein Naturstoff Geschichte schreibt*, vol. 3. oekom Verlag, 2007.

[3] Y. Fors, "Sulfur-Related Conservation Concerns for Marine Archaeological Wood2, 2008.

[4] J. V. Serrão, D. Freire, L. Fernández Prieto, and R. Santos, "Old and New Worlds: The Global Challenges of Rural History. Conference eBook," 2016.

[5] R. W. Haynes, "An analysis of the timber situation in the United States: 1952 to 2050.," *Gen. Tech. Rep. PNW-GTR-560. Portland, OR US Dep. Agric. For. Serv. Pacific Northwest Res. Station*. 254 p, vol. 560, 2003.

[6] B. Waliszewska, W. Pradzynski, M. Zborowska, A. Stachowiak-Wencek, H. Waliszewska, and A. Spak-Dzwigala, "The diversification of chemical composition of pine wood depending on the tree age," *Ann. Warsaw Univ. Life Sci. For. Wood Technol.*, vol. 91, 2015.

[7] J. Perlin, *A forest journey: The story of wood and civilization*. The Countryman Press, 2005.

[8] M. Ek, G. Gellerstedt, and G. Henriksson, *Wood chemistry and biotechnology*, vol. 1. Walter de Gruyter, 2009.

[9] Y. Fors, T. Nilsson, E. D. Risberg, M. Sandström, and P. Torssander, "Sulfur accumulation in pinewood (Pinus sylvestris) induced by bacteria in a simulated seabed environment: Implications for marine archaeological wood and fossil fuels," *Int. Biodeterior. Biodegrad.*, vol. 62, no. 4, pp. 336–347, 2008.

[10] K. Kranitz, "Effect of natural aging on wood," 2014.

[11] D. W. Grattan, "Waterlogged wood," in *Conservation of marine archaeological objects*, Elsevier, pp. 55–67, 1987.

[12] K. Kuroda, "Functions of Parenchyma Cells in Wood; Material Transport and Heartwood Formation," *Mokuzai Gakkaishi*, vol. 61, no. 3, pp. 131–135, 2015.

[13] A. B. Anderson, "The composition and structure of wood." ACS Publications, 1958.

[14] R. M. Rowell, R. Pettersen, J. S. Han, J. S. Rowell, and M. A. Tshabalala, "Cell wall chemistry," *Handb. wood Chem. wood Compos.*, vol. 2, 2005.

[15] P. Basu, *Biomass gasification, pyrolysis, and torrefaction: practical design and theory*. Academic press, 2018.

[16] R. C. Pettersen, "The chemical composition of wood," ACS Publications, 1984.

[17] D. Fengel and G. Wegener, *Wood: chemistry, ultrastructure, reactions*. Walter de Gruyter, 2011.

[18] L. Hrdlička, A. Škulcová, and A. Ház, "Degradation of lignin via Fenton reaction," in *5th International Scientific Conference, Renewable Energy Sources, Tatranské Matliare, Slovakia*, 2014

[19] C. Bonechi, M. Consumi, A. Donati, G. Leone, A. Magnani, G. Tamasi, and C. Rossi, "Biomass: an overview," in *Bioenergy systems for the future*, Elsevier, pp. 3–42, 2017.

[20] M. Z. M. Salem, M. Böhm, P. Šedivka, R. A. Nasser, H. M. Ali, and W. A. Elgat, "Some physico-mechanical characteristics of uncoated OSB ECO-products made from Scots Pine (Pinus sylvestris L.) and bonded with pMDI resin," *BioResources*, vol. 13, no. 1, pp. 1814–1828, 2018.

[21] H. E. Young and V. P. Guinn, "Chemical elements in complete mature trees of seven species in Maine," *Tappi*, vol. 49, no. 5, pp. 190–197, 1966.

[22] C. G. Björdal, "Microbial degradation of waterlogged archaeological wood," *J. Cult. Herit.*, vol. 13, no. 3, pp. S118–S122, 2012.

[23] C. G. Björdal and T. Nilsson, "Waterlogged archaeological wood—a substrate for white rot fungi during drainage of wetlands," *Int. Biodeterior. Biodegradation*, vol. 50, no. 1, pp. 17–23, 2002

[24] C. G. Björdal and T. Nilsson, "Reburial of shipwrecks in marine sediments: a long-term study on wood degradation," *J. Archaeol. Sci.*, vol. 35, no. 4, pp. 862–872, 2008.

[25] M. Sandström, Y. Fors, and I. Persson, *The Vasa's New Battle: Sulfur, Acid and Iron*. National Maritime Museums [Statens maritima museer], 2003.

[26] C. G. Björdal, G. Daniel, and T. Nilsson, "Depth of burial, an important factor in controlling bacterial decay of waterlogged archaeological poles," *Int. Biodeterior. Biodegrad.*, vol. 45, no. 1–2, pp. 15–26, 2000.

[27] R. Mouzouras, A. M. Jones, E. B. G. Jones, and M. H. Rule, "Non-Destructive Evaluation of Hull and Stored Timbers from the Tudor Ship 'Mary Rose,'" *Stud. Conserv.*, vol. 35, no. 4, p. 173, 1990.

[28] R. M. Seborg and R. B. Inverarity, "Preservation of old, waterlogged wood by treatment with polyethylene glycol," *Science* (80-.)., vol. 136, no. 3516, pp. 649–650, 1962.

[29] M. Romagnoli, G. Galotta, F. Antonelli, G. Sidoti, M. Humar, D. Krzisnik, K. Cufar, and B. D. Petriaggi, "Micro-morphological, physical and thermogravimetric analyses of waterlogged archaeological wood from the prehistoric village of Gran Carro (Lake Bolsena-Italy)," *J. Cult. Herit.*, vol. 33, pp. 30–38, 2018.

[30] C. Remazeilles, L. Meunier, F. Lévêque, N. Plasson, E. Conforto, M. Crouzet, P. Refait, and L. Caillat, "Post-treatment Study of Iron/Sulfur-containing Compounds in the Wreck of Lyon Saint-Georges 4 (Second Century ACE)," *Stud. Conserv.*, vol. 65, no. 1, pp. 28–36, 2020.

[31] M. Egloff, "Recent archaeological discoveries in Lake Neuchatel, Switzerland. From the Paleolithic to the Middle Ages," *Wet Site Archaeol.*, pp. 31–42, 1988.

[32] K. Ismail-Meyer, P. Rentzel, and P. Wiemann, "Neolithic lakeshore settlements in

Switzerland: new insights on site formation processes from micromorphology," *Geoarchaeology*, vol. 28, no. 4, pp. 317–339, 2013.

[33] C. M. A. McQueen, D. Tamburini, J. J. Lucejko, S. Braovac, F. Gambineri, F. Modugno, M. P. Colombini, and H. Kutzke, "New insights into the degradation processes and influence of the conservation treatment in alum-treated wood from the Oseberg collection," *Microchem. J.*, vol. 132, pp. 119–129, 2017.

[34] M.-L. E. Florian, "Scope and history of archaeological wood," ACS Publications, 1990.

[35] C. G . Björdal, T. Nilsson, and G. Daniel, "Microbial decay of waterlogged archaeological wood found in Sweden Applicable to archaeology and conservation," *Int. Biodeterior. Biodegradation*, vol. 43, no. 1–2, pp. 63–73, 1999.

[36] Y. S. Kim, A. P. Singh, and T. Nilsson, "Bacteria as Important Degraders in Waterlogged Archaeological Woods," *Holzforschung*, vol. 50, no. 5, pp. 389–392, 1996.

[37] G. Daniel and T. Nilsson, "Developments in the study of soft rot and bacterial decay In: Forest Products Biotechnology (Bruce, A. and Palfreyman, JW, Eds.)." Taylor & Francis, London, 1998.

[38] T. Nilsson and C. G. Björdal, "Culturing wood-degrading erosion bacteria," *Int. Biodeterior. Biodegrad.*, vol. 61, no. 1, pp. 3–10, 2008.

[39] A. P. Singh and J. A. Butcher, "Bacterial degradation of wood cell walls: a review of degradation patterns," *J. Inst. Wood Sci.*, vol. 12, pp. 143–157, 1991.

[40] M. Albelda Berenguer, M. Monachon, C. Jacquet, P. Junier, C. Rémazeilles, E. J. Schofield, and E. Joseph, "Biological oxidation of sulfur compounds in artificially degraded wood," *Int. Biodeterior. Biodegrad.*, vol. 141, pp. 62-70, 2018.

[41] A. Wargin, K. Olańczuk-Neyman, and M. Skucha, "Sulphate-Reducing Bacteria, Their Properties and Methods of Elimination from Groundwater.," *Polish J. Environ. Stud.*, vol. 16, no. 4, 2007.

[42] J. Sørensen, D. Christensen, and B. B. Jørgensen, "Volatile Fatty Acids and Hydrogen as Substrates for Sulfate-Reducing Bacteria in Anaerobic Marine Sediment," *Appl. Environ. Microbiol.*, vol. 42, no. 1, pp. 5–11, 1981.

[43] A. Jongejan, "Observations on a microbial cellulose degradation process that decreases water acidity," *Int. Biodeterior.*, vol. 22, no. 3, pp. 207–211, 1986.

[44] S. Takii, "Amino acids as main substrates for sulfate-reducing bacteria in surface sediment of a eutrophic bay," *J. Gen. Appl. Microbiol.*, vol. 49, no. 6, pp. 329–336, 2003.

[45] J. H. Tuttle, P. R. Dugan, and C. I. Randles, "Microbial sulfate reduction and its potential utility as an acid mine water pollution abatement procedure.," *Appl. Microbiol.*, vol. 17, no. 2, pp. 297–302, 1969.

[46] C. Rémazeilles, K. Tran, E. Guilminot, E. Conforto, and P. Refait, "Study of Fe(II) sulphides in waterlogged archaeological wood," *Stud. Conserv.*, vol. 58, no. 4, pp. 297–307, 2013.

[47] Y. Fors and V. Richards, "The effects of the ammonia neutralizing treatment on marine

archaeological Vasa wood," *Stud. Conserv.*, vol. 55, no. 1, pp. 41–54, 2010.

[48] G. Almkvist, S. Norbakhsh, I. Bjurhager, and K. Varmuza, "Prediction of tensile strength in iron-contaminated archaeological wood by FT-IR spectroscopy-a study of degradation in recent oak and Vasa oak," *Holzforschung*, vol. 70, no. 9, pp. 855–865, 2016.

[49] D. Rickard and G. W. Luther, *Chemistry of iron sulfides*, vol. 107, no. 2. 2007.

[50] J. A. Bourdoiseau, M. Jeannin, R. Sabot, C. Rémazeilles, and P. Refait, "Characterisation of mackinawite by Raman spectroscopy: Effects of crystallisation, drying and oxidation," *Corros. Sci.*, vol. 50, no. 11, pp. 3247–3255, 2008.

[51] K.-Y. L. Julian Bosch Guntram Jordan Kyoung-Woong Kim and Rainer U. Meckenstock, "Anaerobic, Nitrate-Dependent Oxidation of Pyrite Nanoparticles by Thiobacillus denitrificans," *Est*, pp. 1–11, 2012.

[52] W. Sand, T. Gehrke, P.-G. Jozsa, and A. Schippers, "(Bio)chemistry of bacterial leaching—direct vs. indirect bioleaching," *Hydrometallurgy*, vol. 59, no. 2–3, pp. 159–175, 2001.

[53] D. Rickard and G. W. Luther, "Kinetics of pyrite formation by the H2S oxidation of iron (II) monosulfide in aqueous solutions between 25 and 125°C: The mechanism," *Geochim. Cosmochim. Acta*, vol. 61, no. 1, pp. 135–147, 1997.

[54] S. Boursiquot, M. Mullet, M. Abdelmoula, J.-M. Génin, and J.-J. Ehrhardt, "The dry oxidation of tetragonal FeS 1-x mackinawite," *Phys. Chem. Miner.*, vol. 28, no. 9, pp. 600–611, 2001.

[55] G. Da Costa, A. Hofmann, and A. Agangi, "Provenance of Detrital Pyrite in Archean Sedimentary Rocks: Examples From the Witwatersrand Basin," in *Sediment Provenance*, Elsevier, pp. 509–531, 2017.

[56] A. Newman, "Pyrite oxidation and museum collections: a review of theory and conservation treatments," *Geol. curator*, vol. 6, no. 10, pp. 363–371, 1998.

[57] N. R. Larkin, "Pyrite Decay: cause and effect, prevention and cure," *NatSCA News*, vol. 21, pp. 35–43, 2011.

[58] J. Preston, A. D. Smith, E. J. Schofield, A. V. Chadwick, M. A. Jones, and J. E. M. Watts, "The effects of Mary Rose conservation treatment on iron oxidation processes and microbial communities contributing to acid production in marine archaeological timbers," *PLoS One*, vol. 9, no. 2, 2014.

[59] M. Sandström, F. Jalilehvand, E. Damian, Y. Fors, U. Gelius, M. Jones, and M. Salomé "Sulfur accumulation in the timbers of King Henry VIII's warship Mary Rose: a pathway in the sulfur cycle of conservation concern.," *Proc. Natl. Acad. Sci. U. S. A.*, vol. 102, no. 40, pp. 14165–70, 2005.

[60] J. A. Emery and H. A. Schroeder, "Iron-catalyzed oxidation of wood carbohydrates," *Wood Sci. Technol.*, vol. 8, no. 2, pp. 123–137, 1974.

[61] H. Y. Jeong, Y.-S. Han, S. W. Park, and K. F. Hayes, "Aerobic oxidation of mackinawite (FeS) and its environmental implication for arsenic mobilization," *Geochim. Cosmochim.*

Acta, vol. 74, no. 11, pp. 3182–3198, 2010.

[62] K. M. Wetherall, R. M. Moss, A. M. Jones, A. D. Smith, T. Skineer, D. M. Pickup, S. W. Goatham, A. V. Chadwick, and R. J. Newport, "Sulfur and iron speciation in recently recovered timbers of the Mary Rose revealed via X-ray absorption spectroscopy," *J. Archaeol. Sci.*, vol. 35, no. 5, pp. 1317–1328, 2008.

[63] C. Rémazeilles, M. Saheb, D. Neff, E. Guilmimot, K. Tran, J.-A. Bourdoiseau, R. Sabot, M. Jeannin, H. Matthiesen, P. Dillmann, and P. Refait, "Microbiologically influenced corrosion of archaeological artefacts:Characterisation of iron(II) sulfides by Raman spectroscopy," J. Raman Spectrosc., vol. 41, no. 11, pp. 1425–1433, 2010.

[64] Y. Fors and M. Sandström, "Sulfur and iron in shipwrecks cause conservation concerns," *Chem. Soc. Rev.*, vol. 35, no. 5, pp. 399–415, 2006.

[65] M. Broda, B. Mazela, and K. Radka, "Methyltrimethoxysilane as a stabilising agent for archaeological waterlogged wood differing in the degree of degradation," *J. Cult. Herit.*, vol. 35, pp. 129-139, 2018.

[66] M. Sandström, F. Jalilehvand, I. Persson, U. Gelius, P. Frank, and I. Hall-Roth, "Deterioration of the seventeenth-century warship Vasa by internal formation of sulphuric acid," *Nature*, vol. 415, no. 6874, pp. 893–897, 2002.

[67] R. Giorgi, D. Chelazzi, and P. Baglioni, "Nanoparticles of calcium hydroxide for wood conservation. The deacidification of the Vasa warship," *Langmuir*, vol. 21, no. 23, pp. 10743–10748, 2005.

[68] A. Tahira, W. Howard, E. R. Pennington, and A. Kennedy, "Mechanical strength studies on degraded waterlogged wood treated with sugars," *Stud. Conserv.*, vol. 62, no. 4, pp. 223–228, 2017.

[69] R. Walker, "Instability of Iron Sulfides on Recently Excavated Artifacts," *Stud. Conserv.*, vol. 46, no. 2, p. 141, 2001.

[70] P. Hoffmann and J. Pätzold, "The stabilisation of wet sediment cores by means of a polyethylene glycol/freeze-drying treatment for display and permanent storage," *GeoMarine Lett.*, vol. 21, no. 4, pp. 245–252, 2001.

[71] W. R. Ambrose, "Application of freeze-drying to archaeological wood," ACS Publications, 1990.

[72] P. Hoffmann, *Conservation of Archaeological Ships and Boats: Personal Experiences*. Archetype Publications, 2013.

[73] G. Giachi, C. Capretti, I. D. Donato, N. Macchioni, and B. Pizzo, "New trials in the consolidation of waterlogged archaeological wood with different acetone-carried products," *J. Archaeol. Sci.*, vol. 38, no. 11, pp. 2957–2967, 2011.

[74] G. Almkvist and I. Persson, "Extraction of iron compounds from wood from the Vasa," *Holzforschung*, vol. 60, no. 6, pp. 678–684, 2006.

[75] E. A. Sanya, S.-A. Rezzoug, and K. Allaf, "A new method for drying waterlogged wooden artefacts: Comparison of cyclical pressure drops with conventional methods,"

Chem. Eng. Res. Des., vol. 81, no. 9, pp. 1243–1249, 2003.

[76] S. Rapti, S. Boyatzis, S. Rivers, A. Velios, and A. Pournou, "Removing iron stains from wood and textile objects: assessing gelled siderophores as novel green chelators," in *International conference Science in Techology, Athens*, 2017.

[77] L. Selwyn, C. Cook, W. R. McKinnon, R. Fairman, and S. Labroche, "Iron stain removal from archaeological composite artifacts made of wood and iron," *J. Can. Assoc. Conserv. J. l'Association Can. pour la Conserv. la Restaur.*, vol. 38, p. p-31, 2013.

[78] A. E. Martell, R. J. Motekaitis, D. Chen, R. D. Hancock, and D. McManus, "Selection of new Fe (III)/Fe (II) chelating agents as catalysts for the oxidation of hydrogen sulfide to sulfur by air," *Can. J. Chem*., vol. 74, no. 10, pp. 1872–1879, 1996.

[79] G. Almkvist, "Iron Removal from Waterlogged Wood." in *12th ICOM-CC Wet Organic Archaeological Materials Working Group Conference, Istanbul, Turkey* 2013.

[80] R. Boxma, "Effect of pH on the behaviour of various iron chelates in sphagnum (moss) peat," *Commununication soil Sci. plant Anal*., vol. 12, no. 8, pp. 755–763, 1981.

[81] W. A. Norvell, "Reactions of metal chelates in soils and nutrient solutions," *Micronutr. Agric*., vol. 4, pp. 187–227, 1991.

[82] H. Burgess, "The use of chelating agents in conservation treatments," *Pap. Conserv*., vol. 15, no. 1, pp. 36–44, 1991.

[83] D. G. Suryawanshi and S. K. Bisaria, "Removing metallic stains from paper objects using chelating agent EDTA," *Restaur. Int. J. Preserv. Libr. Arch. Mater*., vol. 26, no. 4, pp. 276–285, 2005.

[84] S. Irwin, "A comparison of the use of sodium metabisulfite and sodium dithionite for removing rust stains from paper," *B. Pap. Gr. Annu*., vol. 30, no. 37, pp. 37–46, 2011.

[85] A. Berko, A. D. Smith, A. M. Jones, E. J. Schofield, J. F. W. Mosselmans, and A. V Chadwick, "XAS studies of the effectiveness of iron chelating treatments of Mary Rose timbers," in *Journal of Physics: Conference Series*, vol. 190, no. 1, 2009.

[86] C. M. A. McQueen, S. Braovac, J. J. Lucejko, and F. Modugno, "Unexpected ammonium compounds in alum-treated wood from the Oseberg collection," in *14th ICOM-CC Wet Organic Archaeological Materials Working Group Confreence, Portsmouth, United Kingdom* 2019.

[87] C. Brandi and C. Déroche, *Théorie de la restauration*. École nationale du patrimoine, 2001.

[88] B. Appelbaum, "Criteria for treatment: reversibility," *J. Am. Inst. Conserv*., vol. 26, no. 2, pp. 65–73, 1987.

[89] K. Ito, T. Matsui, A. Miyake, and S. Imazu, "The conservation treatment of wood-iron composite objects excavated from marine contexts using the trehalose method: a study of the stabilization of iron after conservation treatment," in *14th ICOM-CC Wet Organic Archaeological Materials Working Group Confreence, Portsmouth*, 2019.

[90] S. Mahapol, "The conservation of ropes from the phanom-surin shipwreck site, Thailand," in *14th ICOM-CC Wet Organic Archaeological Materials Working Group*

Confreence, Portsmouth, 2019.

[91] K. Straetkvern, "From promising theories to praxis - conservation of a large oak barque stern with d-mannitol," in *14th ICOM-CC Wet Organic Archaeological Materials Working Group Confreence, Portsmouth*, 2019.

[92] J. Wakefield, "Investigation of natural polymers for treatments of Oseberg artefacts: review of lab degraded and archaeological wood," in *14th ICOM-CC Wet Organic Archaeological Materials Working Group Confreence, Portsmouth*, 2019.

[93] K. S. Hennum-simmonds, "A Study of Alternatives to Freeze-Drying A Study of Alternatives to Freeze-Drying," 2020.

[94] Á. Tímár-Balázsy and D. Eastop, *Chemical principles of textile conservation*. Routledge, 1998.

[95] M. G. Masciotta, M.J. Morais, L. F. Ramos, D. V. Oliveira, L. J. Sánchez-Aparicio, and D. González-Aguilera, "A Digital-based Integrated Methodology for the Preventive Conservation of Cultural Heritage: The Experience of HeritageCare Project", *Inter. J. Arch. Herit*., pp. 1-20, 2019.

[96] J. Gelbrich and L. Poelmans, "Post-excavation storage of large waterlogged wooden objects – pilot project in monitoring of degradation activity", in *12th ICOM-CC Wet Organic Archaeological Materials (WOAM) Conference Proceedings. Istanbul, Turkey,* 2013.

[97] M. S. Kamal, I. Hussein, M. Mahmoud, A. S. Sultan, and M. A. S. Saad, "Oilfield scale formation and chemical removal: A review," *J. Pet. Sci. Eng*., vol. 171, pp. 127–139, 2018.

[98] M. Mahmoud, I. A. Hussein, A. Sultan, M. A. Saad, W. Buijs, and T. J. H. Vlugt, "Development of efficient formulation for the removal of iron sulphide scale in sour production wells," *Can. J. Chem. Eng*., vol. 96, no. 12, pp. 2526–2533, 2018.

[99] R. Ramanathan and H. Nasr-el-din, "SPE-197891-MS Evaluation of Chelating Agents for Iron Sulfide FeS Scale Removal Chemistry of Polyaminocarboxylic Acid," pp. 16–20, 2019.

[100] C. Pelé, E. Guilminot, S. Labroche, G. Lemoine, and G. Baron, "Iron removal from waterlogged wood : Extraction by electrophoresis and chemical treatments," *Stud. Conserv*., vol. 60, no. 3, pp. 1–17, 2013.

[101] Y. Yuan, H. Tao, J. Fan, and L. Ma, "Degradation of p-chloroaniline by persulfate activated with ferrous sulfide ore particles", *Chemical Engineering J*., vol. 268, pp. 38-46, 2015.

[102] H. Gamal and K. Abdelgawad, "New Environmentally Friendly Acid System for Iron Sulfide Scale Removal," 2019.

[103] M. Rimmer, D. Watkinson, and Q. Wang, "The efficiency of chloride extraction from archaeological iron objects using deoxygenated alkaline solutions," *Stud. Conserv*., vol. 57, no. 1, pp. 29–41, 2012.

[104] E. E. Harris and A. A. Kline, "Hydrolysis of wood cellulose with hydrochloric acid and sulfur dioxide and the decomposition of its hydrolytic products.," *J. Phys. Chem*., vol.

53, no. 3, pp. 344–351, 1949.

[105] G. Taglieri, V. Daniele, L. Macera, R. Schweins, S. Zorzi, M. Capron, G. Chaumat, and C. Mondelli, "Sustainable nanotechnologies for curative and preventive wood deacidification treatments: An eco-friendly and innovative approach," *Nanomaterials*, vol. 10, no. 9, pp. 1–16, 2020.

[106] E. J. Schofield, R. Sarangi, A. Mehta, A. M. Jones, A. Smith, J. F. W. Mosselmans, and A. V. Chadwick, "Strontium carbonate nanoparticles for the surface treatment of problematic sulfur and iron in waterlogged archaeological wood," *J. Cult. Herit.*, vol. 18, pp. 306–312, 2016.

[107] F. Jroundi, A. Fernández-Vivas, C. Rodriguez-Navarro, E. J. Bedmar, and M. T. González-Muñoz, "Bioconservation of deteriorated monumental calcarenite stone and identification of bacteria with carbonatogenic activity," *Microb. Ecol.*, vol. 60, no. 1, pp. 39–54, 2010.

[108] M. del P. Bosch Roig, J. L. Regidor Ros, M. P. Soriano Sancho, and R. M. Montes Estellés, "Biocleaning of animal glue on wall paintings by Pseudomonas stutzeri," *Chim. Oggi–Chemistry Today*, vol. 31, no. 1, pp. 50–53, 2013.

[109] D. Gregory, K. Lyngby, D. Yvonne Shashoua, and N. Braunschweig Hansen, "Anyone for a nice cup of tea? The use of bacterial cellulose for conservation of waterlogged archaeological wood," in *18th ICOM-CC Triennial Conference, Copenhage*, 2017.

[110] K. Tran, N. Bertout, F. Dalard, and J.-P. Magnin, "Trials on chemical and microbiological processes for the oxidation of sulphur compounds in archaeological wood," in *9th ICOM-CC on Wet Organic Archaeological Materials Working Group Conference, Copenhague*, 2004.

[111] M. Monachon, M. Albelda-Berenguer, and E. Joseph, "Biological oxidation of iron sulfides," in *Advances in applied microbiology*, vol. 107, Elsevier, pp. 1–27, 2019.

[112] A. Mahmoud, P. Cézac, A. F. A. Hoadley, F. Contamine, and P. D'Hugues, "A review of sulfide minerals microbially assisted leaching in stirred tank reactors," *Int. Biodeterior. Biodegrad.*, vol. 119, pp. 118–146, 2017.

[113] C. Jacquet, "Applications biotechnologiques à la préservation des biens culturels en bois," 2016.

[114] C. Torrentó, J. Cama, J. Urmeneta, N. Otero, and A. Soler, "Denitrification of groundwater with pyrite and Thiobacillus denitrificans," *Chem. Geol.*, vol. 278, no. 1–2, pp. 80–91, 2010.

[115] C. J. Jørgensen, O. S. Jacobsen, B. Elberling, and J. Aamand, "Microbial oxidation of pyrite coupled to nitrate reduction in anoxic groundwater sediment," *Environ. Sci. Technol.*, vol. 43, no. 13, pp. 4851–4857, 2009.

[116] X. Liu and F. J. Millero, "The solubility of iron in seawater," *Mar. Chem.*, vol. 77, no. 1, pp. 43–54, 2002.

[117] L. O. De Serrano, "Biotechnology of siderophores in high-impact scientific fields," *Biomol. Concepts*, vol. 8, no. 3–4, pp. 169–178, 2017.

[118] T. Yoshida, K. Hayashi, and H. Ohmoto, "Dissolution of iron hydroxides by marine bacterial siderophore," *Chem. Geol*., vol. 184, no. 1–2, pp. 1–9, 2002.

[119] P. U. Reichard, R. Kretzschmar, and S. M. Kraemer, "Dissolution mechanisms of goethite in the presence of siderophores and organic acids," *Geochim. Cosmochim*. Acta, vol. 71, no. 23, pp. 5635–5650, 2007.

Chapter 2: Experimental methods

1 – Samples selection

1.1 – Fresh wood model samples

Model waterlogged archaeological wood (WAW) samples were prepared from fresh wood. One of the objectives of this thesis was to define an artificial degradation and contamination protocol to replicate the characteristics of WAW, *i.e.,* degradation of carbohydrates and iron sulfide contamination.

Different wood species were employed: balsa (*Ochroma pyramidale*), oak (*Quercus* sp.), and pine (*Pinus* sp.). Balsa was selected as it presents a similar porosity to WAW, allowing an easier degradation of the carbohydrates content. However, balsa wood is not reported as substrate of archaeological items, and so its employment during this thesis was purely as a primary step to evaluate the feasibility of the proposed protocols. Oak and pine were chosen as representative species of hard-and softwood respectively but also as they are widely reported as WAW substrates [1]–[3]. In addition, oak wood (*i.e.,* hardwood) is largely investigated for the preparation of WAW model samples [4], [5].

Fresh balsa was commercially provided while oak and pinewood were supplied and cut in 2x2x2 cm^3 cubes by a carpenter (J.P. Liaboeuf, Switzerland). The samples present the three Transversal (Tv), Tangential (Tg), and Radial (Rd) plane sections allowing to study the performances of the protocols in terms of wood shrinkage, content degradation, and depth efficiency. Their light color at the beginning of the experiment can facilitate monitoring the color variation of the samples when artificially contaminated with iron sulfides phases. The samples were kept at room temperature before use.

1.2 – Archaeological wood model samples

Aged model samples were also prepared from WAW samples. These wood samples already present degradation of carbohydrates but the iron and sulfide contamination levels were under the detection threshold or absent according to the applied spot tests. Both hard-and softwood species were selected to produce archaeological wood model samples. A pole of oak and a board of pine were provided by the Archaeological Service of Bern Canton (ADB) from freshwater sites. The oak pole is dated from the Neolithic area while the pine board is from the XIX^{th} century. 2-cm slide was selected from the pole and board surface. This slide represents the earlywood part of oak pole and was more exposed to microbial degradation. Then cubes of 2x2x2 cm^3 were cut in these slides and following the wood ring to have as much as possible homogeneous sample sets. To induce the presence of Fe and S, the samples were then impregnated with the same protocol employed to contaminate fresh wood model samples.

1.3 –Real archaeological wood samples

In addition of the model samples, WAW samples were collected to validate the extraction treatments tested. Three poles of Neolithic oak were provided by ADB and the Swiss National Museum (SNM) and one board of Neolithic pine by ADB, all from freshwater sites. As for archaeological wood model samples, a slide of 2-cm was cut from the poles and board and 2x2x2 cm^3 samples cut in the slides. These archaeological samples present an important

degradation of carbohydrates with a spongy texture. Spot tests to detect iron species (Fe^{2+}/Fe^{3+}) and sulfur speciation (S^{2-}/SO_4^{2-}) were performed and revealed the presence of ferric iron Fe^{3+} and sulfates SO_4^{2-} and in some parts sulfides S^{2-}. The tests were performed with potassium thiocyanate 33% and barium chloride to detect iron and sulfates, respectively. Machery-Nagel® test paper n◦90761 (Fisher Scientific AG, Reinach, Switzerland) was employed for sulfides detection [6].

For all WAW samples (models and real), no bark was present on the samples after cutting. All the samples present the Transversal (Tv), Tangential (Tg) and Radial (Rd) plane sections. The samples were cut at the *Atelier mécanique* of the University of Neuchâtel, Switzerland. To avoid eventual external contamination (from oil or from metal saw), the blade of the metal saw was changed before cutting and cleaned with absolute ethanol between each use.

The different wood samples were either used for modelling WAW or for the evaluation of extraction methods, as summarized in Table 2. A total of 10 sets of 19 samples each were prepared and characterized. The samples will be referred by their set name in the Chapters 3 and 4.

Table 2: Samples information and utilization for the preparation of model samples and the evaluation of extraction methods

Wood samples	Label	Model/real samples	Degradation protocol	Contamination protocol	Extraction method	Stabilization method
Fresh balsa	Set A*	Model	X	X	X	X (ADB/SNM)
Fresh oak	Set B	Model	X	X	X	X (SNM)
Fresh pine	Set E	Model	X	X	X	X (ADB)
Neolithic oak	Set C	Model	-	X	X	X (SNM)
Lake pine	Set F	Model	-	X	X	X (ADB)
Archaeologic oak	Sets D1/D2/G2	Real	-	-	X	X (ADB/SNM/SNM)
Archaeologic pine	Set G1	Real	-	-	X	X (ADB)

**: set A has 38 samples contrary to the other sets. Half of the set was conserved by ADB and the other half by SNM*

All the set samples were labelled depending on the treatment applied on them. For each set, one sample was kept as a reference (R) in the laboratory while the other samples were subdivided in three groups: biologically treated (BT), chemically treated (CT), and untreated (NT) samples. Each group contain six samples, labelled BT-1 to BT-6, CT-1 to CT-6, and NT-1 to NT-6, respectively. At each step of the conservation procedure (extraction, consolidation, and freeze-drying), one sample was kept as a reference and removed from the following steps. The labelling assigned to each set is presented in Table 3:

Table 3: Example of labelling on sets C (model) and D1 (real) archaeological samples for the different step of the MICMAC project

	Set C – archaeological model samples			**Set D1 – archaeological samples**		
	BT	*CT*	*NT*	*BT*	*CT*	*NT*
Fresh/Recovered samples	C-R			D1-R		
Extracted and stabilized samples	C-BT-1 C-BT-2 C-BT-3	C-CT-1 C-CT-2 C-CT-3	C-NT-1 C-NT-2 C-NT-3	D1-BT-1 D1-BT-2 D1-BT-3	D1-CT-1 D1-CT-2 D1-CT-3	D1-NT-1 D1-NT-2 D1-NT-3
Extracted reference	C-BT-4	C-CT-4	C-NT-4	D1-BT-4	D1-CT-4	D1-NT-4
Consolidated reference	C-BT-5	C-CT-5	C-NT-5	D1-BT-5	D1-CT-5	D1-NT-5
Stabilized reference	C-BT-6	C-CT-6	C-NT-6	D1-BT-6	D1-CT-6	D1-NT-6

2 – Selection of protocols and conservation methods

2.1 –Degradation protocols

Six degradation protocols were investigated to determine the most efficient regarding the degradation of carbohydrates: five chemical protocols (T1-T5) and a biological protocol (T6). Among the five chemical degradation protocols studied, three were adapted from literature. The two others were adapted or designed by the University of Neuchâtel. Untreated samples (T0) were kept as reference to evaluate the different degradation protocols. All the protocols were performed on fresh wood to ascertain the reliability and reproducibility of the results. Furthermore, similar analytical protocol was performed on the samples to have comparable results as the research on which some protocols are adapted employed different characterization methods and the results cannot be comparable among them. For each degradation protocol, six samples from sets B and E (fresh oak and fresh pine) were used. The samples were first weighted and distributed into different groups based on their mass in order to have homogeneous representative experimental groups with similar variation within each group. All the protocols evaluated are described in Table 4.

Table 4: Degradation protocols performed on fresh wood

Label	Degradation Protocol	Reference
T0	Untreated samples.	
T1	Samples were immersed into 1.6 L deionized water. Vacuum of -0.6 bars was applied. Immersion under vacuum lasted for 1 week.	[7]
T2	Samples were placed in a climatic chamber at 25 °C, 50% RH, 100% fanning and with UV light. Exposition lasted for 3 weeks.	[8]
T3	Samples were pre-immersed into 1.6 L deionized water for 24 hours prior being placed in an empty desiccator without water. Vacuum of -0.2 bars was applied then desiccator filled with nitrogen N_2. Cycle vacuum/N_2 was performed 5 times. Protocol lasted 2 days.	[4]
T4	Samples were poured into a solution of H_2O_2 30%: NH_4OH 25% (5:1) for 4 weeks.	[9]
T5	Stainless steel needles were hammered in two faces (Tv and Tg) of the samples. Then the T1 protocol was applied.	
T6	Samples were placed on a malt-agar culture of the fungal strain *Chaetomium globosum*. Petri dishes were put in a desiccator containing 64%(w/w) glycerol solution to control the relative humidity (at 70% RH) for 21 weeks.	[10]

T6 (fungal degradation) samples were autoclaved when the degradation protocol ended. All samples were conserved in Ziplock bags in the dark and at room temperature before analyses. The results of degradation of carbohydrates are discussed in Chapter 3.

2.2 –Contamination protocol

Three contamination protocols were selected from literature and applied on fresh balsa wood (set A. All the protocols evaluated are described in Table 5.

Table 5: Contamination protocols performed on fresh wood

Label	Contamination Protocol	Reference
IP1	4 h immersion into 0.8 L $FeCl_2{\cdot}4H_2O$ 0.5 M solution under vacuum (-600 mbars). Overnight drying at 50 °C. 4 h immersion into 0.8 L $Na_2S{\cdot}9H_2O$ 0.5 M solution under vacuum (-0.6 bars)	[7]
IP2	Immersion in artificial seawater in presence of archaeological nails*. Immersion time of 18 or 60 days. Optional vacuum (-0.6 bars)	[11]
IP3	8 h immersion into 0.8 L $Na_2S{\cdot}9H_2O$ 0.12 M solution neutralized with HCl. Addition of 0.8 L $FeCl_2{\cdot}4H_2O$ 0.09 M solution	[12]

**: 5-7 cm terrestrial nails excavated from chalky soil in Champagne region, France, dating from the late Roman period (300 AD) presenting a corrosion layer composed of a mixture of goethite (α-FeOOH) and lepidocrocite (γ-FeOOH) identified by Raman spectroscopy*

The most promising protocol was then applied on artificially degraded fresh oak (set B) and fresh pine (set E). All samples were conserved in Ziplock bags filled with deionized water flushed with N_2, in the dark and at room temperature before analyses.

2.3 – Preventive extraction methods

Two preventive methods for the extraction of iron Fe and sulfur S species were investigated and evaluated on model (fresh and archaeological) and real WAW samples: a biological extraction method (BT) and a chemical extraction method (CT). Before extraction, the samples were put in 400 ml of deionized water and sonicated for 2 min and then 4 min. The water was changed between the two-sonication baths. The sonication allows removing the chemicals employed during the previous artificial contamination. Two baths were necessary to have a clear solution.

2.3.1 – Untreated samples

Six samples per set were kept as reference (NT) samples in the laboratory. After being cut and/or contaminated, NT samples were conserved in Ziplock bags filled with deionized water flushed by N_2, until the characterization campaign begins. The Ziplock bags were stored in a fridge at 4 °C.

2.3.2 – Biological treatment

The biological treatment (BT) was developed by the University of Neuchâtel, during the PhD thesis of Magdalena Albelda-Berenguer [13]. A two-step extraction protocol was established, based on the properties of desferoxamine (DFO) siderophores molecules and *T. denitrificans* strain . DFO was purchased as Desferal® (Novartis Pharma Schweiz AG, Basel, Switzerland). *T. denitrificans* (DSMZ 12475) was obtained from the German Collection of Microorganisms and Cell Cultures (DMSZ, Braunschweig, Germany). The strain was cultivated using standard anaerobic techniques at 30 °C using a medium 113 (2010 DMSZ) in the dark.

T. denitrificans was selected as this bacterium proved its efficiency regarding dissolution of iron sulfide compounds. It is a chemolithoautotrophic bacterium discovered to be able to grow on inorganic sulfur and to use it as an energy source [14], [15]. This bacterium derives their energy by the reduction of reduced sulfur compounds in anaerobic conditions. However, the oxidation can also occur under denitrifying conditions. The bacteria grow on inorganic sulfur substrates with the use of different nitrogen compounds (NO_3^-, NO_2, N_2O) as terminal respiratory oxidants [15]. The microbial reduction process leads then to the formation of sulfates [16], [17]. Under anaerobic conditions, any iron sulfides present, as mackinawite FeS or pyrite FeS_2, offer an alternative for NO_3^- reduction [14], [18], [19]. *T. denitrificans* grows at a neutral pH [20], in a range between 6.8 and 7.4 [15] and at a temperature range between 28 and 35 °C, with an optimum temperature of 30 °C. In addition, a preliminary study regarding the utilization of this bacterium on WAW showed that no wood degradation was induced [7]. *T. denitrificans* was considered then a perfect candidate regarding extraction of iron sulfide compounds.

Siderophores primary function is to sequester iron from the environment, allowing the development of microorganisms. In oxic environments, iron is mainly found as iron oxides and oxyhydroxides while in reducing environments like waterlogged soils, iron can be found as ferrous soluble species but also as iron sulfide such as pyrite FeS_2 [21]. Siderophores are produced by microorganisms to make the iron present in the minerals bioavailable. Indeed, the access of iron may be problematic for living organisms due to the low solubility and

dissolution kinetics of the iron phases [22].The dissolution of iron minerals is promoted by the production of siderophores. Furthermore, siderophores form stable complexes with ferric iron with an efficiency to remove iron corrosion superior to common chemical extractive agents, *i.e.* EDTA and DTPA [23]. DFO was selected for its properties regarding iron sequestration. DFO were not produced in laboratory but commercially purchased, allowing to have large quantity of siderophores. Siderophores are employed in agriculture applications and no study reported the degradation of plant components [22]. Yet, some studies have reported the utilization of siderophores molecules to bleach paper [24], [25].

BT samples were immersed in a solution of DFO 84 mM for 10 days. Samples were kept at room temperature under orbital agitation (100 rpm). After rinsing with deionized water, the samples were immersed with *T. denitrificans* for 20 days. Samples inoculated with the bacteria were incubated at 30 °C in medium 113 in darkness without agitation. The volume of immersion solution was set to 200 ml.

2.3.2 – Chemical treatment

The chemical treatment (CT) was developed and proposed by the conservation and research laboratory Arc'Antique (France) [26]. As for BT, CT is a two-step extraction protocol by a first immersion in sodium persulfate $Na_2S_2O_8$ followed by a second immersion in ethylenediaminetetraacetic acid (EDTA). Sodium persulfate and EDTA were purchased from Merck as puriss chemical.

As discussed in Chapter 1, paragraph 2.4.2, ethylenediaminetetraacetic acid (EDTA) is commonly employed in the field of heritage conservation as chelating agent. It is employed for paper or textile conservation [68]. Indeed, EDTA forms strong complexes with ferrous and ferric iron [69]. Among the different chelating agents proposed in the field of paper and textile conservation, EDTA was preferred to diethylethylenetriamine pentaacetic acid (DTPA) or ethylenediiminobis (2-hydroxy-4-methyl-phenyl) acetic acid (EDMA) as the treatment presents few advantages such as i) occurring under alkaline conditions, permitting to neutralize the acidic wooden surface, ii) presenting a smaller molecular size accompanied with higher diffusion kinetics, and iii) respecting the appearance of the wood [26]–[28].

Sodium persulfate $Na_2S_2O_8$ was suggested to oxidize iron sulfides as it presented encouraging results [26]. Indeed, it was proven that an initial immersion treatment with $Na_2S_2O_8$ followed by EDTA treatment was efficient regarding iron extraction and could even be more efficient than EDTA immersion alone. Yin et al [29] also demonstrated that $Na_2S_2O_8$ oxidize iron sulfides and form sulfates SO_4^{2-} as well as radicals that induce more iron sulfides oxidation. Therefore, $Na_2S_2O_8$ was employed as initial immersion step to reduce iron sulfides present in waterlogged wood and facilitate Fe and S extraction. If EDTA seems innocuous regarding wood degradation, $Na_2S_2O_8$ is employed as a bleaching agents especially for hair cosmetic [30] but also as degrading agent for organic chemicals like phenols that can be found in wood [31].

CT samples were immersed in $Na_2S_2O_8$ 0.1 M for 1 day to oxidize reduced sulfur species. After rinsing with deionized water, the samples were then immersed in EDTA 0.125 M for 7 days to complex free iron ions. During the whole process, the samples were kept at room temperature without agitation. The volume of immersion solution was set to 200 ml.

2.4 – Stabilization methods

To evaluate the compatibility of the preventive extraction methods with other conservation procedures traditionally applied to WAW, the wood samples were submitted to a stabilization procedure. The samples were split between two wood conservation departments (ADB and SNM)): Sets A1, D1, E, F and G1 were treated at ADB while sets A2, B, C, D2 and G2 were treated at SNM (Table 2).

The same stabilization protocol currently employed by the wood conservators from ADB and SNM was selected. As for the extraction methods, this procedure implied two steps. First, the samples were consolidated with polyethylene glycol then freeze-dried. Nowadays, this methodology is widely applied in the wood conservation field.

2.4.1 – Polyethylene glycol consolidation

Conservators chose to consolidate the samples with PEG 2000 (Omya AG, Switzerland). The consolidation treatment comprised 5 sequential baths of 350 ml, each bath for 28 days. Every 28 day, the PEG bath was renewed, and the PEG concentration increased. Five samples per set per treatment were submitted to this consolidation. The parameters for each consolidation bath are given in Table 6.

Table 6: Polyethylene glycol (PEG) consolidation baths parameters used during the 5-months consolidation treatment

PEG 2000 bath	PEG 2000 bath concentration	Deionized Water (L)	PEG 2000 (g)
#1	8%	5.09	440
#2	16%	4.68	880
#3	24%	4.25	1320
#4	32%	3.85	1760
#5	40%	3.45	2200

At the end of the different baths, the used PEG solutions were kept in plastic bottle at room temperature prior analyses. One wood sample per set per treatment was kept as reference for the consolidation step and was stored in PEG solution at room temperature (Table 3).

2.4.2 – Freeze-drying

The excess of PEG solution was removed from the samples before freeze-drying by wood conservators. Four samples per set per treatment were placed in the chamber to freeze-dry. Then the samples were cooled at 4 °C for 24 hours. Freeze-drying lasted for 10 days with the following settings: vacuum of -0.00012 bars and condenser temperature sets at -50 °C (ADB) and -85 °C (SNM). The eutectic temperature for the wood sample was set at -22 °C. Five thermocouples were used to measure the temperature in the whole chamber on selected samples (sets A, C and E). Weight of D1 at ADB and G2 at SNM samples (both archaeologic oak) was continuously measured during freeze-drying. Once the weight stabilized, the temperature of the chamber was gradually raised until room temperature was reached. At the end, one sample per treatment and set was kept as final reference and stored in Ziplock bag at room temperature.

3 – Analytical protocol

A specific analytical protocol was defined to properly characterize artificially degraded and contaminated samples as well as extracted and stabilized samples. The selection of characterization methods was based on common techniques reported in literature for the conservation of WAW artefacts (Maximum Water Content, Raman and Infrared spectroscopies) [32]–[35]. An important parameter was considered to select the different characterization methods: as far as possible, non-invasive, and non-destructive methods were preferred. In general, these methods do not require samples preparation, which allow to be performed by conservators. Yet, some destructive methods were necessary, such as Inductively Coupled Plasma-Optical Emission Spectroscopy, to evaluate the total iron and sulfur concentration within the samples.

The methods employed informed about the state of degradation and contamination of the artefacts. In addition, analytical methods can ascertain the efficiency of investigated methods. Criteria have been defined in the field of heritage conservation, in order to validate a treatment: respect of aesthetic and historical value, harmless for the artefacts, efficiency of the method, harmless for the artefacts, and reversibility/retreatability [36]–[38]. Further criteria were defined by the persons involved in the project such as safety for users and environment and durability.

The different analyses performed and described in the following paragraphs should validate that these criteria are respected. The different characterization techniques employed to validate the proposed model samples and the extraction methods studied are summarized in Table 7.

Table 7: Characterizations performed on the different sets

Wood samples	Label	Model/real samples	Fresh/Recovered	Degradation protocol	Contamination protocol	Extraction method	Stabilization method
Fresh balsa	Set A	Model	Documentation Colorimetry pH MWC ATR-FIR Raman		Documentation Colorimetry pH MWC ATR-FTIR Raman ICP-OES	Documentation Colorimetry pH MWC ATR-FTIR Raman ICP-OES	Documentation Colorimetry MWC ATR-FTIR Raman
Fresh oak	Set B	Model	Documentation Colorimetry pH MWC ATR-FTIR Raman	Documentation Colorimetry pH MWC ATR-FTIR Raman Wood content	Documentation Colorimetry pH MWC ATR-FTIR Raman ICP-OES Wood content	Documentation Colorimetry pH MWC ATR-FTIR Raman ICP-OES	Documentation Colorimetry MWC ATR-FTIR Raman
Fresh pine	Set E	Model	Documentation Colorimetry pH MWC ATR-FTIR Raman	Documentation Colorimetry pH MWC ATR-FTIR Raman Wood content	Documentation Colorimetry pH MWC ATR-FTIR Raman ICP-OES Wood content	Documentation Colorimetry pH MWC ATR-FTIR Raman ICP-OES	Documentation Colorimetry MWC ATR-FTIR Raman

Continuation Table 7

Neolithic oak	**Set C**	**Model**	Documentation Colorimetry pH MWC ATR-FTIR Raman ICP-OES	Documentation Colorimetry pH MWC ATR-FTIR Raman ICP-OES SEM-EDS	Documentation Colorimetry pH MWC ATR-FTIR Raman ICP-OES	Documentation Colorimetry MWC ATR-FTIR Raman ICP-OES
Lake pine	Set F	Model	Documentation Colorimetry pH MWC ATR-FTIR Raman ICP-OES	Documentation Colorimetry pH MWC ATR-FTIR Raman ICP-OES SEM-EDS	Documentation Colorimetry pH MWC ATR-FTIR Raman ICP-OES	Documentation Colorimetry MWC ATR-FTIR Raman ICP-OES

Continuation Table 7

Archaeological oak	**Sets D1/D2/G2**	**Real**	Documentation Colorimetry pH MWC ATR-FTIR Raman ICP-OES SEM-EDS Wood content	Documentation Colorimetry pH ATR-FTIR Raman ICP-OES	Documentation Colorimetry MWC ATR-FTIR Raman
Archaeological pine	Set G1	Real	Documentation Colorimetry pH MWC ATR-FTIR Raman ICP-OES SEM-EDS Wood content	Documentation Colorimetry pH ATR-FTIR Raman ICP-OES	Documentation Colorimetry MWC ATR-FTIR Raman

**MWC: Maximum Water Content; ATR-FTIR: Attenuated Total Reflectance FourierTransform Infrared Spectroscopy; ICP-OES: Inductively Coupled Plasma-Optical Emission Spectroscopy; SEM-EDS: Scanning Electron Microscopy coupled with Energy Dispersive X-ray Spectroscopy*

3.1 – Physical characterization

3.1.1 – Documentation

All the sets were photographed with a Canon Power Shot G5X camera with a magnitude of 4.2x, a field of 400 cm-□, and in auto mode (F/4 focal, 1/100 sec exposition time, ISO-125, 37 mm focal distance, 2.97 maximal opening, auto white balance). The samples were placed on a white background in a white chamber (48x48 cm), special for photography. The sets were illuminated with 2 halogen lights (23W/lamp) (Figure 10a). All the faces of the samples were documented, and the samples always places on the same position (Figure 10b). White balance correction was applied with Photoshop® based on a color scale placed on each photograph.

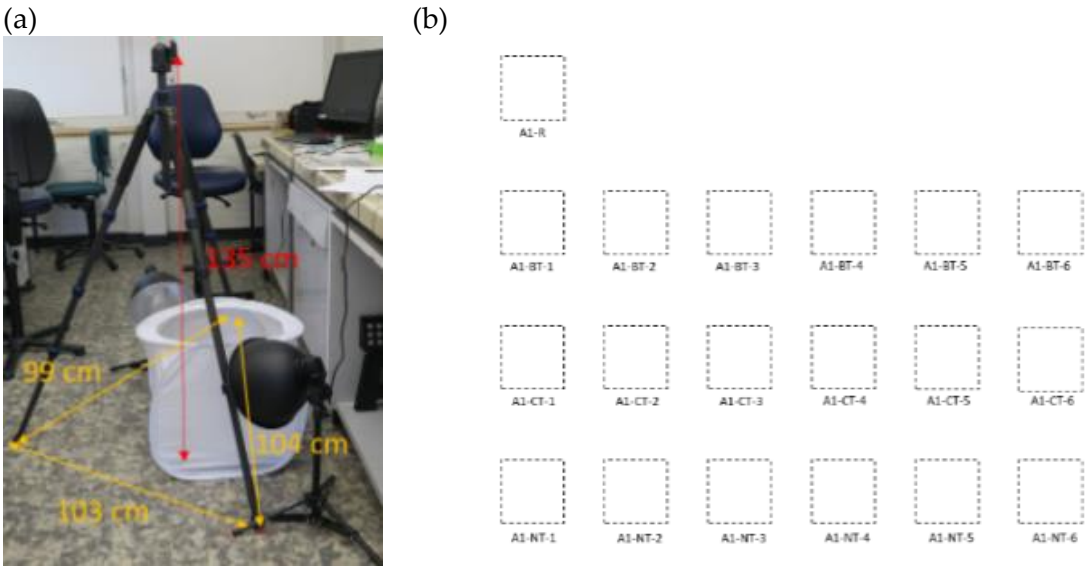

Figure 10: (a) Documentation settings and (b) samples position

3.1.2 – Colorimetric measurements

A Minolta CM-508D spectrophotometer was used for the color measurements, with the following parameters: Specular Component Included (SCI), Illuminant D65 (daylight containing UV component, color T 6504K), d/8° geometry, 10° observer, measurement area diameter 10 mm, illumination with Xe flashlight source, 100% UV containing all UV components or 0% UV containing no UV components, CIELab 1976 color space. L* represents the brightness axis (0 for black and 1 for white), a* the green to magenta axis (-128 for green and +127 for magenta) and b* the blue to yellow axis (-128 for blue and +127 for yellow) [39].

All the different sets were characterized. For each sample, one measurement was carried out through plastic film at the center of each cube face. The mean values of the colorimetric coordinates L*, a* and b* for each sample was then calculated and associated with its standard error. The color variation was also calculated, according to the equation $\Delta E^* = \sqrt{(\Delta L^*)^2 + (\Delta a)^2 + (\Delta b^*)^2}$

3.1.3 – pH measurements

pH was measured at the surface of the wood samples and within the solutions used for the biological and chemical extraction methods. A 691 Meter Metrohm standard pHmeter (Metrohm AG, Herisau, Switzerland) was used with a surface electrode (flat membrane

electrode 6.0256.100) and an ionic electrode (unitrode 6.0259.100) calibrated with pH = 4, pH = 7 and pH = 9 buffer solutions.

3.1.4 – Maximum Water Content

Maximum water content (MWC) was measured for all samples of each sets. The samples were placed in a vacuum chamber (Gallen Kamp) for twice 20 min. The air content of the samples was replaced by water (Figure 11a). When the samples floated, the samples weight was measured with a KERN ALS/A01 precision balance. The samples were weighted above and within the water, as illustrated in Figure 11b.

(a)

(b)

Figure 11: (a) Pictures of vacuum chamber. (b) Pictures of wood samples weight measurements above and within water

The MWC was calculated according to the formula :

$$MWC\ (\%) = \frac{W_{air} - 3W_{water}}{3W_{water}} \times 100$$

where MWC represents the maximal water content, W_{air} the weight of the cube above water and W_{water} the weight within water. The state of wood degradation was determined according to Macchioni et al [32]. Five degradation grades were hence defined:

- Grade 0: no sign of decay
- Grade 1: low decay
- Grade 2: initial decay
- Grade 3: high decay
- Grade 4: important decay

3.2 – Spectroscopic analyses

3.2.1 – Infrared spectroscopy

Wood degradation was evaluated by Fourier Transform Infrared (FTIR) spectroscopy. Wood samples were characterized in the 4000–650 cm^{-1} range using a Nicolet iS5 instrument (Thermo Fisher Scientific, Waltham, MA, USA) equipped with an Attenuated Total Reflectance (ATR) accessory. Spectra were acquired on an area of 62.5 µm with 16 scans and at a resolution of 4 cm^{-1} . Three ratios were calculated based on the height of vibrational bands at 1034 cm^{-1} assigned to holocellulose Ho and lignin Li, 1158 and 1374 cm^{-1} assigned to Ho and cellulose Ce and 1506 cm^{-1} assigned to Li, according to literature [35], [36]:

- R1 = I(1158)/I(1506),
- R2 = I(1374)/I(1506),
- R3 = I(1034)/I(1506)

These ratios permit determining if the wood components were affected by the treatments and thus the state of wood degradation. After correction with a polynomial function, and the normalization of the spectra, the height of the selected bands was measured using Rstudio v3.6.3 software (Rstudio, Boston, MA, USA) and ChemoSpec package (Bryan A. Hanson, DePauw University, https: //bryanhanson.github.io/ChemoSpec/index.html). In addition, the variation within the ratios calculated was calculated according to the formula $\frac{Rb-Ra}{Rb} \times 100$ with Rb the ATR-FTIR ratios (R1, R2, R3) before treatment (*i.e.*, degradation, contamination) and Ra the ATR-FTIR ratios after treatment.

For fresh wood model samples, three samples were analyzed and four spectra of each cutting section (Tg, Tv and Rd) were recorded. As well, two samples per model samples were cut in half following the Tg plane section and four spectra of per core recorded (Figure 12a).

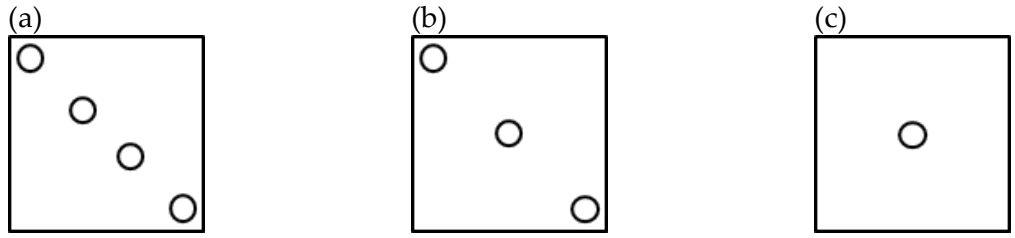

Figure 12: Masks employed for (a) fresh wood ATR-FTIR analyses, (b) treated samples ATR-FTIR analyses and (c) treated samples Raman analyses

Two samples per extraction method per set were analyzed and three spectra for each of the six faces were recorded (Figure 12b).

3.2.2 – Raman spectroscopy

Compounds present in the wood samples were identified by Raman spectroscopy. Analyses were carried out using a LabRam Aramis Horiba instrument (HORIBA Jobin Yvon GmbH, Bensheim, Germany) and LabSpec 5 software with a 632.8 nm laser, in the range 100–1500 cm^{-1}, with 100× objective (numerical aperture of 0.9) and laser power of 0.99 mW at the surface of the sample (D1 filter, 10%), 1800 lines/mm grating, 1000 µm confocal pinhole and 100 µm spectrometer entrance slit. One spectrum at the center of three faces corresponding to each cutting section (Tv, Tg and Rd) was recorded (Figure 12c): two routine spectra on Tg and Rd sections (10 acquisitions of 5 s) and a third spectrum on Tv section with a long acquisition (25 × 10 secs). Two samples per extraction method per set were analyzed, before and after extraction as well as after stabilization.

Before and after application of the extraction methods, the samples were wet and thus the analyses were performed in the samples immersed in their stock solution (deionized water flushed with N_2). This methodology allows avoiding the overwarming of the samples during measurement that would induce a possible modification of the compounds under the laser excitation.

After stabilization, the samples were dry and thus the samples were characterized without sample preparation.

In parallel, reference compounds (mackinawite FeS, goethite α-FeOOH, hematite Fe_2O_3) were synthetized according to Bourdoiseau et al. [40] and Schwertmann [41]. These precipitates as well as sulfur (Sigma, α-S_8) and pyrite (http://www.pierrequiroule.ch/ , FeS_2) were used to create a reference spectral dataset. Spectra were acquired with the same parameters as above. In addition, water pre-immersed fresh and archaeological samples of different wood species were analyzed to obtain reference spectra of the wood substrates.

3.2.3 – Inductively Coupled Plasma-Optical Emission Spectroscopy

Mainly used for environmental analysis, this analytical method allows a detection of several elements, in a low concentration range. An Optima 2100 Perkin-Elmer (Waltham, Massachusetts, United-States) was employed for the determination of the concentration in iron and sulfur within wood samples, extraction, and consolidation solutions. Wood samples were digested in nitric acid HNO_3 (65%, Suprapur, Merck KGaA) by reflux for 24 hours. The

digested wood, extraction, and consolidation solutions were diluted 100 to 200 times before being examined.

Before application of extraction methods, three samples were digested and investigated for iron and sulfur content. Due to the limitation of archaeological samples, only one extracted sample was digested at the end of the preventive methods.

3.2.4 – Scanning Electron Microscopy coupled with Energy Dispersive X-ray Spectroscopy

Wood degradation as well as elemental analyses were evaluated with Scanning Electron Microscopy coupled with Energy Dispersive X-Ray Spectroscopy (SEM-EDS). A Scios 2 DualBeam (Thermo Fisher Scientific, Waltham, MA, USA) scanning electron microscope equipped with an energy-dispersive X-ray analyzer was used to obtain high-resolution images and to determine the elemental composition of the compounds present in wood samples as well as the wood state of degradation. Observations were performed on lyophilized thin cross-sections mounted on a carbon conductive tape and covered with a thin gold layer by use of an SDS050 Sputter Coater (Leica, Wetzlar, Germany). Thin cross-sections of fresh wood were obtained with a Leica RM 2145 microtome (Leica, Wetzlar, Germany). Thin cross-sections of degraded and wet wood were cut manually with a razor blade. One sample was characterized per degradation protocol and per set before extraction.

3.3 – Wood composition

The contents in lignin, cellulose, and holocellulose were determined for each wood specie, before and after degradation and contamination protocols. To have similar moisture content, the samples were dried at 60°C to slowly evaporate free water until constant weight. Then, the samples were grinded with a Retsch grinding machine RM 200 (RETSCH GmbH, Haan, Germany) with hard porcelain mortar and grinder. The grinding session lasted 3 minutes for oakwood and 6 minutes for pinewood, and the scraper pressure was switched from 5 to 8 to reach the smallest wood particles. This sample preparation respects the ASTM standard E 1757 *Lignin in Wood and Pulp* [42]. For each degradation protocol, duplicates were prepared. It is worth mentioning that these analyses were not planned from the beginning and most of the samples were employed for other analyses and/or for the preparation of model samples.

3.3.1 – Lignin extraction

The acid-insoluble lignin content (called Klason lignin) was determined according to the standard ASTM-D 1106-56 *Standard Test Method for Acid-Insoluble Lignin in Wood* [43], [44].

0.5 g of material was dissolved in 10 ml of 67% of sulfuric acid (Fisher, Analytical Reagent Grade, >95%) previously cooled at 0°C. After being stored at room temperature for 16 hours, 315 ml of deionized water were added to the mixture. The mixture was refluxed for 5 hours. The lignin precipitate was vacuum filtrated over a G4 frit (10-16 µm pore size) and washed with water until filtrate pH reached 7.0. The precipitate was oven-dried until constant weight. Lignin content (LC) was calculated with equation $LC = \frac{m_L}{m_i} \times 100$ with m_L being the weight of dried lignin and m_i the weight of initial sample.

3.3.2 – Cellulose extraction

The cellulose content was determined according to the method developed by Kürchner-Hoffer [45].

1 g of material was refluxed for 1 hour with 25 ml of nitration solution (1 vol HNO_3:4 vol EtOH) (HNO_3 Honeywell, puriss p.a.; EtOH Fisher, Analytical Reagent Grade, 99.8%). The mixture was vacuum filtered over a G3 frit (16-40 μm pore size) before being add to another 25 ml of nitration solution. The mixture was refluxed three times for 1 hour with nitration solution then washed with ethanol and deionized water. The remaining cellulose precipitate was refluxed with deionized water for 30 minutes then filtered with hot deionized water until the filtrate was at neutral pH. The precipitate was oven-dried, and the cellulose content (CC) calculated: $CC = \frac{m_C}{m_i} \times 100$ with m_C being the weight of dried cellulose and m_i the weight of initial sample.

3.3.3 – Holocellulose extraction

The holocellulose content was determined according to the method developed by Poljak [46].

0.5g of material was added to 10 ml of a 10% solution of sodium acetate (ACROS, ACS reagent, >99%) in concentrate acetic acid (VWR, 99.9%). The mixture was dissolved in 6 ml of 40% peracetic acid (Sigma) then refluxed for 1 hour at 70°C. 50 ml of deionized water were added to the cooled mixture. The mixture was then vacuum filtered over a G2 frit (40-100 μm pore size) and washed until acid-free. The holocellulose precipitate was oven-dried and the holocellulose content (HC) calculated: $HC = \frac{m_H}{m_i} \times 100$ with m_H being the weight of dried holocellulose and m_i the weight of initial sample.

4 – Chemometrics approach

Complementary approaches to classical analysis were performed on the results obtained. Specific chemometrics approaches were selected based on their reliability and previous applications in different conservation studies. The term chemometrics appeared in the beginning of 1970s and was introduced by Wold and Kowalski [47]–[49]. The discipline applies for the development of evaluation of analytical chemical data and quantitative structure. If chemometrics was originally developed for organic chemistry and is widely used for pharmaceutical research, it proves to be a powerful tool also in the field of the conservation and preservation of cultural heritage. Its application was extended for many heritage materials such as paper [50], [51], pigments [52], colorants [53] or metals [54], but also for many techniques like Raman [55] and FTIR [56], [57] spectroscopies as well as for imaging analyses [58], [59]. Archaeological and waterlogged wood preservation was also investigated through chemometric approach. An Italian research group has worked on archaeological and waterlogged wood for over a decade, at the *Instituto per la Valorizzazione del Legno e delle Specie Arboree*, Sesto Fiorentino, Italy. They studied the degradation state and wood properties to understand the mechanics occurring. Their research, based on spectroscopic, microscopic, and physical analyses, allowed to classify wood in different degradation ranks [32], [60]. Their investigations to classify and predict the decay rank, wood species (hard-and softwood) as well as the location of sampling were validated by several analyses. RStudio, a free software,

was employed to run chemometrics analyses but also to produce the graphs displayed in Chapters 3 and 4.

4.1 – Experimental design

Experimental design is one of the main approach to apply the different statistic methods employed [46]. This method allows determining the main factors influencing the experiment and then to reduce the number of experiments to perform and thus to gain time [61]. Factors could be quantitative, such as the concentration, the temperature, or the pH of the experiment; but can also be categorical, like a specie or a brand. The differences among the factors are called levels (m). For example, if one evaluates different species, each specie will be represented by a level (specie A, specie B…). The experiment is a combination of all levels. Each factor can interact with the other ones. We talk then of interaction effects. Interaction between factors $p1$ and $p2$ is based on the non-addition of the effects, meaning that effect of $p1$ depend on $p2$ level m.

In this thesis, most of the factors were categorical, in particular when evaluating the degradation protocols or the extraction treatments. In this case, we talk of factorial design. Most of the factors studied during the thesis present more than two levels. Thus, Plackett Burman approach, with "low" and "top" levels for the factors, is not adequate for our case study [61], [62]. For an approach with $p = 3$ factors and level m is undefined, we talk of Latin squares. If $p = 4$, the plan is called Mutually Orthogonal Latin Squares and is the superposition of two Latin squares [63]. These two approaches are well described in literature and could be employed to evaluate many experimental designs.

Yet, it could happen that the p factors studied do not have all the same m levels. In this later case, the experimental design is referred as asymmetric plans and no general method is provided. This was generally the case in this thesis. For instance, regarding the preparation of WAW model samples in Chapter 3, three factors $p = 3$, for treatment, wood species and contamination, of different levels were evaluated: 7 treatments (6 chemicals *vs* 1 biological, m = 7) for two wood species (oak and pine, $m = 2$) and depending on an artificial contamination protocol (yes or no, $m = 2$). Concerning the evaluation of the proposed bio-based extraction treatment (Chapter 4), p = 4 factors were gauged: wood species (balsa, oak and pine, $m = 3$), type (fresh *vs* archaeological, $m = 2$), the application of an artificial contamination protocol (yes or no, $m = 2$) as well as the treatment applied (bio-based extraction, chemical extraction and untreated, $m = 3$). For each factor evaluated, the responses were the results of the different analytical measurements obtained (*i.e.*, colorimetric coordinates, ATR-FTIR vibrational bands intensity, pH values…).

The results obtained and discussed in Chapters 3 and 4 are then based on an asymmetric experimental design and were all verified by a statistician from the University of Neuchâtel.

4.2 – Spectroscopic data pre-processing

4.2.1 – Baseline correction

Baseline correction is usually performed as primary data pre-processing [64]. The main goal of the process is to remove the background effects from the spectroscopic data set, in regard to regression or classification methods [65].

Among the correction approaches, the modified polynomial fitting method was employed for the different ATR-FTIR and Raman data sets. The *polynomial fitting* (polyfit) method curves the spectrum according to Zhao's method [66], [67] and is proposed in the ***ChemoSpec*** package. This approach allows to correct the baseline of the original spectrum. Therefore, the noise effect is considered to avoid a false interpretation of the peaks, possibly due to the noise. The residual spectral R(x) is calculated from the polynomial fitting P(x) of the original spectral O(x) as well as the standard deviation SD, according to equations (1) and (2) respectively:

$$R(x) = O(x) - P(x) \quad (1)$$

$$SD = \sqrt{\frac{(R_1-\bar{R})^2+(R_2-\bar{R})^2+\cdots+(R_n-\bar{R})^2}{n-1}} \quad (2)$$

The final corrected spectrum is reached after several iterations on the original spectrum. The number of iterations is defined by the package.

4.2.2 – Binning

The binning of the spectroscopic data sets is another important pre-processing and is proposed in ***ChemoSpec*** package. The main advantage of binning is to compact large data sets and to reduce the effects of minor observation errors [64], [68]. The data spacing is influenced by the spectral resolution. Binning method groups the frequencies in one frequency value without losing spectral resolution. The corresponding intensities of the spectra are them summed [64]. The method allows reducing the computational burden when classification and multivariate analyses are conducted. The binning factor is chosen based on the spectral settings. A correct factor is required to avoid the splitting of important peaks and bands. For the analyses described in Chapters 3 and 4, the binning factor was set at 2, meaning that every 2 data points the values are averaged. Binning of the spectroscopic data was performed to fasten the analyses without reducing the reliability of the results obtained.

4.2.3 – Normalization

This pre-processing step is employed for comparative purpose and is proposed by ***ChemoSpec*** package. By normalizing the spectral data set, the characteristics bands observed on the spectra can be compared as well as ratios calculated. Among several normalization methods, the *Probabilistic Quotient Normalization* (PQN) was selected. This approach assumes that change of the matrix does not only influence some parts of the spectrum but the complete spectrum [69]. This method is a suitable option for many data sets [64]. A normalization factor is calculated between the signals of corresponding and original spectra. This allows to determine the most probable quotient that derived from the distribution of signals of spectra divided by the corresponding spectrum of the original spectrum [69]. Quotient normalization can be applied either on raw data or a binned data set. Normalization was performed on binned data set and

the quotient defined by the ***ChemoSpec*** package. *Total Integration* (TotInt) was not selected to avoid misinterpretation as TotInt assumes that the concentration giving by some peaks does not vary among the samples, which is not the case evaluating wood degradation [64].

4.2.4 – Savitzky-Golay filter

The Savitzky-Golay (SG) filter was initially performed in 1964 to smooth and differentiate the data with a filtering algorithm [70]–[72]. In addition to smothering the spectrum data, SG permits attenuated the noise while preserving important chemical signals[73], [74]. This data pre-processing is proposed on ***ChemoSpec*** package. SG is based on the least square fitting principle where the fitting numerical values are employed instead of the original spectral data sequence [70]. High frequency noise points are removed, and the original sequence is flattened. This method was proven to be effective for spectroscopic data as it preserves the higher moments of the peak. SG filter was applied on baseline corrected, binned, and normalized spectra for ATR-FTIR and Raman data set, leading to uniform spectra.

4.3 – Principal Component Analysis

Principal Component Analysis (PCA) was applied as clustering method on physical measurements as well as on spectroscopic data. The aim was to gather treatments and/or sample sets that present similar results or responses based on the experimental design applied. Physical measurements (*i.e.,* colorimetric coordinates, pH values, MWC values) were investigated with ***ggplot2*** and ***ggfortify*** packages while spectroscopic data (*i.e.,* ATR-FTIR and Raman) were visualized with ***ChemoSpec*** package.

Several clustering methods can be applied on spectroscopic data set: classical or robust. Classical method computes all data while robust method down weights some samples. Concerning the spectroscopic systems, the PCA classical approach was employed. This method uses all the data provided to calculate the scores and loadings. Contrary to robust PCA, no sample is down weighted when finding the components explaining as much as possible the variability of the data set. *Pareto* scaling method was also chosen to perform PCA. This scaling method is in between the no scaling and autoscaling methods. With *Pareto* scaling, the largest peaks contribute strongly for the data grouping , but the weaker ones also weight in PCA [64].

Depending on the information required, PCA analyses were presented as 2D or 3D score plot with the loadings (PCs) giving more information as axes. For spectroscopic analysis, the clusters, or confident ellipses, are provided by ***ChemoSpec*** package while clusters regarding physical measurements are defined by ***car*** package.

4.4 – Analysis of Variance

Analysis of Variance, simplified as ANOVA, is one of the most used statistical method [75]. This approach covers numerous experimental designs with the aim to assess the effects of factors on the responses. ANOVA was performed on the different responses obtained to observe the variability among the groups analyzed (*i.e.,* degradation protocols, extraction treatments). Based on the variance of the group, p-value (*p-val*) was calculated and showed if two or more groups are significantly similar ($p\text{-}val > 0.05$) or different ($p\text{-}val < 0.05$). In addition,

the interaction between the factors (treatments, and wood species for instance) was investigated to determine if all protocols and treatments applied gave significant similar results for any wood species. In addition of classical approach, ANOVA could discard or validate some parameters for the treatments applied regarding the preservation of WAW.

References

[1] J. Preston, A. D. Smith, E. J. Schofield, A. V. Chadwick, M. A. Jones, and J. E. M. Watts, "The effects of Mary Rose conservation treatment on iron oxidation processes and microbial communities contributing to acid production in marine archaeological timbers," *PLoS One*, vol. 9, no. 2, 2014.

[2] Y. Fors, H. Grudd, A. Rindby, F. Jalilehvand, M. Sandstrom, I. Cato, and L. Bornmalm, "Sulfur and iron accumulation in three marine-archaeological shipwrecks in the Baltic Sea: The Ghost, the Crown and the Sword," *Sci. Rep*., vol. 4, no. 1, p. 4222, 2015.

[3] B. A. Jordan, "Site characteristics impacting the survival of historic waterlogged wood: A review," *Int. Biodeterior. Biodegrad*., vol. 47, no. 1, pp. 47–54, 2001.

[4] S. Norbakhsh, I. Bjurhager, and G. Almkvist, "Impact of iron (II) and oxygen on degradation of oak – modeling of the Vasa wood," *Holzforschung*, vol. 68, no. 6, pp. 649–655, 2014.

[5] S. Norbakhsh, I. Bjurhager, and G. Almkvist, "Mimicking of the strength loss in the Vasa: model experiments with iron-impregnated recent oak," *Holzforschung*, vol. 67, no. 6, pp. 707–714, 2013.

[6] N. Odegaard, S. Carroll, and W. S. Zimmt, *Material characterization tests for objects of art and archaeology*. 2000.

[7] M. Albelda Berenguer, M. Monachon, C. Jacquet, P. Junier, C. Rémazeilles, E. J. Schofield and E. Joseph., "Biological oxidation of sulfur compounds in artificially degraded wood," *Int. Biodeterior. Biodegrad*., vol. 141, pp. 62-70, 2018.

[8] C. Pelosi, G. Agresti, L. Calienno, A. Lo Monaco, R. Picchio, U. Santamaria and V. Vinciguerra., "Application of spectroscopic techniques for the study of the surface changes in poplar wood and possible implications in conservation of wooden artefacts," in *Optics for Arts, Architecture, and Archaeology IV*, vol. 8790, p. 879014, 2013.

[9] P. Pullanikat, S. J. Jung, K. S. Yoo, and K. W. Jung, "Oxidative degradation of reducing carbohydrates to ammonium formate with H_2O_2 and NH_4OH," *Tetrahedron Lett*., vol. 51, no. 47, pp. 6192–6194, 2010.

[10] N. MacChioni, S. Palanti, and P. Rozenberg, "Measurements of fungal wood decay on Scots pine and beech by means of X-ray microdensitometry," *Wood Sci. Technol*., vol. 41, no. 5, pp. 417–426, 2007.

[11] E. Franceschi, I. Cascone, and D. Nole, "Thermal, XRD and spectrophotometric study on artificially degraded woods," *J. Therm. Anal. Calorim*., vol. 91, no. 1, pp. 119–123, 2008.

[12] S. Vaclavkova, N. Schultz-Jensen, O. S. Jacobsen, B. Elberling, and J. Aamand, "NitrateControlled Anaerobic Oxidation of Pyrite by Thiobacillus Cultures," *Geomicrobiol. J*., vol. 32, no. 5, pp. 412–419, 2015.

[13] M. Albelda-Berenguer, "Biological strategies for the preservation of waterlogged archaeological wood," Universtiy of Neuchâtel, 2020.

[14] H. R. Beller, P. S. G. Chain, T. E. Letain, A. Chakicherla, F. W. Larimer, P. M. Richardson,

M. A. Coleman, A. P. Wood, and D. P. Kell, "The genome sequence of the obligately chemolithoautotrophic, facultatively anaerobic bacterium Thiobacillus denitrificans," *J. Bacteriol.*, vol. 188, no. 4, pp. 1473–1488, 2006.

[15] D. P. Kelly and A. P. Wood, "Confirmation of Thiobacillus denitrificans as a species of the genus Thiobacillus, in the beta-subclass of the Proteobacteria, with strain NCIMB 9548 as the type strain," *Int. J. Syst. Evol. Microbiol.*, vol. 50, no. 2000, pp. 547–550, 2000.

[16] C. Juncher Jørgensen, O. S. Jacobsen, B. Elberling, and J. Aamand, "Microbial oxidation of pyrite coupled to nitrate reduction in anoxic groundwater sediment," *Environ. Sci. Technol.*, vol. 43, no. 13, pp. 4851–4857, 2009.

[17] R. C. Brunet and L. J. Garcia-Gil, "Sulfide-induced dissimilatory nitrate reduction to ammonia in anaerobic freshwater sediments," *FEMS Micorbiol. Ecol.*, vol. 21, pp. 131–138, 1996.

[18] K. L. Straub, M. Benz, B. Schink, and E. Widdel, "Anaerobic, nitrate-dependent oxidation of ferrous iron," *Appl. Environ. Microbiol.*, vol. 62, no. 4, pp. 1458–1460, 1996.

[19] H. Pauwels, W. Kloppmann, J. Foucher, and A. Martelat, "Field tracer test for denitirfication in apyrite-bearing schist aquifer," *Appl. Geochemistry*, vol. 13, no. 6, pp. 767–778, 1998.

[20] K.-Y. L. Julian Bosch Guntram Jordan Kyoung-Woong Kim and Rainer U. Meckenstock, "Anaerobic, Nitrate-Dependent Oxidation of Pyrite Nanoparticles by Thiobacillus denitrificans," *Est*, pp. 1–11, 2012.

[21] S. M. Kraemer, "Iron oxide dissolution and solubility in the presence of siderophores," *Aquat. Sci.*, vol. 66, no. 1, pp. 3–18, 2004.

[22] M. Albelda-Berenguer, M. Monachon, and E. Joseph, "Siderophores: From natural roles to potential applications," *Adv. Appl. Microbiol.*, vol. 106, p. 193, 2019.

[23] S. Rapti, S. Boyatzis, S. Rivers, A. Velios, and A. Pournou, "Removing iron stains from wood and textile objects: assessing gelled siderophores as novel green chelators," in *International conference Science in Technology, Athens* 2017.

[24] J. Li and Z. Chi, "Siderophores from marine microorganisms and their applications," *J. Ocean Univ. China*, vol. 3, no. 1, pp. 40–47, 2004.

[25] E. Ahmed and S. J. M. Holmström, "Siderophores in environmental research: roles and applications," *Microb. Biotechnol.*, vol. 7, no. 3, pp. 196–208, 2014.

[26] C. Pelé, E. Guilminot, S. Labroche, G. Lemoine, and G. Baron, "Iron removal from waterlogged wood : Extraction by electrophoresis and chemical treatments," *Stud. Conserv.*, vol. 60, no. 3, pp. 1–17, 2013.

[27] F. Jalilehvand, M. Sandstrom, I. Persson, U. Gelius, and P. Frank, "Acidity and Salt Precipitation on the Vasa; The Sulfur Problem," 2001.

[28] G. Almkvist, "Iron Removal from Waterlogged Wood." in *12th ICOM-CC Wet Organic Archaeological Materials Working Group Conference, Istanbul, Turkey* 2013

[29] R. Yin, C. Fan, J. Sun, and C. Shang, "Oxidation of iron sulfide and surface-bound iron

to regenerate granular ferric hydroxide for in-situ hydrogen sulfide control by persulfate, chlorine and peroxide," *Chem. Eng. J.*, vol. 336, pp. 587–594, 2018.

[30] E. M. Gargano, G. F. Mangiatordi, I. Weber, C. Goebel, D. Alberga, O. Nicolotti, W. Ruess, and S. Wierlacher, "Persulfate Reaction in a Hair-Bleaching Formula: Unveiling the Unconventional Reactivity of 1, 13-Diamino-4, 7, 10-Trioxatridecane," *ChemistryOpen*, vol. 7, no. 5, pp. 319–322, 2018.

[31] L. W. Matzek and K. E. Carter, "Activated persulfate for organic chemical degradation: a review," *Chemosphere*, vol. 151, pp. 178–188, 2016.

[32] N. Macchioni, C. Capretti, L. Sozzi, and B. Pizzo, "Grading the decay of waterlogged archaeological wood according toanatomical characterisation. The case of the Fiavé site (N-E Italy)," *Int. Biodeterior. Biodegrad.*, vol. 84, pp. 54–64, 2013.

[33] J. A. Bourdoiseau, M. Jeannin, R. Sabot, C. Rémazeilles, and P. Refait, "Characterisation of mackinawite by Raman spectroscopy: Effects of crystallisation, drying and oxidation," *Corros. Sci.*, vol. 50, no. 11, pp. 3247–3255, 2008.

[34] I. Dobrică, P. Bugheanu, I. Stănculescu, and C. Ponta, "FT-IR spectral data of wood used in Romanian," *Analele Univ. din Bucuresti*, vol. I, pp. 33–37, 2008.

[35] G. Almkvist and I. Persson, "Extraction of iron compounds from wood from the Vasa," *Holzforschung*, vol. 60, no. 6, pp. 678–684, 2006.

[36] B. Appelbaum, "Criteria for treatment: reversibility," *J. Am. Inst. Conserv.*, vol. 26, no. 2, pp. 65–73, 1987.

[37] C. Brandi and C. Déroche, *Théorie de la restauration*. École nationale du patrimoine, 2001.

[38] D. W. Grattan and R. W. Clarke, "Conservation of waterlogged wood," in *Conservation of marine archaeological objects*, Elsevier, pp. 164–206, 1987.

[39] W. S. Mokrzycki and M. Tatol, "Colour differenceΔ E-A survey," *Mach. Graph. Vis.*, vol. 20, no. 4, pp. 383–411, 2011.

[40] J. A. Bourdoiseau, M. Jeannin, C. Rémazeilles, R. Sabot, and P. Refait, "The transformation of mackinawite into greigite studied by Raman spectroscopy," *J. Raman Spectrosc.*, vol. 42, no. 3, pp. 496–504, 2011.

[41] R. M. Cornell and U. Schwertmann, *The iron oxides: structure, properties, reactions, occurrences and uses. John Wiley & Sons*, 2003.

[42] B. Hames, R. Ruiz, C. Scarlata, A. Sluiter, J. Sluiter, and D. Templeton, "Preparation of samples for compositional analysis," *Lab. Anal. Proced.*, vol. 1617, 2008.

[43] S. Tachibana, "Decomposition of lignin and holocellulose on Acacia mangium leaves and twigs by six fungal isolates from nature.," *Pak. J. Biol. Sci.*, vol. 13, no. 12, pp. 604–610, 2010.

[44] Tappi, "Lignin in Wood and Pulp," *T222 Om-02*, pp. 1–7, 2011, doi: 10.1023/a:1019003230537.

[45] K. Kürschner, "Einige kritische Erwägungen zur Analyse von Hölzern," *Holz als Roh-*

und Werkst., vol. 16, no. 8, p. 288, 1958.

[46] A. Poljak, "Holzaufschluss mit Peressigsäure," *Angew. Chemie*, vol. 60, no. 2, pp. 45–46, 1948.

[47] K. Héberger, "Chemoinformatics—multivariate mathematical–statistical methods for data evaluation," in *Medical Applications of Mass Spectrometry*, Elsevier, pp. 141–169, 2008.

[48] S. D. Sarker and L. Nahar, "Applications of high performance liquid chromatography in the analysis of herbal products," in *Evidence-Based Validation of Herbal Medicine*, Elsevier, pp. 405–425, 2015.

[49] H. T. L. dos Santos, A. M. de Oliveira, P. G. de Melo, W. Freitas, and A. P. R. de Freitas, "Chemometrics: Theory and application," *Multivar. Anal. Manag. Eng. Sci.*, p. 121, 2013.

[50] T. Trafela, M. Strlič, J. Kolar, D. A. Lichtblau, M. Anders, D. P. Mencigar, and B. Pihlar, "Nondestructive analysis and dating of historical paper based on IR spectroscopy and chemometric data evaluation," *Anal. Chem.*, vol. 79, no. 16, pp. 6319–6323, 2007.

[51] D. Lichtblau, M. Strlič, T. Trafela, J. Kolar, and M. Anders, "Determination of mechanical properties of historical paper based on NIR spectroscopy and chemometrics–a new instrument," *Appl. Phys. A*, vol. 92, no. 1, p. 191, 2008.

[52] S. Duchêne, V. Detalle, R. Bruder, and J. B. Sirven, "Chemometrics and laser induced breakdown spectroscopy (LIBS) analyses for identification of wall paintings pigments," *Curr. Anal. Chem.*, vol. 6, no. 1, pp. 60–65, 2010.

[53] M. Manfredi, E. Barberis, M. Aceto, and E. Marengo, "Non-invasive characterization of colorants by portable diffuse reflectance infrared Fourier transform (DRIFT) spectroscopy and chemometrics," *Spectrochim. Acta Part A Mol. Biomol. Spectrosc.*, vol. 181, pp. 171–179, 2017.

[54] G. Visco, S. H. Plattner, G. Guida, S. Ridolfi, and G. E. Gigante, "Rings or daggers, axes or fibulae have a different composition? A multivariate study on Central Italy bronzes from eneolithic to early iron age," *Chem. Cent. J.*, vol. 9, no. 1, p. 15, 2015.

[55] M. D. Peris-Díaz, B. Łydżba-Kopczyńska, and E. Sentandreu, "Raman spectroscopy coupled to chemometrics to discriminate provenance and geological age of amber," *J. Raman Spectrosc.*, vol. 49, no. 5, pp. 842–851, 2018.

[56] G. Capobianco, M. P. Bracciale, D. Sali, F. Sbardella, P. G. Bonifazi, S. Serranti, M. L. Santarelli, and M. C. Guidi, "Chemometrics approach to FT-IR hyperspectral imaging analysis of degradation products in artwork cross-section," *Microchem. J.*, vol. 132, pp. 69–76, 2017.

[57] A. S. Luna and J. S. de Gois, "Application of Chemometric Methods Coupled With Vibrational Spectroscopy for the Discrimination of Plant Cultivars and to Predict Physicochemical Properties Using R," in *Comprehensive Analytical Chemistry*, vol. 80, Elsevier, pp. 165–194, 2018.

[58] P. Geladi, J. Swerts, and F. Lindgren, "Multiwavelength microscopic image analysis of a piece of painted chinaware: Classification and regression," *Chemom. Intell. Lab. Syst.*,

vol. 24, no. 2, pp. 145–167, 1994.

[59] C. R. Cork, W. D. Cooke, and J.-P. Wild, "The use of image analysis to determine yarn twist level in archaeological textiles," *Archaeometry*, vol. 38, no. 2, pp. 337–345, 1996.

[60] B. Pizzo, E. Pecoraro, A. Alves, N. Macchioni, and J. C. Rodrigues, "Quantitative evaluation by attenuated total reflectance infrared (ATR-FTIR) spectroscopy of the chemical composition of decayed wood preserved in waterlogged conditions," *Talanta*, vol. 131, pp. 14–20, 2015.

[61] R. G. Brereton, J. Jansen, J. Lopes, F. Marini, A. Pomerantsev, O. Rodionova, J. M. Roger, B. Walczak, and R. Tauler, "Chemometrics in analytical chemistry—part I: history, experimental design and data analysis tools," *Anal. Bioanal. Chem.*, vol. 409, no. 25, pp. 5891–5899, 2017.

[62] J.-J. Droesbeke, J. Fine, and G. Saporta, *Plans d'expériences: applications à l'entreprise*. Editions technip, 1997.

[63] D. Raghavarao and L. V Padgett, *Block designs: analysis, combinatorics, and applications*, vol. 17. World Scientific, 2005.

[64] B. A. Hanson, "An Introduction to ChemoSpec," pp. 1–19, 2018.

[65] K. H. Liland, B.-H. Mevik, and R. Canteri, "Package 'baseline.'" 2015.

[66] J. Zhao, H. Lui, D. I. McLean, and H. Zeng, "Automated autofluorescence background subtraction algorithm for biomedical Raman spectroscopy," *Appl. Spectrosc.*, vol. 61, no. 11, pp. 1225–1232, 2007.

[67] H. Hu, J. Bai, G. Xia, W. Zhang, and Y. Ma, "Improved baseline correction method based on polynomial fitting for Raman spectroscopy," *Photonic Sensors*, vol. 8, no. 4, pp. 332–340, 2018.

[68] H. J. Butler, B. R. Smith, R. Fritzsch, P. Radhakrishnan, D. S. Palmer, and M. J. Baker, "Optimised spectral pre-processing for discrimination of biofluids via ATR-FTIR spectroscopy," *Analyst*, vol. 143, no. 24, pp. 6121–6134, 2018.

[69] F. Dieterle, A. Ross, G. Schlotterbeck, and H. Senn, "Probabilistic quotient normalization as robust method to account for dilution of complex biological mixtures. Application in 1H NMR metabonomics," *Anal. Chem.*, vol. 78, no. 13, pp. 4281–4290, 2006.

[70] A.-X. Zhao, X.-J. Tang, Z.-H. Zhang, and J.-H. Liu, "The parameters optimization selection of Savitzky-Golay filter and its application in smoothing pretreatment for FTIR spectra," in *9th IEEE Conference on Industrial Electronics and Applications*, 2014.

[71] J. Luo, K. Ying, and J. Bai, "Savitzky–Golay smoothing and differentiation filter for even number data," *Signal Processing*, vol. 85, no. 7, pp. 1429–1434, 2005.

[72] A. R. M. Radzol, K. Y. Lee, W. Mansor, and A. Azman, "Optimization of Savitzky-Golay smoothing filter for salivary surface enhanced Raman spectra of non structural protein 1," in *TENCON 2014-2014 IEEE Region 10 Conference*, 2014.

[73] B. Zimmermann and A. Kohler, "Optimizing Savitzky-Golay parameters for improving

spectral resolution and quantification in infrared spectroscopy," *Appl. Spectrosc.*, vol. 67, no. 8, pp. 892–902, 2013.

[74] J. Serafinczuk, J. Pietrucha, G. Schroeder, and T. P. Gotszalk, "Thin film thickness determination using X-ray reflectivity and Savitzky-Golay algorithm," *Opt. Appl.*, vol. 41, no. 2, pp. 315–322, 2011.

[75] L. Stahle and S. Wold, "Analysis of variance (ANOVA)," *Chemom. Intell. Lab. Syst.*, vol. 6, no. 4, pp. 259–272, 1989.

Chapter 3: Results of degradation and contamination protocols to model waterlogged wood

1 – Real archaeologic samples

Archaeological oak poles and pine board were donated from Swiss collaborators: Swiss National Museum (SNM) and Archaeological Service of Bern Canton (ADB). The poles and board were stored in water in sealed containers prior to being cut and characterized. These wood items representative of freshwater sites were characterized and their properties defined as reference criteria in the design of model WAW samples. 2-cm slices were cut from the poles and board and then cubes of 2x2x2 cm^3 were shaped on the external layer of the slices, following the wood ring to have homogeneous samples sets.

1.1 – Appearance and colorimetry

All real waterlogged archaeological wood (WAW) oak samples (sets D1, D2, G2) presented a dark appearance while real WAW pine samples (set G1) were brownish (Figure 13a).

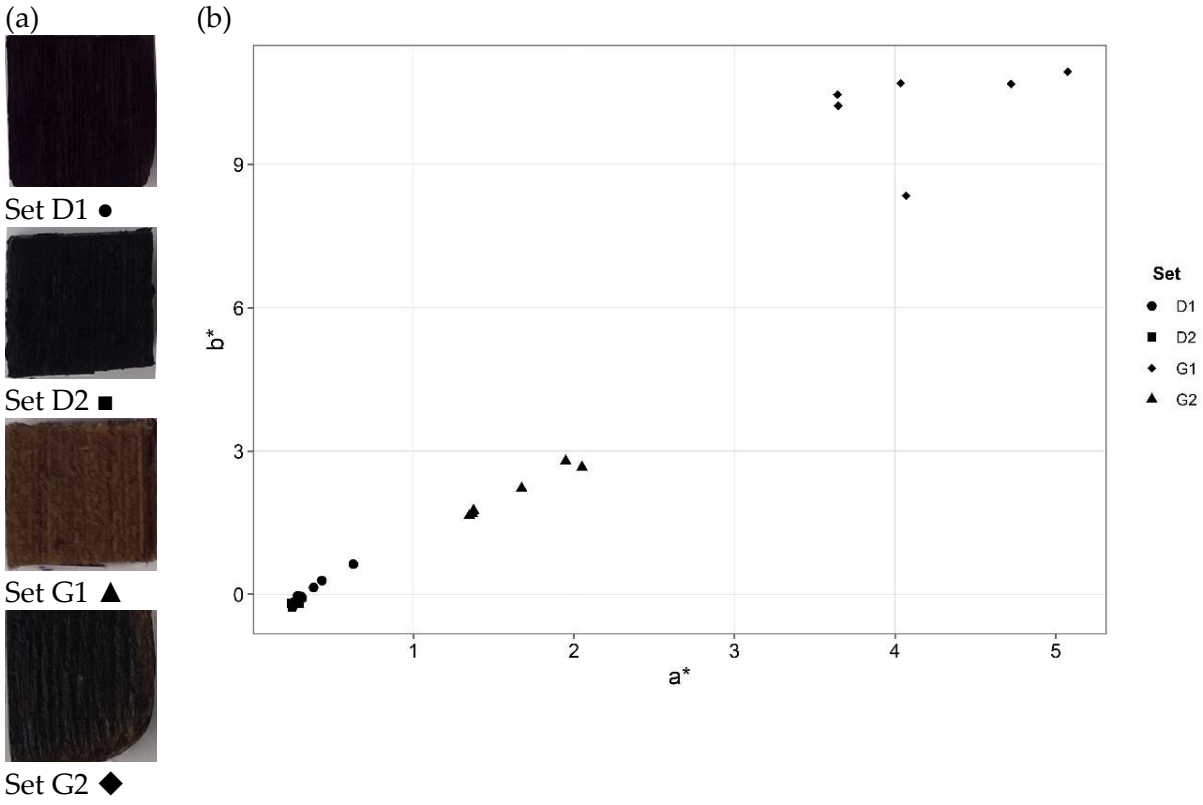

Figure 13: (a) Appearance of archaeological oak (sets D1, D2, G2) and pine (Set G1) wood samples when recovered. (b) Colorimetric coordinates a and b* of archaeologic oak (set D1, ●; set D2, ■; set G2, ▲) and pine (Set G1, ◆) wood samples*

Regarding colorimetric coordinates a* and b*, sets D1 and D2 gathered (Figure 13b, circles, and squares) with set G2 not far from this cluster (Figure 13b, triangles). All these sets are WAW oak. Samples from set G1 (pine) were farther from the other samples (Figure 13b, diamonds). Real WAW hard- and softwood samples presented indeed a different appearance that should be maintained after the application of the different conservation interventions in order to respect artefacts aesthetic values [1]–[3].

1.2 – State of conservation

1.2.1 - Wood degradation

The state of conservation of sets D1, D2, G1 and G2 was investigated. First, Attenuated Total Reflectance Fourier Transformed Infrared (ATR-FTIR) spectroscopy was carried out to determine which wood components were degraded. The characteristic infrared bands assigned to wood are reported in Table 8.

Table 8: Assignment characteristic FTIR vibrational bands in wood

Band position (cm^{-1})	**Assignment**	**Reference**
1738/1734	Xylan (hemicellulose) unconjugated C=O stretching	[4], [5]
1650	Water adsorption H-O-H deformation	[4]
1595	Lignin skeleton C=C stretching	[4]
1506	Lignin skeleton C=C stretching	[4], [5]
1374	Cellulose and xylan CH deformation	[4], [5]
1268	Lignin (guaiacyl ring, softwood) Xylan C-O stretching Cellulose and xylan CH and OH wagging	[4]
1237	Lignin (syringyl ring, hardwood) Xylan C-O stretching	[6], [7]
1158	Holocellulose C-O-C vibration	[5]
1112	Lignin aromatic skeletal Holocellulose C–O stretching	[6]
1059	Holocellulose C-O stretching	[7]
1034	Holocellulose C-O stretching	[8]
898	Cellulose C-H deformation	[5]

Analyses were performed at the surface of the wood's samples, on the three plane sections.

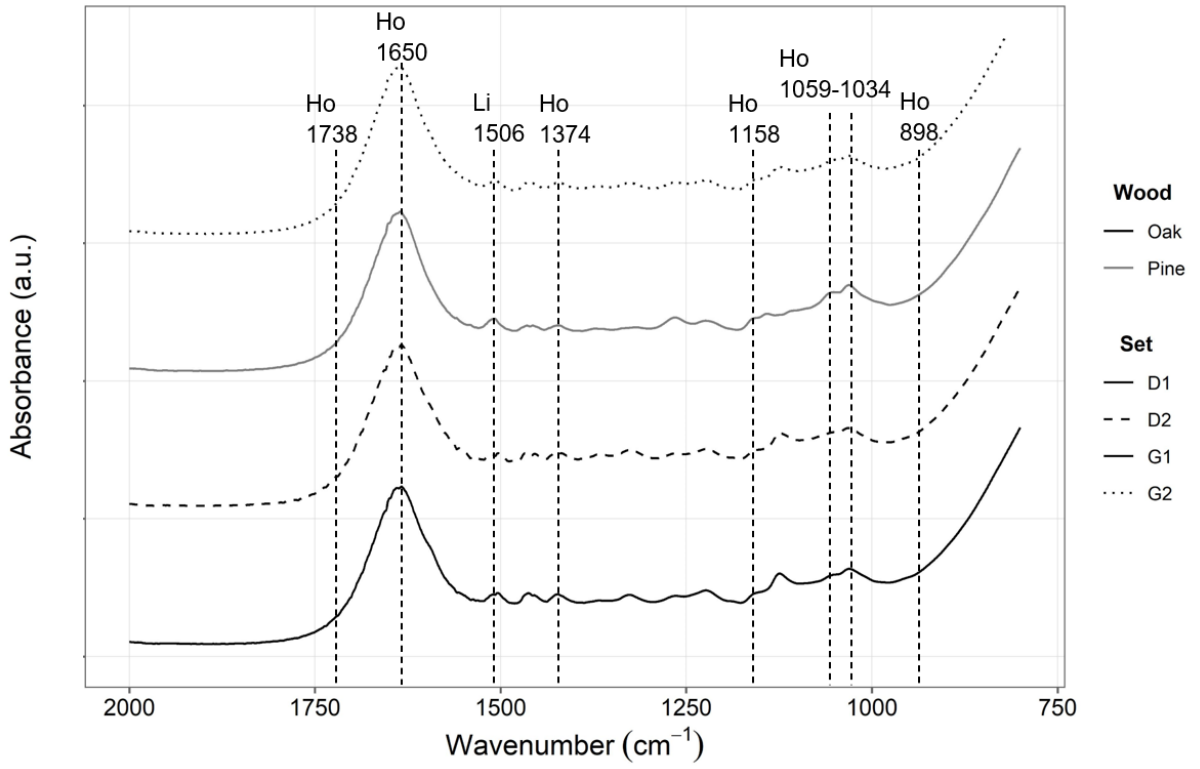

Figure 14: Representative ATR-FTIR spectra of archaeological oak (set D1, black solid line; set D2, black dash line; set G2, black dot line) and pine (set G1, grey line) with characteristic wood vibrational bands of holocellulose (Ho) and lignin (Li) indicated with dashed lines

The vibrational bands at 898, 1034, 1059, 1158, 1374 and 1738 cm^{-1}, characteristic of holocellulose, were not visible or very weak on the spectra (Figure 14) [5], [8]. This was the same for both wood species. Thus, the carbohydrates content was very low. The poles and board were recovered from different waterlogged sites, but all presented a high degradation state. In addition, a vibrational band at 1650 cm^{-1} was observed for all samples. This band is assigned to water adsorption [4].

Furthermore, the ATR-FTIR ratios R1, R2, and R3 calculated showed values lower than 1, usually correlated to important degradation of carbohydrates (Table 8) [9]. No clear difference was observed between the ratios of buried hard- and softwood samples. It seemed most probably that after a certain amount of time buried, the type of wood species does not affect the degradation of carbohydrates. Additional Maximum Water Content (MWC) measurements were performed. MWC is a method to categorized archaeological wood depending on the degree of degradation and is part of the Italian standard UNI 11250:2007 for wood characterization [10]. MWC is calculated based on the weight of the wood samples above and within water. Five ranks exist to classify wood from not decayed (0) to importantly decayed (4) [11], [12]. Based on MWC values, sets D1 and G2 were categorized in rank 4 and sets D2 and G1 in rank 3 (Table 9). These samples were classified as highly decayed.

Table 9: ATR-FTIR ratios R1, R2 and R3 and maximum water content (MWC) calculated for archaeological oak (sets D1, D2, G2) and pine (set G1) wood samples, with standard deviation indicated in brackets. R1 = I(1158)/I81506), R2 = I(1374)/I81506) and R3 = I(1034)/I(1506)

Samples		R1	R2	R3	MWC rank
Archaeological oak	*Set D1*	0.90 (± 0.01)	0.92 (± 0.01)	1.01 (± 0.03)	4
	Set D2	0.85 (± 0.02)	0.92 (± 0.00)	0.91 (± 0.04)	3
	Set G2	0.83 (± 0.00)	0.92 (± 0.01)	0.84 (± 0.03)	3
Archaeological pine	*Set G1*	0.84 (± 0.01)	0.92 (± 0.01)	0.90 (± 0.06)	4

1.2.2 - Presence of harmful species

Microchemical spot test were carried out to determine wood contamination by iron and sulfur species. Iron species were detected on archaeological oak thanks to the phenanthroline method though no sulfur speciation was identified [13]. The wood samples were dated from 3840 BC, before Iron Age, thus the iron contamination should be originated from the surrounding environment (*i.e.*, sediments). Also, the spot tests were performed on the surface of the poles and board, and we cannot ascertain the presence of iron and sulfur specie within these items.

Raman spectroscopy was thus performed on the samples once cut in cubes of 2x2x2 cm^3. No Raman shifts related to reduced sulfur species were identified on the samples. The bands observed in the range 600-1500 cm^{-1} were assigned to wood components (*i.e.*, lignin, cellulose and hemicellulose) [14]. Therefore, we concluded that all sets D1, D2, G1 and G2 were free of any contamination from iron or sulfur species. Though, spot tests detected iron within the WAW samples. To complete Raman analyses carried out on narrow spots, SEM-EDS measurements were also performed on thin cross-sections.

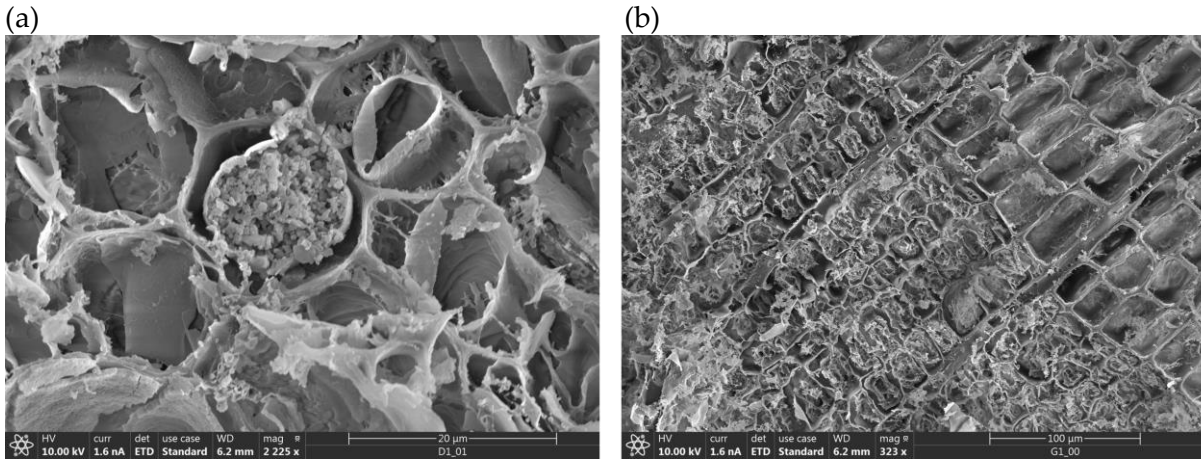

Figure 15: SEM micrographs of (a) archaeological oak (set D1) and (b) pine (set G1) cross section

One can observe that the cell walls were degraded during the burial time, with the accumulation within the wood cells (vessels and tracheids) of amorphous cellulose that is characteristic of exposition to erosion bacteria (Figure 15) [15].

Also, EDS analyses revealed the presence of calcium Ca as main element, both on WAW oak and pine sections. Calcium is naturally present in wood, under the form of ash content, allowing tree growth [16]. Complementary Inductively Coupled Plasma-Optical Emission Spectroscopy (ICP-OES) analyses on different wood samples from the D1 burial site indicated a mean concentration of 90.0 (± 2.7) g of Ca per kg of oak wood. The high Ca concentration observed can be due to the presence of sediments within the wood samples. Other elements were also detected, either by EDS or ICP-OES analyses. For instance, sodium Na, potassium K, magnesium Mg, and aluminium Al were detected for both hard-and softwood species. Their concentration was higher for hardwood, with for example 800 mg of Na per kg of oak wood compared to 400 mg of Na per kg of pine wood. All these species are naturally present in the wood and should not interfere with any conservation procedures.

Finally, iron and sulfur species were also detected on the samples but in lower proportions. ICP-OES analyses carried out on some samples revealed a concentration of 1.38 mg of Fe and 2.11 mg of S per g of WAW oak and 0.30 mg of Fe and 3.82 mg of S per g of WAW pine. Compared to calcium and sodium, these species concentrations were very low, which may explain why no iron and sulfur were detected by spot tests, Raman, and EDS analyses. In addition, analyses of the water collected on the burial site and in which the wood pieces are stored revealed a low iron concentration but an important concentration in sulfates SO_4^{2-}, with a mean value of 21.0 (± 2.9) mg of SO_4^{2-} per liter. Iron contamination may then come from the sediments surrounding the objects while the natural sulfur cycle occurring in such environments may explain the presence of sulfur within the wood samples.

WAW oak and pine samples characterized here present the highest degree of degradation reported in literature [10], [11]. However, the iron and sulfur contamination were quite low. Therefore, even if these samples are real WAW, they may not be representative enough of the problematic WAW objects. In addition, real WAW samples are valuable items and cannot be employed to experiment new extraction and stabilization methods. Thus, model samples replicating main characteristics of WAW samples should be prepared from selected degradation and contamination protocols. Such protocols should allow to reach the same degree of degradation than real WAW samples displayed (poor holocellulose content) as well as contamination with main iron sulfide compounds identified on WAW artefacts (*i.e.*, mackinawite FeS, greigite Fe_3S_4, pyrite FeS_2) [17], [18].

1.3 – Summary of research

All WAW samples collected (sets D1, D2, G1 and G2) presented a low state of conservation, independently of the type of wood species under study. Both hard- and softwood samples were decayed by erosion bacteria during their burial time, with conversion of cellulose into an amorphous substance in the degraded cells. Even if their concentration levels were low, iron and sulfur species were detected in the samples or their environments. These samples will be

referred as reference samples in order to develop degradation and contamination protocols mimicking WAW samples characteristics.

2 – Modelling waterlogged wood

Different degradation and contamination protocols were studied on different wood samples, with the goal to mimic the state of real WAW. In the section above, it was concluded that real WAW samples were highly decayed and presented a little contamination with iron and sulfur species. The protocols foreseen should then allow degrading holocellulose content as well as contaminating wood with iron and/or sulfur species.

2.1 – Degradation protocols

First, chemical, and biological degradation protocols were performed on fresh wood samples. Fresh oak (*Quercus* sp.) and fresh pine (*Pinus* sp.) were selected as representative species of hard- and softwood species.

2.1.1 – Appearance and colorimetry

The samples were documented at the end of each degradation protocol. It could be observed that the degradation protocols here studied impacted hard- and softwood species differently. In general, oak (hardwood) samples (Figure 16) were darker than pinewood (softwood) samples (Figure S 1).

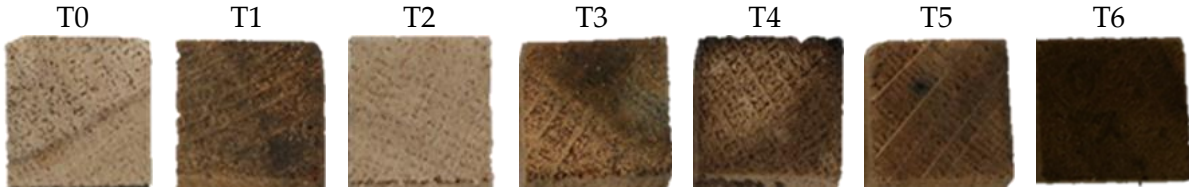

Figure 16: Oak wood samples, either untreated (T0) or after degradation protocols (T1: H_2O+vacuum; T2: UV; T3: N_2+vacuum; T4: H_2O_2:NH_4OH; T5: T1+metal; T6: fungi)

First observations showed that the appearance of the samples changed except for samples degraded with T2 (UV exposition). To ascertain this statement, colorimetric measurements were performed and a* and b* coordinates were obtained in the CIELab color space for untreated (T0) and degraded (T1-T6) samples.

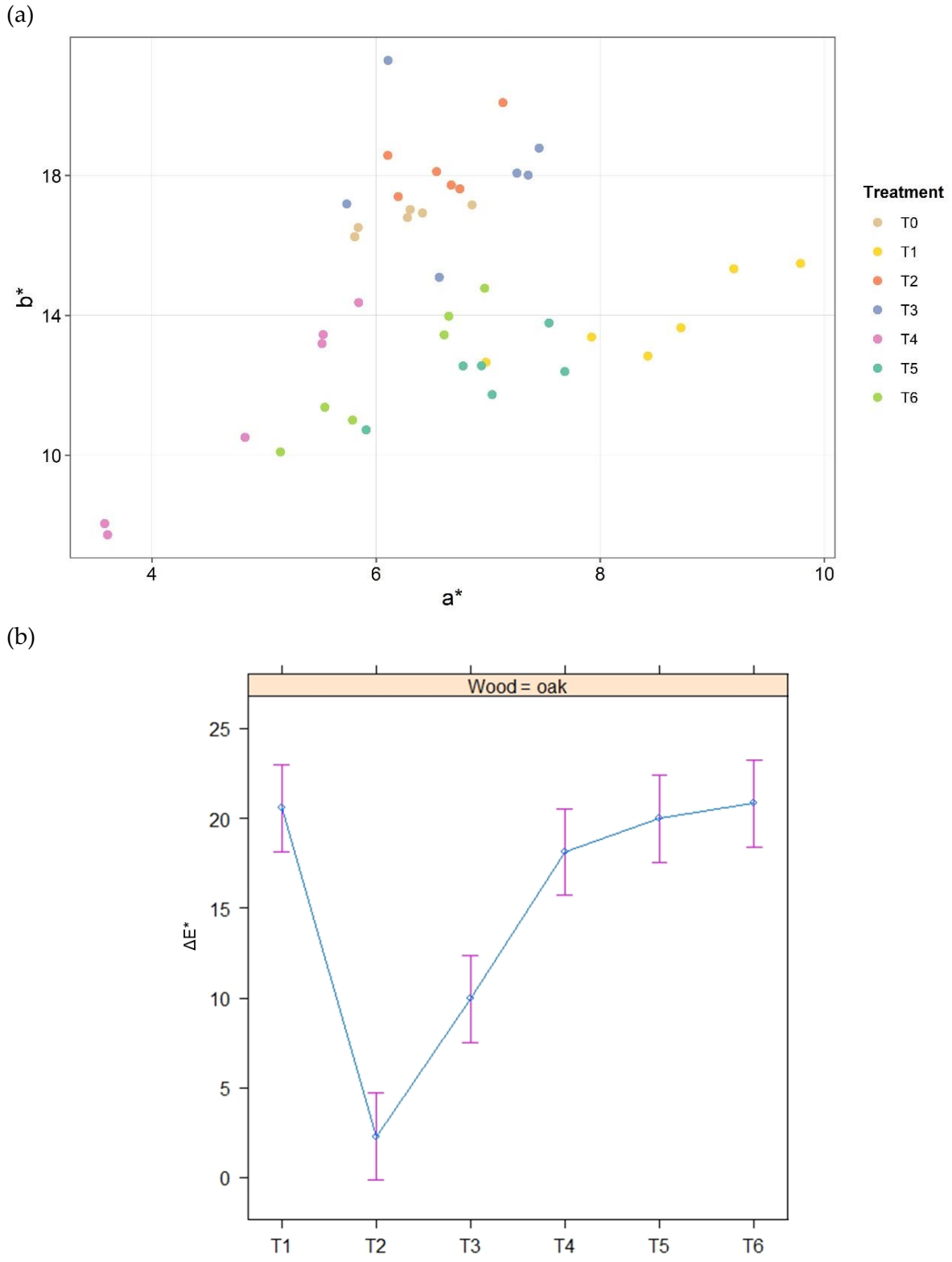

Figure 17: (a) Colorimetric coordinates a and b* for oak untreated (T0) and degraded (T1-T6) wood samples. (b) ANOVA results of color variation (ΔE*) depending on degradation protocols (T1-T6) for oak wood species*

From colorimetric coordinates, one can observed that T0 and T2 samples gathered (Figure 17a and Figure S 2a). Therefore, the UV exposure did not induce a color variation, as expected and demonstrated in the work of Pelosi et al [19]. Indeed, some studies demonstrated a possible correlation between the wood degradation state and visual appearance [20]. Here, no color

variation was observed applying T2 protocol and thus, this implies that the T2 protocol did not enhance any wood decay. In other words, a UV exposure of fresh wood cannot be considered as an efficient protocol to replicate WAW. Furthermore, it is worth mentioning that ultraviolet light only penetrates few microns (80 μm) of wood due to the presence of chromophoric groups at the surface [21], [22]. Then, UV exposition could enhance a degradation but would probably not be sufficient to decay carbohydrates within the whole wood sample. Additionally, such exposition may induce an important decrease of the lignin content compared to holocellulose, going in the opposite direction of our study goal [23]. Regarding the other protocols, differences were observed based on the type of wood species. Indeed, oak samples submitted to T3 (N_2+vacuum) protocol also gathered with T0 and T2 samples while oak samples submitted to T1 (H_2O+vacuum), T4 (H_2O_2:NH_4OH), T5 (T1+metal) and T6 (fungi) protocols clustered together (Figure 17a). Thus, the distance between the two clusters is narrow, implying that the variation is not as important as suggested by the visual observations in Figure 16. Concerning pinewood, all samples, except T2 samples, were far from T0 untreated pine samples, T1 samples giving the farther points along the a* axis (Figure S 2a). Contrary to the visual observations that showed darker oak than pine samples after degradation, pine samples presented a more important color variation according to measured colorimetric data. Colorimetric measurements and calculation of the color variation may be hence a more reliable method to evaluate the effective degradation of wood. Modelling WAW with degradation of fresh samples from pine or softwood species may also be more easily interpreted, with a higher color variation observed.

To validate these results, ANOVA analysis was carried out on the color variation ΔE* calculated for each degradation protocol. It resulted that T2 (UV) samples were significantly different from the other degraded samples and similar to untreated T0 samples for both oak and pine (Figure 17b and Figure S 2b). Thus, the T2 degradation protocol could be actually discarded and will not be discussed in the following paragraphs. Regarding the other degradation protocols, T3 oak samples were also significantly different from those treated with the other protocols (T1, T4, T5 and T6) while for pine, T3 and T4 samples were significantly similar (Figure S 2b). ΔE* for T3-pine samples was higher than ΔE* for T3-oak samples. If it is assumed that an important color variation ΔE* is correlated with an important wood degradation, T3 protocol (water immersion under vacuum followed by N_2/vacuum cycles) altered more softwood than hardwood. T1, T4, T5 and T6 protocols presented the highest ΔE* implying that their degradation was the most important and were significantly similar together according to ANOVA analyses ($p\text{-val} < 0.05$).

2.1.2 – ATR-FTIR spectroscopy

If the visual appearance of samples could be a first indication of their degradation, ATR-FTIR spectroscopy facilitates to quantify this wood degradation. In particular, this method allows to determine which components of the wood were altered. Wood degradation was observed on the spectra collected at the samples' surface.

(a)

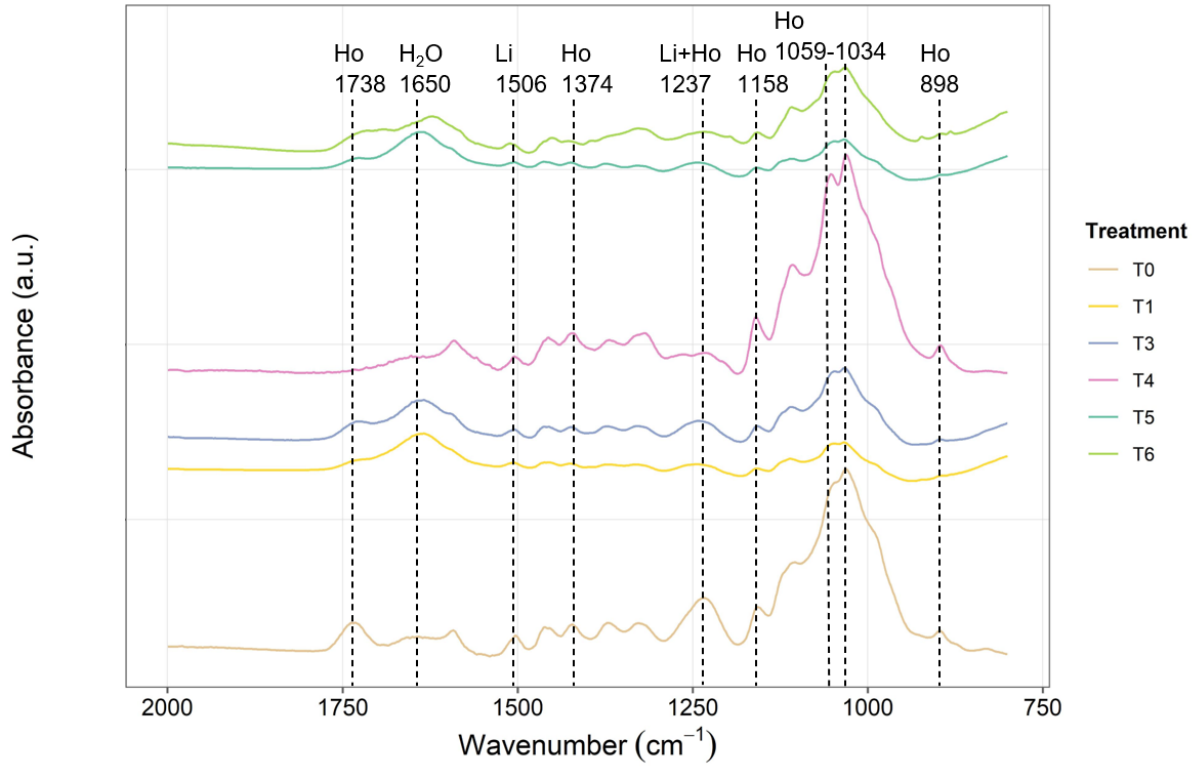

(b)

Vibrational bands	T0	T1	T3	T4	T5	T6
1237	1.33	0.76	0.91	0.89	0.80	0.84
1506	0.80	0.81	0.80	0.90	0.78	0.65

Figure 18: (a) Representative ATR-FTIR spectra for oak untreated (T0) and degraded (T1-T6) samples with characteristic vibrational bands of holocellulose (Ho) and lignin (Li) indicated with dashed lines. (b) Mean height of characteristic hardwood lignin vibrational bands for each degradation protocol

First, the vibrational band at 1738 cm^{-1} presented a decrease in intensity for all degradation protocols (Figure 18a and Figure S 3a). This band is associated with the xylan content that is part of hemicellulose (Table 8) [4], [5]. Therefore, this means that all the protocols investigated may induce hemicellulose and thus holocellulose decay. The decreased intensity of the 1374 cm^{-1} band, assigned to cellulose and xylan deformation, confirmed the holocellulose decay [4], [5]. Yet, this decrease in intensity was only observed for oak samples submitted to T1 (H_2O+vacuum), T5 (T1+metal) and T6 (fungi) degradation protocols (Figure 18a). On the contrary, all pine samples presented a decreased intensity at 1374 cm^{-1} whatever the degradation protocol applied (Figure S 3a). Similarly, to that could be deduced from colorimetric measurements, pine decayed more easily than oak. The four other vibrational bands associated with holocellulose content (*i.e.*, 1158, 1059, 1034 and 898 cm^{-1}) also presented a decrease in intensity after degradation with T1, T3, T5 and T6 protocols for both oak and pine wood.

Two other bands at 1268 and 1237 cm^{-1} can be assigned to xylan content and thus to its degradation [5], [6]. However, these bands can also be assigned to lignin content and more precisely with 1268 $cm^{-1}$and 1237 cm^{-1} assigned to softwood (pine) and hardwood (oak) lignin, respectively. Concerning oak (hardwood), a decrease of 1237 cm^{-1} band intensity was observed for samples degraded with T1, T4, T5 and T6 protocols (Figure 18a), while all pine (softwood) samples presented less intense 1268 cm^{-1} vibrational band (Figure S 3a). To determine if lignin content was also affected during the degradation protocols, intensity of the band at 1506 cm^{-1} was considered [4], [5]. The mean height of the vibrational bands at 1237, 1268 and 1506 cm^{-1} was compared among the different protocols applied (Figure 18b). It was observed that the bands at 1237 and 1268 cm^{-1} did decrease in intensity after all protocols. On the contrary, the band at 1506 cm^{-1} slightly decreased or remained in the same range for protocols T1, T3 and T4, while the mean height was lower for T5 and T6 protocols. This was observed for oak and pine wood samples. The band at 1506 cm^{-1} is only assigned to lignin content while the two others at 1237 and 1268 cm^{-1} are also attributed to holocellulose content. Therefore, lignin was affected when the samples were treated with T5 and T6 protocols as only the height of band at 1506 cm^{-1} decreased for these protocols.

(a)

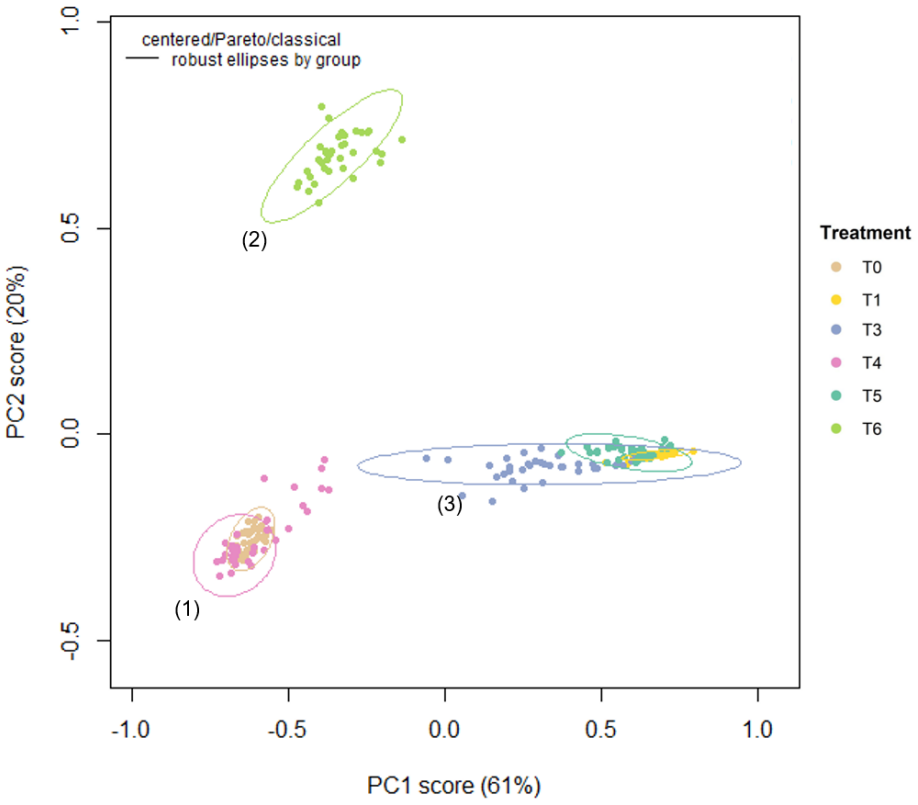

(b)

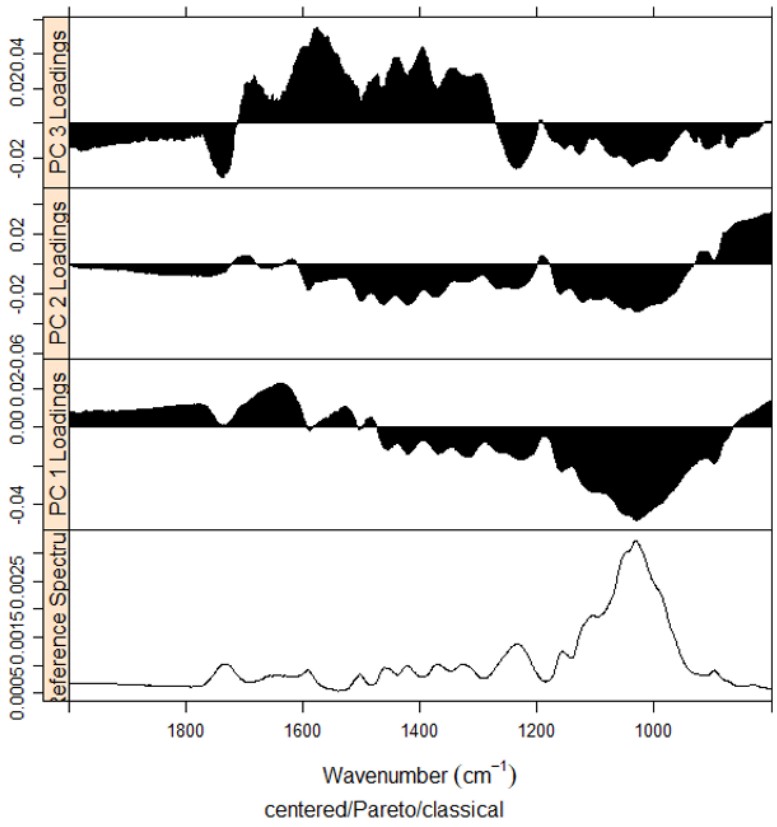

Figure 19: (a) PCA score plot of ATR-FTIR spectra for untreated (T0) and degraded (T1-T6) oak samples. (b) PCA loadings of ATR-FTIR spectra in the range 2000-800 cm^{-1} with fresh oak as reference sample

PCA analysis was performed on all spectra. Figure 19a only showed results from oak wood samples but a similar score plot was obtained for pine wood samples (and data are presented in supplementary material 1, Figure S 3b). Three clusters were observed on the PCA score plot (Figure 19a). In the first one (1) are gathered T0 and T4-samples. Cluster (2) only gathered T6-samples while cluster (3) assembled T1, T3 and T5-samples. If from the interpretation of ATR-FTIR spectra, T4 protocol seemed to decay wood samples as efficiently as the other protocols, PCA analysis demonstrated the contrary. This approach implies that T0 and T4-samples are significantly similar and thus that T4 degradation protocol may not be appropriate for the degradation of carbohydrates from fresh wood. The three clusters were distributed along PC1, which compiles 59% of total variability. Clusters (1) and (2) were mainly in the negative part of PC1 while cluster (3) was in the positive part. Looking more carefully at PC1 loading, we observed that the holocellulose bands in the range 1400-850 cm^{-1} negatively affected the loading (Figure 19b). This means that the samples in clusters (1) and (2) were gathered based on these bands and thus based on the holocellulose content. This suggested that holocellulose was less decayed for T0 and T4- samples and in minor proportion for T6-samples. Also, the vibrational band at 1506 cm^{-1} (lignin content) positively affected PC1 but with a lower contribution. T1, T3 and T5-samples gathered in cluster (3) in the positive part of PC1. The vibrational band at 1506 cm^{-1} showed similar intensity for T0, T1, T3 and T5-samples though the holocellulose bands for T1, T3 and T5-samples were less intense than T0-samples, explaining the distribution of the samples in the score plot. In addition, one can observed that clusters (1) and (3) are in the negative part of PC2 (16% total variability) and cluster (2) in the positive part (Figure 19a). PC2 loading profile showed positive score for the vibrational band at 898 cm^{-1}, band assigned to CH deformation in cellulose (Figure 19b) [44]. Only T6-samples clustered in the positive part of PC2 though cluster (3) gathering T1, T3 and T5-samples also tend to positive scores of PC2. In general, cellulose degradation differed between chemical (T1, T3, T4, T5) and biological (T6) protocols.

Then, we quantified wood degradation through calculation of three ratios: R1 = I(1158)/I81506), R2 = I(1374)/I81506) and R3 = I(1034)/I(1506). Ratios were calculated for each of the three plane sections of the different samples analyzed (triplicates per set and protocol evaluated). It resulted that the ratios were similar for all plane sections, suggesting that the degradation was homogeneous within wood, along the three wood directions. The mean ratios obtained for oak wood are presented in Table 10 and mean values for pine wood in supplementary material (Table S 1).

Table 10: ATR-FTIR ratios calculated for oak untreated (T0) and degraded (T1-T6) samples. Mean values of the ratios obtained on three plane sections are presented with the corresponding standard deviation indicated with brackets. R1 = I(1158)/I81506), R2 = I(1374)/I81506) and R3 = I(1034)/I(1506)

Wood species	Degradation protocol	R1	R2	R3
Oak	*T0*	1.52 (± 0.06)	1.24 (± 0.03)	3.85 (± 0.23)
	T1	0.89 (± 0.03)	0.98 (± 0.02)	1.30 (± 0.17)
	T3	1.07 (± 0.1)	1.08 (± 0.05)	2.11 (± 0.37)
	T4	1.32 (± 0.27)	1.20 (± 0.06)	3.30 (± 0.87)
	T5	0.96 (± 0.05)	1.03 (± 0.04)	1.57 (± 0.20)
	T6	1.32 (± 0.09)	1.16 (± 0.04)	2.87 (± 0.35)

As observed on Table 10, the standard error was low, proving the reproducibility of each degradation protocol. In general, the following rank is noticed for both wood species: T1 < T5 < T3 < T6 < T4 < T0. R1 and R3 evaluate holocellulose (hemicellulose + cellulose) degradation while R2 cellulose degradation only. The three ratios assessed then carbohydrates decay. It seemed that T1, T3 and T5 degradation protocols can be considered more efficient regarding holocellulose (hemicellulose and cellulose) degradation based on PCA and ratios analyses.

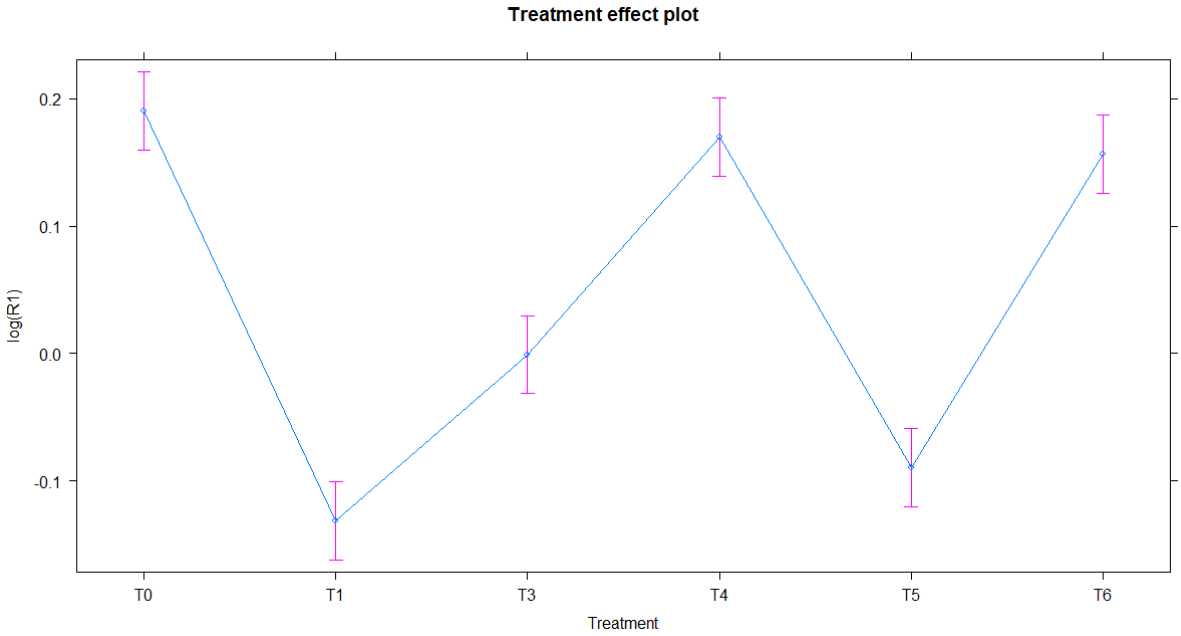

Figure 20: ANOVA results of ATR-FTIR R1 ratio for untreated (T0) and degraded (T1-T6) wood samples

ANOVA validated ATR-FTIR observations with T1 (H_2O+vacuum), T3 (N_2/vacuum cycles) and T5 (T1+metal) protocols being significantly different of untreated (T0) samples (Figure 20). Yet, T1 and T5 mean values were lower than T3 mean value. Only ANOVA for R1 ratio is presented but the same was observed for R2 and R3 ratios (supplementary material 1 Figure S 4).

T1, T3 and T5 protocols all included a water immersion step under vacuum. However, the conditions of immersion were slightly different between the protocols. For instance, T3 lasted

only 24 hours and with vacuum set at -0.2 bars while T1 and T5 lasted a week with vacuum set at -0.6 bars. One can then conclude here that water immersion and vacuum application may be key factors to reproduce the carbohydrates content degradation within fresh wood in order to replicate WAW artefacts. Moreover, the longer the immersion lasted, the higher the degradation was. Indeed, it was proven that water weaken the wood structure and specially the secondary bonding [24]. This bond held together the cellulosic chains. Therefore, water immersion induce a diminution of the wood stiffness [25], [26]. However, it is the lignin content that gives rigidity to the cell wall by acting as a glue between cellulose microfibrils. Then lignin may have been slightly decayed as well, as observed on the ATR-FTIR spectra, to reach the carbohydrates content encrusting in lignin. Even if not reported in literature, the application of vacuum during the immersion step may have also contribute to the degradation of the carbohydrates content. Thus, wood rigidity decreased during immersion in water under vacuum, permitting the reactive to potentially penetrate deeper within the samples and interact with carbohydrates. However, a previous study also reported that cellulose only decays when immersed in strong acidic solutions [24]. R2 ratio allows evaluating this cellulose degradation and we can observe here that R2 presented the lowest variation compared to untreated (T0) samples (Table III. 4). The variation before/after degradation was calculated according to the formula $\frac{Rb-Ra}{Rb} \times 100$ with Rb being ATR-FTIR ratios (R1, R2, R3) before degradation protocol and Ra ATR-FTIR ratios after contamination protocol. Results are reported in Table 11 for oak samples and in Table S 2 for pine samples.

Table 11: Mean variation of the ATR-FTIR ratios R1, R2 and R3 calculated on three plane sections after the application of the different degradation protocols T1-T3-T4-T5-T6 on oak wood samples, with standard error indicated in bracket

Degradation protocol	R1	R2	R3
T1-T0/T0	-41.1 (± 3.1)	-21.2 (± 2.3)	-66.0 (± 5.0)
T3-T0/T0	-29.5 (± 6.9)	-12.6 (± 4.3)	-44.9 (± 10.1)
T4-T0/T0	-12.8 (± 18.2)	-3.0 (± 6.2)	-14.4 (± 22.0)
T5-T0/T0	-36.6 (± 4.4)	-16.8 (± 3.2)	-59.2 (± 5.6)
T6-T0/T0	-12.6 (± 6.0)	-6.1 (± 3.5)	-25.0 (± 9.6)

The lower R2 variation suggests that cellulose is poorly degraded and thus that the main part of holocellulose degraded was hemicellulose for all degradation protocols. This is in line with interpretation of ATR-FTIR spectra where the intensity of vibrational bands of xylan (component of hemicellulose) were less intense after degradation protocols being applied. Even if water immersion may not be enough to degrade cellulose, combined with vacuum the protocols T1 and T5 showed the most promising results in terms of holocellulose degradation, as observed with PCA analysis. Furthermore, T1-samples displayed lower R2 values than T5-samples. The addition of metal pieces in the wood samples did not induce further degradation, contrary to that suggested by Franceschi research [27], [28]. This is also not in line with that we know from WAW degradation processes. Indeed, metals corrode easily in water, releasing metallic ions that could then react with wood components. The metal pieces used here were steel needles. Many studies reported that iron ions can catalyze wood degradation [29]. Needles present in T5-samples may not get oxidized during the one-week immersion time, as

this period may be too short for iron ions to be produced and catalyze wood degradation. Increasing the immersion time and/or the vacuum level applied may result in a higher degradation of the wood components. T1 protocol seems here efficient regarding enhancing holocellulose degradation, the addition of metal pieces in T5 protocol may then not be essential to achieve proper wood degradation. Using a simpler protocol, such as T1, would then be enough to simulate properly WAW samples from fresh wood.

Samples treated with T4 protocol were also immersed. Though, their immersion solution was a mixture of H_2O_2 and NH_4OH. Pullanikat's research, on which this protocol was based on, observed a degradation of both holocellulose and lignin content [30]. More precisely, their research showed the feasibility to convert glucose into formates. Glucose is the sugar molecule forming the different blocks of cellulose [31]. Immersion in H_2O_2:NH_4OH solution should then principally attacked the cellulose content of fresh wood. When applied here, one can notice that such degradation did not occur. However, the action of ammonia should be stronger than of only water and thus lead to a higher swelling and weakness of the wood structure [32]. Though, Pullanikat did not work with wood samples but pure carbohydrates molecules such as glucose. It must then be easier for the sugar molecule to be converted in small entities such as formates while in real wood, the solution has to penetrate within the cells, reach the layers rich in sugars and break down the long cellulosic polymer chains (*i.e.*, secondary wall) [24]. This may explain why a poor degradation of carbohydrates was observed with T4 protocol. Furthermore, mean values of R2 ratio, evaluating cellulose degradation, were similar to the ones of untreated T0 samples. Cellulose was then not affected by the alkaline conditions employed in T4 protocol. Holocellulose degradation was evaluated by comparing the bands at 1738 (xylan) and 1237 cm^{-1} (lignin/xylan) on the ATR-FTIR spectra after application of T4 protocol. It seemed than xylan (hemicellulose) and lignin were more affected. According to Kim et al [33], alkaline solution has the capacity to remove lignin content. Combined with hydrogen peroxide H_2O_2, the lignin removal is promoted by breaking the bonds between lignin and carbohydrates [33]. Though, previous analyses proved that lignin was not affected during T4 protocol. Even if holocellulose was degraded, chemometrics approaches discriminate T4 as an efficient protocol to model WAW as ATR-FTIR spectra of T4 and untreated (T0) samples clustered in PCA score plot.

Regarding natural wood degraders, the fungal degradation (T6) performed here was not as efficient as expected. Indeed, the capacity of some fungi, such as *Chaetomium globosum*, to degrade wood substrates is known [34]–[36]. *C. globosum* is a soft rot fungi able to degrade holocellulose into soluble carbohydrates through synergistic enzymes without affecting the lignin [34], [37]. Their hyphae (*i.e.*, long filamentous structure of fungi) can penetrate the wood vessels and so enhance the degradation in depth. Natural wood degradation is a slow process and even if T6 lasted for more than 5 months, ATR-FTIR ratios values of T6 and untreated (T0) samples were close. In addition, the vibrational bands at 1738 (xylan C=O stretching) and 898 cm^{-1} (cellulose C-H deformation) were still visible after T6 but less intense, indicating the fungal attack led to partial holocellulose degradation. Furthermore, T6-samples did not cluster with T0-samples on the PCA score plot based on the cellulose deformation (PC2). Thus, even if the mean values of ATR-FTIR ratios were close, T6 samples presented a certain degradation

respect to untreated samples (T0). PC2 that is based on the vibrational band at 898 cm^{-1} allowed to separate T6 samples (positive part of PC2) from the other samples (located in the negative part of PC2). This band was not used to calculate the ATR-FTIR ratios as reported by Dobrica though R2 ratio also evaluate cellulose degradation based on the band intensity at 1374 cm^{-1} (cellulose and xylan C-H deformation) [38]. Also, no significant difference was observed between R2 ratio of T0 and T6-samples based on ANOVA test ($p\text{-val} < 0.05$). The core of the samples was also investigated, as it is reported that the fungal attack occurred more within wood than at the surface [37]. However, ATR-FTIR spectra performed on wood sections and corresponding ratios revealed no degradation of carbohydrates inside T6 samples (Figure S 5). It seemed that cellulose degradation was induced by *C. globosum* but only superficially. Contrary to brown rot fungi that would degrade lignin, *C. globosum* could be used to replicate WAW but after evaluating an extended application time. Also, *C. globosum* may be allergenic for human health [39]. Therefore, a microbial safety cabinet would be needed for the manipulation of this fungi and required an additional autoclaving step to stop the fungal growth afterwards. Thereby, biological degradation may be more complicated to set in real praxis. This parameter should be considered for optimization of the protocol.

Therefore, based on the results obtained, the degradation protocols investigated could be classified from the more efficient to the less, as follow: T1 > T5 > T6 > T3 > T4 > T0. T6 was categorized are more efficient than T3 based on aesthetical criteria and colorimetric measurements.

In general, oak was more degraded than pine, as deduced from the wood composition analyses (Table S 3). Wood composition analyses also revealed that carbohydrates were more degraded with T6 protocol. However, only two samples per protocol were analyzed and the values obtained were not in agreement with that reported in literature, these data should thus be taken with prudence. In any case, the type of wood species seemed to impact the degradation of carbohydrates And it was previously stated than softwood could be generally more complex to decay than hardwood [25], [36]. Optimization of the parameters could therefore be required for pine and other softwood species, applying harsher conditions, such as higher vacuum or longer immersion time in the case of chemical degradation (T1, T3 and T5) [23]. In the case of biological degradation (T6) of softwood species, the addition of certain nutriments such as nitrogen N and phosphates PO_4^{3-} could be useful to ascertain an optimal growth of the fungi employed [36]. It seems that the degradation of the wood may be directly proportional to the concentration of these nutrients within the medium [36]. A possible alternative to degrade softwood would be a combination of chemical and biological protocols. In fact, it is known that cellulose is quite affected by strong acids [40]. Also, it is reported that chlorinated solution under acidic conditions could promote the growth of *C. globosum* on softwood [41]. We could plan to first immerse wood samples in an aqueous solution of HCl, presenting an acidic pH and free Cl^- ions and applying vacuum. Then, the pre-degraded wood samples could be exposed to fungi during few months.

So far, protocols T1, T5 and T6 were considered as the most promising protocols regarding the degradation of carbohydrates content. These protocols were then selected as first step towards obtaining model samples from fresh wood. The following step was the selection of a

contamination protocol to induce the presence of iron and sulfur species within pre-degraded wood samples.

Supplementary material 1

As for oak samples, some protocols altered the appearance of pine samples. However, their appearance is of a lighter hue respect to oak samples.

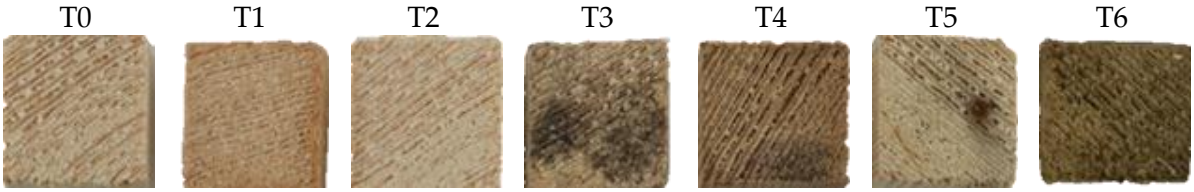

Figure S 1: Pine wood samples, either untreated (T0) or after degradation protocol (T1: H_2O+vacuum; T2: UV; T3: N_2+vacuum; T4: H_2O_2:NH_4OH; T5: T1+metal; T6: fungi)

Colorimetric coordinates of pine samples treated with T1, T3, T4, T5 and T6 protocols were far from untreated samples (T0) but also generally cluster on their own. Based on color variation, T3 and T4 pine samples were significantly similar (p-val < 0.05). This was not observed for oak wood. Therefore, the type of wood species may impact the degradation of carbohydrates. As oak samples, exposition of pine wood samples to UV lights did not induce significant color variation of the samples.

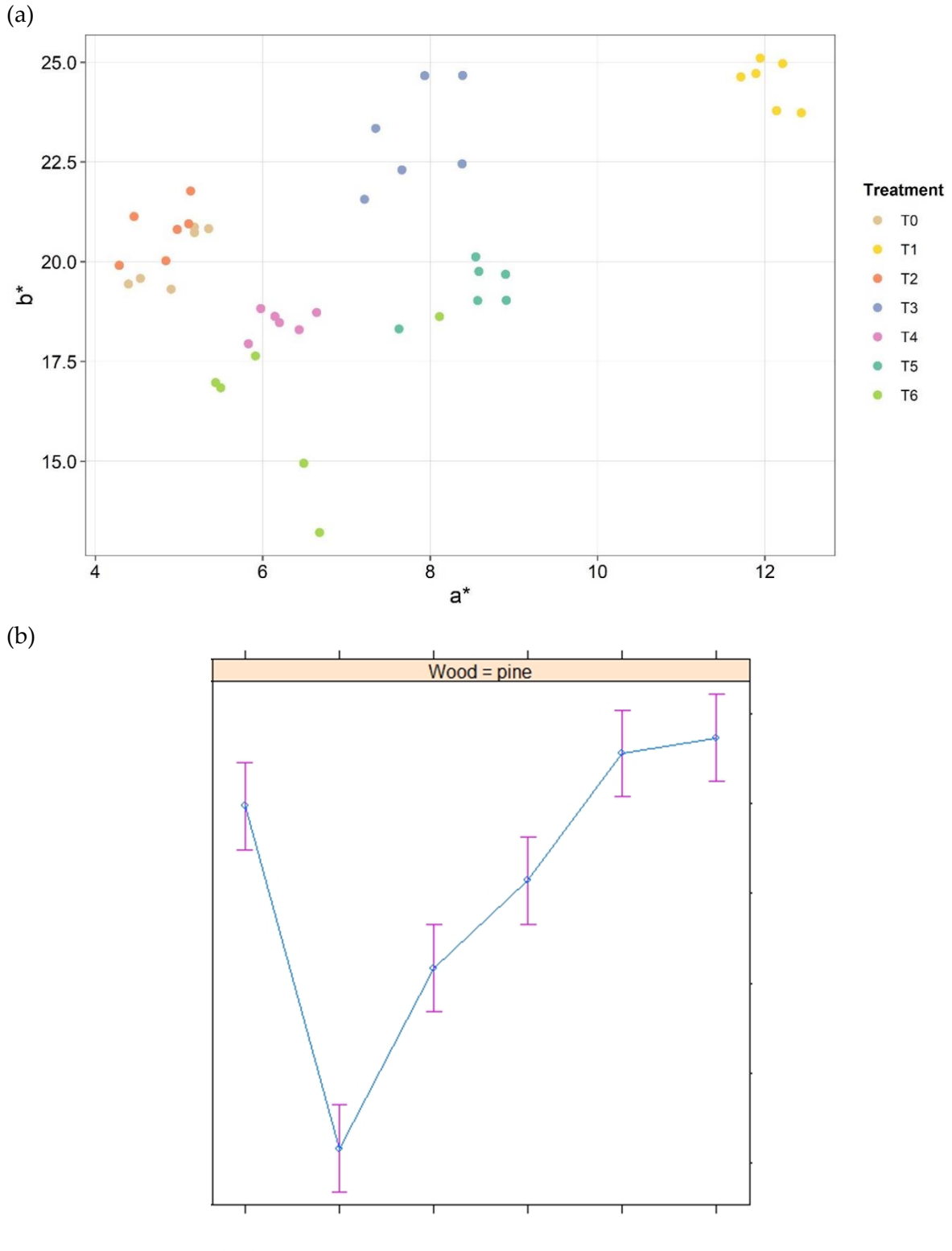

Figure S 2: (a) Colorimetric coordinates a and b* for pine untreated (T0) and degraded (T1-T6) wood samples. (b) ANOVA results of color variation (ΔE*) depending on degradation protocols (T1-T6) applied on pine wood samples*

Holocellulose seemed to be degraded as a decreased intensity of bands at 1738 (xylan C=O stretching) and 898 cm^{-1} (cellulose C-H deformation) was observed for T1, T3, T5 and T6-pine samples. T4 representative spectrum was more similar to T0 spectrum, as it was confirmed by PCA. The other chemical degradation protocols (T1, T3 and T5) all gathered in the same

cluster, in the positive part of PC1 (58% total of variability). As for oak samples, T6-samples clustered on their own in positive part of PC2 (21% total variability).

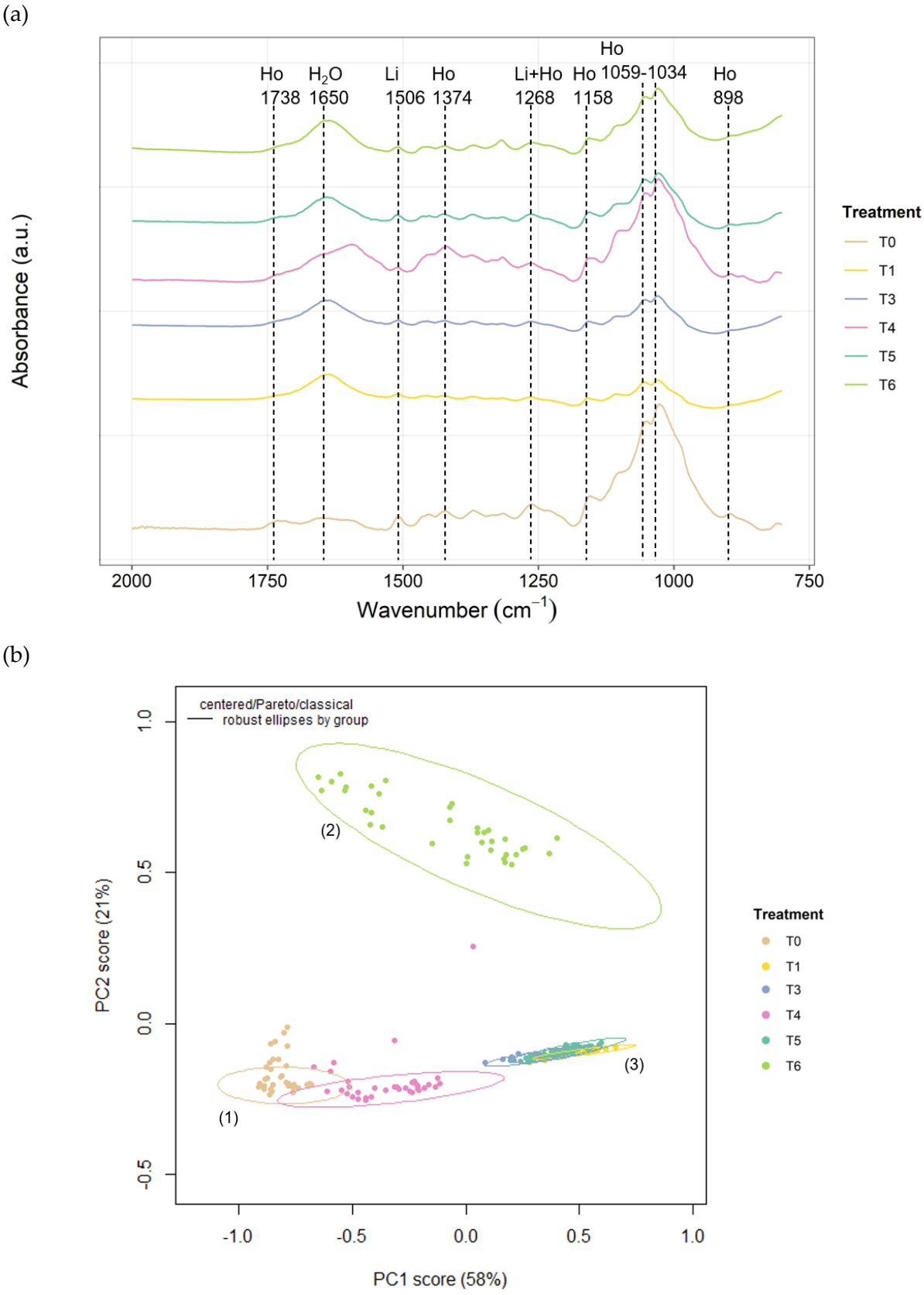

Figure S 3: (a)Representative ATR-FTIR spectra for pine untreated (T0) and degraded (T1-T6) samples with characteristic vibrational bands of holocellulose (Ho) and lignin (Li) indicated with dashed lines. (b) PCA score plot of ATR-FTIR spectra for untreated (T0) and degraded (T1-T6) pine samples.

The degradation protocols were classified from the most efficient to the less, according to the ratios mean values, as follows: T1 < T5 < T3 < T6 < T4 < T0. As for oak, the degradation protocols involving water immersion and vacuum seemed the most efficient protocols to degrade carbohydrates content.

Table S 1: ATR-FTIR ratios calculated for pine untreated (T0) and degraded (T1-T6) samples. Mean values of the ratios obtained on three plane sections are presented with the corresponding standard deviation indicated with brackets. R1 = I(1158)/I81506), R2 = I(1374)/I81506) and R3 = I(1034)/I(1506)

Wood species	Degradation protocol	R1	R2	R3
Pine	*T0*	1.34 (± 0.09)	1.11 (± 0.03)	3.02 (± 0.35)
	T1	0.93 (± 0.06)	0.95 (± 0.02)	1.40 (± 0.24)
	T3	1.03 (± 0.06)	0.98 (± 0.03)	1.84 (± 0.23)
	T4	1.26 (± 0.11)	1.11 (± 0.06)	2.87 (± 0.40)
	T5	0.98 (± 0.07)	0.99 (± 0.02)	1.61 (± 0.26)
	T6	1.15 (± 0.14)	1.02 (± 0.05)	2.36 (± 0.57)

ANOVA analyses performed on the three ATR-FTIR ratios showed that untreated (T0) and T4 (H_2O_2:NH_4OH) and T6 (fungi) samples were significantly similar, implying a poor degradation of carbohydrates. On the contrary, T1 (H_2O+vacuum), T3 (N_2/vacuum cycle) and T5 (T1+metal) samples were significantly different. In particular, T1 and T5-samples were the farthest from T0, suggesting that one-week water immersion under vacuum was the most efficient regarding degradation of carbohydrates.

(a)

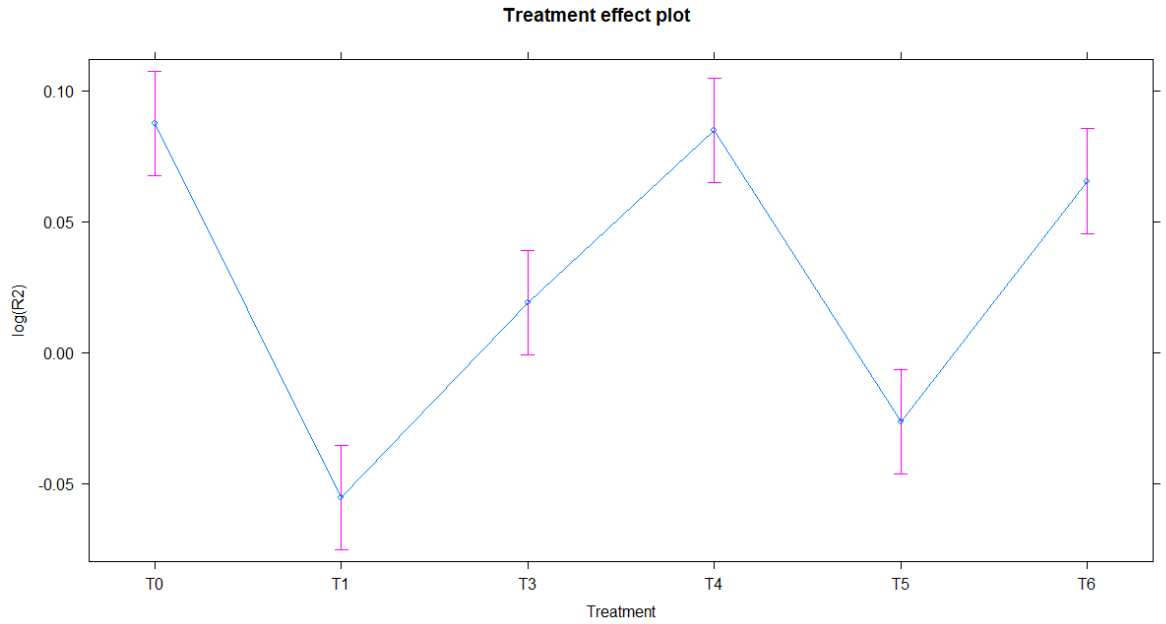

(b)

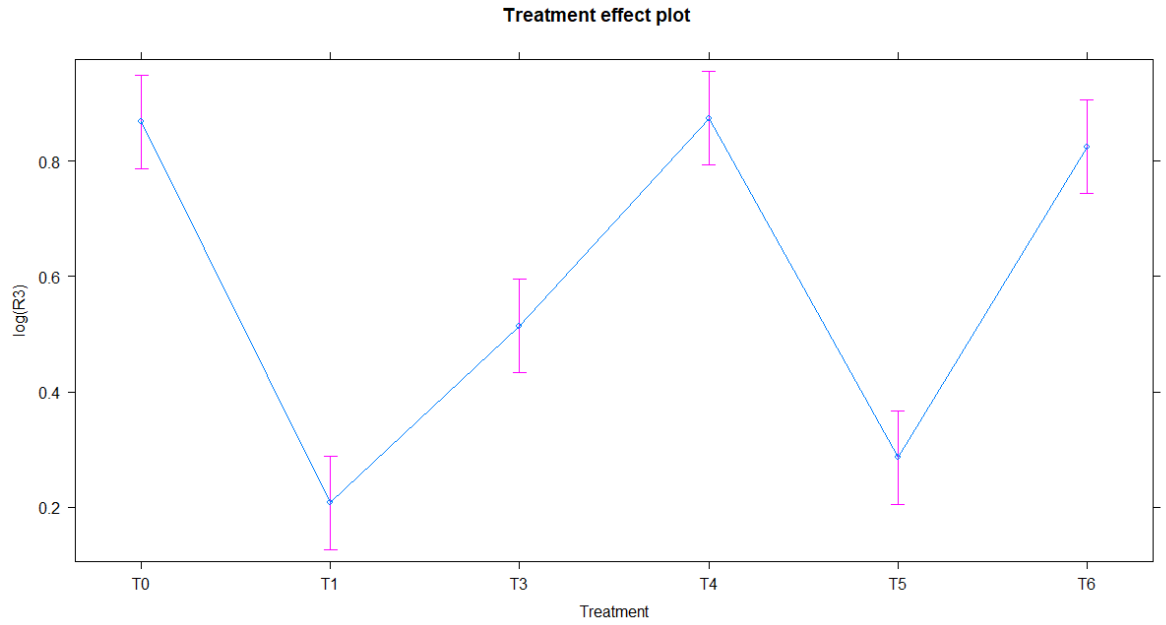

Figure S 4: ANOVA results of ATR-FTIR (a) R2 and (b) R3 ratios for untreated (T0) and degraded (T1-T6) wood samples

The variation before/after contamination was calculated for pine samples to evaluate the degradation of carbohydrates. According to the variations, the degradation protocols were ranked as follow, from the less degraded to the most: T4 > T6 > T3 > T5 > T1.

Table S 2: Mean variation of the ATR-FTIR ratios R1, R2 and R3 calculated on three plane sections after the application of the different degradation protocols T1-T3-T4-T5-T6 on pine wood samples, with standard error indicated in bracket

Degradation protocol	R1	R2	R3
T1-T0/T0	-30.9 (± 6.3)	-14.8 (± 2.6)	-53.0 (± 9.8)
T3-T0/T0	-22.7 (± 7.6)	-11.6 (± 2.9)	-38.1 (± 11.9)
T4-T0/T0	-6.0 (± 10.0)	-0.2 (± 5.2)	-3.7 (± 18.5)
T5-T0/T0	-26.9 (± 5.5)	-11.1 (± 4.1)	-46.5 (± 9.3)
T6-T0/T0	-13.2 (± 11.4)	-8.0 (± 4.3)	-19.1 (± 18.9)

Even if a degradation was observed at the surface of the wood samples, ATR-FTIR measurements of the samples core revealed that wood core was not degraded. Therefore, the degradation protocols efficient in degrading wood surface do not allow a degradation of the wood components in depth within the wood substrate.

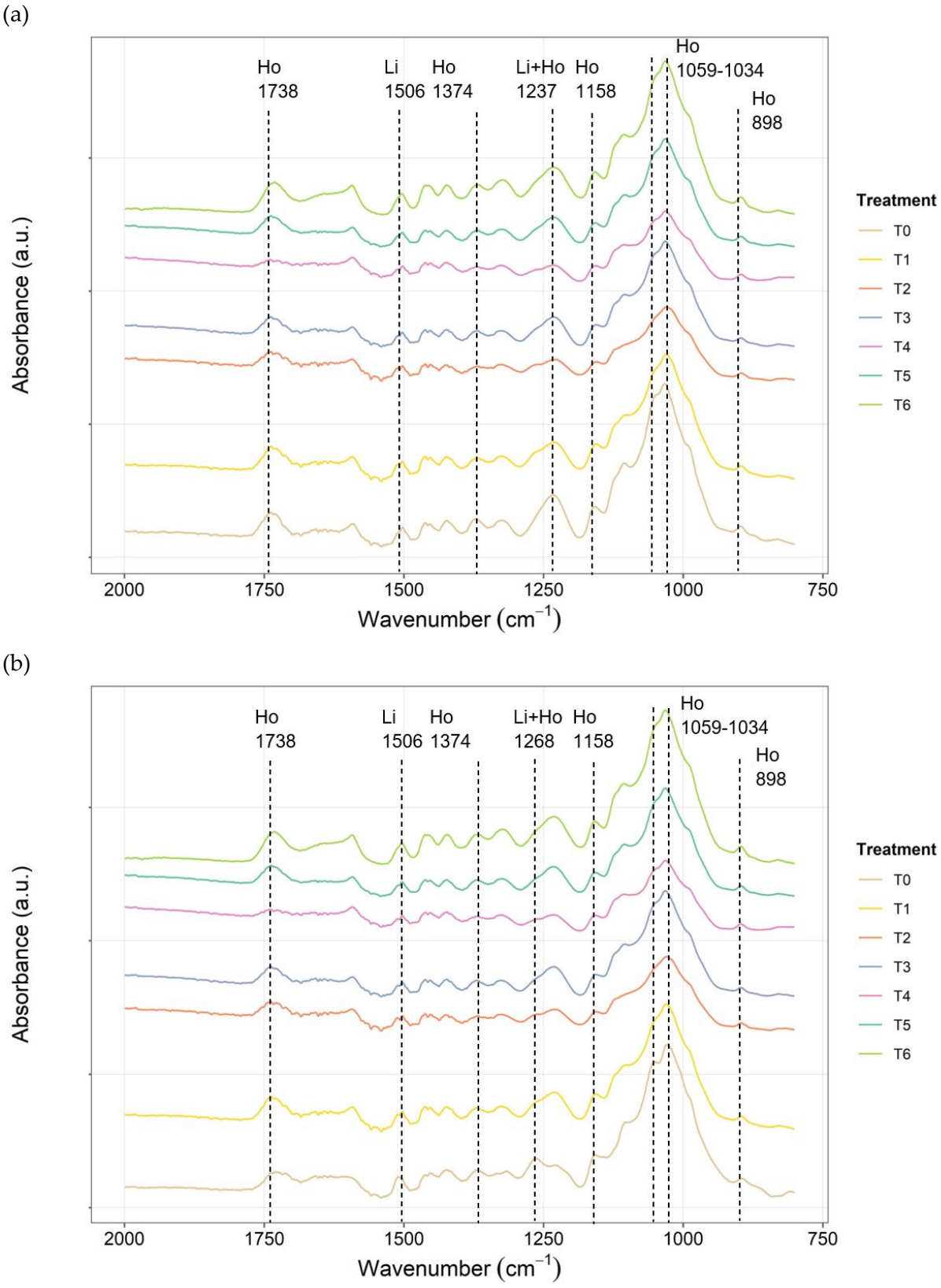

Figure S 5: Representative ATR-FTIR spectra of untreated (T0) and degraded (T1-T6) (a) oak and (b) pine core samples with characteristics vibrational bands of holocellulose (Ho) and lignin (Li) indicated with dashed lines

The samples were first oven-dried until constant weight. No collapse was observed, suggesting that the structure was not deeply affected by any degradation protocol. In general, lignin content (LC) was not affected by any protocol as all the values obtained were in the

same range of untreated T0 samples (Table S 2). Regarding cellulose content (CC) and holocellulose content (HC), T6 (fungi)-samples presented lower values than untreated (T0) samples. Thus, this protocol was considered more efficient to degrade the cellulosic part of fresh wood.

Table S 3: Percentage of lignin (LC), cellulose (CC) and holocellulose (HC) contents for untreated (T0) and degraded (T1, T3, T4, T5 and T6) oak and pine wood samples, with standard error indicated with brackets

Wood species	Degradation protocol	LC (%)	CC (%)	HC (%)
Oak	*T0*	40.0 (± 0.1)	36.4 (± 0.9)	39.7 (± 9.1)
	T1	42.9 (± 1.3)	35.4 (± 3.9)	42.4 (± 6.8)
	T3	54.7 (± 18.7)	30.6 (± 4.6)	42.2 (± 4.3)
	T5	72.2 (± 13.4)	37.5 (± 2.8)	41.4 (± 3.6)
	T6	43.2 (± 2.8)	24.2 (± 3.5)	31.1 (± 3.0)
Pine	*T0*	47.9 (± 12.1)	47.5 (± 3.7)	48.0 (± 0.4)
	T1	42.0 (± 5.8)	46.2 (± 4.8)	49.2 (± 0.3)
	T3	41.3 (± 6.6)	43.1 (± 4.6)	50.8 (± 5.4)
	T5	39.1 (± 3.4)	46.8 (± 7.2)	45.1 (± 1.6)
	T6	39.8 (± 1.0)	40.7 (± 1.3)	42.9 (± 1.4)

2.2 – Contamination protocols

2.2.1 – Proof of concept

Three contamination protocols based on literature study were first studied on raw balsa wood samples. The goal of this first step was to identify the compounds formed during the selected protocols before their application on artificially pre-degraded and naturally pre-degraded wood free of Fe and S to model WAW. These protocols were named impregnation protocol and labelled as IP.

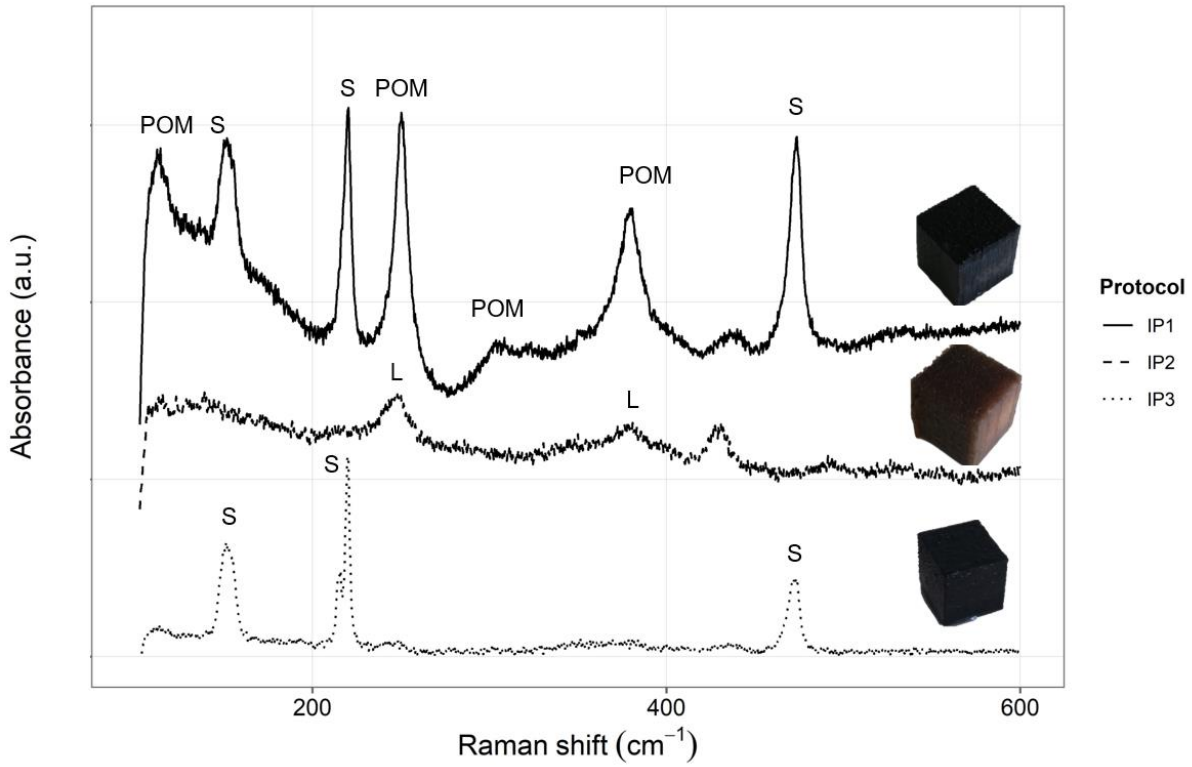

Figure 21: Representative Raman spectra of impregnated balsa samples (IP1 —, IP2 --- and IP3 ···) with characteristic bands labelled for partially oxidized mackinawite (POM), lepidocrocite (L) and sulfur (S) and embedded images of the samples for each impregnation protocol

For both IP1 and IP3, reduced sulfur compounds were identified by Raman spectroscopy (Figure 21). For IP1, the observed bands at 119, 247, 303 and 362 cm^{-1} cannot not be attributed to only mackinawite (FeS) or greigite (Fe_3S_4), but some bands could be attributed to both minerals [42]. It was then deduced that an intermediary phase named as partially oxidized mackinawite ($Fe_{1-x}S$, POM) was formed. Characteristic bands of elemental sulfur (S) at 152, 220 and 473 cm^{-1} were mainly identified on IP3 samples. For IP2 samples, only iron oxides were identified as lepidocrocite (L) with bands at 252, 379 and 530 cm^{-1} [43]. In terms of appearance, IP1 and IP3 protocols provided a black hue to wood while IP2 samples presented a brownish aspect, both present as natural hue on WAW artefacts [15].

ATR-FTIR spectroscopy was also carried out on the samples to evaluate wood degradation. Only the ratio R1 (I(1158)/I(1506)) was calculated, for this preliminary study. Values obtained are as reported in Table 12.

Table 12: Mean ATR-FTIR ratio values R1 = I(1158)/I(1506) for balsa untreated (T0) or contaminated (IP1-IP3) wood samples, with standard deviation indicated between brackets

Contamination protocol	R1
T0	2.67 (± 0.37)
IP1	1.41 (± 0.14)
IP2	4.45 (± 0.50)
IP3	1.55 (± 0.09)

It resulted that, in addition to form reduced sulfur compounds, IP1 and IP3 also degraded holocellulose content with respective R1 value (1.41 and 1.55) lower than the R1 value = 2.67 for untreated (T0) samples. On the contrary, IP2 tended to decay lignin content as R1 value (R1 = 4.45) was higher compared to T0 value. Given these promising results obtained in terms of iron sulfides formation and cellulosic content degradation, IP1 protocol was selected to pursuit the preparation of model samples as it formed partially oxidized mackinawite ($Fe_{1-x}S$, POM) compounds as well as inducing more degradation of carbohydrates.

2.2.2 – Contamination of artificially pre-degraded fresh wood

IP1 protocol was applied on fresh wood samples previously degraded with T1, T5, and T6-protocols. Untreated (T0) fresh oak and pine samples were also contaminated with IP1, to evaluate IP1 impact on raw wood.

2.2.2.1. Appearance and colorimetry

After application of IP1, oak samples were photographed. They all presented a dark hue, similar to the one observed on balsa wood samples and gathered with pine samples in the same part of the CIELab color space ,whatever the degradation protocol (T1-T5-T6) applied previously (Figure 22a). Also, it appeared that the type of wood species may not affect the final appearance after impregnation as the colorimetric coordinates a* and b* were similar for oak and pine samples (Figure S 6a).

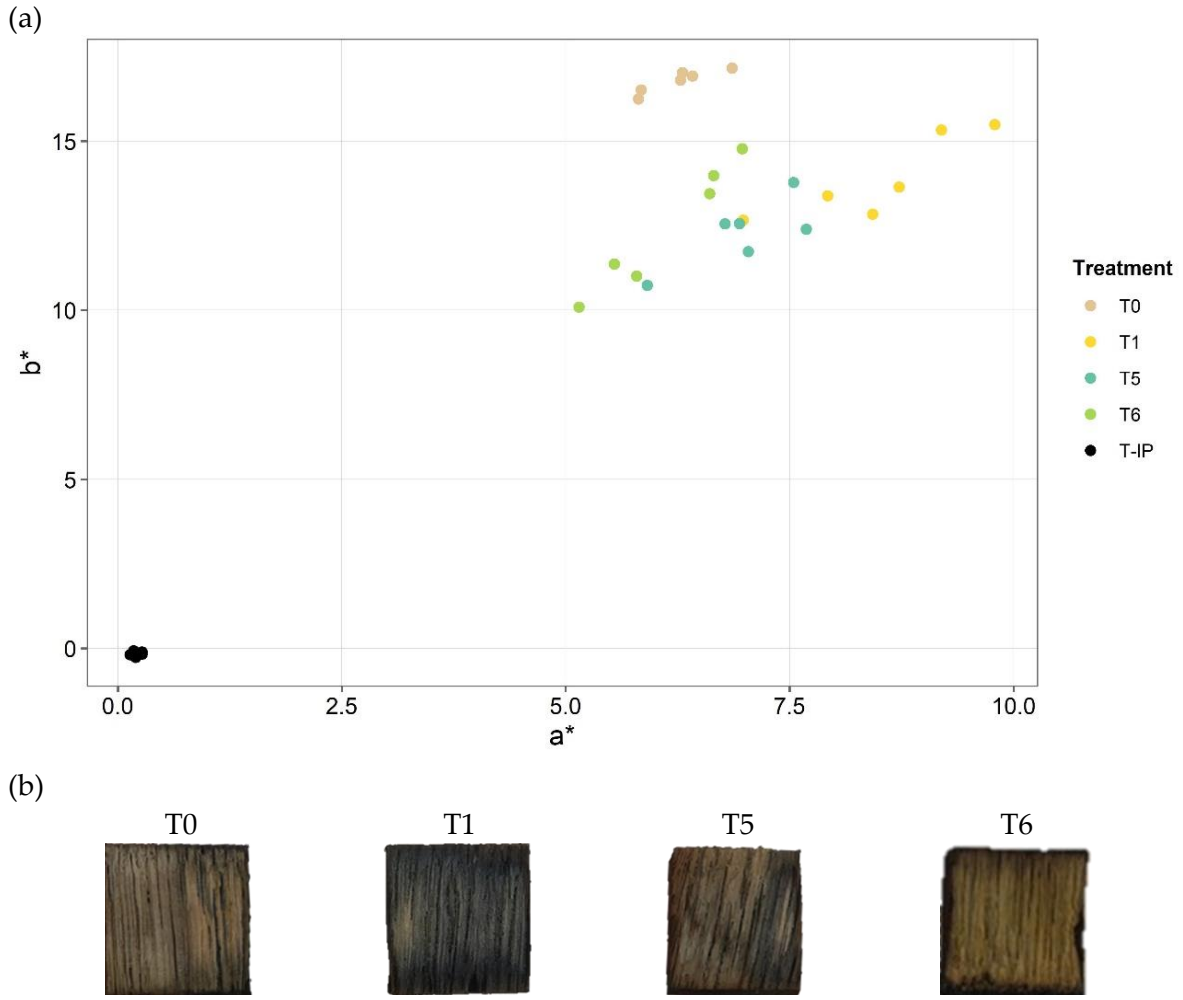

Figure 22: (a) Colorimetric coordinates a and b* for oak untreated (T0), degraded (T1-T5-T6) and contaminated (IP) wood samples. (b) Core Tg plane section of contaminated untreated (T0) and degraded (T1-T5-T6) oak wood samples after impregnation with IP1 protocol*

The samples were cut following tangential Tg plane section to evaluate the depth of efficiency of IP1 depending on the degradation protocol (T1-T5-T6) applied previously. One can observe that all oak samples were completely contaminated till the core. A different behavior was observed for pine with only T6 (fungi)-treated pine samples showing a complete darker aspect after impregnation (Figure S 6b). This suggested that the diffusion of impregnation reagents may be different according to the type of wood species treated, as wood cell structures differ between hard- and softwood. In fact, tracheids are present on softwood and observed on Tv plane section and provide the conductive and mechanical functions of to the softwood [24]. The water flowing through these tracheids takes a sinuous path to go from one cell to another, passing wood cells that are resistant to water [16]. Due to the difference in the wood structure, the artificial contamination solution can penetrate more easily oak (hardwood) than pinewood (softwood). Why only T6 pine samples seemed to be as impregnated as oak could be explained by the degraded cellulosic content present in these samples and observed in the previous section regarding the definition of a degradation protocol. In fact, investigation of degraded samples showed that T6 samples presented a lower holocellulose content after T6 degradation protocol being applied, suggesting that some cell walls may have been thus degraded and allowed the impregnation solution to penetrate deeper in the wood substrate. In order to

achieve a full impregnation of the other pre-degraded pine samples, one can modify the experimental conditions with prolonged immersion.

2.2.2.3 – Raman spectroscopy

An identification of compounds formed after the application of IP1 on oak and pine samples was performed.

Compared to contaminated balsa with IP1, a similar appearance was observed. However, the compound identified on oak samples differed from the one identified on pine samples. The representative Raman spectra obtained are illustrated in Figure 23 and Figure S 7.

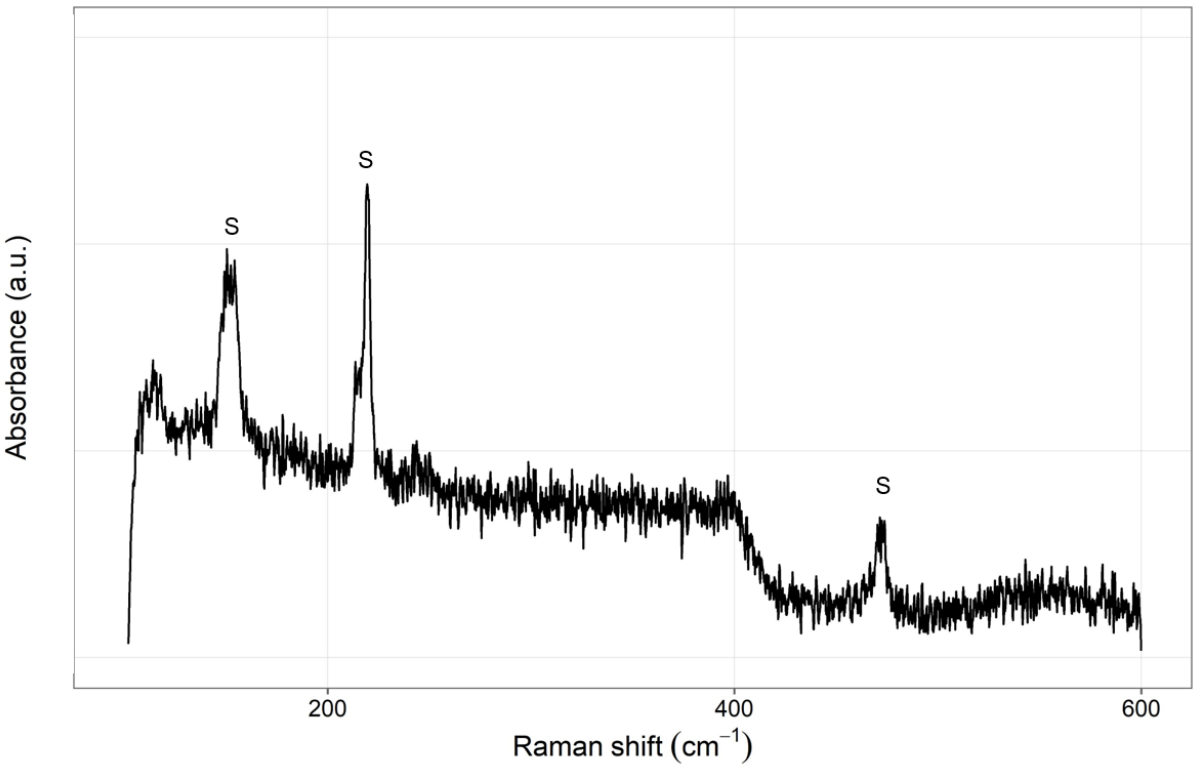

Figure 23: Representative Raman spectrum of compounds identified at the surface of oak samples with bands of elemental sulfur (S) indicated

The same compounds were identified within each oak or pine sample set, independently of the previous degradation protocol applied showing the versatility of the IP1 impregnation protocol. Concerning oak, only elemental sulfur α-S_8 was identified at the surface with its characteristic bands at 152, 220 and 473 cm^{-1} [17], [42], [44]. The precipitation of α-S_8 at the surface of oak wood could be explained by the wood composition. Indeed, even if hardwood present less extractives than softwood, the large presence of tannins may interfere with the formation of iron sulfides [40]. Indeed, tannins were released during T1 (H_2O+vacuum) and T5 (T1+metal) degradation protocols, with mean value of 12.9 mg/l (± 0.4) for oak and 3.1 mg/l (± 0.1) for pine. It is well known that tannins react with iron to form iron-tannins complexes, as observed on paper objects [45], [46]. If tannins were liberated during previous T1 and T5 degradation protocols, most probably they were also released during IP1, which also includes an immersion step. In particular, tannins could react with Fe^{2+} ions coming from the

$FeCl_2 \cdot 4H_2O$ 0.5 M solution employed in IP1. However, Fe^{2+}-tannin complexes are colorless and their formation may not be rapidly detected during IP1 [47].

Raman analyses carried out on the core of the samples revealed that the compounds formed only at the surface of the samples and not in depth. Therefore, by optimizing the degradation of holocellulose content, the contamination reagents could penetrate deeper and completely contaminated the samples. However, no pyrite was observed after application of IP1.

Some reasons may explain why pyrite was not identified during Raman analyses. In fact, few spectra were recorded at the center of three faces of the samples and the narrow area analyzed may not contain all compounds being present on the wood samples. To remediate to this drawback, Raman mapping could then be considered to investigate larger areas. Also, it is known that the intensity of pyrite Raman shifts are quite low compared to mackinawite [17]. This can be showed on reference spectra collected on synthetized mackinawite and natural pyrite with the same parameters (Figure 24). One can observe that the characteristic bands of pyrite, at 344 and 379 cm^{-1} are of weak intensity respect to the bands corresponding to synthetized mackinawite. In case pyrite and mackinawite would be associated in wood, these bands assigned to pyrite would be overlapped with the broad band at 360 cm^{-1} of mackinawite. Therefore, identifying pyrite in presence of mackinawite may be difficult to achieve by Raman spectroscopy.

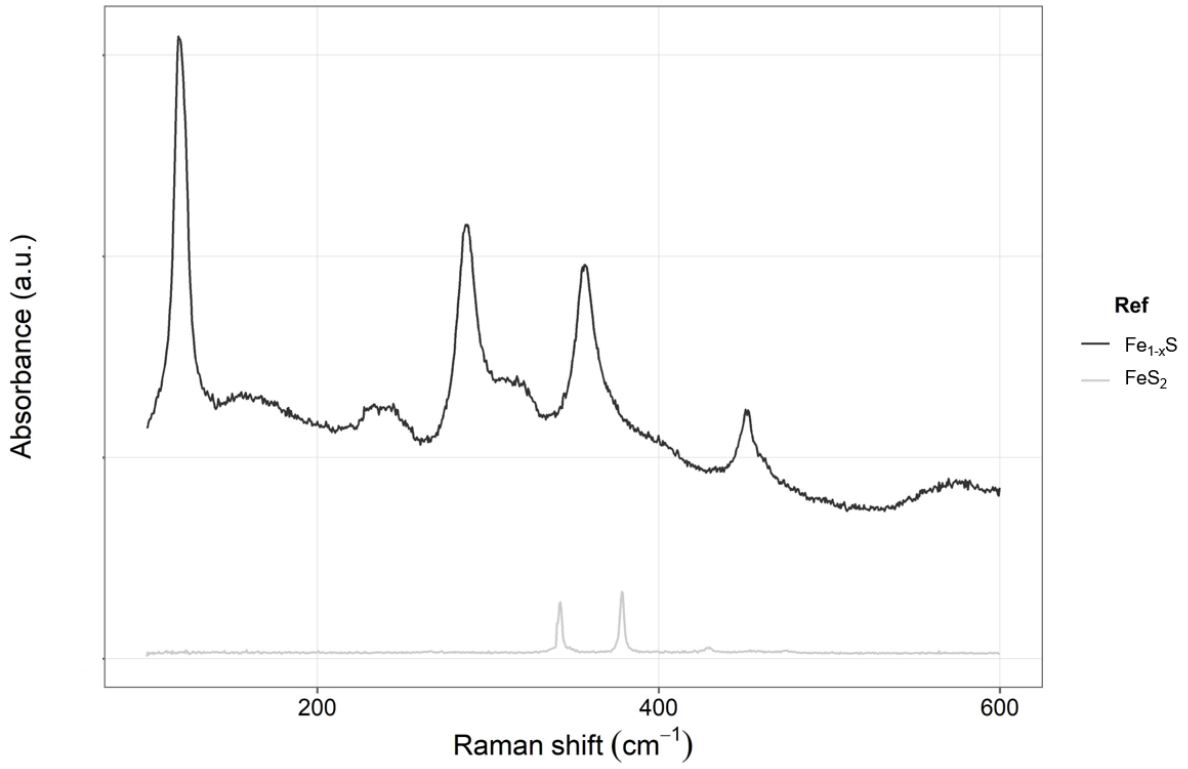

Figure 24: Raman spectra of synthetized mackinawite ($Fe_{1-x}S$, black) and mineral pyrite (FeS_2, grey)

However, many WAW artefacts are mainly made of oak [4], [48]–[50]. Thus, optimization of IP1 should be performed for oak and any hardwood species. As even water immersed wood seemed to released tannins, a primary step could be to dissolve all tannins and extractives in

general, by immersion in cold water and renew the baths until tannin concentration is constant [24], [51]. In fact, the release of tannins is described as an indicator of wood degradation [52]. Their extraction from fresh wood appears then necessary to properly replicate the characteristics of WAW artefacts and favorize the formation of iron sulfides. In addition, not pure FeS was formed and no FeS_2 were identified at the end of IP1 protocol. Adjusting the concentration of $Na_2S{\cdot}9H_2O$ and of $FeCl_2{\cdot}4H_2O$ solution could be a starting point to form the latter phase and optimization perform to precipitate pure FeS [17].

2.2.2.4 – ATR-FTIR spectroscopy

ATR-FTIR spectroscopy analyses were performed on fresh oak and pine wood as R1 ratio on balsa (proof of concept section) showed that IP1 led to holocellulose degradation.

Spectra were recorded at the surface of the contaminated samples and were compared to spectra of the pre-degraded samples prior application of IP1.

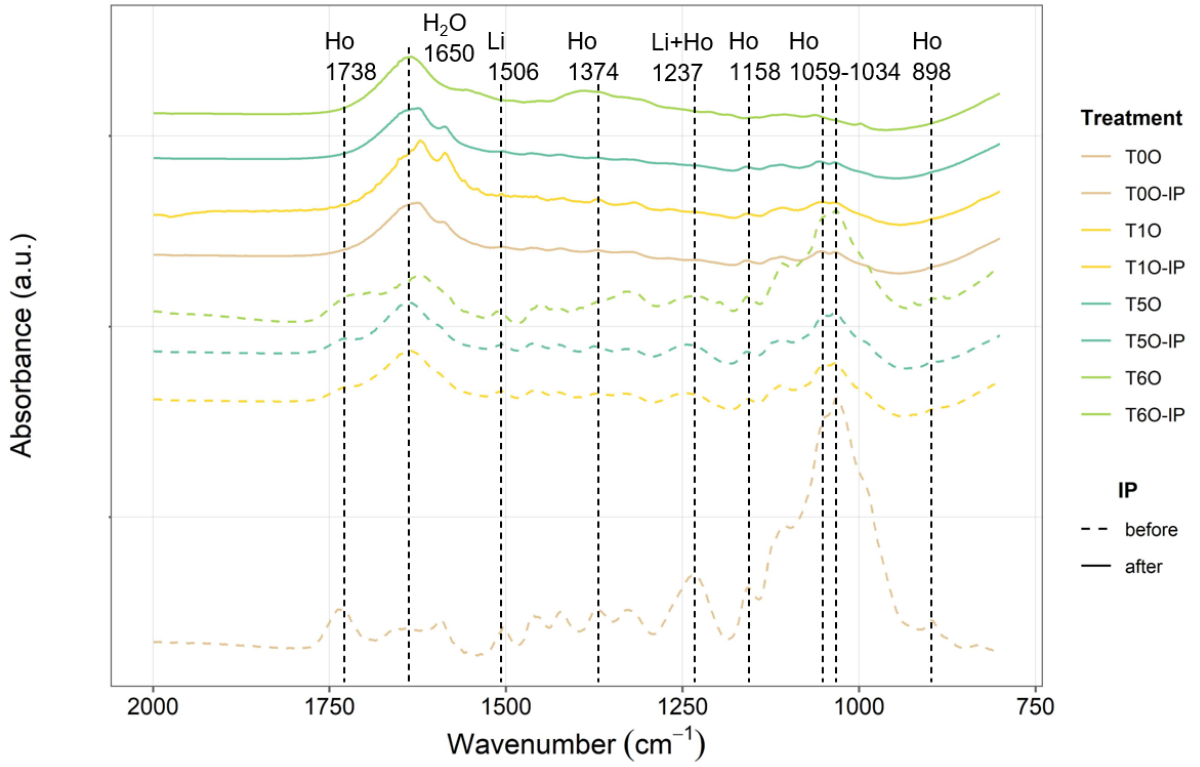

Figure 25: Representative ATR-FTIR spectra for untreated (T0), degraded (T1, T5, T6) and contaminated (IP) oak wood samples with characteristics vibrational bands of holocellulose (Ho) and lignin (Li) indicated with dashed lines

As for balsa wood, the effect of IP1 led to structural modifications. Indeed, after IP1, all the wood-assigned bands in the range 1400-1000 cm^{-1} decreased in intensity suggesting that the application of IP1 led to the degradation of the carbohydrates content. Figure 25 showed that for oak, whatever the previous degradation protocols applied, the intensities of the bands at 1034, 1059 and 1158 cm^{-1} decreased. Especially, the two bands at 1034 and 1059 cm^{-1}, assigned to holocellulose and that were very intense for untreated (T0), were not visible anymore after impregnation (solid-line spectra) [7], [8]. IP1 application affected thus the carbohydrates content by degrading holocellulose content. In addition, the vibrational band at 1738 cm^{-1} (xylan C=O stretching) also disappeared from the spectra after impregnation. Xylan was then

degraded by IP1. In addition to degradation of carbohydrates, the vibrational bands at 1237 and 1268 cm^{-1}, assigned to lignin content, also decreased in intensities after IP1. The application of IP1 may then led to the degradation of the lignin content as well as holocellulose content. Similar results were observed for pine samples (Supplementary material 2, Figure S 8). To ascertain wood degradation, ATR-FTIR ratios were also calculated. From these ratios, the variation before/after contamination was calculated according to the formula $\frac{Rb-Ra}{Rb} \times 100$ with Rb the ATR-FTIR ratios (R1, R2, R3) before contamination protocol and Ra the ATR-FTIR ratios after contamination protocol. The variation values for oak samples are reported in Table 13 and for pine samples in Table S 4.

Table 13: Mean variation within the ATR-FTIR ratios before and after application of contamination protocol IP1 on untreated (T0) and pre-degraded (T1-T5-T6) oak wood samples. R1 = I(1158)/I(1506); R2 = I(1374)/I(1506); R3 = I(1034)/I(1506).

Degradation protocol	**Oak**		
	R1	*R2*	*R3*
T0	-42.8 (± 5.1)	-21.5 (± 3.0)	-70.6 (± 5.6)
T1	-8.3 (± 5.6)	-4.66 (± 2.7)	-21.5 (± 17.3)
T5	-13.6 (± 4.9)	-8.4 (± 3.1)	-40.8 (± 11.7)
T6	-39.4 (± 3.9)	-3.5 (± 3.3)	-70.2 (± 4.2)

One can observe that important variations were obtained for untreated (T0) and biologically degraded (T6) samples after application of IP1. Regarding R1 (holocellulose degradation), the variation was in the range of 30-45%, implying that holocellulose content was degraded after application of IP1. On the contrary, the range was between 8-15% for T1 (H_2O+vacuum) and T5 (T1+metal). Even if partial holocellulose degradation occurred after IP1 for samples previously degraded with T1 and T5, most of them were already degraded before IP1. R3 ratio, also evaluating holocellulose decay, presented the highest variation among the different ratios calculated, around 70% for T0- and T6-oak samples and between 55-60% for the corresponding T0- and T6- pine samples. Once again, the variation for T1 and T5 was lower confirming the previous statement that these two protocols have already degraded carbohydrates before application of IP1. Concerning R2, which evaluates cellulose degradation, the variation was the lowest whatever the degradation protocol applied previously (T1, T5, T6). Only previously untreated samples (T0) presented variation values around 20% after IP1, suggesting that IP1 can be employed for both contamination and degradation purpose. Indeed, it was demonstrated that iron can catalyze cellulose degradation [29]. The degradation occurs through the Fenton reaction (equation (1)):

$$Fe^{2+} + H_2O_2 \rightarrow Fe^{3+} + HO^{\cdot} + HO^{-} \quad (1)$$

In fact, the first step of IP1 is an immersion in $FeCl_2{\cdot}4H_2O$ 0.5 M solution. Many studies regarding model WAW samples include a step with samples immersed in ferrous solution

[48], [53], [54]. It seemed then here that this immersion step in $FeCl_2 \cdot 4H_2O$ 0.5 M could lead to degradation of carbohydrates. While penetrating the wood cells, the solution may react with the cellulose content and enhanced its degradation. Wood composition was also determined after impregnation on two samples for each degradation protocol previously applied to ascertain that IP1 could be considered as degradation protocol as well. It resulted that holocellulose content (hemicellulose and cellulose) was slightly affected after contamination with IP1 (Figure S 9a and Figure S 9b). However, ATR-FTIR analyses were performed at the samples surface and are not sufficient to evaluate the depth efficiency of a treatment, as demonstrated with the ATR-FTIR results obtained on core sections and presented above (supplementary material 2 Figure S 5). Examination of lignin content (LC) also showed a decrease of LC after IP1 (Figure S 9c). However, ANOVA analysis revealed that the decrease of holocellulose and lignin content was not significant (p-val > 0.05). Thereby, IP1 could be considered as a contamination protocol but not as degradation protocol.

2.2.3 - Contamination of naturally pre-degraded wood

Neolithic oak (set C) and lake pine (set F) were employed as naturally degraded wood substrate to produce model samples simulating WAW. These samples were investigated as fresh wood artificially degraded and contaminated were not sufficient to properly model WAW artefacts. These sets were impregnated with the contamination protocol IP1 that was selected based on the contamination experiment conducted on fresh oak and pine presented above. A characterization campaign was carried out to ascertain sets C and F could be effective model samples for WAW.

2.2.3.1 – Appearance and colorimetry

The visual appearance of the sets C and F samples was first compared before and after the application of IP1.

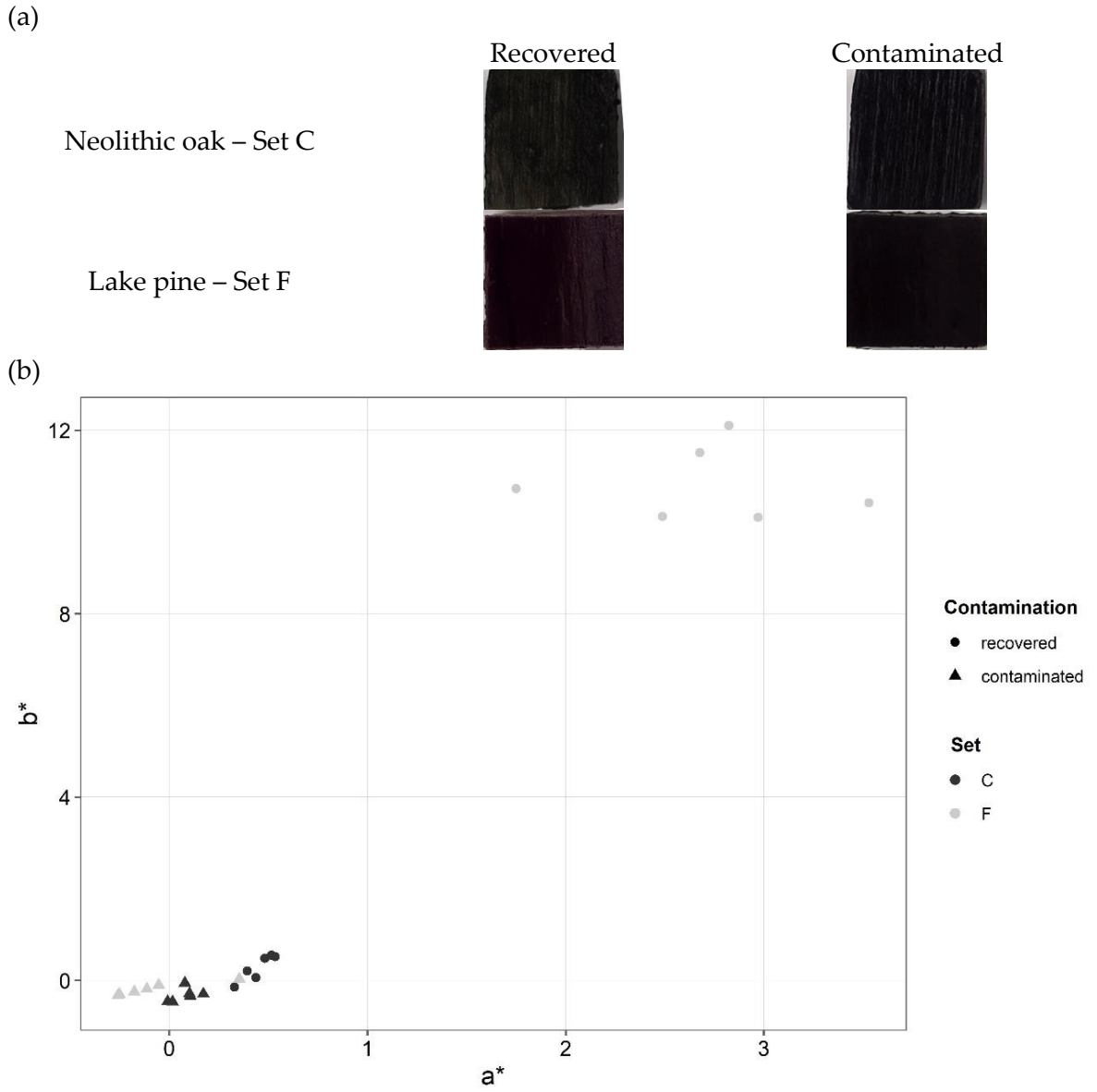

Figure 26: (a) Appearance of Neolithic oak (set C) and lake pine (Set F) when recovered and after contamination with IP1. (b) Colorimetric coordinates a and b* for Neolithic oak (set C, black) and lake pine (Set F, grey) when recovered (●) and after contamination with IP1 (▲)*

When recovered, Neolithic oak (set C) presented a dark appearance as described in literature [1]. Lake pine (set F) was of a lighter hue than set C samples (Figure 26a). This may come from the different type of wood species and burial time. Indeed, set C samples were dated from 2753 BC while set F samples are originated from 1878 AC. As set C remained underwater for a longer period of time more degradation could have occurred. Plotting a* and b* colorimetric coordinates confirmed the difference of hue between set C and set F samples when recovered (Figure 26b squares).

After contamination with IP1, set C samples remained very dark while set F samples were slightly darker than before impregnation. Colorimetric coordinates showed that sets C and F samples gathered after IP1 application (Figure 26b triangles). One can observe that set C samples before and after IP1 application were in the same part of the score plot (black squares

and triangles), implying that IP1 did not alter drastically the appearance and natural hue of ancient oak, obtained after a prolonged burial time.

2.2.3.2 – State of conservation
ATR-FTIR spectroscopy

As for fresh oak and pine samples, ATR-FTIR spectroscopy was performed on sets C and F samples surface.

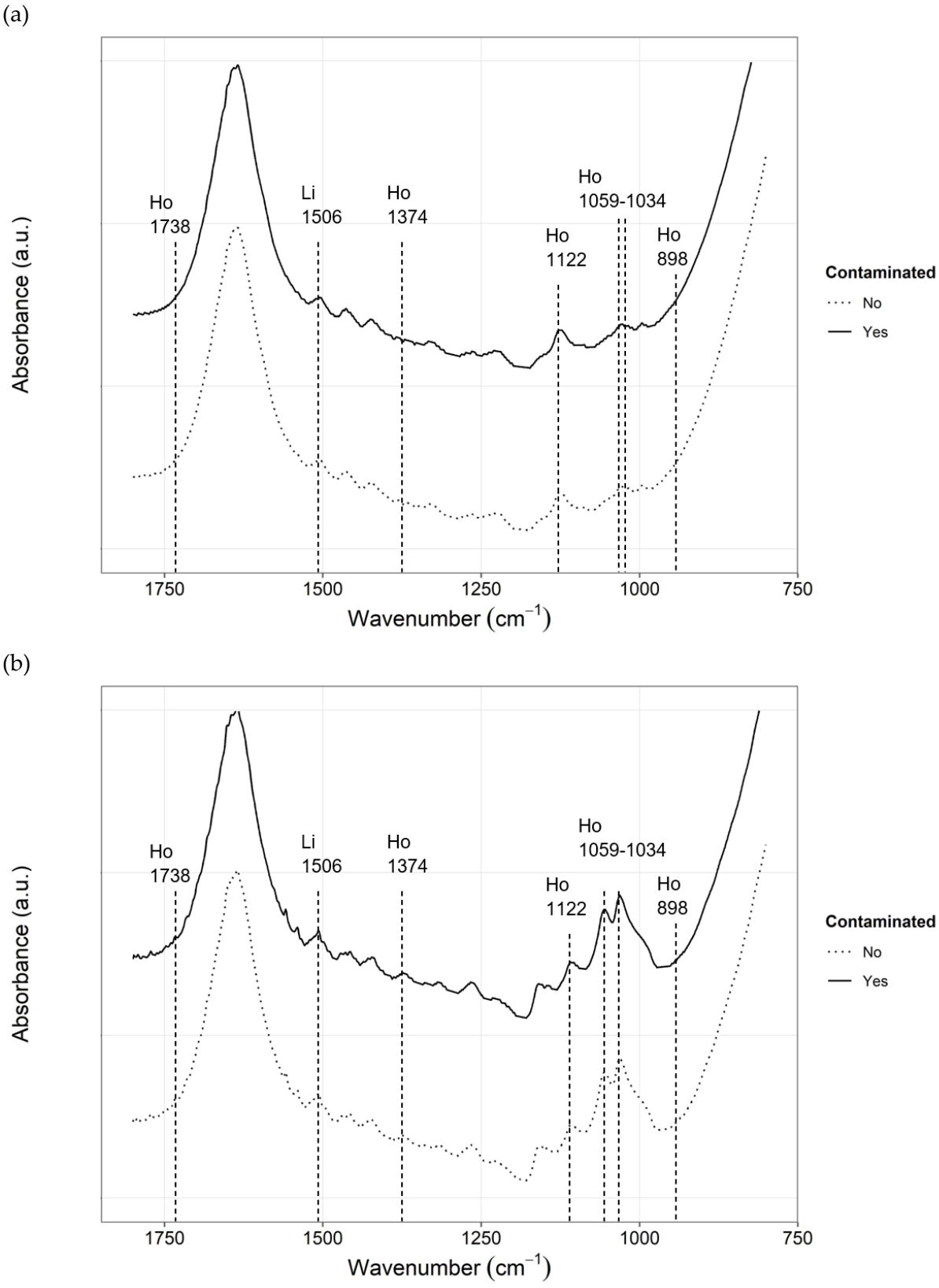

Figure 27: Representative ATR-FTIR of (a) Neolithic oak (set C) and (b) lake pine (set F) samples before (···) and after (—) contamination with IP1 with characteristic vibrational bands of holocellulose (Ho) and lignin (Li) indicated with dashed lines

Recovered samples showed different state of conservation. Neolithic oak (set C) presented less intense vibrational bands at 1034 and 1059 cm^{-1}, assigned to holocellulose C-O stretching, implying that the holocellulose content was more altered for the oak pole than pine board

(Figure 27, solid spectra). Such difference may provide from the different burial time of the two sets. Yet, none of the recovered wood presented a band at 1738 cm^{-1}, assigned to xylan content [4], [7]. Therefore, hemicellulose content was affected for Neolithic oak (set C) and lake pine (set F). In addition, the vibrational band at 1374 cm^{-1}, assigned to cellulose content, was not visible for set C [4]. This implies that all the cellulose content was degraded for the Neolithic oak, as validated by the absence of the vibrational band at 898 cm^{-1}, also assigned to cellulose [5]. The cellulose degradation is also highlighted by the relative intense band present at 1112 cm^{-1} and assigned to lignin content [6]. That was not observed for spectra collected on set F, where the band at 1112 cm^{-1} was not present. After application of IP1, ATR-FTIR spectra were similar to the ones before contamination (Figure 27, solid-line spectra). As previously stated, IP1 can only be regarded as contamination protocol. No degradation of carbohydrates was expected on Neolithic oak and lake pine after application of IP1. ATR-FTIR ratios were calculated on three samples per set and on the three plane sections. Mean values are reported in Table 14.

Table 14: ATR-FTIR mean ratios calculated for Neolithic oak (set C) and lake pine (set F) recovered and contaminated samples, with standard deviation indicated in brackets. R1 = I(1158)/I81506), R2 = I(1374)/I81506) and R3 = I(1034)/I(1506)

Samples		R1	R2	R3
Neolithic oak	*Recovered*	0.87 (± 0.02)	0.91 (± 0.01)	0.95 (± 0.05)
(set C)	*Contaminated*	0.90 (± 0.01)	0.92 (± 0.01)	0.99 (± 0.03)
Lake pine	*Recovered*	0.97 (± 0.08)	0.95 (± 0.03)	1.32 (± 0.33)
(set F)	*Contaminated*	0.98 (± 0.06)	0.95 (± 0.02)	1.27 (± 0.26)

The ATR-FTIR mean ratios confirmed the innocuousness of IP1 regarding wood material as all the calculated mean ratios were in the same range, before and after contamination with IP1. This is in line with the previous results obtained with ATR-FTIR spectra and for fresh wood Even if set F (lake pine) samples did not remain underwater as long as set C (Neolithic oak) samples, it seemed that most of the carbohydrates content degraded during burial. No or very little differences were observed between ATR-FTIR mean ratios of recovered and contaminated samples (Table 14). However, one can observed that the mean ratios of Neolithic oak (set C) tended to be lower than the ones of fresh oak (Table 10) as lake pine (set F) ratios were lower than the ones of fresh pine (Table S 1). It seemed then that the burial time affected the degradation of carbohydrates: when wood remained for a longer period of time in their burial environment, more decay can be induced. The state of conservation could also be due to the type of wood species. For instance, Hedges et al [55] demonstrated that spruce (*Picea* sp.) and alder (*Alnus* sp.) buried for the same period of time in the same site presented different degree of degradation. The former was softwood while the latter hardwood. This study highlighted that the type of wood structure affected the decay processes. Both these parameters (type of wood species and burial time) may explain the differences between the ATR-FTIR ratios.

Maximum water content

In addition, the maximum water content (MWC) was calculated. This characterization method is commonly used to quantify wood degradation [11]. The samples were then classified into five ranks to determine their state of conservation. MWC measurements validated previous ATR-FTIR observations and that set C (Neolithic oak) is more degraded than set F (lake pine). Indeed, set C was categorized in rank 4, the highest possible, while set F fell in rank 2 (Table 15). According to literature, set F samples only presented an initial decay and indeed are in the same rank as fresh oak (set B). Also, fresh pine (set E) was classified in rank 1, defined with a low state of degradation.

Table 15: Wood degradation ranks for artificially degraded (set B and set E) and naturally degraded (set C and set F) samples based on maximum water content (MWC) measurements.0: decay absent; 1: low decay; 2: initial decay; 3: high decay; 4: important decay

Samples	Rank
Set B – Fresh oak model sample	2
Set C – Naturally degraded oak model sample	4
Set E – Fresh pine model sample	1
Set F – Naturally degraded pine mode sample	2

Raman spectroscopy

As for fresh wood, Raman spectroscopy was performed to identify the compounds formed during the contamination protocol IP1. The spectra before and after contamination are presented in Figure 28.

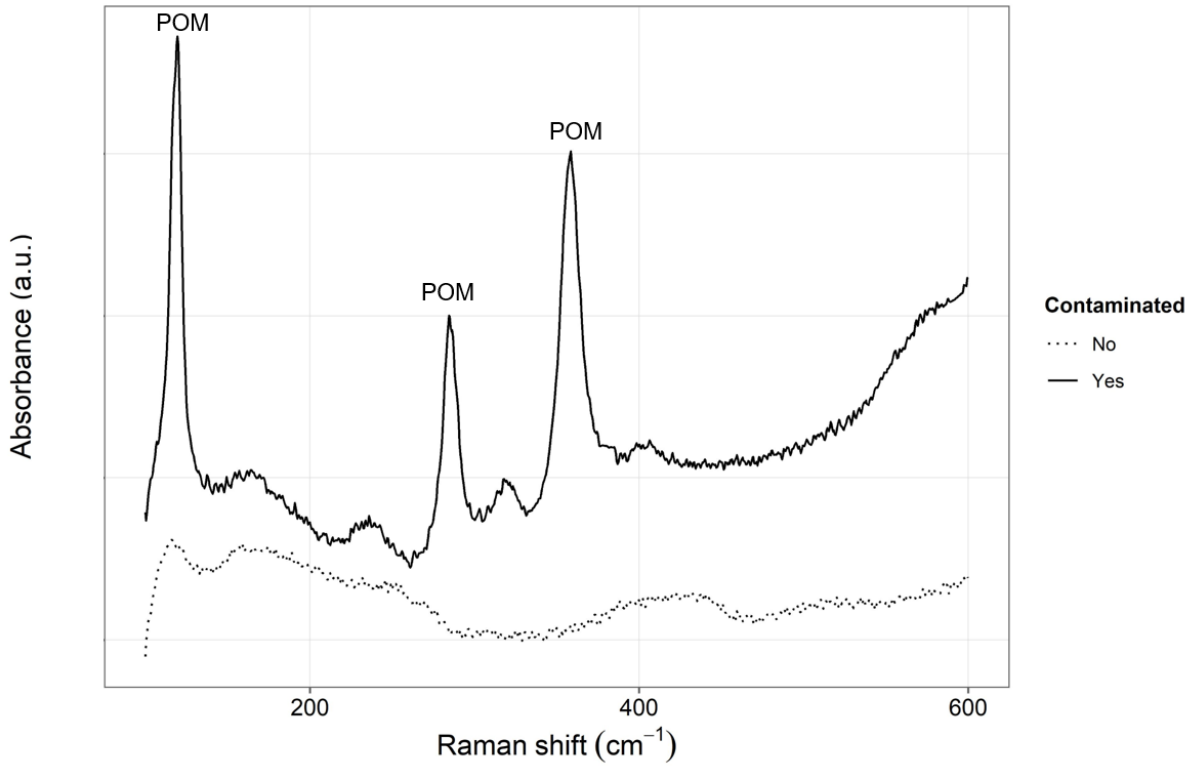

Figure 28: Representative Raman spectra of model samples before (···) and after (—) contamination with IP1 with characteristic partially oxidized mackinawite ($Fe_{1-x}S$, POM) vibrational bands

Before contamination, we ascertained that sets C and F were not contaminated with iron sulfides. Corresponding Raman spectra presented some bands at 1270, 1330 and 1480 cm^{-1} that were identified and assigned to wood components [14]. However, no bands that could be attributed to iron or sulfur species, were visible in the range 100-600 cm^{-1} (Figure 28 dashed-line spectrum).

After application of IP1, bands at 119, 282 and 363 cm^{-1} were observed, as it was the case for balsa and pine wood above (sections proof of concept and contamination of artificially pre-degraded samples). This suggested that partially oxidized mackinawite $Fe_{1-x}S$ formed also on both naturally degraded oak set C and pine set F. Set C samples (Neolithic oak) were buried for a long period of time. Thus, the extractives present may have dissolved during burial and only lignin remained. Contrary to artificially degraded oak, on which it was hypothesized that tannins formed complexes with ferrous iron from $FeCl_2{\cdot}4H_2O$ solution during the contamination protocol IP1, the absence of tannins here may have prevented this reaction to occur. Hence, iron sulfides were formed here on both naturally degraded oak and pine with the same contamination protocol, contrary to that observed on artificially degraded oak and pine.

SEM-EDS analysis

Complementary SEM-EDS allowed to evaluate wood cells degradation as well as to quantify the amount of Fe/S species within the wood sets C and F . Cross sections from surface Tv plane sections were characterized.

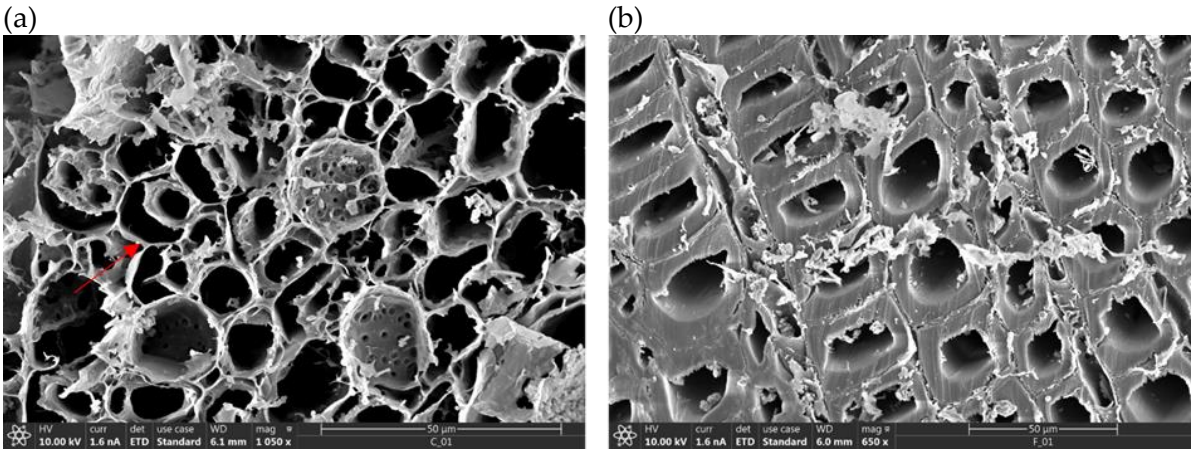

Figure 29: SEM micrographs of (a) Neolithic oak (set C) and (b) lake pine (set F) cross section after contamination with IP1

Vessels were clearly visible on set C (Neolithic oak) samples with the secondary cell wall detaching from the middle lamella (Figure 29a, red arrow). As reported by Macchioni et al, SEM analyses are generally associated to MWC measurements to ascertain the degradation state [11]. Here, both MWC and SEM analyses categorized set C samples into a high state of degradation, as confirmed also with ATR-FTIR spectra obtained. Concerning set F (lake pine) samples, tracheids did not show unattached cells (Figure 29b). This is in line with that observed above through ATR-FTIR and MWC analyses.

However, for both sets, exogenous materials were observed within the degraded wood cells, with an elongated form on set F and as circular aggregates on sets C and F. Lan and Butler showed that pure FeS formed small spheres and/or fine needles when converting into greigite Fe_3S_4 and FeS_2 [56]. However, EDS analyses revealed here a Fe:S ratio consistent with the presence of pyrite FeS_2 for sets C and F. In addition, some spot analyzes also presented a Fe:S ratio more consistent with the presence of mackinawite FeS on set F only.

If EDS analyses reported pyrite formation, the shape of the aggregates is not in line with what described in the literature. The precipitates observed on sets C and F identified as FeS_2 by EDS analysis did not present a framboid shape, usually representative of pyrite formation [57], [58]. However, pyrite can also crystallize as columnar crystals or tortuous filaments [59]. In addition, other compounds present similar Fe:S ratio than pyrite. For instance, marcasite is also reported as iron disulfide [60]. However, marcasite mainly form in acidic environment, which was not the case here [60]. In fact, measurements of pH at the surface of samples from sets C and F revealed a mean pH value around 11. The exact nature of the iron disulfide formed could be investigated through X-Ray Diffraction (XRD). Whatever the species of iron disulfide formed, EDS analyses validated the formation of an iron sulfide phase, identified as partially oxidized mackinawite $Fe_{1-x}S$ with Raman spectroscopy, and iron disulfide, pyrite, or marcasite.

Supplementary material 2

After application of IP1, all pine samples gathered in one cluster. As for oak wood samples, the degradation protocol previously applied did not affect the final appearance of contaminated samples.

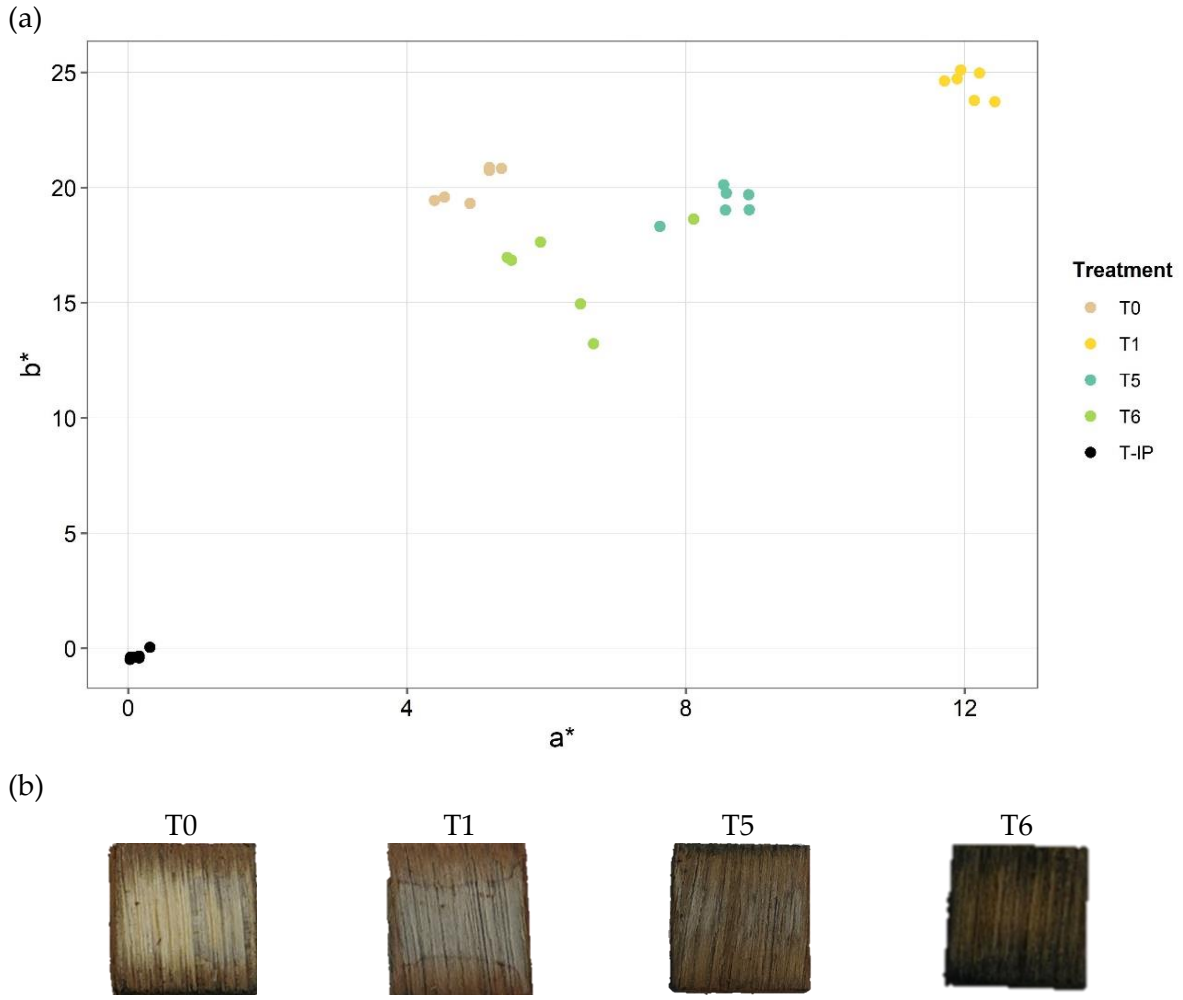

Figure S 6: (a) Colorimetric coordinates a and b* for pine untreated (T0), degraded (T1-T6) and contaminated (IP) wood samples. (b) Core Tg plane section of contaminated untreated (T0) and degraded (T1-T6) pine wood samples*

Partially oxidized mackinawite ($Fe_{1-x}S$, POM) was identified on pre-degraded pine wood contaminated with IP1. This phase was determined due to the vibrational bands at 119, 286 and 362 cm^{-1} observed on pine samples.

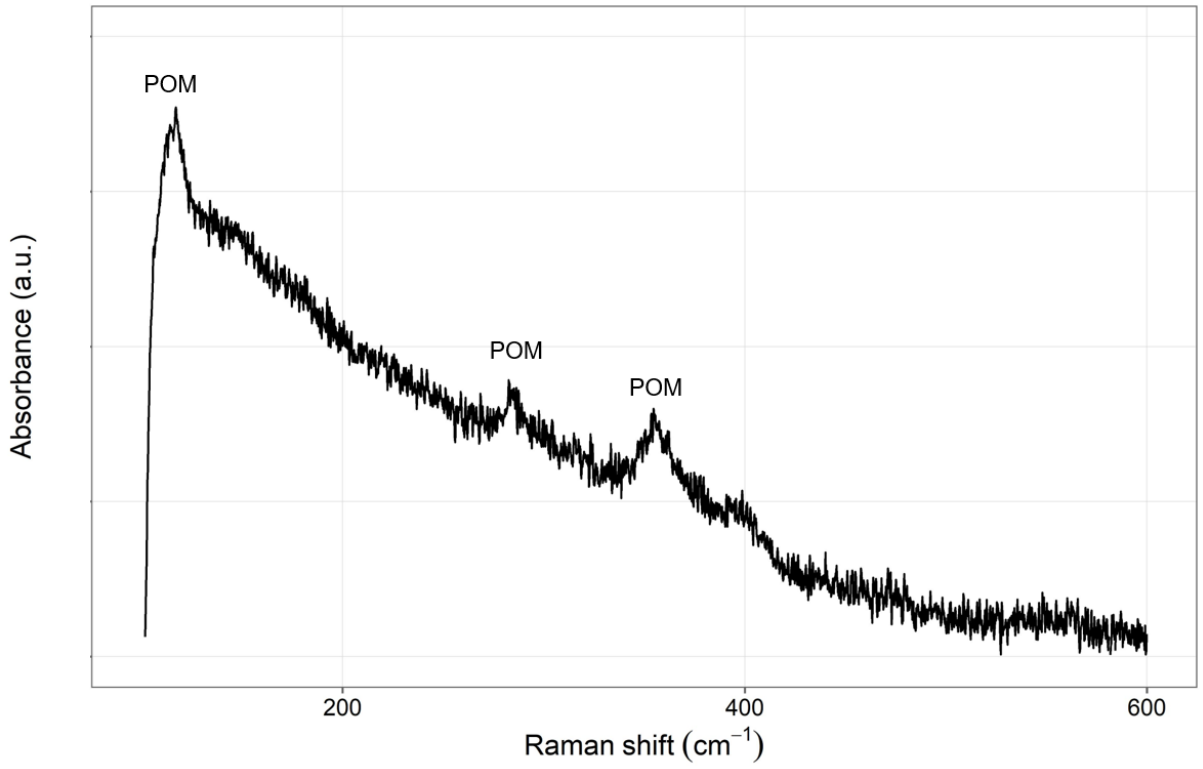

Figure S 7: Representative Raman spectrum of compounds identified at the surface of pine samples with bands of partially oxidized mackinawite (POM) indicated

After contamination with IP1, all the samples showed a degradation of carbohydrates content with the bands at 1738, 1059 and 1034 cm^{-1} less intense than before IP1. These bands are attributed to xylan C=O stretching and holocellulose C-O stretching [7], [8].

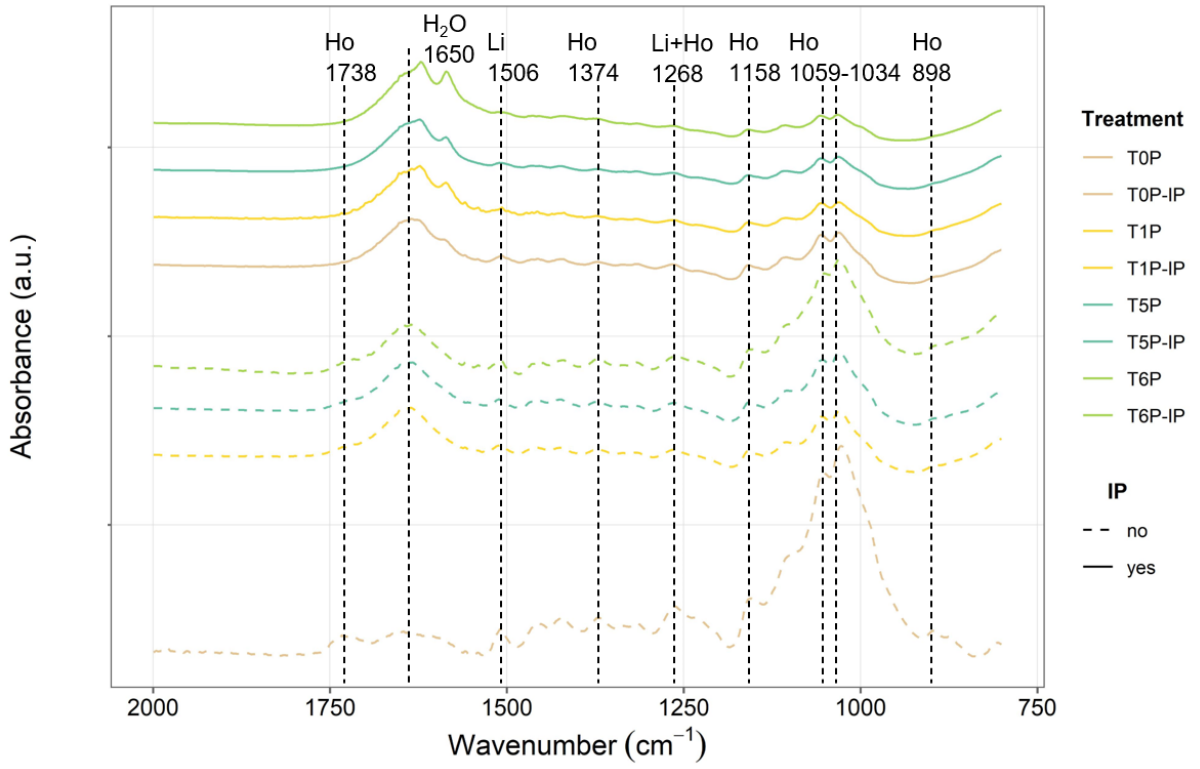

Figure S 8: Representative ATR-FTIR spectra for untreated (T0), degraded (T1-T6) and contaminated (IP) pine wood samples with characteristic vibrational bands of holocellulose (Ho) and lignin (Li) indicated with dashed lines

As for oak samples, untreated (T0) and biologically degraded (T6) pine samples presented the higher variation in ATR-FTIR ratios before and after contamination. It resulted that the chemical protocols (T1 and T5) allowed degradation of carbohydrates that is further enhanced with the application of IP1.

Table S 4: Mean variation within the ATR-FTIR ratios before and after application of contamination protocol IP1, depending on the degradation protocol T1-T5-T6 applied previously for pine wood samples. R1 = I(1158)/I(1506); R2 = I(1374)/I(1506); R3 = I(1034)/I(1506)

Degradation protocols	**Pine**		
	R1	*R2*	*R3*
T0	-35.5 (± 5.5)	-19.5 (± 2.5)	-59.2 (± 8.8)
T1	-12.6 (± 3.9)	-5.9 (± 1.8)	-24.4 (± 10.9)
T5	-13.2 (± 6.0)	-6.5 (± 2.2)	-31.3 (± 11.1)
T6	-31.4 (± 9.6)	-10.5 (± 5.4)	-56.6 (± 17.7)

Wood composition was investigated after application of the contamination protocol IP1. Cellulose was poorly affected contrary to holocellulose and lignin content. Yet, none of the decrease in cellulose, holocellulose and lignin content was significant, as showed with ANOVA analysis.

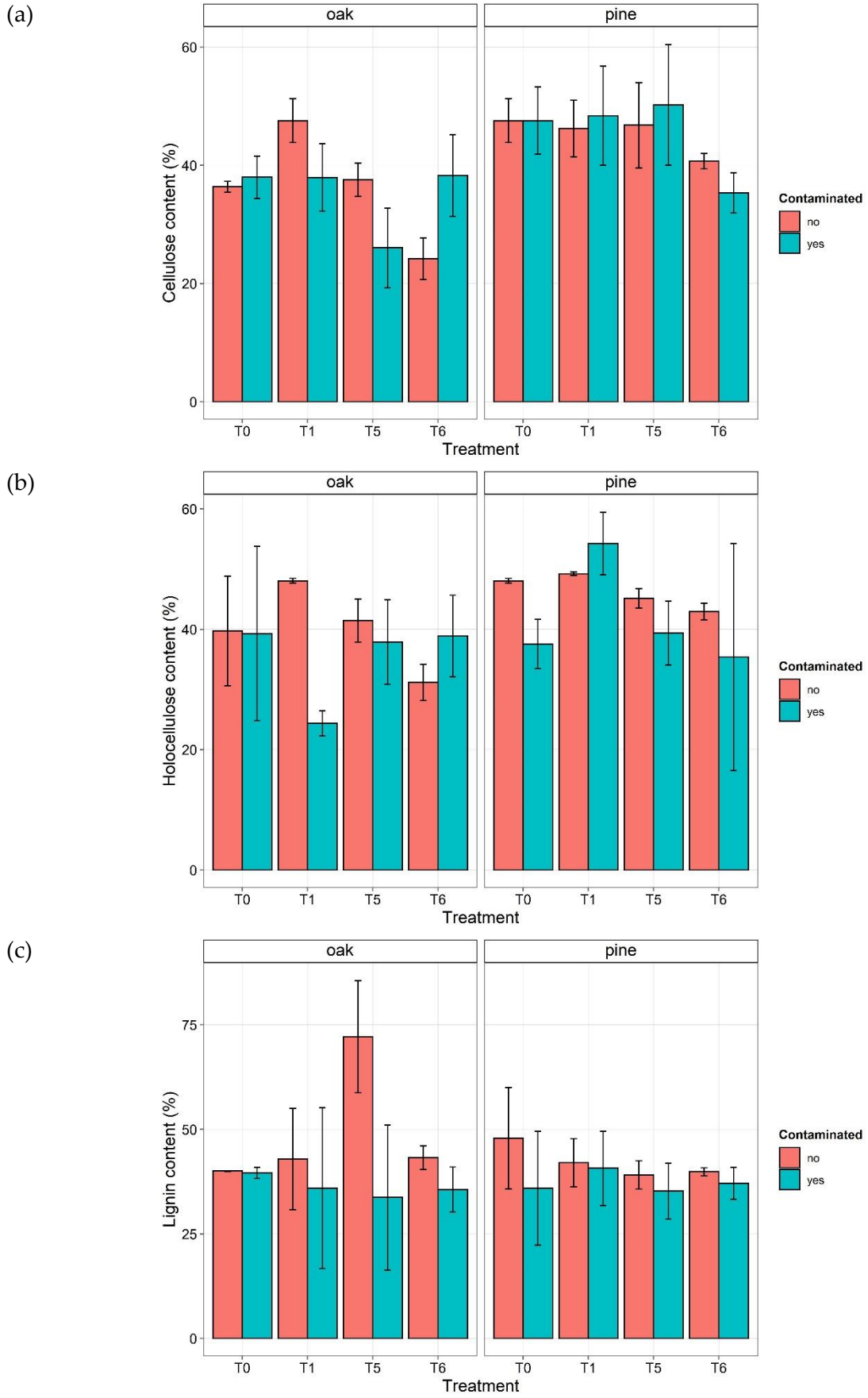

Figure S 9: (a) Cellulose content, (b) holocellulose content and (c) lignin content before (red bars) and after (blue bars) contamination protocol depending on the previous degradation protocol applied.

(a)

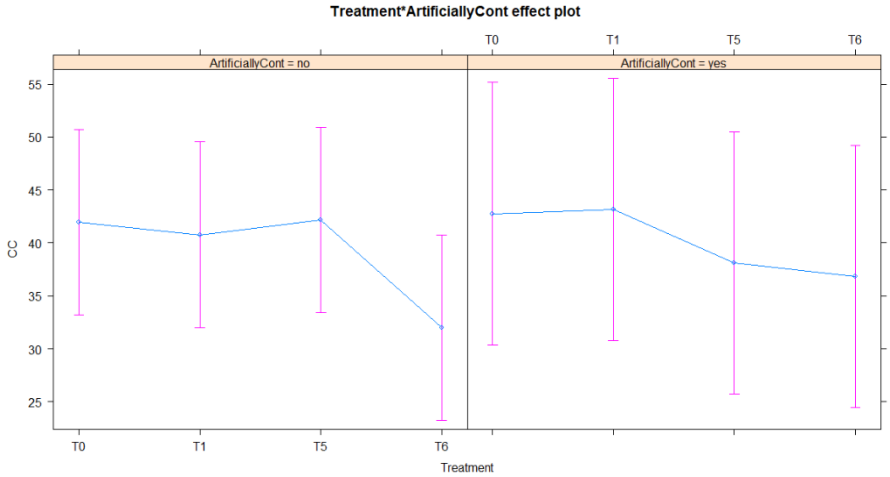

(b)

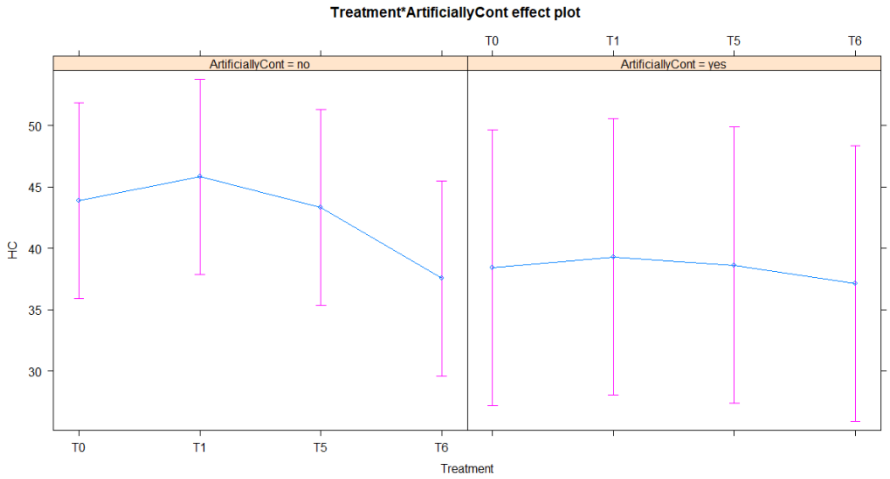

(c)

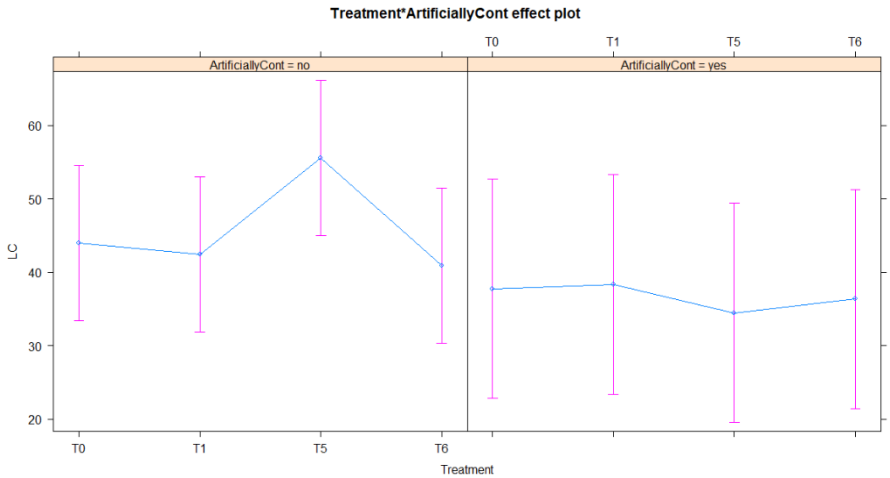

Figure S 10: ANOVA results of (a) cellulose content (CC), (b) holocellulose content (HC) and (c) lignin content (LC) before and after application of contamination protocol IP1 on untreated (T0) and pre-degraded (T1, T5, T6) wood samples

2.3 – Summary of research

To resume the investigations performed on fresh wood samples to simulate WAW characteristics, it appeared that water immersion under vacuum (T1 protocol) was the most effective protocol to enhance degradation of carbohydrates, at least on surface. The presence of metal pieces (T5) did not induce further degradation and so this protocol was discarded. The fungal degradation protocol (T6) was also less efficient regarding carbohydrates even if penetrated more deeply within the samples. Concerning the contamination with iron sulfides, IP1 ($FeCl_2 \cdot 4H_2O$ and $Na_2S \cdot 9H_2O$ 0.5 M solutions, 24 hours immersion under vacuum) presented the most promising results, even if only sulfur precipitates were observed on oak samples. However, this contamination protocol was selected to go further in the investigation of preparing WAW model samples and was then applied on waterlogged wood samples.

Preparation of model samples from naturally pre-degraded wood (sets C and F) seemed possible in terms of degradation of carbohydrates and iron sulfide contamination. As showed by the different analyses carried out, holocellulose was highly degraded, especially for Neolithic oak, due to the prolonged burial time of the two sets studied. This allowed the contamination reagents to easily penetrate within the degraded cells. Both wood species (oak in set C and pine in set F) presented partially oxidized mackinawite $Fe_{1-x}S$ on surface, according to Raman spectroscopy. Also, EDS analyses suggested formation of iron disulfide such as pyrite FeS_2.

3 – Conclusions

Freshwater archaeological wood samples were investigated as reference WAW samples. Two type of wood species were characterized, oak and pine, as representative of hard- and softwood species. As reported in literature, they presented a low carbohydrate content due to their long burial time in anaerobic environment. The different ranks, in which the samples are classified, revealed that these wood samples present a different state of degradation. This is interesting regarding the evaluation of preventive extraction methods, allowing to assess if biological and chemical treatments induce any degradation during their application and if they are efficient whatever the initial degradation state of wood treated. However, these WAW sets exhibited a low iron and sulfur contamination. In particular, microchemical spot tests performed on some wood pieces of wood ascertain the presence of iron but not of sulfur. Therefore, model WAW samples were prepared to form sets with higher contamination levels.

Artificial degradation protocols were thus carried out on fresh oak and fresh pine. Among the different protocols applied, one-week immersion under vacuum (T1) was the most promising protocol regarding enhancing degradation of carbohydrates, as observed on ATR-FTIR spectra. Furthermore, the ATR-FTIR ratios calculated for T1 were in the same range as the one of reference freshwater WAW, which is encouraging to prepare WAW model samples from fresh wood. Yet, evaluation of holocellulose content revealed that T1-protocol was only superficial and could not reach wood core. In addition, the successive application of contamination protocol formed different compounds for the two type of wood species. Elemental sulfur was detected on oak wood while an unstable iron sulfide phase (partially oxidized mackinawite $Fe_{1-x}S$) precipitated on pine wood. Therefore, naturally pre-degraded

Neolithic oak and lake pine were selected to go further in the preparation of WAW model samples. Neolithic oak displayed an important degradation of carbohydrates, such as reference freshwater WAW, due to its long burial time. Lake pine remained buried for a shorter period of time and was less decayed than Neolithic oak but more decayed than fresh pine. $Fe_{1-x}S$ was identified by Raman spectroscopy on Neolithic oak and lake pine. Complementary EDS analyses revealed that iron disulfide FeS_2 phases also have formed. The behavior of both these phases during the application of extraction methods discussed in Chapter 4 will be of great interest to determine if these methods are efficient on acid-soluble (*i.e.*, $Fe_{1-x}S$) and acid-insoluble (*i.e.*, FeS_2) compounds.

Thus, several sets were prepared to evaluate the proposed preventive biological and chemical extraction methods:

- Set C (Neolithic oak) and set F (lake pine) as model WAW samples
- Sets D1, D2, G2 (archaeological oak) and set G1 (archaeological pine) as real WAW samples

Even if considered as not proper model WAW samples, artificially degraded and contaminated fresh wood were also investigated, as complementary results:

- Sets A (fresh balsa), set B (fresh oak) and set E (fresh pine) as simulating WAW samples

References

[1] D. W. Grattan and R. W. Clarke, "Conservation of waterlogged wood," in *Conservation of marine archaeological obj*ects, Elsevier, pp. 164–206, 1987.

[2] B. Appelbaum, "Criteria for treatment: reversibility," *J. Am. Inst. Conserv*., vol. 26, no. 2, pp. 65–73, 1987.

[3] C. Brandi and C. Déroche, *Théorie de la restauration*. École nationale du patrimoine, 2001.

[4] G. Almkvist, S. Norbakhsh, I. Bjurhager, and K. Varmuza, "Prediction of tensile strength in iron-contaminated archaeological wood by FT-IR spectroscopy-a study of degradation in recent oak and Vasa oak," *Holzforschung*, vol. 70, no. 9, pp. 855–865, 2016.

[5] K. K. Pandey and H. C. Nagveni, "Rapid characterisation of brown and white rot degraded chir pine and rubberwood by FTIR spectroscopy," *Holz als Roh- und Werkst*., vol. 65, no. 6, pp. 477–481, 2007.

[6] K. K. Pandey and A. J. Pitman, "FTIR studies of the changes in wood chemistry following decay by brown-rot and white-rot fungi," *Int. Biodeterior. Biodegrad*., vol. 52, no. 3, pp. 151–160, 2003.

[7] K. K. Pandey and K. S. Theagar, "Analysis of wood surfaces and ground wood by diffuse reflectance (DRIFT) and photoacoustic (PAS) Fourier transform infrared spectroscopic techniques," *Holz als Roh- und Werkst*., vol. 55, pp. 383-390, 1997.

[8] B. Pizzo, E. Pecoraro, A. Alves, N. Macchioni, and J. C. Rodrigues, "Quantitative evaluation by attenuated total reflectance infrared (ATR-FTIR) spectroscopy of the chemical composition of decayed wood preserved in waterlogged conditions," *Talanta*, vol. 131, pp. 14–20, 2015.

[9] N. Macchioni, E. Pecoraro, and B. Pizzo, "The measurement of maximum water content (MWC) on waterlogged archaeological wood: A comparison between three different methodologies," *J. Cult. Herit*., vol. 30, pp. 51–56, 2018.

[10] G. Giachi, C. Capretti, N. Macchioni, B. Pizzo, and I. D. Donato, "A methodological approach in the evaluation of the efficacy of treatments for the dimensional stabilisation of waterlogged archaeological wood," *J. Cult. Herit*., vol. 11, no. 1, pp. 91–101, 2010.

[11] N. Macchioni, C. Capretti, L. Sozzi, and B. Pizzo, "Grading the decay of waterlogged archaeological wood according toanatomical characterisation. The case of the Fiavé site (N-E Italy)," *Int. Biodeterior. Biodegrad*., vol. 84, pp. 54–64, 2013.

[12] G. McConnachie, R. Eaton, and M. Jones, "A re-evaluation of the use of maximum moisture content data for assessing the condition of waterlogged archaeological wood," *E-preservation Sci*., vol. 5, pp. 29–35, 2008.

[13] N. Odegaard, S. Carroll, and W. S. Zimmt, *Material characterization tests for objects of art and archaeology*. 2000.

[14] U. P. Agarwal and S. A. Ralph, "FT-Raman Spectroscopy of Wood : Identifying Contributions of Lignin and Carbohydrate Polymers in the Spectrum of Black Spruce (Picea mariana)," *Applied Scpectro.*, vol. 51, no. 11, pp. 1648–1655, 1997.

[15] C. G. Björdal, T. Nilsson, and G. Daniel, "Microbial decay of waterlogged archaeological wood found in Sweden Applicable to archaeology and conservation," *Int. Biodeterior. Biodegradation*, vol. 43, no. 1–2, pp. 63–73, 1999.

[16] A. C. Wiedenhoeft and R. B. Miller, "2. Structure and Function of Wood," *Handb. Wood Chem. Wood Compos.*, 2005.

[17] J. A. Bourdoiseau, M. Jeannin, C. Rémazeilles, R. Sabot, and P. Refait, "The transformation of mackinawite into greigite studied by Raman spectroscopy," *J. Raman Spectrosc.*, vol. 42, no. 3, pp. 496–504, 2011.

[18] C. Remazeilles L. Meunier, F. Lévêque, N. Plasson, E. Conforto, M. Crouzet, P. Refait, and L. Caillat, "Post-treatment Study of Iron/Sulfur-containing Compounds in the Wreck of Lyon Saint-Georges 4 (Second Century ACE)," *Stud. Conserv.*, vol. 65, no. 1, pp. 28–36, 2020.

[19] C. Pelosi, G. Agresti, L. Calienno, A. Lo Monaco, R. Picchio, U. Santamaria and V. Vinciguerra, "Application of spectroscopic techniques for the study of the surface changes in poplar wood and possible implications in conservation of wooden artefacts," in *Optics for Arts, Architecture, and Archaeology IV*, vol. 8790, p. 879014, 2013.

[20] A. J. Varma and V. B. Chavan, "A study of crystallinity changes in oxidised celluloses," *Polym. Degrad. Stab.*, vol. 49, no. 2, pp. 245–250, 1995.

[21] C. A. Teacă, D. Roşu, R. Bodîrlău, and L. Roşu, "Structural changes in wood under artificial UV light irradiation determined by FTIR spectroscopy and color measurements–A brief review," *BioResources*, vol. 8, no. 1, pp. 1478–1507, 2013.

[22] D. N. Hon and S. Chang, "Surface degradation of wood by ultraviolet light," *J. Polym. Sci. Polym. Chem. Ed.*, vol. 22, no. 9, pp. 2227–2241, 1984.

[23] D. N.-S. Hon, "Degradative effects of ultraviolet light and acid rain on wood surface quality," *Wood fiber Sci.*, vol. 26, no. 2, pp. 185–191, 2007.

[24] R. M. Rowell, R. Pettersen, J. S. Han, J. S. Rowell, and M. A. Tshabalala, "Cell wall chemistry," *Handb. wood Chem. wood Compos.*, vol. 2, 2005.

[25] Y. Fors, "Sulfur-Related Conservation Concerns for Marine Archaeological Wood", 2008.

[26] F. F. P. Kollmann, E. W. Kuenzi, and A. J. Stamm, *Principles of Wood Science and Technology: II Wood Based Materials*. Springer Science & Business Media, 2012.

[27] E. Franceschi, I. Cascone, and D. Nole, "Thermal, XRD and spectrophotometric study on artificially degraded woods," *J. Therm. Anal. Calorim.*, vol. 91, no. 1, pp. 119–123, 2008.

[28] E. Franceschi, I. Cascone, and D. Nole, "Study of artificially degraded woods simulating natural ageing of archaeological findings," *J. Therm. Anal. Calorim.*, vol. 92, no. 1, pp. 319–322, 2008.

[29] J. A. Emery and H. A. Schroeder, "Iron-catalyzed oxidation of wood carbohydrates," *Wood Sci. Technol.*, vol. 8, no. 2, pp. 123–137, 1974.

[30] P. Pullanikat, S. J. Jung, K. S. Yoo, and K. W. Jung, "Oxidative degradation of reducing carbohydrates to ammonium formate with H_2O_2 and NH_4OH," *Tetrahedron Lett.*, vol. 51, no. 47, pp. 6192–6194, 2010.

[31] A. B. Anderson, "The composition and structure of wood." ACS Publications, 1958.

[32] R. A. Parham, "Crystallinity and Ultrastructure of Ammoniated Wood: Part 1. X-Ray Crystallinity," *Wood Fiber Sci.*, vol. 2, no. 4, pp. 311–319, 2007.

[33] J. S. Kim, Y. Y. Lee, and T. H. Kim, "A review on alkaline pretreatment technology for bioconversion of lignocellulosic biomass," *Bioresour. Technol.*, vol. 199, pp. 42–48, 2016.

[34] M. P. Levi and R. D. Preston, "A chemical and microscopic examination of the action of the soft-rot fungus Chaetomium globosum on beechwood (Fagus sylv.)," *HolzforschungInternational J. Biol. Chem. Phys. Technol. Wood*, vol. 19, no. 6, pp. 183–190, 1965.

[35] J. G. Savory and L. C. Pinion, "Chemical aspects of decay of beech wood by Chaetomium globosum," *Holzforschung-International J. Biol. Chem. Phys. Technol. Wood*, vol. 12, no. 4, pp. 99–103, 1958.

[36] J. Levy, "The soft rot fungi: their mode of action and significance in the degradation of wood," in *Advances in botanical research*, vol. 2, Elsevier, 1966, pp. 323–357.

[37] C.-M. Popescu, C. Mihaela Tibirna, A. L. Manoliu, P. Gradinariu, and C. Vasile, "Microscopic study of lime wood decayed by Chaetomium globosum," *Cellul. Chem. Technol.*, vol. 45, no. 9, p. 565, 2011.

[38] I. Dobrică, P. Bugheanu, I. Stănculescu, and C. Ponta, "FT-IR spectral data of wood used in Romanian," *Analele Univ. din Bucuresti*, vol. I, pp. 33–37, 2008.

[39] C. L. Biles, D. Wright, M. Fuego, A. Guinn, T. Cluck, J. Young, M. Martin, J. Biles, and S. Poudyal, "Differential chlorate inhibition of Chaetomium globosum germination, hyphal growth, and perithecia synthesis," *Mycopathologia*, vol. 174, no. 5–6, pp. 475–487, 2012.

[40] K. Kranitz, "Effect of natural aging on wood," 2014.

[41] C. G. Duncan, "Wood-attacking capacities and physiology of soft-rot fungi," 1960.

[42] C. Rémazeilles, K. Tran, E. Guilminot, E. Conforto, and P. Refait, "Study of Fe(II) sulphides in waterlogged archaeological wood," *Stud. Conserv.*, vol. 58, no. 4, pp. 297–307, 2013.

[43] M. Bouchard and D. C. Smith, "Catalogue of 45 reference Raman spectra of minerals concerning research in art history or archaeology, especially on corroded metals and coloured glass," *Spectrochim. Acta - Part A Mol. Biomol. Spectrosc.*, vol. 59, no. 10, pp. 2247–2266, 2003.

[44] M. Monachon, M. Albelda Berenguer, T. Lombardo, E. Cornet, F. Moll-Dau, J. Schramm, K. Schmidt-Ott and E. Joseph, "Evaluation of bio-based extraction methods by spectroscopic methods," *Minerals*, vol. 10, no. 2, pp. 1–17, 2020.

[45] M. A. P. C. De Feber, J. B. G. A. Havermans, and P. Defize, "Iron-gall ink corrosion: A compound-effect study," *Restaur. Int. J. Preserv. Libr. Arch. Mater.*, vol. 21, no. 4, pp. 204–212, 2000.

[46] B. Reissland and S. de Groot, "Ink corrosion: comparison of currently used aqueous treatments for paper objects," in *9th International Congress of IADA, Copenhagen*, 1999.

[47] H. Lee, W. I. Kim, W. Youn, T. Park, S. Lee, T.-S. Kim, J. F. Mano, and I. S. Choi, "Iron Gall Ink Revisited: In Situ Oxidation of Fe (II)–Tannin Complex for Fluidic-Interface Engineering," *Adv. Mater.*, vol. 30, no. 49, p. 1805091, 2018.

[48] J. Preston, A. D. Smith, E. J. Schofield, A. V. Chadwick, M. A. Jones, and J. E. M. Watts, "The effects of Mary Rose conservation treatment on iron oxidation processes and microbial communities contributing to acid production in marine archaeological timbers," *PLoS One*, vol. 9, no. 2, 2014.

[49] B. A. Jordan, "Site characteristics impacting the survival of historic waterlogged wood: A review," *Int. Biodeterior. Biodegrad.*, vol. 47, no. 1, pp. 47–54, 2001.

[50] Y. Fors, H. Grudd, A. Rindby, F. Jalilehvand, M. Sandstrom, I. Cato, and L. Bornmalm, "Sulfur and iron accumulation in three marine-archaeological shipwrecks in the Baltic Sea: The Ghost, the Crown and the Sword," *Sci. Rep.*, vol. 4, no. 1, p. 4222, 2015.

[51] G. J. Ritter and L. C. Fleck, "Chemistry of wood," *Ind. Eng. Chem.*, vol. 14, no. 11, pp. 1050–1053, 1922.

[52] C. G. Björdal, T. Nilsson, and R. Petterson, "Preservation, storage and display of waterlogged wood and wrecks in an aquarium:'Project Aquarius,'" *J. Archaeol. Sci.*, vol. 34, no. 7, pp. 1169–1177, 2007.

[53] S. Norbakhsh, I. Bjurhager, and G. Almkvist, "Mimicking of the strength loss in the Vasa: model experiments with iron-impregnated recent oak," *Holzforschung*, vol. 67, no. 6, pp. 707–714, 2013.

[54] S. Norbakhsh, I. Bjurhager, and G. Almkvist, "Impact of iron (II) and oxygen on degradation of oak – modeling of the Vasa wood," *Holzforschung*, vol. 68, no. 6, pp. 649–655, 2014.

[55] J. I. Hedges, G. L. Cowie, J. R. Ertel, R. J. Barbour, and P. G. Hatcher, "Degradation of carbohydrates and lignins in buried woods," *Geochim. Cosmochim. Acta*, vol. 49, no. 3, pp. 701–711, 1985.

[56] Y. Lan and E. C. Butler, "Monitoring the transformation of mackinawite to greigite and pyrite on polymer supports," *Appl. geochemistry*, vol. 50, pp. 1–6, 2014.

[57] R. T. Wilkin, H. L. Barnes, and S. L. Brantley, "The size distribution of framboidal pyrite in modern sediments: An indicator of redox conditions," *Geochim. Cosmochim. Acta*, vol. 60, no. 20, pp. 3897–3912, 1996.

[58] R. T. Wilkin and H. L. Barnes, "Formation processes of framboidal pyrite," *Geochim. Cosmochim. Acta*, vol. 61, no. 2, pp. 323–339, 1997.

[59] I. K. Bonev, J. M. Garcia-Ruiz, R. Atanassova, F. Otalora, and S. Petrussenko, "Genesis of filamentary pyrite associated with calcite crystals," *Eur. J. Mineral.*, vol. 17, no. 6, pp. 905–913, 2005.

[60] D. Rickard and G. W. Luther, *Chemistry of iron sulfides*, vol. 107, no. 2. 2007.

Chapter 4: Evaluation of preventive extraction methods

1 – Surface treatment

Naturally degraded samples which were artificially contaminated (Neolithic oak and lake pine), referred as model samples, and waterlogged archaeological wood (WAW) samples were selected to evaluate the efficiency of the proposed preventive biological (BT) and chemical (CT) extraction methods.

Both BT and CT are two-steps extraction methods. Regarding BT, the samples were first immersed in a solution containing Desferoxamine (DFO) siderophores for 10 days then incubated with *Thiobacillus denitrificans* for 20 days. Concerning CT, the samples were immersed in sodium persulfate for 1 day before being immersed in EDTA for 7 days. In parallel, untreated (NT) samples remained in deionized water until characterization.

Several criteria were defined to assess the efficiency of the proposed preventive biological extraction method. These criteria were defined based on common conservation criteria and evaluate the efficiency of the methods regarding visual aspect, safety for the artefacts and extraction of harmful salts [1], [2]. Innocuousness and extraction were the main criteria to respect in order to prevent further wood degradation. Moreover, the retreatability of the artefacts was also considered as an important parameter for the proposed preventive extraction method [3]. Additional criteria were suggested to validate the proposed preventive biological extraction method. In addition of being harmless for the artefact, the microorganisms employed with BT method should be safe for users and the environment. Finally, the compatibility of BT was examined with common stabilization method. This complementary step will valorize the proposed preventive biological extraction method.

Fresh wood simulating WAW samples were not considered as representative but extraction methods were also applied. These results are presented in supplementary materials 3 and 4.

1.1. Efficiency

1.1.1.– Appearance

BT and CT-samples submitted to biological and chemically extraction method respectively, were compared to untreated (NT) samples.

Figure 30: Visual appearance of model oak (set C) and pine (set F) as recovered, after contamination with IP1 and after extraction with biological (BT) or chemical (CT) method compared with untreated (NT) samples

Regarding model samples (sets C and F), their visual appearance seemed not altered after the biological treatment (Figure 30 BT). On the contrary, model samples chemically treated

displayed an important color shifts with a bleaching of the surface (Figure 30 CT). The discoloration instantly occurred when the samples were poured in sodium persulfate solution. Persulfate $S_2O_8^{2-}$ ions are known to have a bleaching action on some compounds, especially on phenols naturally present in wood [4], [5]. Concerning untreated samples, an important color change towards a reddish hue was also observed with both model sets (Figure 30 NT). In comparison, all fresh balsa, oak, and pine samples simulating WAW treated with BT as well as fresh oak-CT samples conserved a dark appearance (Figure S 11). However, fresh balsa (set A) and pine (set E) presented a bleached appearance after CT.

Figure 31: Visual appearance of model archaeological oak (sets D1, D2 and G2) and pine (set G1) as recovered and after extraction with biological (BT) and chemical (CT) method compared with untreated (NT) samples

Regarding WAW samples, BT and CT seemed to give similar results in terms of appearance for oak samples (Figure 31 sets D1, D2, G2). Indeed, all oak samples conserved a brown-black hue characteristic of WAW after treatment [6]. CT-samples were in general of a light hue respect to BT-samples, but no important color modification was observed as for model samples. Pine WAW (set G1) displayed light hues compared to respective oak WAW samples, whatever the method applied (Figure 31 set G1). Indeed, pine WAW treated with BT seemed completely bleached, CT-pine WAW samples turned red, and the appearance of untreated samples turned towards lighter hue. The final appearance of untreated samples after treatment suggested that some compounds are dissolve with solely water immersion.

Complementary colorimetric measurements were performed on the treated and untreated samples. The color variation (ΔE^*) was calculated before and after application of each extraction method studied.

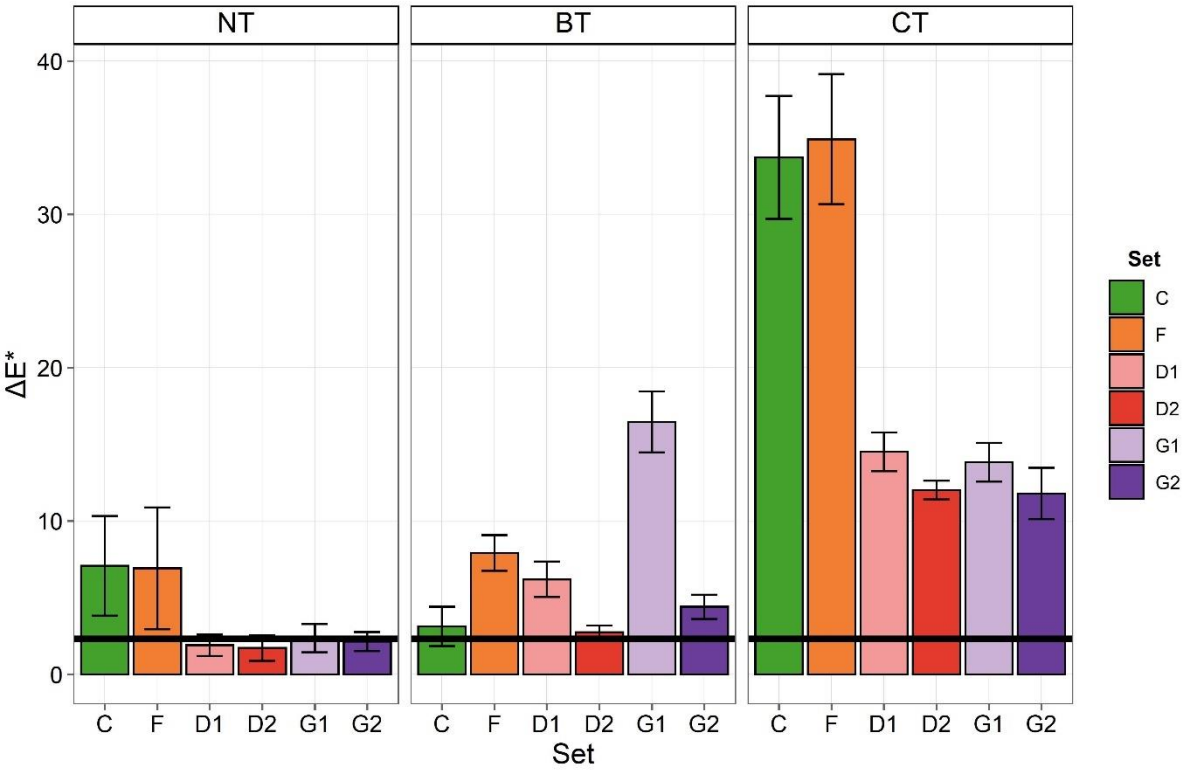

Figure 32: Mean color variation (ΔE) for untreated (NT) samples, model (sets C and F) and WAW (sets D1, D2, G1 and G2) samples, before and after extraction (BT: biological treatment, CT: chemical treatment) , with standard deviation bars and visually perceivable threshold (ΔE* = 2.3, black line) indicated*

ΔE* validated the strong visual modification observed after CT treatment of model samples (Figure 32). Fresh model samples presented even higher values (Figure S 12). Also, this confirmed here that the employment of sodium persulfate on heavily contaminated samples can be considered as too aggressive in terms of color modification. Even if few changes were observed on oak WAW, color variation ΔE* calculated for BT and CT-samples showed values above of ΔE* = 2.3, threshold where color variation detected by human eye [7]. NT-samples presented the lowest ΔE* color variation values after treatment, especially for WAW samples. Even if ΔE* was above the threshold (ΔE* = 2.3), the visual appearance of oak WAW samples treated with BT was approved by wood conservators involved in the MICMAC project.

To go further in the evaluation of the proposed preventive extraction methods, the innocuousness of BT and CT extraction methods was evaluated.

1.1.2 – Risk evaluation

pH at surface of wood was measured to evaluate wood degradation. In fact, it was proven that wood exposed to acidic solutions can degrade with a decrease of its mechanical strength [8].

Table 16: Wood samples mean pH values of model (sets C and F) and (sets D1, D2, G1, G2) WAW samples after biological (BT) and chemical (CT) extraction methods, and of untreated (NT) samples, with standard error indicated with brackets

Sets	BT	CT	NT
Set C	6.17 (± 0.04)	4.05 (± 0.16)	11.44 (± 0.50)
Set D1	5.69 (± 0.01)	3.96 (± 0.20)	6.03 (± 0.13)
Set D2	5.94 (± 0.13)	4.01 (± 0.11)	6.11 (± 0.18)
Set F	5.74 (± 0.01)	4.62 (± 0.63)	11.90 (± 0.11)
Set G1	5.53 (± 0.05)	4.47 (± 0.32)	6.45 (± 0.25)
Set G2	5.83 (± 0.04)	4.14 (± 0.17)	6.43 (± 0.03)

After extraction methods, the samples presented slightly acidic pH values (Table 16 and Table S 5). One can observe that the pH of BT-samples was in the range 5.3-6.2. This is slightly acidic but deionized water pH is in the same range and is around 5.6. On the contrary, CT-samples presented low pH values between 4.0 and 4.9. NT-samples displayed the highest pH values in the range 6.04-11.90.

ATR-FTIR analyses were also carried out before and after extraction on the area. Model (sets C and F) and WAW (sets D1, D2, G1 and G2) samples seemed unaffected by extraction protocols as the corresponding spectra before and after extraction were similar (Figure S 13).

(a)

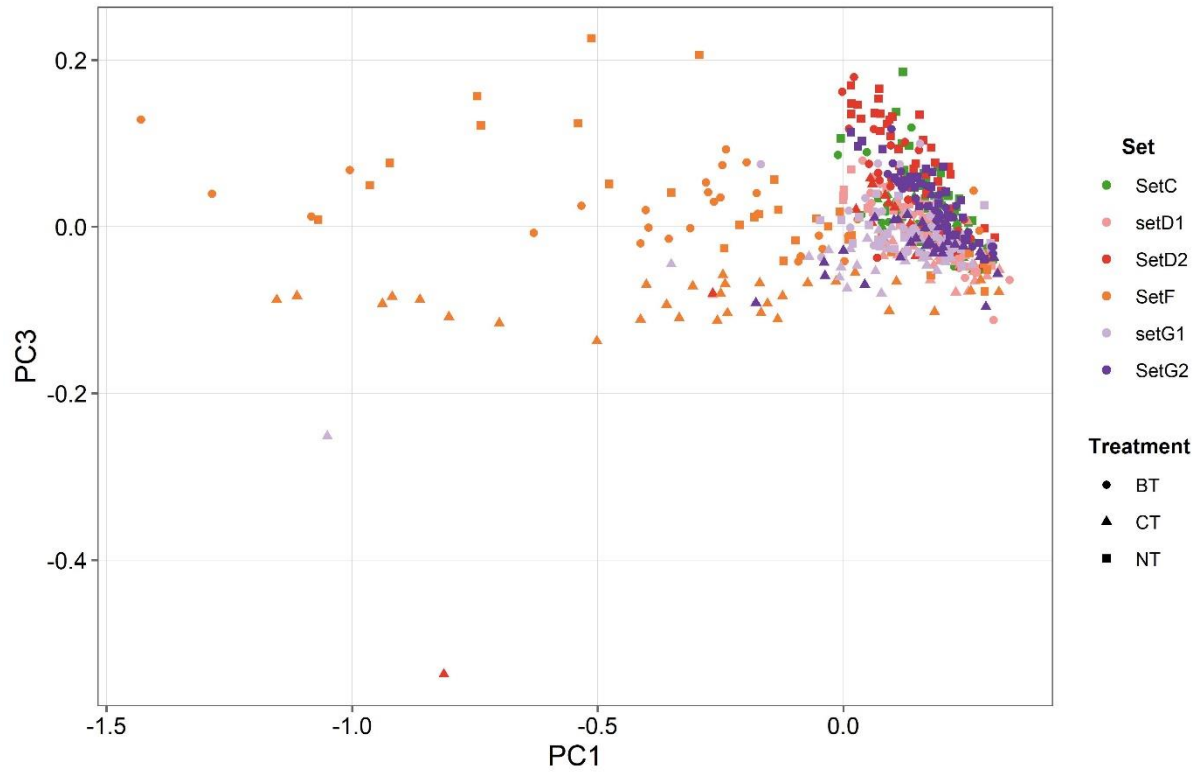

(b)

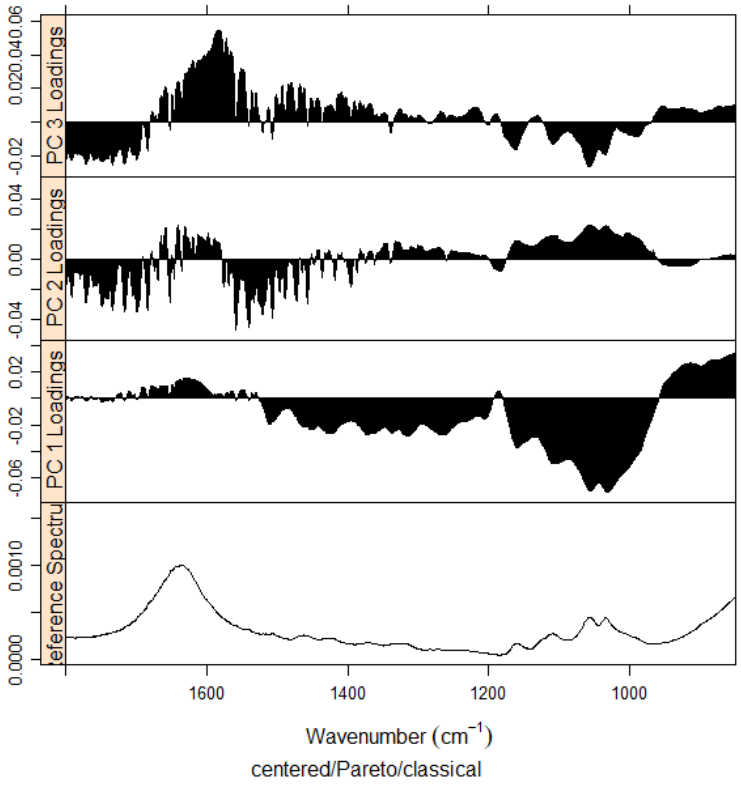

Figure 33: (a) PCA score plot of ATR-FTIR spectra of model (sets C and F) and WAW (sets D1, D2, G1, G2) samples after biological (BT, ●) and chemical (CT, ▲) extraction methods compared with untreated (NT, ■) samples. (b) ATR-FTIR PCA loadings after extraction

This was all confirmed with PCA approach, all spectra gathered in one cluster, as observed on Figure 33a. Indeed, all scores grouped in the positive part of PC1 (53% total variability). According to PC loadings, the lignin bands (1600-1500 cm^{-1}) as well as absorbed water band at 1650 cm^{-1} positively affected PC1 while holocellulose bands negatively affected the same PC1 (Figure 33b). All wood sets seemed to present similar lignin and holocellulose content after extraction. Set F samples (orange scores) were slightly apart from the other scores This could be explained by the fact that this set has been recovered from Biel lake after a 200-years burial and less decayed than the other sets. However, the difference between set F-samples and the other samples was not significant, according to statistical approach (p-val < 0.05). Similar results were observed for fresh wood simulating WAW samples with fresh pine presenting similar scores than lake pine (set F) (Figure S 14a).

Further analyses were performed from ATR-FTIR spectra by calculating R1 = I(1158)/I(1506), R2 = I(1374)/I(1506) and R3 = I(1034)/I(1506) ratios. These ratios support the evaluation of wood state of degradation and thus the efficiency of the proposed preventive extraction methods.

Table 17: ATR-FTIR ratios (R1 = I(1158)/I(1506), R2 = I(1374)/I(1506) and R3 = I(1034)/I(1506)) calculated for model (sets C and F) and WAW (sets D1, D2, G1 and G2) samples after extraction, with standard deviation indicated in brackets

Set	Extraction method	R1	R2	R3
Set C	*BT*	0.87 (± 0.01)	0.91 (± 0.01)	0.95 (± 0.03)
	CT	0.85 (± 0.01)	0.91 (± 0.01)	0.90 (± 0.03)
	NT	0.90 (± 0.01)	0.92 (± 0.01)	0.99 (± 0.03)
Set F	*BT*	0.95 (± 0.09)	0.95 (± 0.03)	1.31 (± 0.37)
	CT	0.98 (± 0.09)	0.96 (± 0.03)	1.37 (± 0.34)
	NT	0.98 (± 0.06)	0.95 (± 0.02)	1.27 (± 0.26)
Set D1	*BT*	0.89 (± 0.02)	0.91 (± 0.01)	0.98 (± 0.03)
	CT	0.88 (± 0.03)	0.91 (± 0.01)	0.95 (± 0.08)
	NT	0.90 (± 0.01)	0.92 (± 0.01)	1.01 (± 0.03)
Set D2	*BT*	0.86 (± 0.01)	0.91 (± 0.01)	0.94 (± 0.03)
	CT	0.87 (± 0.06)	0.92 (± 0.03)	0.96 (± 0.12)
	NT	0.85 (± 0.02)	0.92 (± 0.00)	0.91 (± 0.04)
Set G1	*BT*	0.85 (± 0.02)	0.92 (± 0.01)	0.93 (± 0.07)
	CT	0.87 (± 0.04)	0.93 (± 0.02)	0.98 (± 0.10)
	NT	0.84 (± 0.01)	0.92 (± 0.01)	0.90 (± 0.06)
Set G2	*BT*	0.85 (± 0.01)	0.91 (± 0.01)	0.89 (± 0.02)
	CT	0.88 (± 0.03)	0.91 (± 0.01)	0.95 (± 0.09)
	NT	0.83 (± 0.00)	0.92 (± 0.01)	0.84 (± 0.03)

Whatever the extraction methods employed, the ATR-FTIR ratios remained in the same range for model and WAW samples (Table 17). Being more recent, the values for set F-samples were higher than for the other sets. ANOVA was carried out on these ATR-FTIR ratios. All the ratios were significantly similar for BT and CT-samples (p-val < 0.05). On the contrary, set F-NT samples were significantly different than the other samples (p-val > 0.05).

Concerning fresh wood simulating WAW, no degradation was observed on the ATR-FTIR spectra, with the vibrational bands at 1059 and 1034 cm^{-1} being as intense as before extraction (Figure S 14b). In addition, the three ratios remained in the same range, validating the innocuousness of BT and CT toward wood material (Table S 6). As for model and WAW samples, pH values were slightly acidic for BT-samples (in the same range as WAW samples) and pH of CT-samples was in more acidic range (Supplementary material 3). Even if not representative of WAW samples, fresh wood samples could be reliable samples to test some new conservation methods as the results for fresh, model, and WAW samples followed the same pattern here.

1.1.3 –Salts extraction

Raman spectroscopy was carried out at the surface of the wood samples to identify the phases eventually present after treatment with BT and CT extraction methods.

No reduced sulfur compounds were detected at the surface of model oak and pine samples treated with BT extraction method (Figure 34a, green spectrum). On the contrary, elemental sulfur was identified for model samples treated with CT, with its characteristic bands observed at 152, 220 and 473 cm^{-1} (Figure 34a, blue spectrum). Also, partially oxidized mackinawite was identified for untreated (NT) samples (Figure 34a, grey spectrum) [9], [10]. Concerning WAW samples, spectra presented the same pattern before and after BT and CT extraction methods without sulfur compounds detected (Figure 34b).

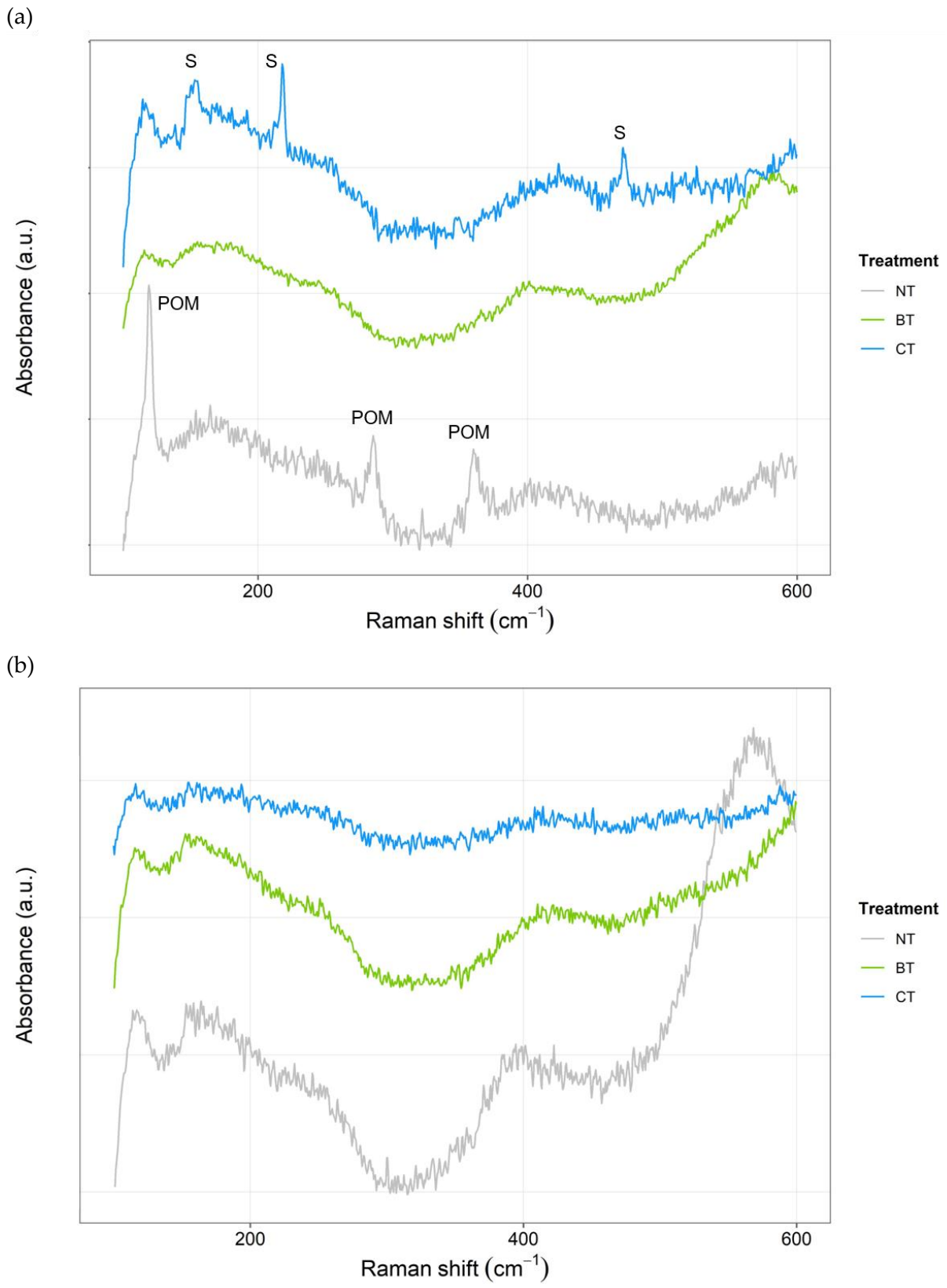

Figure 34: Representative Raman spectra for (a) model (set C) and (b) WAW (set D1) samples, after extraction with BT (green) and CT (blue) method, compared to untreated (NT, grey spectra) samples

Appearance

The application of BT biological extraction method on model WAW samples and oak WAW samples showed that these samples conserved their visual appearance after treatment. However, pine WAW samples were affected by BT extraction method with samples presenting a bleaching appearance. As no discoloration was observed during the preliminary studies when wood was immersed with *Thiobacillus denitrificans* culture, the bleaching of BT-pine WAW samples may result most probably from immersion with siderophores deferoxamine (DFO) [11]. It is known that some siderophores are employed in the paper industry to bio-bleach the wood pulp content [12], [13]. In addition, the different preliminary tests conducted with different siderophores on fresh balsa contaminated with IP1[1] also showed a discoloration [14]. Furthermore, such bleaching process is generally accompanied with degradation of either lignin or holocellulose content [13]. As oak WAW was not visually altered, pine WAW may present more sensitive molecules or parts than oak WAW towards siderophores, explaining such discoloration. The type of wood (hardwood *vs* softwood) seemed then to impact BT method. For instance, Granholm et al demonstrated that EDTA concentration should be adapted when extracting manganese Mn from hard- or softwood pulp [15]. The same could be true for other complexing agents, such as siderophores. An alternative would be to employ another siderophore type. In her PhD thesis research, Albelda-Berenguer proved that the siderophore pyoverdine (PVD) allowed contaminated balsa to conserve a brown appearance [14]. Even if less stable than commercial DFO, its action on softwood species could be investigated to prevent discoloration. Though, model pine WAW samples (set F), which is dated from a more recent period and thus less degraded, was more contaminated than pine WAW samples (set G1). Set F-samples have a mean iron concentration of 7.69 ± 1.12 mf of Fe per g of wood while set G1-samples have a lower mean iron concentration (0.30 ± 0.01 mg of Fe per g of wood). The quantity of harmful species within wood may impact the final visual appearance of treated samples. To prevent pine discoloration, DFO concentration could then be adjusted.

In general, the application of chemical CT extraction method tended to discolor the samples. It was proven that sodium persulfate concentration rapidly decreases in presence of ferrous Fe^{2+} ions. The oxidation of Fe^{2+} ions led to the formation of sulfate ions and sulfate radicals (equation (1)) [16]. Another study showed that when Fe^{2+} is easily accessible, addition of persulfates in solution led to a 50% bleaching of the solution within 30 seconds [17].

$$S_2O_8^{2-} + Fe^{2+} \rightarrow SO_4^{\cdot-} + SO_4^{2-} + Fe^{3+} \quad (1)$$

Indeed, persulfates are activated by some metals such as iron [17]. As some dissolved iron species (from left contamination solution within wood) were released during extraction of model samples (sets C and F), the iron species are easily accessible and can thus react with persulfate ions. As described in the work of Bennedsen et al, the discoloration and bleaching of the wood samples occurred in the first instants of immersion [17]. In addition to the visual modification, set F (lake pine) samples presented a slight orange hue after CT treatment. If

[1] IP1: 4 hours immersion in $FeCl_2{\cdot}4H_2O$ 0.5 M under vacuum (-600 mbars) followed by 4 hours immersion in $Na_2S{\cdot}9H_2O$ 0.5 M under vacuum (-600 mbars)

ferric Fe^{3+} ions were produced by the reaction of persulfates with Fe^{2+} ions, this may explain the observed orange staining of set F samples due to the precipitation of the produced Fe^{3+} species at the surface of the samples [8], [9]. The iron species present in the WAW samples (sets D1,D2,G1,G2)were not readily soluble and, therefore, they were not as affected by bleaching induced with persulfate. This could raise questions about the extraction of all iron species from WAW artefacts. Indeed, the analyses performed prior extraction revealed the presence of iron but in very low concentrations range (0.30-3.00 mg of Fe per g of wood) for WAW samples. On the contrary, model WAW samples (sets C and F) were artificially contaminated with iron species to ascertain its presence (concentrations range 7.50 – 15.00 mg of Fe per g of wood) were observed. Therefore, oak WAW samples conserved a dark appearance while pine WAW samples tended to a reddish hue. Such as for BT method, the type of wood species (hardwood *vs* softwood) impacts the appearance of the treated samples. Alternative extraction method should be considered for softwood samples species. Some laboratories employed hydrogen peroxide H_2O_2 instead of sodium persulfate [18], [19]. However, ferric ions in presence of H_2O_2 can promote the formation of hydroxyl radical OH^- that can decay cellulose fibers [20]. If ferrous ions oxidize during the extraction method, the production of ferric ions could be problematic towards the cellulosic wood content for the stability of the artefacts. Another possibility would be to directly extract iron species with solely EDTA instead of a two-steps protocol involving sodium persulfate and then EDTA but the extraction rate for this method is lower [21]. CT method may then be too aggressive in terms of color modification when wood is heavily contaminated with iron concentrations being very important or for softwood species. Yet, to respect the artefacts appearance, a threshold of iron contamination in WAW should be defined when considering sodium persulfate as extraction method. If the iron concentration is above this defined threshold, sodium persulfate immersion should be avoided and replaced by EDTA. Regarding softwood species, further experiments should be achieved to ascertain which method between sodium persulfate/EDTA or EDTA would induce less modification.

Safety for the wood

BT-solution displayed a neutral pH (pH = 7.46 ± 0.06) from the beginning until the end (pH 7.39 ± 0.22) of the 2nd step of the extraction protocol. The stability of the solution over time resulted of the employment of a buffer for the immersion of *T. denitrificans* culture, allowing an optimal bacterial growth and also preventing an acid hydrolysis of wood during BT extraction [22], [23]. As WAW samples treated with BT presented similar pH to untreated samples, it is unlikely that BT treatment induce any wood degradation. Concerning CT, both step of the two-steps preventive method may be aggressive for wood material. In the 1st step, sodium persulfate is employed, and sulfate radicals are produced (equation (1)). The production of sulfate radicals may be problematic as these radicals could degrade organic compounds, such as carbohydrates [16]. In addition, pH of EDTA solution employed for the 2nd step of this protocol was around pH = 3.88 ± 0.13 at the beginning of immersion and reached a final pH value of pH = 3.72 ± 0.24. With the acidic pH values, extraction with CT method could induce a further degradation of the wood substrate. However, the duration of this 2nd step of immersion in EDTA lasted one week, preventing an important degradation of wood

content to occur. In addition, no study reported EDTA as a potential degrading agent for organic materials. On the contrary, EDTA is employed in pulp and paper industry to prevent transition metals, such as iron, to form free radicals that could attack cellulose [24]. Therefore, despite sulfate radicals production, low pH values and visual modification observed, wood samples should not degrade during CT extraction method. Untreated (NT) model samples presented strong alkaline pH while NT WAW samples conserved a neutral to slightly acidic pH. Alkaline conditions could be as destructive as acidic pH for wood material [25]. However, wood degradation in such alkaline or acidic conditions occurred over a long period of time and is quite unlikely to arise during a few-months water immersion as applied here. Also, these high pH values measured on model samples (sets C and F) is not in line with their appearance. In fact, based on their visual appearance, one can postulated that iron oxides were formed and expected acidic pH values, as reported for the oxidation of iron sulfides into iron oxides [8]. So, alkaline pH measured of model set F-samples may result from residues of contamination solution remained within wood substrate. Indeed, sodium sulfide is an alkaline solution [26].

Complementary ATR-FTIR analyses were carried out. It resulted from the interpretation of ATR-FTIR spectra, PCA and calculated ratios that neither BT nor CT extraction method induce further degradation of the wood material, as suggested by pH values presented above. Contrary to these results, ANOVA analyses suggested that BT and CT extraction methods may degraded model pine WAW samples (set F). Yet, mean values calculated by ANOVA test before extraction were higher than after extraction. Thereby, this suggested that BT and CT extraction methods do induce degradation of the wood substrate. As PCA and ANOVA results diverged, another chemometrics approach could be considered to ascertain the innocuousness of the proposed preventive extraction methods such as Partial Least Square (PLS) regression method which is commonly used on infrared spectroscopy [27], [28].

Harmful salts extraction

In addition to the potential innocuousness for wood substrate, BT method appeared efficient in terms of extraction of iron Fe and sulfur S species. Indeed, no reduced sulfur compounds was identified at the surface of model and WAW samples, for both wood species (*i.e.*, oak and pine). In fact, in the first step of the BT extraction method, iron species present in wood were complexed by siderophores (DFO). Indeed, siderophores are known to present the highest affinity with ferric iron (log Kf = 30.6) and lowest for ferrous iron (log Kf = 10.29), compared to iron chelators such as EDTA (log Kf (Fe^{3+}) = 25.1 and log Kf (Fe^{2+}) = 14.30) [29]–[31]. In particular, DFO can thus solubilize iron sulfide phases, as observed by Albelda-Berenguer during her PhD thesis project [14]. As no iron species were identified on BT model and WAW samples surfaces, one can assume that iron was extracted. Regarding sulfur moieties, generally sulfate ions SO_4^{2-} could then be released but reduced sulfur species could also precipitate in the wood substrate. Here, in the 2nd step of BT extraction method, *T. denitrificans* was employed to oxidize the eventually remaining reduced sulfur species according to equation (2) [32].

$$5S + 6NO_3^- + 2H_2O \rightarrow 5SO_4^{2-} + 3N_2 + 4H^+ \quad (2)$$

T. denitrificans allowed then to solubilize solid forms of sulfur permitting to extract all sulfur species from WAW. Thus, it resulted that at the end of BT extraction method, both iron and sulfur moieties of iron sulfide phases seemed extracted from wood.

Concerning CT, elemental sulfur α-S_8 was still detected at the end of extraction method. It was discussed above that persulfate $S_2O_8^{2-}$ reacted with Fe^{2+} ions and produced sulfates SO_4^{2-} and Fe^{3+} ions, as illustrated in equation (1). Sodium persulfate was suggested to facilitate dissolution of iron sulfides and thus their extraction from WAW [21]. As no iron was detected after CT treatment, it resulted that iron sulfides were dissolved by sodium persulfate solution. The ferric ions Fe^{3+} released during the first step (immersion in sodium persulfate solution) were then complexed by EDTA, and washed out from the samples [33]. However, no step regarding sulfur dissolution or encapsulation was foreseen during CT method. Once iron complexed, the eventual remained sulfur or reactive sulfate radicals $SO_4^{\cdot-}$ may have led to the formation of reduced sulfur species on wood surface, as detected by Raman spectroscopy (Figure 34). However, Almkvist and Persson reported that sulfates were detected in the extractive solutions at the end of treatment of WAW objects with EDTA derivatives [33]. Therefore, immersion in solely EDTA could be sufficient to extract both complexed Fe and dissolved S species. Sodium persulfate immersion was proposed here as first immersion step as it was demonstrated that iron complexation was fasten by the sue of persulfate and then EDTA solutions [21]. In addition, CT extraction method is of a relatively short duration (8 days). One can suggest using EDTA, which does not induce wood degradation or considerable visual modifications. By removing the step with sodium persulfate solution and increasing the immersion time in EDTA, CT extraction method could allow to obtain both iron and sulfur soluble species that would be easily washed out and thus be more efficient.

Finally, the necessity of treating WAW artefacts was highlighted by the results obtained on untreated (NT) samples. Indeed, these samples still presented iron sulfide phases on model samples (Figure 34a, grey spectrum). One can notice some inconsistencies between the different spectra collected. Model samples presented an orange appearance (Figure 30) with an acidic pH but no wood degradation was noticed (Table 17). However, few spectra were recorded and given the high spatial resolution of Raman spectroscopy, may not be representative enough to track iron and sulfur compounds present in a whole sample. It is thus possible that harmful iron and sulfur salts remained and could lead to wood degradation.

Fresh wood treated with BT and CT presented similar results (Supplementary material 3 Table S 7). Though, some differences could be observed. Indeed, fresh oak (set B) was mainly contaminated with elemental sulfur, as discussed in Chapter 3, while the other fresh wood samples (sets A and E) presented iron sulfide phases. After CT treatment, set B-samples did not present any sulfur compounds contrary to the other sets artificially contaminated (fresh and model samples) and treated with CT. Thus, when only elemental sulfur is present, successive immersion in sodium persulfate and EDTA allowed the extraction of reduced sulfur phases. In addition, set A1 (fresh balsa) was free of any iron and sulfur compounds at the end

of CT treatment, unlike the twin set A2 (fresh balsa). Two reasons may explain the differences between these sets, which are identical and treated the same way:

1) the proposed extraction method is not reproducible. This shows a potential limitation of CT method and thus an optimization should be required, as discussed above.
2) the settings chosen for the Raman characterization are inappropriate. Only central area of three faces of the samples were investigated and the spectra obtained may not be representative enough. Additional measurements should be performed to track all iron and sulfur species still present.

From the different analyses carried out on the treated (BT and CT) and untreated (NT) samples, it resulted that BT was more efficient as preventive extraction method. BT fulfilled all the criteria listed at the beginning of the Chapter, meaning efficiency in terms of appearance, wood composition and salts extraction.

1.2 – Compatibility

To validate BT, the samples were stabilized with common conservation procedures, *i.e.*, PEG consolidation followed by freeze-drying. The appearance was first evaluated to ascertain the compatibility of the proposed preventive methods.

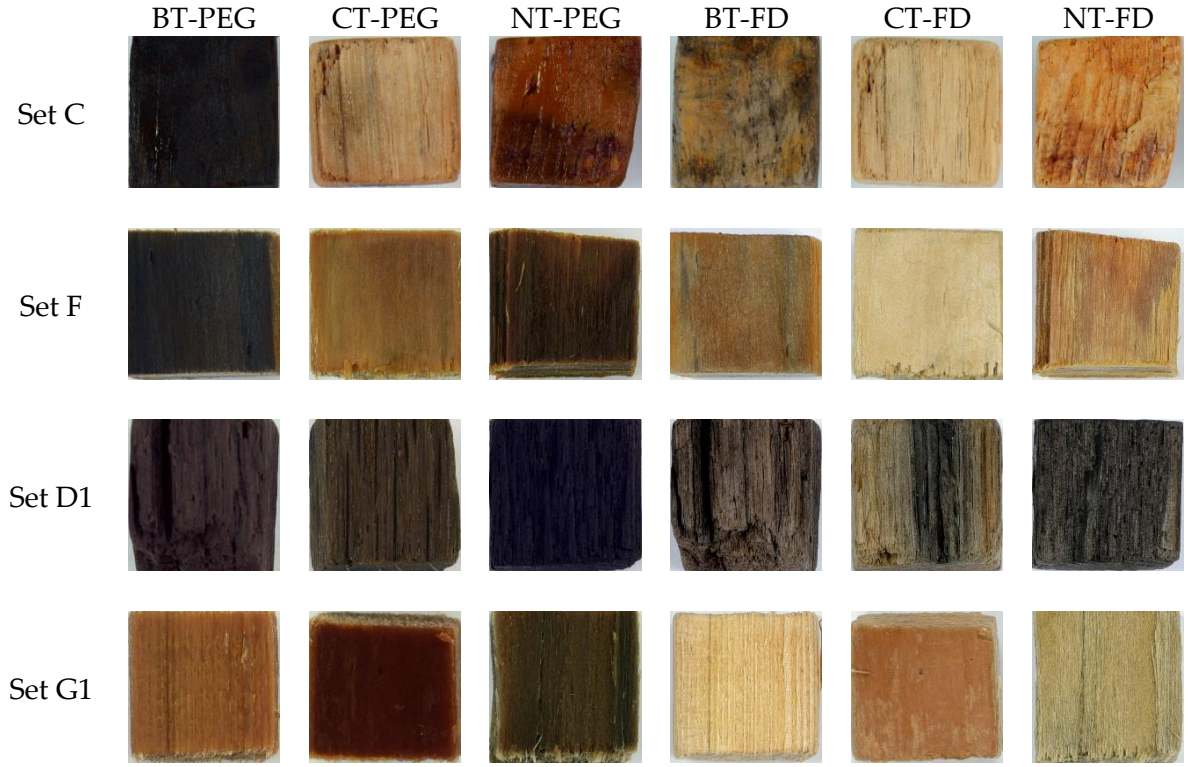

Figure 35: Visual appearance of model oak (set C) and pine (set F) and oak (set D1) and pine (set G1) WAW samples after consolidation with PEG and after freeze-drying (FD) for biological (BT) and chemical (CT) methods compared with untreated (NT) samples

Compared to the visual appearance of the samples after extraction (Figure 30 and Figure 31), the consolidation step in polyethylene glycol (PEG) did not alter the samples visual aspect (Figure 35 PEG). After 5 successive immersion baths in PEG, the samples were placed in

lyophilization chamber in order to dry them. At the end of freeze-drying, one can observe that all samples were visually altered. It seemed that model samples (sets C and F) were more altered as they present a bleached appearance respect to WAW samples (sets D1 and G1). WAW pine (set G1) was more altered that WAW oak (set D1).

Based on color variation ΔE*, one can notice that model (sets C and F) and pine WAW (set G1) samples displayed the highest color variation between before and after conservation procedures (Figure 36). The visual aspect of all samples, model and WAW, was highly affected by the stabilization method employed resulting in color variation ΔE* above 20. Yet, the variations were similar between NT, BT, and CT-samples of each set and thus visual modification is then comparable for the extracted and control samples. It was also observed that some sets presented very high error bars, such as set C-CT samples. The discoloration was not equally observed among the CT set, explaining the large color variation measured.

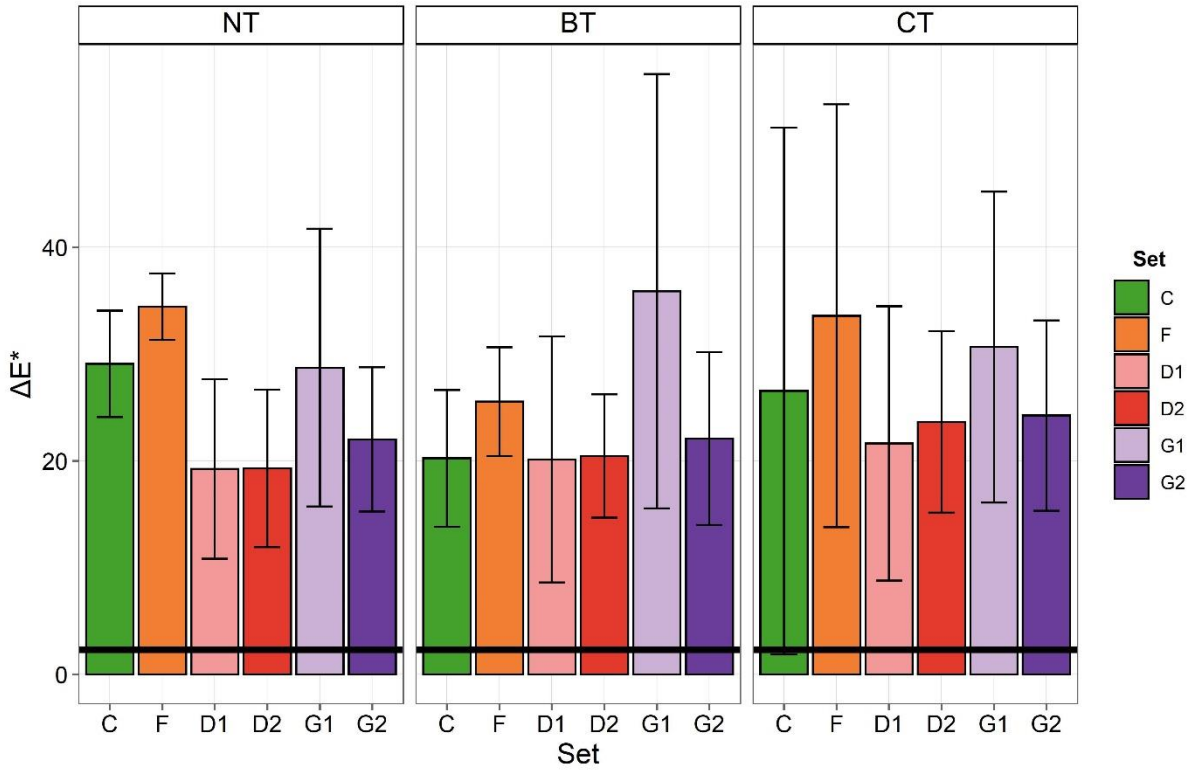

Figure 36: Mean color variation (ΔE) for model (sets C and F) and WAW (sets D1, D2, G1 and G2) samples, after previous extraction with BT and CT method and stabilization method (PEG + freeze-drying) and , with untreated (NT) samples, indicating standard deviation and visual perceivable threshold (ΔE* = 2.3, black line)*

In addition to discoloration, some untreated NT samples presented orange spots, suggesting an oxidation of iron sulfides present (Figure S 15 set G2) [8], [9]. Samples treated with BT also showed an orange hue (set F) (Figure S 16). An oxidation occurred during the stabilization protocol, suggesting that not all iron and sulfur compounds were extracted. Raman spectroscopy was then carried out to identify these potentially harmful corrosion products.

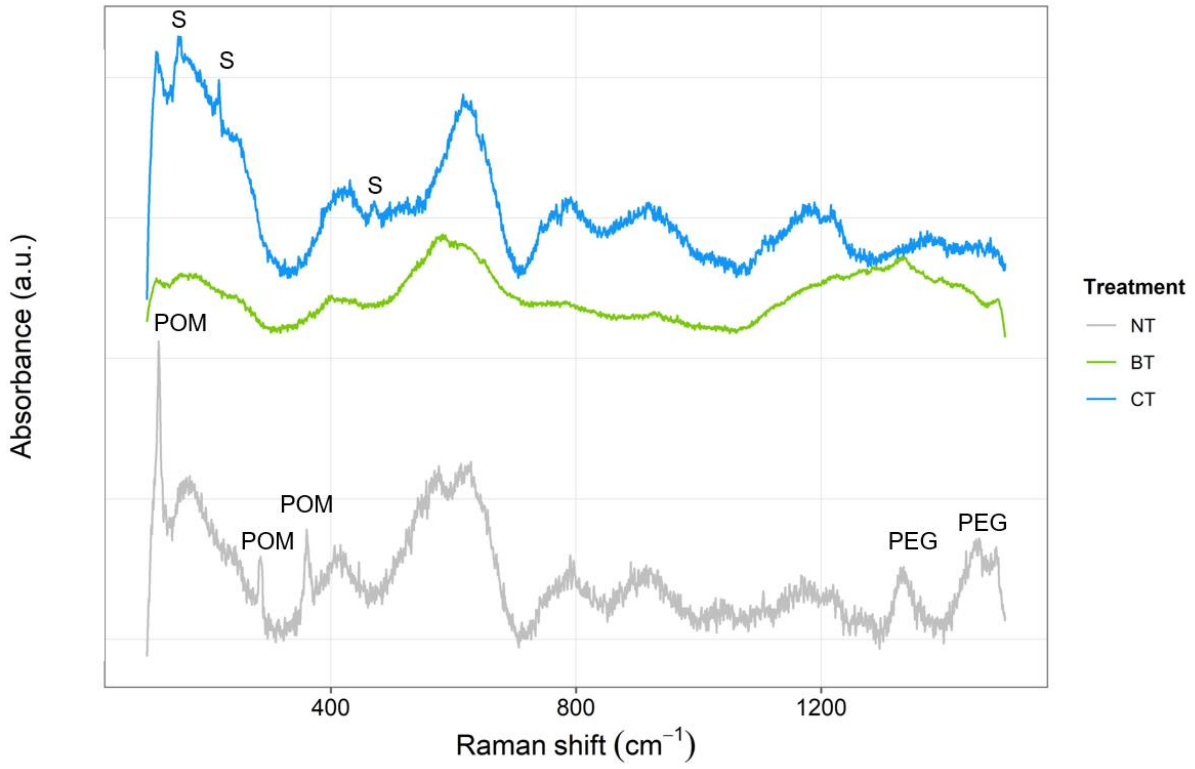

Figure 37: Representative Raman spectra for model (set C) oak WAW samples after stabilization method, for BT (green), CT (blue) and NT (grey) samples with characteristic bands for partially oxidized mackinawite (POM, elemental sulfur (S) and polyethylene glycol (PEG)

PEG characteristic bands were observed for most of the samples [34]. PEG being an organic compound, its vibrational bands were mainly in the high Raman shifts range and did not overlap with common iron corrosion products Raman bands. It allows identifying some characteristic bands of elemental sulfur on set C-CT samples (Figure 37 blue spectrum) or iron sulfides on C.NT samples (Figure 37, grey spectrum). All the other oak WAW samples did not show reduced sulfur compounds at the end of stabilization while iron oxide (lepidocrocite) was identified on set F-BT samples. Concerning fresh wood simulating WAW, some sets presented harmful products such as elemental sulfur for set A1-CT samples or lepidocrocite for set E-BT samples (Supplementary material 3 Table S 7).

If BT was considered as an efficient preventive extraction method, its compatibility with common stabilization method is here questioned. Even if no reduced sulfur compounds were identified on model and WAW samples, it seemed that their condition was different before stabilization. Indeed, for model samples, which where artificially contaminated with iron and sulfur, the final appearance after freeze-drying showed bleached samples with some grey areas at the samples surface. WAW samples also present a clearer appearance though the color variation seemed less important than for model samples and less evident grey areas were observed. The reason of a stronger visual modification for model samples may come from the degree of contamination at the beginning at the extraction protocols. The grey areas observed on model samples could remind the salts efflorescence reported on some WAW artefacts [8].

Similar observations could be made for CT and NT samples. Though, no grey areas were observed on CT model samples and the orange hue persisted for some NT model samples after freeze-drying. Sanya et al demonstrated that a discoloration occurred when oak and pine WAW is freeze-dried [35]. This was confirmed by the stabilization of untreated (NT) samples with D1-, D2- and G2-NT samples being clearer after lyophilization (Figure 35 and Figure S 13). These three sets are from oak species. The visual modification seemed more important for pine species as set G1-NT samples were very light color at the end of stabilization protocol. As oak samples were less visually altered, the parameters selected here for the drying of the consolidated samples may not be adapted for pine and softwood species in general. Indeed, monitoring of the freeze-drying step was performed by evaluating the weight of sets D1 and G2 samples, both from oak species. Thus, the monitoring of softwood species should be deeper investigated, and eutectic temperature, pressure and drying duration modified for softwood species, to prevent such unwanted discoloration.

Furthermore, the conservation procedures proved that not all the harmful species were extracted during BT and CT extraction methods. Indeed, some elemental sulfur (α-S_8) was still detected on samples treated with CT method and lepidocrocite (γ-FeOOH) on BT samples. The identification of these products implies that iron and sulfur were still present within the samples. It is possible that some compounds were skipped during the Raman analyses performed, as only a single point was characterized. Yet, the same area was investigated after conservation procedures. It could be possible that some iron and sulfur species were still present at the core of the samples and migrated towards the samples surface during stabilization. When reaching the surface, the species would then have oxidized and formed iron oxyhydroxides. The detection of such compounds may endanger the long-term stability of the samples. Compared to initial iron sulfide phases, iron oxyhydroxides are more voluminous [8], [36]. To better understand such salts precipitation, further investigation was carried out.

Supplementary material 3

As observed for WAW samples, the type of wood species impacted the extraction methods efficiency. Fresh Balsa (set A) and pine (set E) showed light colored appearance for CT and NT-samples while oak (set B) remained dark. NT samples were reddish such as model samples.

Figure S 11: Visual appearance of fresh balsa (set A), oak (set B) and pine (set E) as fresh, after contaminated with IP1 to simulate WAW and after extraction with biological (BT) and chemical (CT) treatments compared with untreated (NT) samples

Colorimetric measurements validated the previous observations, with BT-samples presenting low color variation values respect to CT-samples. NT-samples presented important differences within the individual sets, with significant standard error bars.

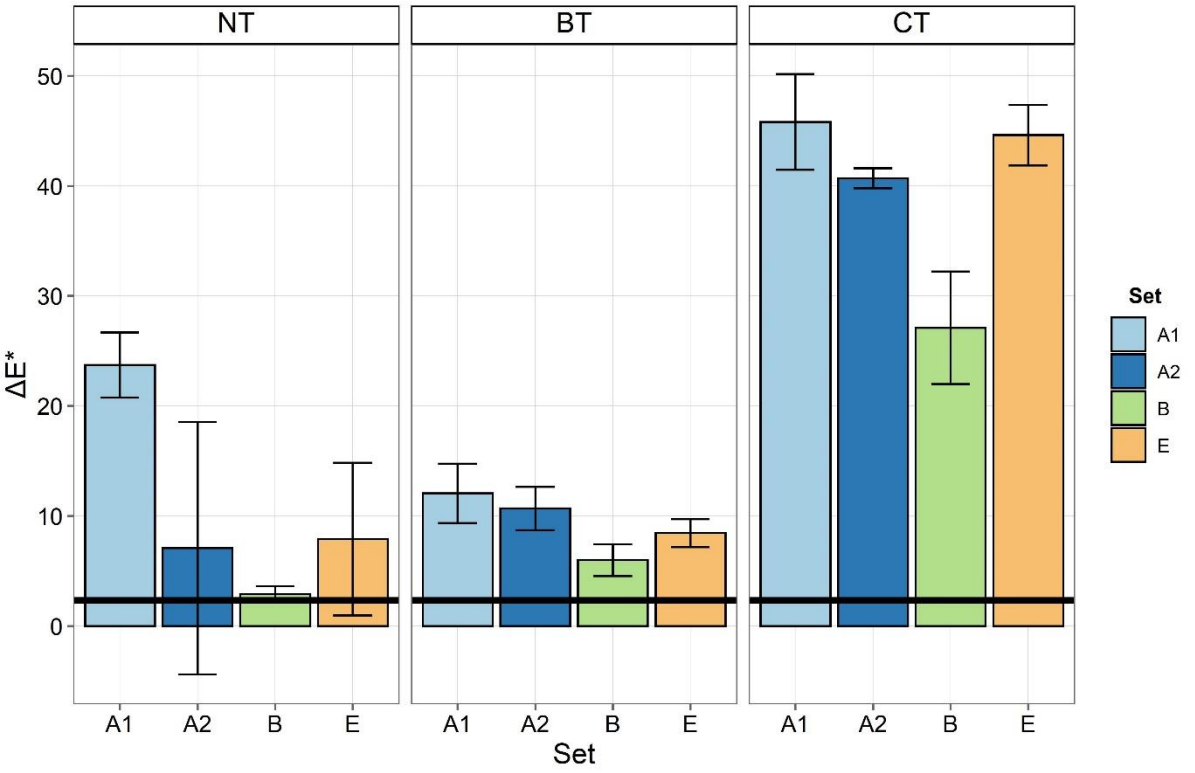

Figure S 12: Mean color variation (ΔE) for untreated (NT) samples, fresh wood simulating WAW, before and after extraction (BT: biological treatment, CT: chemical treatment) with, standard deviation bars and visually perceivable threshold (ΔE* = 2.3, black line) indicated*

Fresh wood simulating WAW samples followed the same tendency than model and WAW samples. At the end of BT method, samples pH was slightly acidic, due to the buffer employed during the treatment while CT-samples were in more acidic range. NT-samples also showed alkaline pH though their values were lower than for model samples.

Table S 5: Wood samples mean pH values for fresh samples after biological (BT) and chemical (CT) extraction methods, and of untreated (NT) samples, with standard error indicated with brackets

Sets	BT	CT	NT
Set A1	5.50 (± 0.04)	4.32 (± 0.02)	8.84 (± 0.95)
Set A2	5.84 (± 0.03)	4.30 (± 0.01)	10.71 (± 1.54)
Set B	5.33 (± 0.04)	4.26 (± 0.02)	8.78 (± 2.67)
Set E	6.00 (± 0.04)	4.86 (± 0.42)	10.18 (± 0.64)

ATR-FTIR spectra of model and WAW samples revealed no differences after BT and CT extraction methods compared to untreated samples (NT) samples.

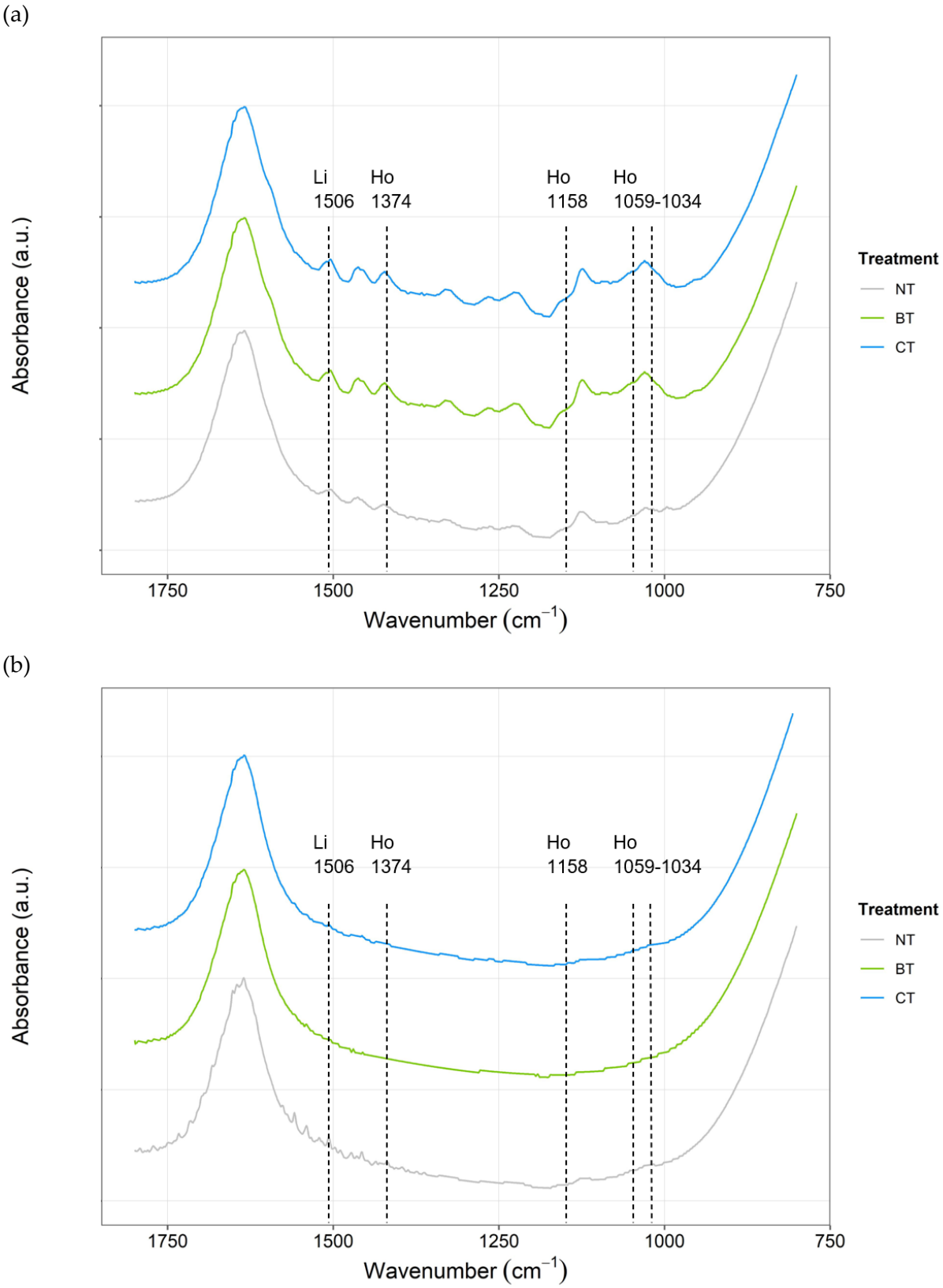

Figure S 13:Representative ATR-FTIR spectra for (a) model (set C) and (b) WAW (set D1) oak samples after biological (BT) and chemical (CT) extraction methods and for untreated (NT) samples with characteristic vibrational bands of holocellulose (Ho) and lignin (Li) indicated with dashed lines

Fresh wood scores gathered in PCA score plot, independently of the extraction methods applied. No decrease in bands intensity was observed on ATR-FTIR spectra collected after

extraction. The sets (A, B and E) still presented intense holocellulose bands at 1059 and 1034 cm^{-1}.

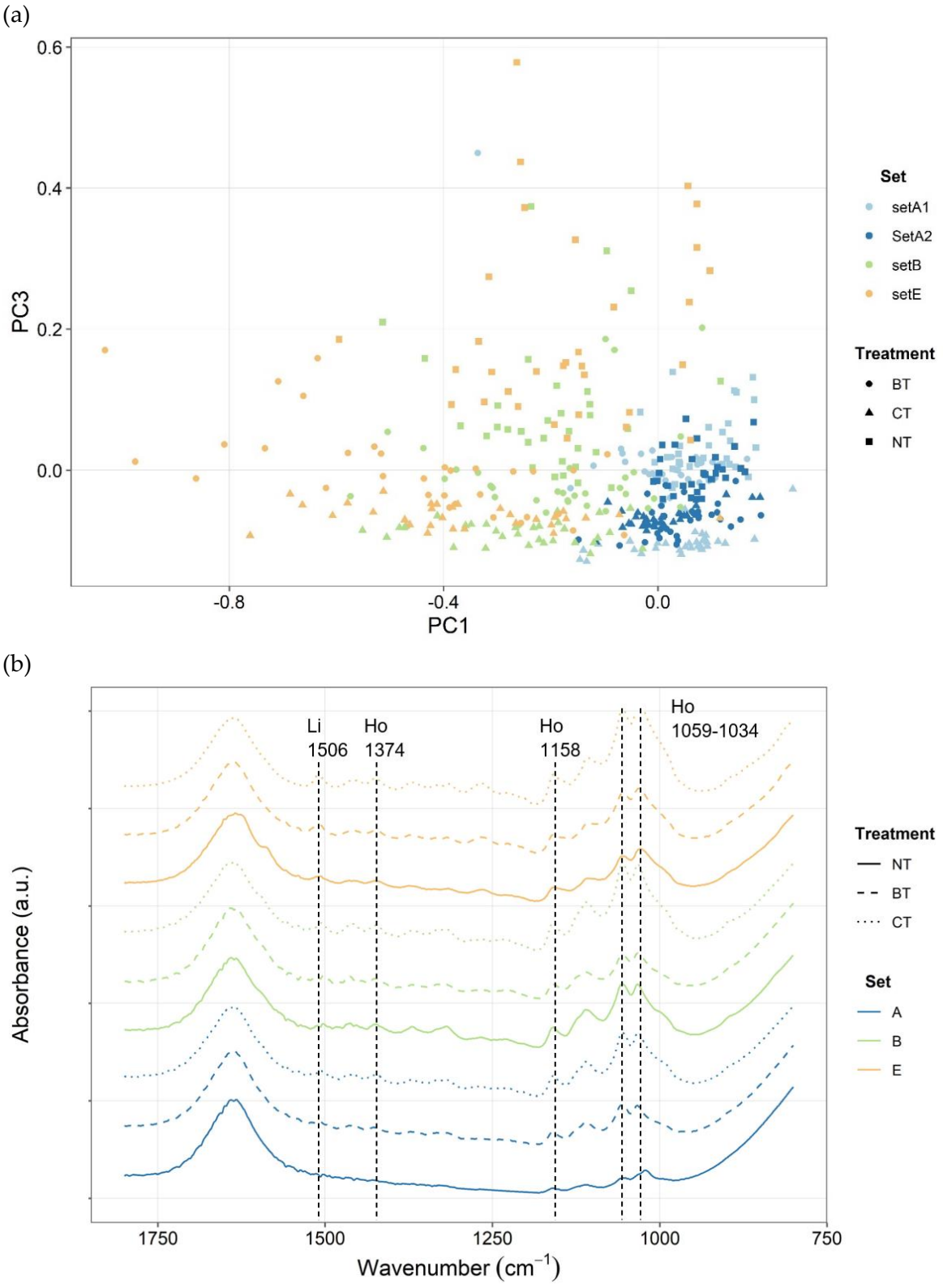

Figure S 14: (a) PCA score plot of ATR-FTIR spectra of contaminated (sets A1, A2, B, E) samples after biological (BT, ●) and chemical (CT, ▲) extraction methods compared with untreated (NT, ■) samples (b)Representative ATR-FTIR spectra fresh model WAW samples (sets A, B and E) after biological (BT) and chemical (CT) extraction methods, compared to untreated (NT) samples with characterized vibrational bands of holocellulose (Ho) and lignin (Li) indicated with dashed lines

The calculated ATR-FTIR ratios remained in the same range of untreated (NT) samples after biological (BT) and chemical (CT) extraction methods.

Table S 6: ATR-FTIR ratios calculated for contaminated (sets A1. A2, B, E) samples after extraction, with standard deviation indicated in brackets

Set	Extraction method	R1	R2	R3
Set A1	*BT*	0.91 (± 0.03)	0.94 (± 0.01)	1.05 (± 0.07)
	CT	0.93 (± 0.02)	0.94 (± 0.00)	1.10 (± 0.07)
	NT	0.88 (± 0.02)	0.93 (± 0.01)	0.97 (± 0.05)
Set A2	*BT*	0.93 (± 0.02)	0.94 (± 0.01)	1.07 (± 0.07)
	CT	0.92 (± 0.03)	0.95 (± 0.01)	1.07 (± 0.07)
	NT	0.89 (± 0.02)	0.94 (± 0.01)	0.99 (± 0.05)
Set B	*BT*	0.95 (± 0.04)	0.94 (± 0.01)	1.21 (± 0.13)
	CT	0.98 (± 0.03)	0.94 (± 0.03)	1.30 (± 0.11)
	NT	0.92 (± 0.04)	0.98 (± 0.01)	1.17 (± 0.11)
Set E	*BT*	1.01 (± 0.06)	0.97 (± 0.02)	1.47 (± 0.20)
	CT	1.00 (± 0.05)	0.96 (± 0.02)	1.42 (± 0.18)
	NT	0.97 (± 0.03)	0.95 (± 0.01)	1.24 (± 0.11)

Reduced sulfur phases were identified on all contaminated and model samples before extraction. After extraction, no reduced samples were detected on BT-samples while elemental sulfur was still identified on CT-samples. After stabilization, PEG was identified on most of the samples. elemental sulfur was still identified on some CT-samples and some iron oxyhydroxides, lepidocrocite, identified on recent pine (sets E and F).

Table S 7: Raman compounds identified for each set biologically (BT) and chemically (CT) extracted with untreated (NT) samples, before and after extraction and after stabilization

Set	Treatment	Before extraction	After extraction	After stabilization
Contaminated fresh balsa – Set A1	NT	POM, S	POM, S	PEG
	BT	POM	S	PEG
	CT	POM	S	S, PEG
Contaminated fresh balsa – Set A2	NT	POM	POM	PEG
	BT	POM		PEG
	CT	POM	S	PEG
Contaminated fresh oak – Set B	NT	S	S	PEG
	BT	S		
	CT	S		
Contaminated fresh pine – Set E	NT	POM, S	POM, S	S, PEG
	BT	POM		S, PEG, L
	CT	POM	S	PEG
Model oak – Set C	NT	POM	POM	PEG
	BT	POM		
	CT	POM	S	
Model pine – Set F	NT	POM	POM	PEG, L
	BT	POM		PEG
	CT	POM	S	PEG
Archaeological oak – Sets D1, D2, G2	NT			
	BT			
	CT			PEG
Archaeological pine - Set G1	NT			PEG
	BT			PEG
	CT			PEG

POM: partially oxidized mackinawite; S: elemental sulfur; PEG: polyethylene glycol; L: lepidocrocite

PEG consolidation maintained the dark appearance of WAW samples. though, after freeze-drying, BT and CT-samples discolored. Regarding NT-samples, some orange stains were observed on set G2-samples.

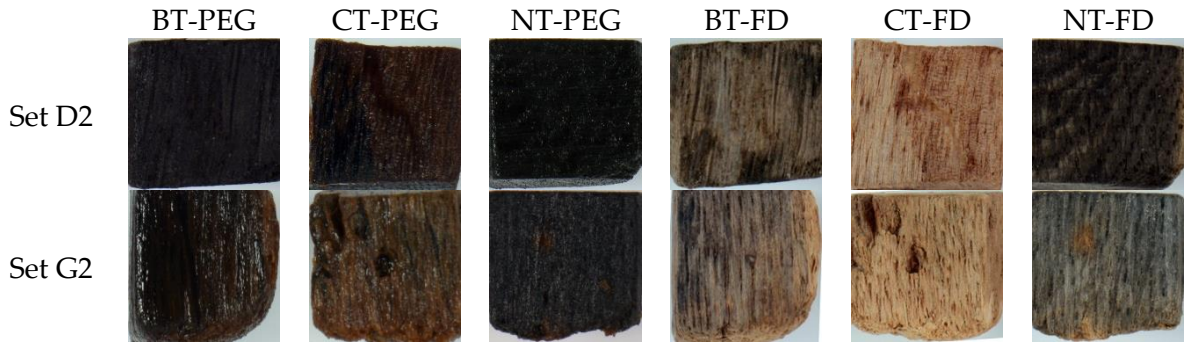

Figure S 15:Visual appearance of oak WAW (sets D2, G2) samples after consolidation with PEG and after freeze-drying (FD) for biological (BT) and chemical (CT) methods compared with untreated (NT) samples

Contaminated fresh wood samples also conserved similar hue after PEG consolidation than the one observed after extraction. However, the visual appearance was altered after freeze-drying.

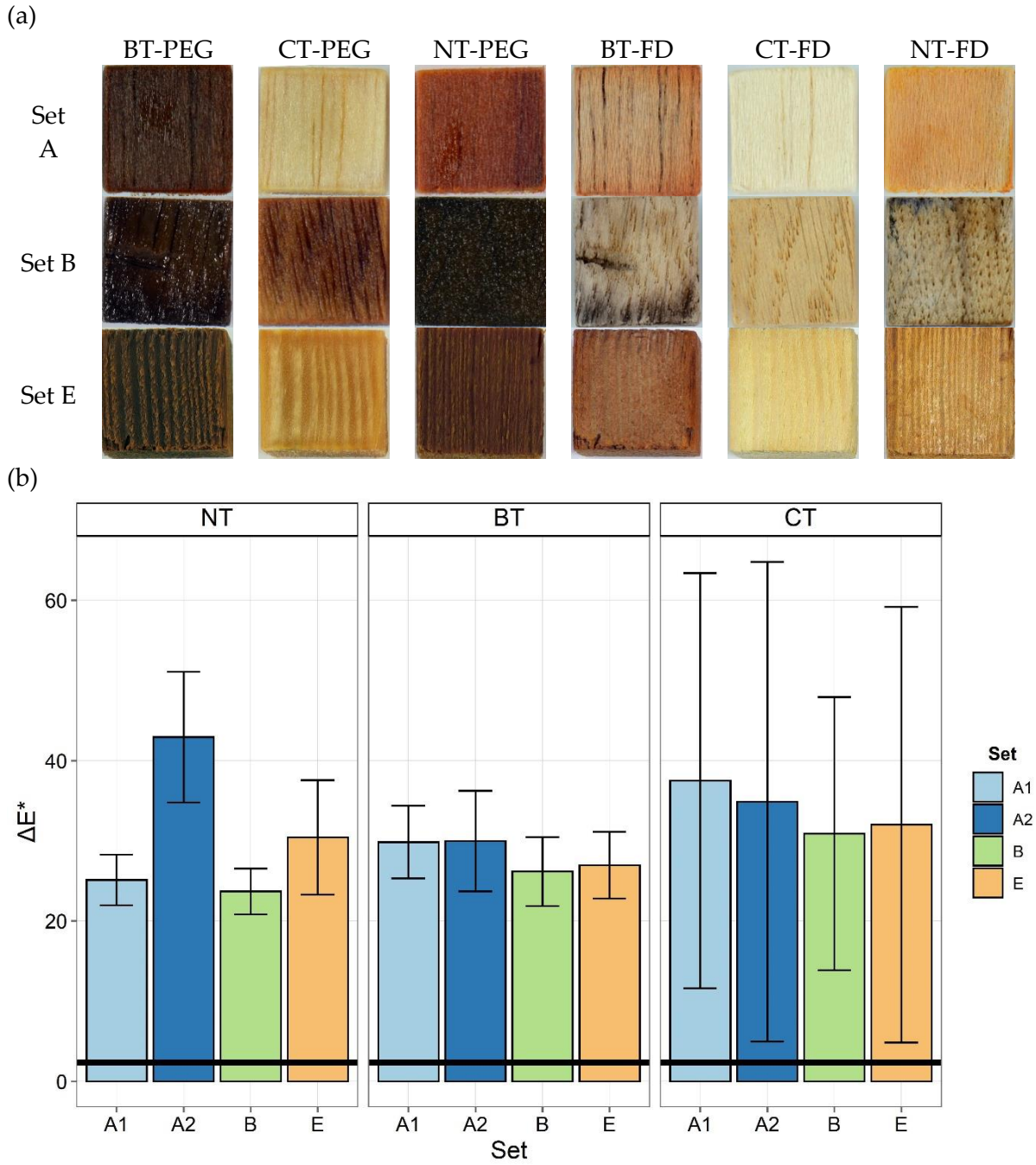

Figure S 16: Mean color variation (ΔE) for contaminated fresh (sets A1, A2, B, E) samples after previous extraction with BT and CT methods and stabilization method (PEG + freeze-drying) with untreated (NT) samples, standard deviation and visual perceivable threshold (ΔE* = 2.3, black line) indicated*

2 – Treatment action in depth

2.1 – Extraction rate

If Raman investigations at the surface on the samples suggested that BT was efficient, characterization of stabilized samples seemed to show otherwise. In addition, it was noticed that some PEG baths get colored during consolidation process. Thus, iron and sulfur content within wood before and after extraction as well as within first PEG consolidation bath were investigated.

To determine the extraction rates for BT and CT methods, one sample per set per treatment was digested in concentrated HNO_3 and the solution analyzed by Inductively Coupled Plasma-Optical Emission Spectroscopy (ICP-OES). The extraction rates for iron and sulfur were calculated based on the concentration of these elements present within wood before and after extraction. The results were compared with data of untreated (NT) samples, as detailed in Table 18.

Table 18: Percentage of iron and sulfur extracted for model oak (set C) and pine (set F) and oak (set D1) and pine (Set G1) WAW samples, depending on the extraction method (BT and CT) applied or for untreated (NT) samples, with standard error indicated in brackets

Set	Iron extracted (%)			Sulfur extracted (%)		
	BT	*CT*	*NT*	*BT*	*CT*	*NT*
Model oak Set C	49.46 (± 0.84)	99.63 (± 0.01)	3.95 (± 1.59)	0.01 (± 0.00)	10.51 (± 7.80)	0.00 (± 0.00)
Model pine Set F	74.59 (± 3.45)	15.75 (± 11.45)	0.00 (± 0.00)	66.66 (± 20.39)	43.30 (± 34.68)	1.82 (± 60.04)
Archaeological oak Set D1	65.15 (± 4.82)	6.56 (± 12.92)	0.00 (± 0.00)	32.12 (± 5.30)	0.00 (± 0.00)	0.00 (± 0.00)
Archaeological pine Set G1	46.16 (± 2.24)	0.00 (± 0.00)	0.00 (± 0.00)	0.00 (± 0.00)	7.26 (± 3.10)	0.0 (± 0.00)

Iron extraction rate was first examined. Regarding BT extraction method, most of the sets presented a rate around or superior to 50 %. The only exception was set D2 (oak WAW) with an extraction rate around 27% (Table S 6). Even if extraction was not complete, these results were promising. Concerning CT extraction method, iron extraction rates were generally higher than those obtained with BT method. Indeed, most of the sets displayed nearly to complete extraction (Table 18 and Table S 6). CT method seemed then generally more efficient for iron extraction than BT method. One can notice that some untreated (NT) samples also displayed iron extraction (sets C and G2), indicating that iron species present get dissolved during the solely immersion in deionized water.

Regarding sulfur extraction, most of the sets treated with BT method presented a rate between 30% and 67%. Only sets C (oak model), D2 (oak WAW) and G1 (pine WAW) presented no sulfur extraction. Quite similar results were observed for CT samples. Indeed, after CT extraction, all oak WAW samples (sets D1, D2 and G2) presented no sulfur extraction while pine WAW (set G1) showed a low extraction rate, around 7% (Table S 8). Therefore, sulfur

extraction seemed more complicated on WAW samples. Concerning the model samples contaminated with IP1, sulfur extraction was around or below 50%, with only exception for fresh balsa (set A, Table S 6). In addition, set A NT samples also displayed an important sulfur extraction (Table S 8). The natural porous structure of balsa may explain these high sulfur extraction rates.

Then, iron and sulfur concentrations were measured within 8% PEG bath used first for consolidation of wood. The consolidation step of the project revealed then that either present Fe and S compounds oxidized (fresh wood samples) or were washed out (model and WAW samples). Indeed, some PEG baths get colored suggesting that some iron and sulfur species were released during consolidation (Figure S 17). Regarding model samples, 8% PEG bath of BT and NT samples were turned brown to orange. CT baths were clear, suggesting that less species may have been released from CT model samples. Regarding WAW samples, PEG bath of CT samples was very dark for oak WAW(sets D1, D2 and G2) and PEG bath of BT samples was orange. The orange coloration is usually associated with iron, Fe content within PEG bath was measured with ICP-OES [37].

Table 19: Iron Fe and sulfur S concentration (mg/l) within 8% PEG bath for model oak (set C) and pine (set F) and oak (set D1) and pine (set G1) WAW samples, depending on the extraction method (BT and CT) applied compared with untreated (NT) samples

Set	**[Fe] (mg/l)**			**[S] (mg/l)**		
	BT	*CT*	*NT*	*BT*	*CT*	*NT*
Model oak – Set C	3.56	0.10	20.02	615.91	682.36	669.99
Model pine – Set F	9.28	0.06	7.70	24.56	76.25	17.83
Archaeological oak – Set D1	0.97	0.84	0.20	47.88	94.04	15.77
Archaeological pine – Set G1	0.03	0.09	0.05	54.21	65.04	27.43

Comparing ICP-OES results obtained, more iron was released in PEG bath by sets C and F model samples, either untreated (NT) or biologically treated (BT) (Table 19). This analysis could imply that not all iron species were extracted during BT method and that the remaining species get extracted by osmotic diffusion during the following consolidation step. Not all sulfur species were extracted either as sulfur was detected in PEG bath (Table 19 and Table S 9). Unlike iron, sulfur was detected in the PEG baths for BT- and CT-treated as well as untreated samples and in high concentration for set C. This is in line with Raman analyses performed. Elemental sulfur was detected on CT samples after extraction and consolidation. Therefore, it appeared that BT and CT extraction methods were efficient in surface but not in depth.

One sample was analyzed per set per protocol and may not be representative of the whole set, explaining the disparity of extraction rates observed between the two extraction methods. To have more representative results, at least two samples should be employed for ICP-OES analyses to avoid mis-interpretation. A reference sample was conserved after extraction methods (samples X-BT-4 and X-CT-4). This sample could be employed for confirmation of the ICP-OES results obtained and validate the tendency observed. An alternative could be to calculate the theoretical sulfur content (g/kg of wood) according to the work of Almkvist et

Persson [33]. Based on the percentage of iron extracted, the theoretical extracted sulfur could be calculated with equation (3).

$$[S]\left(\frac{g}{kg} of\ wood\right) = \frac{109.94 - Fe(\%)}{10.035} \quad (3)$$

As only one samples per method per set was digested, such calculation was not performed, preventing mis interpretation of the results. Thus, if at least two samples are characterized by ICP-OES, salts extraction efficiency could be confirmed. Another possibility to evaluate extracted sulfur would be to calculate the ratio $[SO_4^{2-}]/[S_2O_8^{2-}]$. *T. denitrificans* efficacity to oxidize iron sulfur compounds is measured by calculating the ratio $[SO_4^{2-}]/[NO_3^-]$ [38]. The theorical value of this ratio is set at 1.6 [39]. By measuring the concentration of sulfates and nitrates at the beginning and at the end of the biological extraction, $[SO_4^{2-}]/[NO_3^-]$ is calculated and iron sulfides dissolution ascertained when $[SO_4^{2-}]/[NO_3^-]$ is close to 1.6. The calculation of a similar ratio could be considered to evaluate chemical extraction method. Sulfates and persulfates concentration could be measured at the beginning and the end of chemical extraction method. Theoretical value of $[SO_4^{2-}]/[S_2O_8^{2-}]$ ratio is 0.4. If calculated ratio is close to the theoretical value, one can assume that the iron sulfides dissolution was complete.

Careful interpretation of the ICP-OES data indicated that no correlation could be achieved between the amount of harmful species present and the iron extraction rates measured. Indeed, the model samples (sets C and F) presented iron extraction rates in the same range than WAW samples (sets D1, D2, G1, G2). This pointed out that the proposed BT and CT preventive extraction methods allowed extracting iron even if iron concentration is very low, as it was the case for WAW samples, and so that these preventive extraction methods are both promising. For sulfur extraction, the type of wood species may affect the performances of the extraction methods and not the amount of harmful species present. Even if not all sulfur was extracted, BT and CT presented encouraging results. In addition, BT method seemed to dissolve both acid soluble and insoluble iron sulfides. Raman spectroscopy and SEM-EDS analyses performed on model samples (sets C and F) showed that $Fe_{1-x}S$ and FeS_2 compounds were present on wood. $Fe_{1-x}S$ is classified as acid-soluble phase while FeS_2 as an acid-insoluble one [40]. pH measurements showed that BT occurred at neutral pH. Therefore, $Fe_{1-x}S$ phases should be stable and not dissolved during BT extraction method. Thus, BT displayed encouraging iron extraction rates as no $Fe_{1-x}S$ were identified at the end of biological extraction method. Therefore, employment of siderophores DFO was able to complex iron species from $Fe_{1-x}S$ phases without being in the acidic range. However, not all iron seemed extracted, and SEM-EDS analyses could not be performed at the end of BT method due to instrumental issues. Investigations of phases remaining should be achieved to determine if biological extraction can indeed dissolve acid-soluble iron sulfides, such as partially oxidized mackinawite $Fe_{1-x}S$, and that acid-insoluble phases, such as pyrite FeS_2, were dissolved. On the contrary, CT method occurred at acidic pH also explaining the high iron extraction rate. However, FeS_2 phases were not identified with Raman spectroscopy, but only $Fe_{1-x}S$. Application of SEM-EDS, which detected FeS_2 before extraction methods, would confirm the dissolution of acid-soluble and acid-insoluble iron sulfides.

Still, the results are even more encouraging regarding BT method. As generally no color modification and wood degradation were observed, it would be possible to retreat the samples, with the same extraction method to remove additional harmful iron and sulfur species. Retreatability is a criterium suggested by Appelbaüm when discussing about conservation methodology and BT method fulfill this criterium and thus could be considered to conserve WAW artefacts [3].

To evaluate the depth efficiency of each reagents used in the BT and CT extraction method (DFO and *T. denitrificans* or sodium persulfate and EDTA respectively), sacrificial samples could be cut in half at each extraction step and Raman mapping and/or SEM-EDS analyses carried out on the sections.

2.2 – State of degradation

For consolidation purpose, the samples were immersed in successive PEG solutions with increased concentration (8-40%). However, characteristic bands of PEG overlapped with the characteristic bands of wood on ATR-FTIR spectra (Figure 37). Therefore, it was not possible to calculate the ATR-FTIR ratios and thus to evaluate the effect of the stabilization method on the degradation state of the wood samples. As alternative, maximum water content (MWC) measurements were carried out to evaluate in depth the impact of BT and CT extraction methods toward wood material. Maximum water content (MWC) is a measurement widely employed to evaluate the degree of degradation of waterlogged wood [41], [42]. MWC was calculated after extraction and after stabilization for model and WAW samples and compared with untreated samples (Table 20).

Table 20: Wood degradation grades for model oak (set C) and pine (set F) and oak (set D1) and pine (set G1) WAW samples based on maximum water content (MWC) measurements (0: decay absent; 1: low decay;2: initial decay;3: high decay;4: important decay)

Set	**MWC after extraction**			**MWC after stabilization**		
	BT	*CT*	*NT*	*BT*	*CT*	*NT*
Model oak Set C	4	4	4	2	2	2
Model pine Set F	1	1	2	0	0	0
Archaeological oak Set D1	4	4	4	2	2	2
Archaeological pine Set G1	4	4	4	2	2	1

Characterization of model and WAW samples before being extracted were categorized as highly decayed (Chapter 3). The only exception was set F, due to its relative short burial duration, which was categorized with initial decay (grade 2). After application of the preventive extraction methods (BT and CT), the samples remained in the same category, excepted set F sorted in grade 1 (Table 20). This validated the previous ATR-FTIR ratios calculated (Table 17). After stabilization, all the sets MWC values decreased to lower grade. All the samples previously categorized with important decay (grade 4) were now classified

with grade2, and samples previously categorized in grade 2 (initial decay) were in grade 0 (no decay) after stabilization (Table 20 and Table S 10). Regarding fresh wood simulating WAW samples, balsa followed the same pattern than oak WAW (sets D1, D2, G2) samples while fresh oak and fresh pine displayed lower grades, such as set F (Table S 10).

MWC is based on the weight of the samples above and inside water. To ascertain that the samples do not float during measurement, they were previously placed under vacuum to replace air in the wood pores by water. Despite, balsa samples floated during measurements even if fresh balsa was graded in the same category than WAW samples (sets D1, D2, G1, G2) and presented similar low wood density [42], [43]. The results obtained for WAW samples were then more reliable than for fresh balsa. This observation validated the non-representativity of fresh balsa to simulate WAW. As mentioned in Chapter 3, fresh balsa could eventually be employed to test some degradation or contamination protocols but should be avoided ascertaining novel conservation methods under development.

Model oak and WAW samples remained of the same weight and in the same MWC grade before and after extraction. Set C (oak model) displayed a lower weight m = 0.53 g ± 0.07 in water than set F (pine model) with a weight m = 0.81 g ± 0.12. This is explained by the fact that set F was less decayed. Therefore, MWC seemed a valid complementary method to ATR-FTIR spectroscopy to evaluate wood state of degradation.

However, after stabilization all the samples displayed a lower MWC grade. It could first be assumed that the samples were less decayed after consolidation and freeze-drying. However, this conservation method does not renew degraded wood cells but reinforce wood structure by replacing water with PEG in the wood pores. Immersion in PEG solution resulted the consolidated samples to be heavier and thus having decreased MWC values, as reported in literature [44], [45]. Therefore, MWC measurements performed after stabilization allowed to ascertain that consolidated samples were well impregnated with PEG but not wood degradation state.

Complementary analyses are necessary to determine the impact of stabilization method on the wood substrate. Indeed, the samples were visually altered after freeze-drying (Figure 35). The color change could be due to the deterioration of the wood materials. Therefore, some investigation on the wood composition during and after stabilization were performed. If the presence of iron and sulfur is detected, it is possible that resulting wood degradation also occurs. In particular, tannins concentration was evaluated within 8%PEG bath, where samples were first immersed after extraction. From preliminary analyses carried out, it resulted that tannins were detected in these consolidation baths of both model and WAW samples. Tannin components are water soluble and thus could be released in PEG aqueous solution [46], [47]. Björdal et al already mentioned the release of tannins during consolidation step [48]. This released was characterized by a dark coloration of the PEG solution, as it was observed in some of PEG baths of this study (Figure S 17). Therefore, the stabilization method could damage the wood samples. The purpose of the stabilization method is to conserve the samples and artefacts in their conditions. This discoloration may question the consolidation method employed. Perhaps an alternative procedure should be considered. In fact, oak WAW NT-

samples present a strong discoloration during immersion in 8% PEG solution, even if few could be released within PEG bath as Fe to be extracted was inferior to 0.2 mg/l, which represent less than 1% of iron extracted. In their research, Nguyen et al compared the consolidation of WAW samples with PEG, trehalose and keratin [49]. However, no information about the consolidation bath color and thus a potential release of wood components and wood degradation was mentioned. Therefore, it would be interesting to investigate different consolidation methods in terms of visual modifications and evaluate if one is more appropriate than the others. Also, it would be interesting to determine if the same stabilization method can be applied for all type of wood species (hardwood *vs* softwood).

To better assess the depth of penetration of extraction and wood degradation, further characterization could be also carried out through Raman spectroscopy SEM-EDS, or wood composition analysis. Gierlinger and Schwanninger employed confocal Raman microscopy to observe the composition of the different cell wood layers, as wood Raman bands are well documented [50], [51]. Thereby, it would be for example possible to characterize wood sections before and after extraction by Raman mapping. By comparing the chemical maps obtained, we could evaluate the depth efficiency of extraction and also better ascertain eventual wood degradation occurring at this stage. Moreover, it would be possible to carry out the same analytical protocol on stabilized wood for the determination of wood degradation after stabilization. Observations of the wood cells and unattached cell walls by SEM analyses would also permit to evaluate a potential wood degradation during stabilization. As freeze-drying induce discoloration of wood, it would be interesting to characterize the samples before and after drying. However, wood degradation is not reported after freeze-drying [52]. Yet, tannins are parts of the wood extractives and extractives give their color to wood species [53]. 8% PEG bath analyses showed that some tannins were released during consolidation. During drying, tannins could be trapped in the ice formed and removed by sublimation. This could explain the final visual appearance of stabilized samples. Finally, wood composition could be investigated. Holocellulose and lignin as well as extractives content could be evaluated and ratios Ho/Li (holocellulose content / lignin content) E/Li (extractive content / lignin content) calculated according to literature [42], [54], [55]. By comparing wood content before and after stabilization, we could ascertain the innocuousness of the stabilization method regarding WAW artefacts. All these supplementary investigations could assist wood conservators in selecting the best consolidation and drying method for their purpose. All the proposed analyses are destructive and thus were not deeply investigated during this PhD project, as one of the goals was to define an analytical protocol based on non-invasive and non-destructive methods that could be applied on WAW artefacts. These complementary analyses should be however carried out to better understand ongoing processes during WAW conservation.

Supplementary material 4

CT method displayed generally higher iron extraction rate values compared to BT extraction method. Regarding sulfur, BT extraction method showed more encouraging rates than CT method. As NT-samples also showed some iron and sulfur extraction, the species contained within the impregnated fresh samples may be amorphous compounds that can be easily washed out.

Table S 8: Percentage of iron and sulfur extracted for fresh balsa (set A), oak (set B) and pine (set E) and oak WAW (sets D2 and G2) samples depending on the extraction method (BT and CT) applied or for untreated (NT) samples, with standard error indicated in brackets

Set	Iron extracted (%)			Sulfur extracted (%)		
	BT	*CT*	*NT*	*BT*	*CT*	*NT*
Contaminated fresh balsa Set A	61.97 (± 3.22)	99.88 (± 0.01)	1.26 (± 8.37)	53.37 (± 4.76)	83.07 (± 1.73)	45.75 (± 5.54)
Contaminated fresh oak Set B	72.91 (± 6.11)	62.89 (± 8.37)	0.00 (± 0.00)	41.51 (± 4.30)	0.00 (± 0.00)	0.00 (± 0.00)
Contaminated fresh pine Set E	64.07 (± 3.45)	99.78 (± 0.03)	0.00 (± 0.00)	44.21 (± 6.07)	40.64 (± 6.46)	16.15 (± 9.13)
Archaeological oak Set D2	27.14 (± 5.50)	95.99 (± 0.30)	0.00 (± 0.00)	0.00 (± 0.00)	0.00 (± 0.00)	0.00 (± 0.00)
Archaeological oak Set G2	65.75 (± 6.40)	97.50 (± 0.47)	65.75 (± 6.40)	54.89 (± 1.13)	0.00 (± 0.00)	0.00 (± 0.00)

The PEG solutions get colored independently of the extraction method previously applied. For samples, which were artificially contaminated (represented here by set C), BT and NT PEG solutions turned brown-orange. WAW samples (represented here by set D1) showed less coloration.

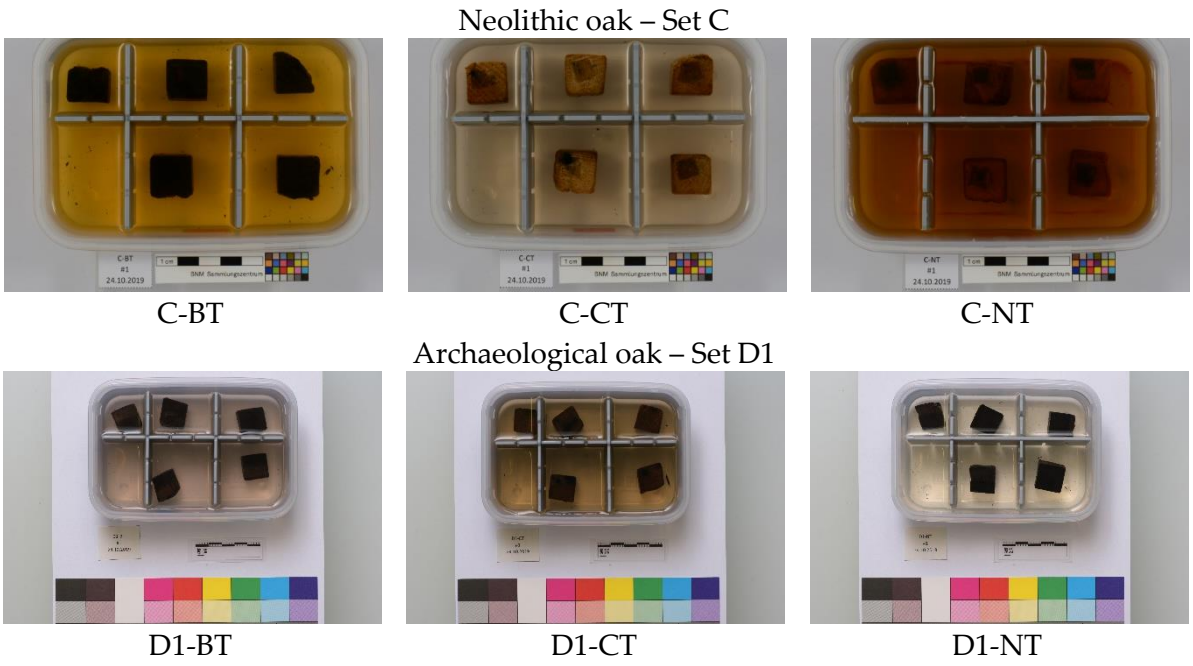

Figure S 17: PEG consolidation first bath for model (set C) and (set D1) WAW oak

Iron was released in 8% PEG bath for contaminated fresh wood samples treated with BT. Regarding CT-samples, iron concentration was very low. Concerning sulfur species, the concentrations measured within 8% PEG bath were important for BT and CT-samples, as well as for NT-samples.

Table S 9: Iron Fe and sulfur S concentration (mg/L) within 8% PEG bath for contaminated fresh (sets A1, A2, B, E) and oak WAW (sets D2, G2) samples, depending on the extraction method (BT and CT) applied compared with untreated (NT) samples

Set	[Fe] (mg/l)			[S] (mg/l)		
	BT	*CT*	*NT*	*BT*	*CT*	*NT*
Contaminated fresh balsa – Set A1	39.91	0.04	1.02	86.34	16.61	8.96
Contaminated fresh balsa – Set A2	18.10	0.02	0.96	859.30	278.52	756.34
Contaminated fresh oak – Set B	5.52	0.20	4.29	620.68	967.01	704.34
Contaminated fresh pine – Set E	11.21	0.04	0.92	587.27	141.71	55.68
Archaeological oak – Set D2	2.10	1.11	0.18	569.89	194.30	181.85
Archaeological oak – Set G2	0.82	0.20	0.36	180.86	462.73	543.72

Wood vibrational bands were not easily identified on stabilized samples as they overlapped some PEG vibrational bands. However, some bands in the range 1600-1500 cm^{-1} could be clearly assigned to lignin but did not allow to calculate ATR-FTIR Ho/Li or Ce/Li ratios and evaluate wood degradation.

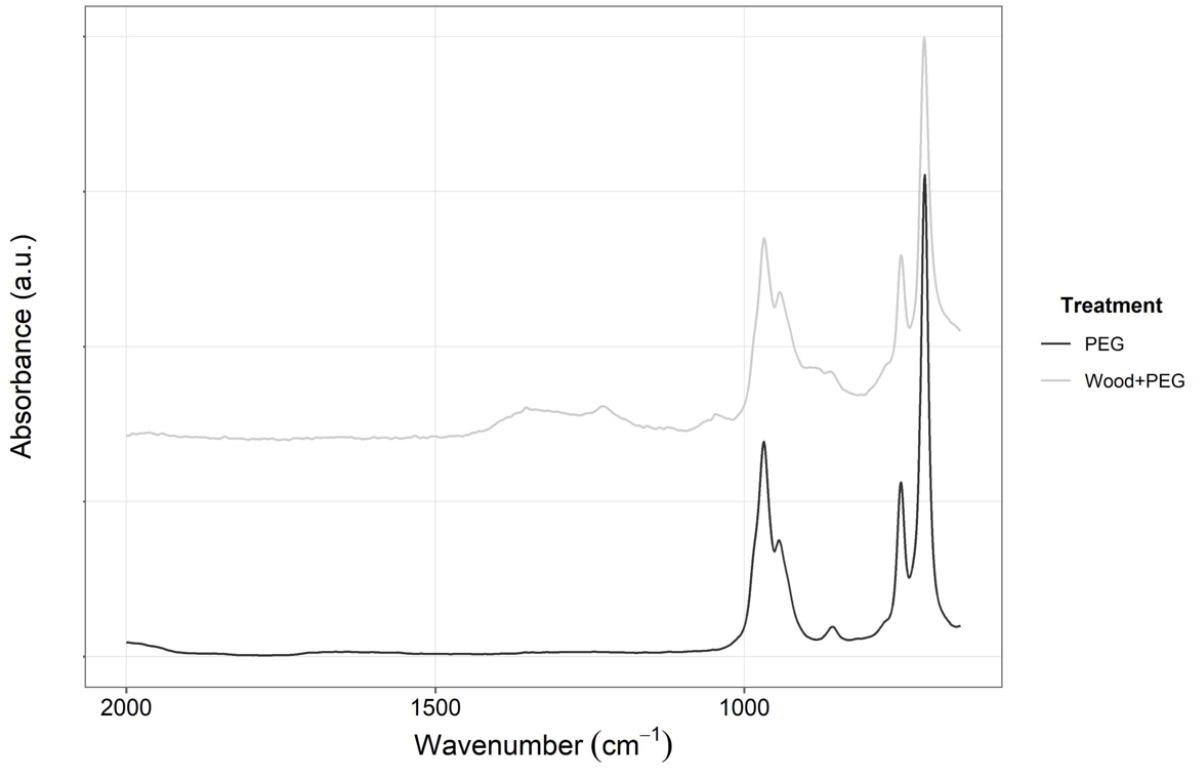

Figure S 18: ATR-FTIR spectrum of PEG polymer (black spectrum) and representative ATR-FTIR spectrum of consolidated wood (grey spectrum)

Fresh oak and fresh pine simulating WAW samples were categorized with initial decay grade (grade 2) while fresh balsa was sorted as grade 4, with WAW samples. As mentioned above, stabilization process decreased the MWC grade, due to the consolidation with PEG that increases samples' weight.

Table S 10: Wood degradation grades for fresh balsa (set A), oak (set B) and pine (set E) and oak WAW (sets D2 and G2) samples based on maximum water content (MWC) measurements (0: decay absent; 1: low decay;2: initial decay;3: high decay;4: important decay)

Set	MWC after extraction			MWC after stabilization		
	BT	*CT*	*NT*	*BT*	*CT*	*NT*
Contaminated fresh balsa Set A	4	4	4	2	2	2
Contaminated fresh oak Set B	1	2	2	2	0	0
Contaminated fresh pine Set E	1	1	1	0	0	0
Archaeological oak Set D2	3	4	3	1	2	1
Archaeological oak Set G2	4	4	4	2	1	2

3 – Evaluation of treatment's efficiency

As defined at the beginning of the Chapter, several criteria were defined to evaluate the efficiency of the proposed preventive extraction methods. Efficiency in terms of visual appearance, wood composition and salts extraction was mainly investigated, as well as retreatability [2], [3]. Yet, other criteria were evaluated, such as the safety towards environment and/or users as well as the cost of each preventive extraction methods. A last point was assessed regarding the acceptation by wood conservators to employ microorganisms to conserve WAW artefacts.

If BT and CT extraction methods comply with appearance criteria of WAW samples, this was not the case for model samples. Indeed, bleaching of CT samples was observed, right after immersion in sodium persulfate solution. Persulfates are known to degrade organic compounds [4]. Also, free iron species released during treatment could catalyze bleaching [16]. In addition, sodium persulfate can induce skin reactions, such as redness or papules [56]. Also, regarding CT method, even if EDTA did not alter wood appearance, its utilization is subject to discussion. Indeed, EDTA and its derivatives (diethylenetriaminepentaacetic acid DTPA and ethylenediamine-N,N′-bis(2-hydroxyphenylacetic acid) EDDHA) present environmental and health issues [20], [57]. Therefore with the view of proposing suitable treatments safe for humans and environment, more eco-friendly and green alternatives could be considered [21], [58]. However, other chelating agents such as oxalic acid or citrates have lower iron extraction rates [21]. Siderophores, such as DFO, are natural iron chelating agents, and not reported as harmful for users. They present then a green alternative to common chelating agents used in the conservation field.

Raman analyses showed that BT extraction method was more efficient than CT as no reduced sulfur compounds were observed. In addition to respect the appearance criteria, the proposed biological preventive method also extracted all iron and sulfur from model and WAW samples. Though, deeper analyses revealed that BT efficiency was only superficial. Indeed, CT displayed higher iron extraction rates with values over 95%. Even if siderophores possess the highest iron affinity, CT was more efficient than BT to chelate and extract iron from model and WAW samples [29], [59]. Two hypotheses could explain such results. The first one is the different diffusion rate of EDTA and DFO. Monitoring of the chelation process showed that EDTA chelated all iron within two days while it took two weeks with DFO to reach similar extraction values [14]. Therefore, EDTA diffuses more easily inside wood due to its low molecular volume respect to siderophores. High diffusion rate could then be considered as a key point for an efficient iron extraction [60]. A prolonged extraction time with DFO would allow a better diffusion of siderophores within wood and thus an increased iron extraction rate. Another possibility would be the different chelating agents concentration. EDTA concentration was higher than DFO (0.125 M *vs* 0.84 mM). EDTA is commercially available with relatively low costs while siderophores are expensive: 1 g of DFO for 140 CHF while a 1 kg of EDTA costs 188 CHF (sigmaaldrich.com/catalog). The elevated price of DFO is a limitation and was the reason of the low concentration employed. As siderophores are naturally produced by bacteria and fungi in iron-deficient environments, one possibility would be to produce siderophores by isolating them from these sources [61]–[63]. However,

this is a long process with a low to median yield and this alternative may not be the easiest to apply by wood conservation departments due to the lack of adequate equipment. Employment of natural chelators may be more respectful of the samples appearance, environment, and users though may not be affordable by all laboratories, unlike CT method.

Unfortunately, if CT was considered more efficient for iron extraction, the same was not true regarding sulfur extraction. Indeed, elemental sulfur was still identified at the surface of CT samples. Except model pine samples contaminated with IP1, no sulfur extraction was observed with CT. Thus, it seemed that the wood type (wood species) affected the sulfur extraction rates observed with CT. Plants require sulfur as nutrient [64]. Sulfur concentration within plants is determined by the uptake of sulfates via the roots or by reduction of sulfates into sulfides [65]. Wood species (hardwood *vs* softwood) seemed to differently interact with the sulfur nutrition process. Thus, sulfur may have more affinity for hardwood species, such as oak, explaining why sulfur was mainly extracted from softwood samples, *i.e.* pine.

On the contrary, BT samples displayed more consistent sulfur extraction rates. Incubation with *T. denitrificans* bacteria allowed dissolution of reduced sulfur species into sulfates ions as described in equation (2). Sulfates are water soluble and can thus be extracted from wood. As strong oxidant, sodium persulfate immersion was proposed to catalyze the dissolution of iron sulfides, converting them into sulfate ions, in the same manner as *T. denitrificans* (equation (1)). It seemed that applying sodium persulfate before EDTA, dissolved sulfate ions may have precipitated as elemental sulfur. It would be interesting to invert the order of sodium persulfate and EDTA in CT protocol. Wood could first be immersed in EDTA solution that will chelate iron present and result in the release of sulfide ions, that should oxidize into sulfate. Immersion in persulfate could then be avoided, as well as the potential bleaching of highly contaminated WAW samples.

If both methods showed their limitations (diffusion rate, cost, discoloration), BT and CT extraction methods have the advantage not to degrade the wood substrate and appeared innocuous as preventive extraction methods. As BT extraction method was not completely efficient but did not induce neither wood degradation, we could envisage to retreat wood and apply different cycles of BT. On the contrary, CT method altered the visual aspect of model samples and to retreat the samples may not be possible without inducing further bleaching. An optimization of the CT method should then be considered. The chemometric approaches carried out on the treated samples gave divergent results. Regarding PCA analysis, BT, CT, and NT samples all gathered in the same cluster, independently of the type of wood species and the amount of harmful salts present. PCA proved that none of the evaluated methods induced wood degradation, unlike ANOVA approach. This second chemometric approach implied that wood material was decayed after treatment. However, ANOVA was performed on the ATR-FTIR ratios of selection vibrational bands while PCA was applied on the whole ATR-FTIR spectra, allowing probably to obtain more reliable classification. To ascertain that the proposed extraction methods did not degrade wood materials, further investigation should be performed, through classical (SEM-EDS) or chemometric (PLS) approaches [66]. Gathering a maximum of information would allow to have a more pertinent evaluation of the

preventive extraction methods and thus allow to convert these methods into real praxis in wood conservation departments.

As the defined preventive extraction methods showed promising results, treated samples were then stabilized with the methods currently used by wood conservators. The samples were consolidated with successive PEG baths for five months and their appearance was not altered. Yet, iron and sulfur were not completely extracted and remained harmful species were released during PEG immersion. Even if the samples were rinsed prior to being consolidated, the rinsing protocol applied was probably not enough. Indeed, it was decided to cease rinsing when constant pH and conductivity reached the values observed for deionized water (pH=5.6, $\Omega_{measured}$ = 1 µS/cm). In addition of optimizing extraction methods, the rinsing part should then not be neglected in future experiments. However, the drying phase of the stabilization method also raised concerns. Indeed, at the end of the treatment, samples discolored while they should conserve their visual aspect.

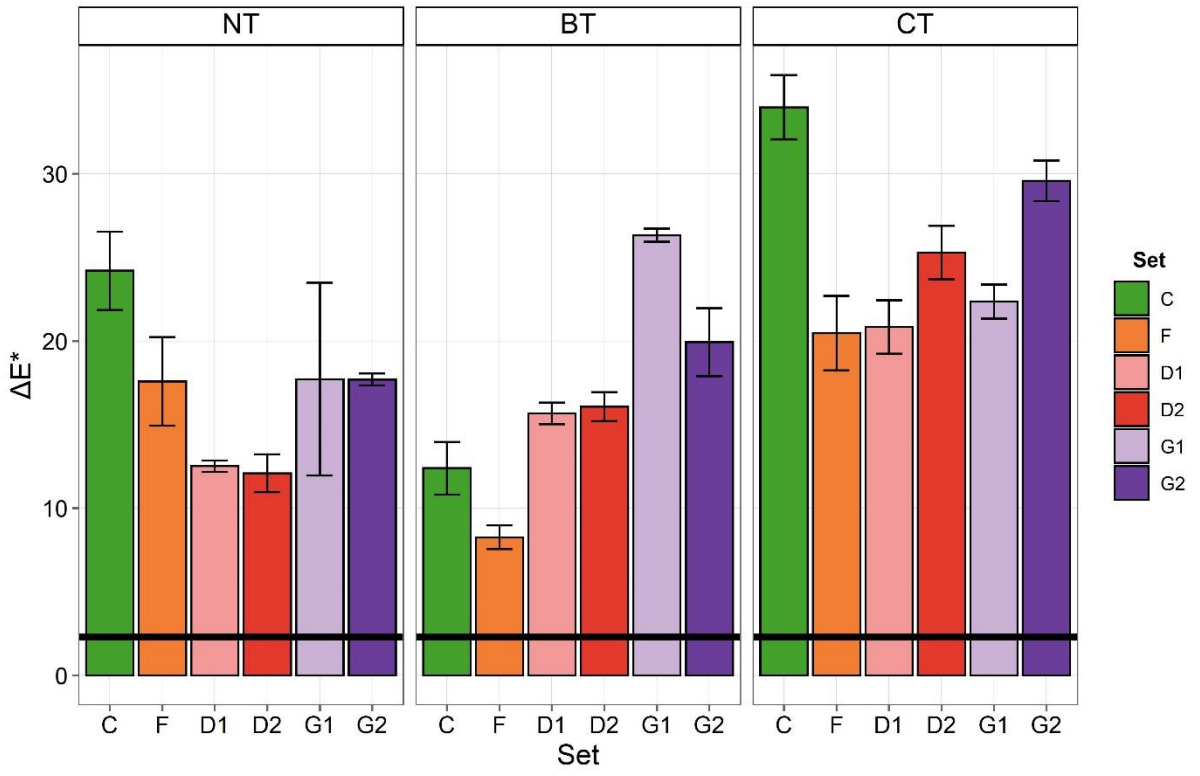

Figure 38: Mean color variation (ΔE) for model oak (set C) and pine (set F) and oak (set D1) and pine (set G1) WAW samples, between extraction (BT: biological treatment, CT: chemical treatment) and stabilization steps with untreated (NT) samples, with standard deviation and visual perceivable threshold (ΔE* = 2.3, black line) indicated*

One can observe on Figure 38 that the drying process induce a visual modification of the samples. Comparing to color variation ΔE* values obtained between before and after extraction (Figure 31), a general increase of ΔE* values was observed. This modification was due to the freeze-drying step. Freeze-drying was selected and performed based on literature study and as a reliable drying process currently used to stabilize WAW artefacts [67]–[69].

Alternatives of freeze-drying are under study. Drying process by dehydration with cyclical pressure drops is a faster drying method though present shrinkage in the same range as freeze-

drying [35]. A recent master thesis performed at the University of Oslo defined also air-drying as an alternative to freeze-drying [70]. However, drying of WAW has to be performed under controlled conditions, to avoid severe and irreversible damages to occur to the wood [8], [71]. Uncontrolled air-drying would imply a collapse of the wood structure due to water evaporation. With an average temperature of 20.8 °C and a relative humidity set at 76%, controlled air-drying would allow to maintain the visual aspect of WAW oak samples. Another study performed on scot pine WAW also demonstrated the efficiency of controlled air-drying method on consolidated samples [72]. Contrary to the study carried out in Oslo, the relative humidity was set at 44% with temperature of the same order. Relative humidity could thus be adapted according to the type of wood species (hardwood *vs* softwood) to avoid discoloration and collapse of the structure. Compared to freeze-drying, this methodology is longer as it lasted 7 weeks for oak WAW and 10 weeks for pine WAW [70], [72]. Though, the results were encouraging.

In particular, it was noticed that the type of wood species influenced the results (ANOVA > 0.05). The optimization of extraction and stabilization methods should take into account this parameter by amending extraction reagents concentration or extraction duration as well as the drying settings. As set G1 samples (pine WAW) discolored after BT and CT extraction methods, an optimization could be considered for the two proposed methods bearing in mind the differences between hard- and softwood species. Wood extractives are responsible for its aspect and their concentration is higher for softwood species [46], [73]. As BT samples bleached, it is possible that some extractives were washed out during this extraction protocol. DFO siderophores showed that they could also lead to some discoloration. Assays on balsa wood samples showed a more important discoloration when the iron was extracted with DFO instead of with pyoverdine (PVD), another siderophores type [14]. By employing PVD instead of DFO, pine WAW may conserve their appearance. However, the time of extraction should be reconsidered as well as PVD may chelate iron differently. In fact Albelda-Berenguer showed that DFO siderophores could reach the samples core, unlike PVD siderophores [14]. Thus, extended extraction times should be considered if PVD is specifically employed for pine WAW. Regarding CT extraction method, the appearance of pine WAW samples showed a reddish hue due to extraction method. Such coloration was already observed in the past on pine WAW treated with different EDTA and derivatives [74]. An appropriate rinsing would remediate to this coloration. Also Almkvist showed that the type of wood species affected extraction rates [60]. Pine wood presented a faster iron extraction compared to oak when treated with DTPA or EDDHA. As for BT method, CT should be optimized for pine wood species. The extraction time could be reduced, preventing an eventual discoloration.

Finally, biotechnologies are more and more applied for the conservation of cultural heritage [75]–[77]. The wood conservators involved in the project supported the use of biological extraction methods. Compared to common chemical extraction method, BT method was quite similar. Conservators approved BT method due to its ease of application combined with the encouraging results obtained. The proposed biological extraction method was performed in laboratories and not in conservation facilities. For conservators to have access to this innovative method, development of a kit could be considered. This kit would contain two

containers, one with siderophores and one with *T. denitrificans*. According to the volume of the object to treat, the quantity of siderophores and bacteria to send should be adjusted. In addition, the conditions of storage of the kit should be determined, to ascertain the efficiency of the biological extraction.

4. Conclusions

The proposed biological (BT) and chemical (CT)preventive extraction methods showed promising results for the preservation of waterlogged archaeological wood. These encouraging results proved the feasibility of extracting iron and sulfur from waterlogged archaeological wood (WAW) fulfilling conservation ethics criteria. In particular, BT extraction method tends to be more efficient. Even if CT showed higher iron extraction rates, BT presented reproductible extraction rates for both iron and sulfur species. The employment of microorganisms regarding the safeguard of WAW proved to be a paradigm towards heritage stakeholders apprehension regards microbial processes. However, BT showed some limitations, such as costs or incomplete extraction, resulting in the oxidation of harmful products still present during following stabilization step. In addition, it resulted that the type of wood species (hardwood *vs* softwood) was an important parameter to consider in order to adjust the extraction parameters. The results presented in this Chapter derived from experiments conducted for the first time, pointing out limitations of BT and CT , but also paving the way to preventive extraction methods as well as eco-friendly and green protocols for WAW conservation.

References

[1] M.-L. E. Florian, "Scope and history of archaeological wood," ACS Publications, 1990.

[2] C. Brandi and C. Déroche, *Théorie de la restauration*. École nationale du patrimoine, 2001.

[3] B. Appelbaum, "Criteria for treatment: reversibility," *J. Am. Inst. Conserv.*, vol. 26, no. 2, pp. 65–73, 1987.

[4] E. M. , G. F. Mangiatordi, I. Weber, C. Goebel, D. Alberga, O. Nicolotti, W. Ruess, and S. Wierlacher, "Persulfate Reaction in a Hair-Bleaching Formula: Unveiling the Unconventional Reactivity of 1, 13-Diamino-4, 7, 10-Trioxatridecane," *ChemistryOpen*, vol. 7, no. 5, pp. 319–322, 2018.

[5] L. W. Matzek and K. E. Carter, "Activated persulfate for organic chemical degradation: a review," *Chemosphere*, vol. 151, pp. 178–188, 2016.

[6] C. G. Björdal, T. Nilsson, and G. Daniel, "Microbial decay of waterlogged archaeological wood found in Sweden Applicable to archaeology and conservation," *Int. Biodeterior. Biodegradation*, vol. 43, no. 1–2, pp. 63–73, 1999.

[7] W. S. Mokrzycki and M. Tatol, "Colour differenceΔ E-A survey," *Mach. Graph. Vis.*, vol. 20, no. 4, pp. 383–411, 2011.

[8] K. M. Wetherall, R. M. Moss, A. M. Jones, A. D. Smith, T. Skineer, D. M. Pickup, S. W. Goatham, A. V. Chadwick, and R. J. Newport, "Sulfur and iron speciation in recently recovered timbers of the Mary Rose revealed via X-ray absorption spectroscopy," *J. Archaeol. Sci.*, vol. 35, no. 5, pp. 1317–1328, 2008.

[9] C. Rémazeilles, K. Tran, E. Guilminot, E. Conforto, and P. Refait, "Study of Fe(II) sulphides in waterlogged archaeological wood," *Stud. Conserv.*, vol. 58, no. 4, pp. 297–307, 2013.

[10] M. Monachon, M. Albelda Berenguer, T. Lombardo, E. Cornet, F. Moll-Dau, J. Schramm, K. Schmidt-Ott, and E. Joseph, "Evaluation of bio-based extraction methods by spectroscopic methods," *Minerals*, vol. 10, no. 2, pp. 1–17, 2020.

[11] M. Albelda Berenguer, M. Monachon, C. Jacquet, P. Junier, C. Rémazeilles, E. J. Schofield and E. Joseph., "Biological oxidation of sulfur compounds in artificially degraded wood," *Int. Biodeterior. Biodegrad.*, vol. 141, pp. 62-70, 2018.

[12] V. Arantes and A. M. F. Milagres, "The effect of a catecholate chelator as a redox agent in Fenton-based reactions on degradation of lignin-model substrates and on COD removal from effluent of an ECF kraft pulp mill," *J. Hazard. Mater.*, vol. 141, no. 1, pp. 273–279, 2007.

[13] L. Wang, W. Yan, J. Chen, F. Huang, and P. Gao, "Function of the iron-binding chelator produced by Coriolus versicolor in lignin biodegradation," *Sci. China Ser. C Life Sci.*, vol. 51, no. 3, pp. 214–221, 2008.

[14] M. Albelda-Berenguer, "Biological strategies for the preservation of waterlogged archaeological wood," Universtiy of Neuchâtel, 2020.

[15] K. Granholm, L. Harju, and A. Ivaska, "Desorption of metal ions from kraft pulps. Part 1. Chelation of hardwood and softwood kraft pulp with EDTA," *BioResources*, vol. 5, no. 1, pp. 206–226, 2010.

[16] G. P. Anipsitakis and D. D. Dionysiou, "Radical generation by the interaction of transition metals with common oxidants," *Environ. Sci. Technol.*, vol. 38, no. 13, pp. 3705– 3712, 2004.

[17] L. R. Bennedsen, J. Muff, and E. G. Søgaard, "Influence of chloride and carbonates on the reactivity of activated persulfate," *Chemosphere*, vol. 86, no. 11, pp. 1092–1097, 2012.

[18] G. Taglieri, V. Daniele, L. Macera, R. Schweins, S. Zorzi, M. Capron, G. Chaumat, and C. Mondelli, "Sustainable nanotechnologies for curative and preventive wood deacidification treatments: An eco-friendly and innovative approach," *Nanomaterials*, vol. 10, no. 9, pp. 1–16, 2020.

[19] S. Fierro-Mircovich, K. Tran, G. Chaumat, and T. Guiblin, "Pyrite removal on small sized archaeological artefacts: the aresquiers 10 bilge pump example," in *14th ICOMCC Wet Organic Archaeological Materials Working Group Confreence, Portsmouth*, 2019.

[20] C. Oviedo and J. Rodríguez, "EDTA: the chelating agent under environmental scrutiny," *Quim. Nova*, vol. 26, no. 6, pp. 901–905, 2003.

[21] C. Pelé, E. Guilminot, S. Labroche, G. Lemoine, and G. Baron, "Iron removal from waterlogged wood : Extraction by electrophoresis and chemical treatments," *Stud. Conserv.*, vol. 60, no. 3, pp. 1–17, 2013.

[22] K.-Y. L. Julian Bosch Guntram Jordan Kyoung-Woong Kim and Rainer U. Meckenstock, "Anaerobic, Nitrate-Dependent Oxidation of Pyrite Nanoparticles by Thiobacillus denitrificans," *Est*, pp. 1–11, 2012.

[23] M. Monachon, M. Albelda-Berenguer, and E. Joseph, "Biological oxidation of iron sulfides," in *Advances in applied microbiology*, vol. 107, Elsevier, pp. 1–27, 2019.

[24] C. Baeza, C. Oviedo, C. Zaror, J. Rodríguez, and J. Freer, "Degradation of EDTA in a total chlorine free cellulose pulp bleaching effluent by UV/H2O2 treatment," *J. Chil. Chem. Soc.*, vol. 52, no. 1, pp. 1069–1072, 2007.

[25] S. Thorgeirsdottir, "Desalination of Archaeological Composite Objects Consisting of Wrought Iron and Wood/Bone. With Focus on the Iron Component.," 2015.

[26] B. MEYER, "Chapter 12 - Industrial Uses of Sulfur and Its Compounds," *B. B. T.-S. MEYER Energy, and Environment*, Ed. Elsevier, pp. 279–290, 1977.

[27] G. Almkvist, S. Norbakhsh, I. Bjurhager, and K. Varmuza, "Prediction of tensile strength in iron-contaminated archaeological wood by FT-IR spectroscopy-a study of

degradation in recent oak and Vasa oak," *Holzforschung*, vol. 70, no. 9, pp. 855–865, 2016.

[28] E. Pecoraro, B. Pizzo, A. Alves, N. Macchioni, and J. C. Rodrigues, "Measuring the chemical composition of waterlogged decayed wood by near infrared spectroscopy," *Microchem. J.*, vol. 122, pp. 176–188, 2015.

[29] M. Albelda-Berenguer, M. Monachon, and E. Joseph, "Siderophores: From natural roles to potential applications," *Adv. Appl. Microbiol.*, vol. 106, p. 193, 2019.

[30] B.-Z. Zhu, J.-G. Zhu, R.-M. Fan, and L. Mao, "Metal-independent pathways of chlorinated phenol/quinone toxicity," in *Advances in Molecular Toxicology*, vol. 5, Elsevier, pp. 1–43, 2011.

[31] H. Boukhalfa and A. L. Crumbliss, "Chemical aspects of siderophore mediated iron transport," *Biometals*, vol. 15, no. 4, pp. 325–339, 2002.

[32] M. I. M. Soares, "Denitrification of groundwater with elemental sulfur," *Water Res.*, vol. 36, no. 5, pp. 1392–1395, 2002.

[33] G. Almkvist and I. Persson, "Extraction of iron compounds from wood from the Vasa," *Holzforschung*, vol. 60, no. 6, pp. 678–684, 2006.

[34] A. León, , P. Reuquen, C. Garín, R. Segura, P. Vargas, P. Zapata, and P. A. Orihuela, "FTIR and Raman characterization of TiO2 nanoparticles coated with polyethylene glycol as carrier for 2-methoxyestradiol," *Appl. Sci.*, vol. 7, no. 1, p. 49, 2017.

[35] E. A. Sanya, S.-A. Rezzoug, and K. Allaf, "A new method for drying waterlogged wooden artefacts: Comparison of cyclical pressure drops with conventional methods," *Chem. Eng. Res. Des.*, vol. 81, no. 9, pp. 1243–1249, 2003.

[36] Y. Fors, "Sulfur-Related Conservation Concerns for Marine Archaeological Wood,. 2008.

[37] A. C. Scheinost and U. Schwertmann, "Color identification of iron oxides and hydroxysulfates: use and limitations," *Soil Sci. Soc. Am. J.*, vol. 63, no. 5, pp. 1463–1471, 1999.

[38] S. Vaclavkova, C. J. J??rgensen, O. S. Jacobsen, J. Aamand, and B. Elberling, "The Importance of Microbial Iron Sulfide Oxidation for Nitrate Depletion in Anoxic Danish Sediments," *Aquat. Geochemistry*, vol. 20, no. 4, pp. 419–435, 2014.

[39] P. Justin and D. P. Kelly, "Growth kinetics of Thiobacillus denitrificans in anaerobic and aerobic chemostat culture," *Microbiology*, vol. 107, no. 1, pp. 123–130, 1978.

[40] D. Rickard and G. W. Luther, "Chemistry of Iron Sulfides," *Chem. Rev.*, vol. 107, no. 2, pp. 514–562, 2007.

[41] N. Macchioni, C. Capretti, L. Sozzi, and B. Pizzo, "Grading the decay of waterlogged archaeological wood according toanatomical characterisation. The case of the Fiavé site (N-E Italy)," *Int. Biodeterior. Biodegrad.*, vol. 84, pp. 54–64, 2013.

[42] G. Giachi, C. Capretti, N. Macchioni, B. Pizzo, and I. D. Donato, "A methodological approach in the evaluation of the efficacy of treatments for the dimensional stabilisation of waterlogged archaeological wood," *J. Cult. Herit.*, vol. 11, no. 1, pp. 91–101, 2010.

[43] M. Borrega, P. Ahvenainen, R. Serimaa, and L. Gibson, "Composition and structure of balsa (Ochroma pyramidale) wood," *Wood Sci. Technol.*, vol. 49, no. 2, pp. 403–420, 2015.

[44] M. Broda, B. Mazela, and K. Radka, "Methyltrimethoxysilane as a stabilising agent for archaeological waterlogged wood differing in the degree of degradation," *J. Cult. Herit.*, vol. 35,pp. 129-139, 2018.

[45] G. Giachi, C. Capretti, I. D. Donato, N. Macchioni, and B. Pizzo, "New trials in the consolidation of waterlogged archaeological wood with different acetone-carried products," *J. Archaeol. Sci.*, vol. 38, no. 11, pp. 2957–2967, 2011.

[46] R. M. Rowell, R. Pettersen, J. S. Han, J. S. Rowell, and M. A. Tshabalala, "Cell wall chemistry," *Handb. wood Chem. wood Compos.*, vol. 2, 2005.

[47] G. J. Ritter and L. C. Fleck, "Chemistry of wood," *Ind. Eng. Chem.*, vol. 14, no. 11, pp. 1050–1053, 1922.

[48] C. G. Björdal, T. Nilsson, and R. Petterson, "Preservation, storage and display of waterlogged wood and wrecks in an aquarium:'Project Aquarius,'" *J. Archaeol. Sci.*, vol. 34, no. 7, pp. 1169–1177, 2007.

[49] T. D. Nguyen, Y. Kohdzuma, R. Endo, and J. Sugiyama, "Evaluation of chemical treatments on dimensional stabilization of archeological waterlogged hardwoods obtained from the Thang Long Imperial Citadel site, Vietnam," *J. Wood Sci.*, vol. 64, no. 4, pp. 436–443, 2018.

[50] N. Gierlinger and M. Schwanninger, "Chemical imaging of poplar wood cell walls by confocal Raman microscopy," *Plant Physiol.*, vol. 140, no. 4, pp. 1246–1254, 2006.

[51] U. P. Agarwal and S. A. Ralph, "FT-Raman Spectroscopy of Wood : Identifying Contributions of Lignin and Carbohydrate Polymers in the Spectrum of Black Spruce (Picea mariana)," *Applied Scpectro.*, vol. 51, no. 11, pp. 1648–1655, 1997.

[52] L. Babiński, "Influence of pre-treatment on shrinkage of freeze-dried archaeological oak-wood," *Acta Sci. Pol. Silv. Colendar. Rat. Ind. Lignar*, 2007.

[53] A. C. Wiedenhoeft and R. B. Miller, "2. Structure and Function of Wood," *Handb. Wood Chem. Wood Compos.*, 2005.

[54] Tappi, "Lignin in Wood and Pulp," *T222 Om-02*, pp. 1–7, 2011, doi: 10.1023/a:1019003230537.

[55] P. Basu, *Biomass gasification, pyrolysis, and torrefaction: practical design and theory*. Academic press, 2018.

[56] S. Pang and M. Z. Fiume, "Final report on the safety assessment of Ammonium, Potassium, and Sodium Persulfate.," *Int. J. Toxicol.*, vol. 20, pp. 7–21, 2001.

[57] J. Arts, S. Bade, M. Badrinas, N. Ball, and S. Hindle, "Should DTPA, an Aminocarboxylic acid (ethylenediamine-based) chelating agent, be considered a developmental toxicant?," *Regul. Toxicol. Pharmacol.*, vol. 97, pp. 197–208, 2018.

[58] P. da Rocha Patrício, M. C. Mesquita, L. H. M. da Silva, and M. C. H. da Silva, "Application of aqueous two-phase systems for the development of a new method of cobalt (II), iron (III) and nickel (II) extraction: A green chemistry approach," *J. Hazard. Mater.*, vol. 193, pp. 311–318, 2011.

[59] J. B. Neilands, "Siderophores: structure and function of microbial iron transport compounds," *J. Biol. Chem.*, vol. 270, no. 45, pp. 26723–26726, 1995.

[60] G. Almkvist, *The chemistry of the Vasa*. 2008.

[61] E. Butaitė, J. Kramer, S. Wyder, and R. Kümmerli, "Environmental determinants of pyoverdine production, exploitation and competition in natural Pseudomonas communities," *Environ. Microbiol.*, vol. 20, no. 10, pp. 3629–3642, 2018.

[62] M. Chiani, A. Akbarzadeh, A. Farangi, M. Mazinani, Z. Saffari, K. Emadzadeh, and M. R. Mehradi, "Optimization of culture medium to increase the production of desferrioxamine B (Desferal) in Streptomyces pilosus.," *Pakistan J. Biol. Sci. PJBS*, vol. 13, no. 11, pp. 546–550, 2010.

[63] M. Chiani, A. Akbarzadeh, A. Farhangi, and M. R. Mehrabi, "Production of desferrioxamine B (Desferal) using corn steep liquor in Streptomyces pilosus.," *Pakistan J. Biol. Sci. PJBS*, vol. 13, no. 23, pp. 1151–1155, 2010.

[64] H. Rennenberg, S. Schneider, and P. Weber, "Analysis of uptake and allocation of nitrogen and sulphur compounds by trees in the field," *J. Exp. Bot.*, vol. 47, no. 10, pp. 1491–1498, 1996.

[65] H. Rennenberg, "The significance of ectomycorrhizal fungi for sulfur nutrition of trees," *Plant Soil*, vol. 215, no. 2, pp. 115–122, 1999.

[66] M. Cocchi, A. Biancolillo, and F. Marini, "Chapter Ten - Chemometric Methods for Classification and Feature Selection," in *Data Analysis for Omic Sciences: Methods and Applications*, vol. 82, J. Jaumot, C. Bedia, and R. B. T.-C. A. C. Tauler, Eds. Elsevier, pp. 265–299, 2018.

[67] U. Schnell and P. Jensen, "Determination of maximum freeze drying temperature for PEG-impregnated archaeological wood," *Stud. Conserv.*, vol. 52, no. 1, pp. 50–58, 2007.

[68] K. Straetkvern, "From promising theories to praxis - conservation of a large oak barque stern with d-mannitol," in *14th ICOM-CC Wet Organic Archaeological Materials Working Group Confreence, Portsmouth*, 2019.

[69] D. Gregory, P. Jensen, and K. Strætkvern, "Conservation and in situ preservation of wooden shipwrecks from marine environments," *J. Cult. Herit.*, vol. 13, no. 3 SUPPL., pp. S139–S148, 2012.

[70] K. S. Hennum-simmonds, "A Study of Alternatives to Freeze-Drying A Study of Alternatives to Freeze-Drying," 2020.

[71] D. W. Grattan and R. W. Clarke, "Conservation of waterlogged wood," in *Conservation of marine archaeological objects*, Elsevier, pp. 164–206, 1987.

[72] M. Fejfer, J. Majka, and M. Zborowska, "Dimensional Stability of Waterlogged Scots Pine Wood Treated with PEG and Dried Using an Alternative Approach," *Forests*, vol. 11, no. 12, p. 1254, 2020.

[73] M. Ek, G. Gellerstedt, and G. Henriksson, *Wood chemistry and biotechnology*, vol. 1. Walter de Gruyter, 2009.

[74] G. Almkvist, "Iron Removal from Waterlogged Wood." in *12th ICOM-CC Wet Organic Archaeological Materials Working Group Conference, Istanbul, Turkey* 2013.

[75] E. Joseph and P. Junier, "Metabolic processes applied to endangered metal and wood heritage objects: Call a microbial plumber!," *N. Biotechnol.*, vol. 56, pp. 21–26, 2020.

[76] F. Palla and G. Barresi, *Biotechnology and conservation of cultural heritage*. Springer, 2017.

[77] G. Ranalli, G. Alfano, C. Belli, G. Lustrato, M. P. Colombini, I. Bonaduce, E. Zanardini, P. Abbruscato, F. Cappitelli, and C. Sorlini, "Biotechnology applied to cultural heritage: biorestoration of frescoes using viable bacterial cells and enzymes," *J. Appl. Microbiol.*, vol. 98, no. 1, pp. 73–83, 2005.

Chapter 5:Conclusions and perspectives

Waterlogged archaeological wood (WAW) present severe conservation issues. Iron and sulfur species accumulated during burial time and oxidized once the artefacts are recovered and exposed to different oxygen concentration and relative humidity [1]. Acidification and salts efflorescence are produced, compromising artefacts' structure [2]. Therefore, the extraction of these harmful species is imperative to preserve the recovered WAW artefacts.

Over the last decade, several treatments were tested, employing alkaline conditions or strong iron chelating agents [3], [4]. Facing their limits, alternative treatments were also investigated [5]–[7]. In particular, the utilization of microorganisms for the conservation of cultural heritage materials raised more and more interest [8].

MICMAC (Microbes for Archaeological wood Conservation) is an interdisciplinary project which aims to develop an innovative bio-based extraction method for iron and sulfur species present within WAW before objects stabilization. This eco-friendly approach aims to respect the integrity of the artefacts, be innocuous for users and the environment, as well as stable in time or retreatable [9], [10]. To evaluate the feasibility of the proposed biological extraction method (BT), a chemical extraction method (CT) was also investigated for comparison. The effects of BT and CT extraction methods were examined on selected WAW samples, based on a specific analytical protocol [11]–[14]. To ascertain the different results obtained, a chemometrics approach was performed.

This PhD thesis was involved in the development of a protocol to prepare WAW mock-ups (*i.e.*, degradation of carbohydrates and iron sulfides contamination) and in the evaluation of preventive biological and chemical extraction methods. To build a robust chemometrics approach, specific experimental design and data pre-processing were achieved.

A specific analytical protocol was also developed with the objective of being applied by end-users and thus relied mainly on non-destructive and non-invasive characterization methods, such as colorimetry measurements and ATR-FTIR spectroscopy.

The preparation of WAW model samples was studied. These samples would replicate the main characteristics of WAW artefacts, meaning a low carbohydrates content and accumulation of iron and sulfur species within wood substrate.

Poles of oak and board of pine recovered from freshwater sites in Switzerland were characterized beforehand and were considered as WAW reference samples (Chapter III). As reported in literature, reference WAW samples showed a decay pattern typical of erosion bacteria with characteristic holocellulose vibrational bands being weak or absent from ATR-FTIR spectra [12], [15]–[18]. However, iron and sulfur concentration was low to null, unlike the estimated content in the *Vasa* warship about 2 tons of sulfur and 5 tons of iron [4], [19].

Chemical and biological degradation protocols were then studied to induce degradation of carbohydrates on fresh oak and pine in order to replicate WAW samples. These wood species were selected as representative of hardwood and softwood species mainly reported on WAW artefacts [20]–[22]. It revealed that one-week water immersion under vacuum (chemical protocol) enhanced the degradation of carbohydrates, as validated by chemometrics approach. Contrary to that reported in literature, the presence of metal pieces did not cause further

degradation [23]. Fungal degradation (biological protocol) was less efficient than this chemical protocol to degrade carbohydrates content though penetrating deeper within the wood samples. In general, it was observed that oak wood samples were more degraded than pine samples. Thus, the studied degradation protocols were more efficient on hardwood species, as previously reported in literature [24], [25]. However, even if ATR-FTIR spectra showed an intensity decrease of vibrational bands of holocellulose, deeper investigation conducted on degraded samples demonstrated that this degradation was limited to wood surface. Holocellulose content (HC) of degraded samples was in the same range as HC of untreated fresh samples. Therefore, the developed chemical degradation protocol investigated is encouraging as it enables the preparation of WAW model samples from fresh wood. Though, some optimization should be considered. Hence, naturally degraded samples (Neolithic oak and lake pine) were selected to go further in the modelling of WAW. Neolithic oak was recovered from a freshwater site, such as reference WAW samples. As for reference WAW, the content of carbohydrates was low such as the contamination content. On the contrary, lake pine showed a lower degradation of carbohydrates than oak but still present some iron and sulfur species. Such differences could be explained by their respective burial time. Indeed, Neolithic oak was dated from 2753 BC while lake pine from 1878 AC. This was also observed with ATR-FTIR spectroscopy, where intense holocellulose bands at 1059 and 1034 cm^{-1} were still identified for lake pine samples but not for Neolithic oak [18]. Yet, both naturally degraded sets did not show vibrational bands at 1738 and 898 cm^{-1}, attributed to xylan stretching and cellulose deformation, respectively, indicating a degradation of carbohydrates also for lake pine samples [26].

In addition to degradation of carbohydrates, WAW model samples were artificially contaminated with iron and sulfur species. Contamination protocol was applied on artificially and naturally degraded wood samples. The selected contamination protocol proved its efficiency to form iron sulfide phases and was referred to as IP1 [7], [27]. When applied to artificially degraded fresh oak and pine, major differences were observed. Raman spectroscopy allowed to identify elemental sulfur (α-S_8) on oak samples while partially oxidized mackinawite ($Fe_{1-x}S$) was identified on pine samples. It seemed the type of wood species impacted on which phase was formed. However, $Fe_{1-x}S$ was only detected for naturally degraded samples. Complementary EDS analyses suggested the formation of iron disulfides, such as pyrite or marcasite (FeS_2). The absence of $Fe_{1-x}S$ phases on fresh oak may be explained by the extractives content, such as tannins that can interact with ferrous iron and form Fe^{2+}-tannins complexes [28]. Tannins being soluble in cold water were probably released during the one-week water immersion under vacuum or during the following immersion in $FeCl_2 \cdot 4H_2O$ 0.5 M used in IP1 protocol, compromising the formation of iron sulfides. Therefore, tannins should be all extracted from fresh oak before the application of degradation and contamination protocols. This would allow to degrade wood and prevent the precipitation of elemental sulfur instead of iron sulfides. It resulted from the investigation that naturally degraded samples were more representative model WAW samples.

Further investigations on fresh wood species could be performed to optimize the degradation of carbohydrates content. It was demonstrated that cellulose degrades under acidic conditions

[29]. Therefore, fresh oak and pine could be immersed in an acidic solution under vacuum, to induce further degradation of carbohydrates. As fungal degradation penetrated deeper within wood, a combination of chemical and biological protocols could be considered. It was reported that the growth of *Chaetonium globosum*, employed for biological degradation, is enhanced by chlorinated acidic solution [30]. It would be then possible to immerse fresh wood in HCl solution under vacuum and to then expose them to fungi degradation. In addition, immersion in aqueous HCl solution would allow the release of tannins in solution, promoting degradation of carbohydrates. The current setting envisaged one-week immersion could be extended, renewing HCl every week, until the solution remained colorless. This would indicate that no more tannins are released and thus that iron sulfides could form, especially for hardwood species (*i.e.*, oak). Additional assays with other hardwood and softwood species, such as beech (*Fagus*)or spruce (*Picea*), could be performed, to determine if all hardwood and softwood species behave the same or if other parameters should be considered, when artificially degrading fresh wood. Furthermore, only an unstable iron sulfide phase $Fe_{1-x}S$ was identified on WAW model samples but is not observed on WAW artefacts. Instead, the formation of iron sulfide FeS and iron disulfide FeS_2 phases should be investigated. For instance, $Na_2S{\cdot}9H_2O$ solution concentration could be amended so iron/sulfur (Fe:S) ratio is set to Fe:S = 1:1 for mackinawite (FeS) and to Fe:S = 1:2 for pyrite (FeS_2) [14]. Other contamination protocols could be explored as well. Hence, Rickard et Luther reported that mackinawite (FeS) could form when metallic iron is poured in sulfides solution [31].

Once the reference samples were characterized and WAW model samples prepared, sets were formed to evaluate the proposed preventive biological and chemical extraction methods (Chapter IV):

- Artificially degraded samples: sets A (fresh balsa), set B (fresh oak) and set E (fresh pine)
- Naturally degraded model samples: set C (Neolithic oak) and set F (lake pine)
- WAW samples: sets D1, D2, G2 (archaeological WAW oak) and set G1 (archaeological WAW pine)

Sets C, D1, D2, F, G1 and G2 were mainly investigated, being more representative of WAW artefacts. For each set, six samples were employed per investigated extraction method, and six samples remained as untreated (NT) samples in deionized water, for a total of eighteen samples.

The appearance of BT samples remained dark, with a low color variation ΔE^*, except for pine WAW (set G1). This set displayed an altered appearance, with a light hue. In fact, siderophores can be employed as bio-bleaching agents [32]. Desferoxamine (DFO) siderophores were used for BT extraction method. DFO seemed then innocuous regarding hardwood species, such as oak, but more aggressive towards softwood species (pine). Other siderophores such as pyoverdine could be also employed depending on the type of wood species to prevent the discoloration of pine WAW. Regarding CT extraction method, model samples (sets C and F) presented a bleached appearance while WAW samples (sets D1, D2, G1, G2) were slightly of light color . Such discoloration was observed when CT samples were immersed with sodium

persulfate solution. Persulfate $S_2O_8^{2-}$ ions are known as bleaching agents, whose action is catalyzed in presence of iron [33]. Model samples (sets C and F) had a high iron concentration in wood, that can catalyze a bleaching action of persulfates, explaining why these samples were more visually altered than WAW samples. Thus prior to treat WAW samples with persulfates, a maximum iron concentration could be defined to avoid bleaching. As observed with BT, pine WAW (set G1) final hue differed from oak WAW. While G1-BT presented a light hue, G1 CT samples presented a red hue, usually observed on WAW artefacts treated with ethylenediaminetetraacetic acid (EDTA) and its derivatives [4]. Such staining can be remediated by rinsing the samples with deionized water. Nevertheless, if some samples were visually altered, none of the evaluated extraction methods showed a degradation of wood content. ATR-FTIR spectra of BT, CT and NT-samples clustered in the PCA score plot, proving the proposed preventive extraction methods being harmless for wood materials.

Still, the evaluated extraction methods presented some limitations. If BT generally respects the visual aspect of the samples and was innocuous for wood materials, the extraction of iron and sulfur species was not completely achieved. Iron extraction rate was in the range 30-70%, lower than rates generally obtained with current chemical methods, as observed on some CT samples [4], [34]. Indeed, iron extraction rates of CT method was over 90% for sets C, D2 and G2 (oak model and oak WAW). The other sets (pine model and pine WAW) presented minor or no extraction. Despite its low iron extraction rate, BT method was more reproducible than CT application and was thus encouraging. Concerning sulfur extraction, 30 to 65% of sulfur was extracted with BT method while only few sets showed sulfur extraction after CT application. Therefore, BT extraction method was more efficient than CT method to remove the harmful species from model and WAW samples. The microorganisms employed during BT method permitted to chelate iron (DFO siderophores) as to dissolve iron sulfides and/or elemental sulfur (*Thiobacillus denitrificans* strain) [35], [36]. Once DFO complexed iron, *T. denitrificans* could interact remaining with the sulfur phases or moieties and convert them into soluble sulfates ions. On the contrary, sulfur species remained present on CT samples, as showed by Raman spectroscopy. Sodium persulfate immersion was performed to enhance iron sulfides dissolution into sulfate ions and EDTA is known to be a strong iron chelating agent. Though, the sulfur species were neither solubilized nor extracted. By changing the order of immersion, EDTA/sodium persulfate instead of sodium persulfate/EDTA, most of iron could be removed from wood and then the remaining reduced sulfur phases or moieties present would be converted to sulfates. In addition, by removing iron with EDTA prior sodium persulfate immersion, bleaching of wood could be avoided. Furthermore, untreated NT samples generally displayed no iron or sulfur extraction. This implies that the phases present in these samples were quite stable and poorly dissolved in solely deionized water.

This study proved that the preservation of WAW samples with bio-based method is a promising alternative to current chemical method. Unlike CT method, the microorganisms employed during BT were not reported as harmful for users and environment. Indeed, wood was then less altered than with chemical reagents, and no degradation of carbohydrates was induced. Yet, the obtained extraction rates showed that not all targeted species were removed. This was also highlighted during the stabilization of the samples with corrosion products such

as lepidocrocite (γ-FeOOH) identified on some BT samples. A possibility would be to retreat the samples, with BT. As BT extraction method showed its innocuousness toward wood material, having a second biological extraction could be foreseen. Retreatability is one criteria defined in conservation ethics when proposing new treatments [10]. One has to remember that a perfect solution does not exist, and every proposed method has its limit. Thus, a complete iron and sulfur extraction may not be achieved. However, as for desalination of archaeological iron objects, a threshold of remaining iron and sulfur species could be determined [37].

Therefore, BT could be considered as a potential preventive extraction method to conserve WAW artefacts. To ascertain the versatility of the proposed BT extraction method, other WAW samples should be treated. For instance, marine WAW artefacts present different state of degradation and contamination degree[21]. Applying BT on marine WAW samples would validate the feasibility of BT for any type of WAW artefacts. In addition, the depth of penetration could be evaluated. On real WAW artefacts, iron and sulfur contamination was mainly detected in the two first centimeters of the artefacts [4]. The samples employed in this study were wood cubes of 2x2x2 cm^3. Thereby, it was not possible to determine if DFO and *T. denitrificans* could reach 2-cm depth, and which extraction parameters (time, concentration) could be adapted to optimize reagents penetration.

This study also accentuated the limitation of freeze-drying conservation method. As already observed, application of freeze-drying of WAW samples altered their visual appearance [38]. Thereby, alternative, such as controlled air drying, could be examined [39]. Furthermore, freeze-drying is an energy-cost process [40]. Controlled air drying may then be a greener stabilization method. In addition, freeze-drying was monitored only on oak WAW samples and not pine. As it was demonstrated, the protocols tested affected differently hard- and softwood species. Thus, a specific stabilization protocol for softwood species should be defined to prevent further visual alteration. For instance, a study showed that scot pine wood samples could be stabilized at room temperature and with a relative humidity of 44%, while oak wood samples were stabilized at room temperature but at 76% of relative humidity [39], [41]. Further investigation regarding the stabilization of the different wood species should be carried out in order to conserve the dark appearance characteristic of WAW artefacts.
To go further in an entirely sustainable protocol, we could imagine stabilizing WAW with a bio-consolidation method instead of PEG. In their research, Gregory et al showed the feasibility to produce bacterial cellulose [6]. The experiments were carried out in a liquid medium and at room temperature with *Acetobacter xylinum* strain. This study also demonstrated that *A. xylinum* still grew and produced bacterial cellulose, even when potential competing bacteria were present inside wood. Therefore, this bio-consolidation step could be applied after BT extraction method and should be compatible with *T. denitrificans*, if still present inside treated wood. Thus, no drying step was performed during Gregory et al research end so the compatibility of this bio-consolidation with freeze-drying or air-drying methods. Furthermore, PEG is a low cost, recyclable, easily degradable and a stable polymer [42]. PEG utilization satisfies wood conservators and its compatibility with the proposed biological method was proven during this study. In addition, PEG is a faster procedure and

more easily appliable for large WAW objects. Bio-consolidation could thus be suggested for small artefacts, with PEG remaining the most reliable and easy consolidation method.

Chemometrics approach permitted to discard or validate some protocols. In particular, PCA and ANOVA validated water immersion under vacuum to induce degradation of carbohydrates from fresh oak and fresh pine samples. ANOVA also validated that this protocol could be applied for both type of wood species. Though, chemometrics approach also showed the limitation of this degradation protocol, as only holocellulose content was degraded at the surface of the wood samples. Still, these results were encouraging to model WAW samples from fresh wood species and thus for the development and investigation of new extraction and stabilization methods. Regarding the evaluation of bio-based extraction method, PCA analysis of spectroscopic data proved the feasibility of the proposed preventive biological method without degrading wood materials. Chemometrics was then a powerful complementary characterization method and was first applied to evaluate a biological preventive extraction method on WAW.

Deeper investigation regarding artificial degradation and contamination of fresh wood as well as preventive biological extraction method will be carried out in the next years, and divided as follows:

WP1 – Study of the relevant chemical processes in microorganisms

- Adaptation of the siderophores to the type of wood species
- Screening of other potential bacterial candidates, *i.e,* aerobic strains
- Application on highly contaminated woods and/or larger samples (*i,e,* 5x5x5cm3)
- Evaluation of a bio-based curative extraction method on previously consolidated objects
- Definition of a user-friendly kit for wood conservation departments

WP2 – Definition of an application protocol on model samples

- Optimization of degradation protocol according to the type of wood species
- Evaluation of additional degradation protocols, such as a combination of acidic digestion and fungal decay
- Assays on other hard- and softwood species to ascertain versatility of the method
- Optimization of contamination protocol to form pure FeS, Fe_3S_4 and FeS_2, *i.e,* immersion in sulfide solution with addition of metallic iron

WP3 – Evaluation of the treatment's performances: efficiency, durability, and impact

- Definition of a kit to "colorimetrically" determine iron and sulfur concentration
- Optimization of BT/CT extraction methods according to the targeted species present (concentration, type)
- Statistical evaluation of the versatility of BT on freshwater or marine WAW
- Assays of bio-consolidation as alternative to PEG consolidation, to move towards a complete green strategy for preservation of WAW artefacts
- Assays of alternative drying methods, *i.e,* controlled air drying, according to the type of wood species

References

[1] K. M. Wetherall, R. M. Moss, A. M. Jones, A. D. Smith, T. Skineer, D. M. Pickup, S. W. Goatham, A. V. Chadwick, and R. J. Newport, "Sulfur and iron speciation in recently recovered timbers of the Mary Rose revealed via X-ray absorption spectroscopy," *J. Archaeol. Sci*., vol. 35, no. 5, pp. 1317–1328, 2008.

[2] C. Rémazeilles, K. Tran, E. Guilminot, E. Conforto, and P. Refait, "Study of Fe(II) sulphides in waterlogged archaeological wood," *Stud. Conserv*., vol. 58, no. 4, pp. 297–307, 2013.

[3] Y. Fors and V. Richards, "The effects of the ammonia neutralizing treatment on marine archaeological Vasa wood," *Stud. Conserv*., vol. 55, no. 1, pp. 41–54, 2010.

[4] G. Almkvist and I. Persson, "Extraction of iron compounds from wood from the Vasa," *Holzforschung*, vol. 60, no. 6, pp. 678–684, 2006.

[5] A. Tahira, W. Howard, E. R. Pennington, and A. Kennedy, "Mechanical strength studies on degraded waterlogged wood treated with sugars," *Stud. Conserv*., vol. 62, no. 4, pp. 223–228, 20174.

[6] D. Gregory, K. Lyngby, D. Yvonne Shashoua, and N. Braunschweig Hansen, "Anyone for a nice cup of tea? The use of bacterial cellulose for conservation of waterlogged archaeological wood," in *18th ICOM-CC Triennial Conference, Copenhage*, 2017.

[7] M. Albelda Berenguer, M. Monachon, C. Jacquet, P. Junier, C. Rémazeilles, E. J. Schofield and E. Joseph., "Biological oxidation of sulfur compounds in artificially degraded wood," *Int. Biodeterior. Biodegrad*., vol. 141, pp. 62-70, 2018.

[8] E. Joseph and P. Junier, "Metabolic processes applied to endangered metal and wood heritage objects: Call a microbial plumber!," *N. Biotechnol*., vol. 56, pp. 21–26, 2020.

[9] D. W. Grattan and R. W. Clarke, "Conservation of waterlogged wood," in *Conservation of marine archaeological objects*, Elsevier, pp. 164–206, 1987.

[10] B. Appelbaum, "Criteria for treatment: reversibility," *J. Am. Inst. Conserv*., vol. 26, no. 2, pp. 65–73, 1987.

[11] N. Macchioni, C. Capretti, L. Sozzi, and B. Pizzo, "Grading the decay of waterlogged archaeological wood according toanatomical characterisation. The case of the Fiavé site (N-E Italy)," *Int. Biodeterior. Biodegrad*., vol. 84, pp. 54–64, 2013.

[12] G. Almkvist, S. Norbakhsh, I. Bjurhager, and K. Varmuza, "Prediction of tensile strength in iron-contaminated archaeological wood by FT-IR spectroscopy-a study of degradation in recent oak and Vasa oak," *Holzforschung*, vol. 70, no. 9, pp. 855–865, 2016.

[13] I. Dobrică, P. Bugheanu, I. Stănculescu, and C. Ponta, "FT-IR spectral data of wood used in Romanian," *Analele Univ. din Bucuresti*, vol. I, pp. 33–37, 2008.

[14] J. A. Bourdoiseau, M. Jeannin, C. Rémazeilles, R. Sabot, and P. Refait, "The transformation of mackinawite into greigite studied by Raman spectroscopy," *J. Raman Spectrosc.*, vol. 42, no. 3, pp. 496–504, 2011.

[15] C. G. Björdal, T. Nilsson, and G. Daniel, "Microbial decay of waterlogged archaeological wood found in Sweden Applicable to archaeology and conservation," *Int. Biodeterior. Biodegradation*, vol. 43, no. 1–2, pp. 63–73, 1999.

[16] K. K. Pandey and A. J. Pitman, "FTIR studies of the changes in wood chemistry following decay by brown-rot and white-rot fungi," *Int. Biodeterior. Biodegrad.*, vol. 52, no. 3, pp. 151–160, 2003.

[17] K. K. Pandey and K. S. Theagar, "Analysis of wood surfaces and ground wood by diffuse reflectance (DRIFT) and photoacoustic (PAS) Fourier transform infrared spectroscopic techniques," *Holz als Roh- und Werkst.*, vol. 55, pp. 383-390, 1997.

[18] B. Pizzo, E. Pecoraro, A. Alves, N. Macchioni, and J. C. Rodrigues, "Quantitative evaluation by attenuated total reflectance infrared (ATR-FTIR) spectroscopy of the chemical composition of decayed wood preserved in waterlogged conditions," *Talanta*, vol. 131, pp. 14–20, 2015.

[19] M. Sandström, F. Jalilehvand, E. Damian, Y. Fors, U. Gelius, M. Jones, and M. Salomé "Sulfur accumulation in the timbers of King Henry VIII's warship Mary Rose: a pathway in the sulfur cycle of conservation concern.," *Proc. Natl. Acad. Sci. U. S. A.*, vol. 102, no. 40, pp. 14165–70, 2005.

[20] J. Preston, A. D. Smith, E. J. Schofield, A. V. Chadwick, M. A. Jones, and J. E. M. Watts, "The effects of Mary Rose conservation treatment on iron oxidation processes and microbial communities contributing to acid production in marine archaeological timbers," *PLoS One*, vol. 9, no. 2, 2014.

[21] Y. Fors, H. Grudd, A. Rindby, F. Jalilehvand, M. Sandstrom, I. Cato, and L. Bornmalm, "Sulfur and iron accumulation in three marine-archaeological shipwrecks in the Baltic Sea: The Ghost, the Crown and the Sword," *Sci. Rep.*, vol. 4, no. 1, p. 4222, 2015.

[22] B. A. Jordan, "Site characteristics impacting the survival of historic waterlogged wood: A review," *Int. Biodeterior. Biodegrad.*, vol. 47, no. 1, pp. 47–54, 2001.

[23] E. Franceschi, I. Cascone, and D. Nole, "Thermal, XRD and spectrophotometric study on artificially degraded woods," *J. Therm. Anal. Calorim.*, vol. 91, no. 1, pp. 119–123, 2008.

[24] Y. Fors, "Sulfur-Related Conservation Concerns for Marine Archaeological Wood", 2008.

[25] J. Levy, "The soft rot fungi: their mode of action and significance in the degradation of wood," in *Advances in botanical research*, vol. 2, Elsevier, pp. 323–357, 1966.

[26] K. K. Pandey and H. C. Nagveni, "Rapid characterisation of brown and white rot degraded chir pine and rubberwood by FTIR spectroscopy," *Holz als Roh- und Werkst.*, vol. 65, no. 6, pp. 477–481, 2007.

[27] M. Monachon, M. Albelda Berenguer, C. Pelé, E. cornet, E. Guilminot, C. Rémazeilles and E. Joseph, "Characterization of model samples simulating degradation processes induced by iron and sulfur species on waterlogged wood," *Microchem. J.*, vol. 155, p. 104756, 2020.

[28] H. Lee, W. I. Kim, W. Youn, T. Park, S. Lee, T.-S. Kim, J. F. Mano, and I. S. Choi, "Iron Gall Ink Revisited: In Situ Oxidation of Fe (II)–Tannin Complex for Fluidic-Interface Engineering," *Adv. Mater.*, vol. 30, no. 49, p. 1805091, 2018.

[29] K. Kranitz, "Effect of natural aging on wood," 2014.

[30] C. G. Duncan, "Wood-attacking capacities and physiology of soft-rot fungi," 1960.

[31] D. Rickard and G. W. Luther, *Chemistry of iron sulfides*, vol. 107, no. 2. 2007.

[32] V. Arantes and A. M. F. Milagres, "The effect of a catecholate chelator as a redox agent in Fenton-based reactions on degradation of lignin-model substrates and on COD removal from effluent of an ECF kraft pulp mill," *J. Hazard. Mater.*, vol. 141, no. 1, pp. 273–279, 2007.

[33] L. R. Bennedsen, J. Muff, and E. G. Søgaard, "Influence of chloride and carbonates on the reactivity of activated persulfate," *Chemosphere*, vol. 86, no. 11, pp. 1092–1097, 2012.

[34] C. Pelé, E. Guilminot, S. Labroche, G. Lemoine, and G. Baron, "Iron removal from waterlogged wood : Extraction by electrophoresis and chemical treatments," *Stud. Conserv.*, vol. 60, no. 3, pp. 1–17, 2013.

[35] S. Vaclavkova, N. Schultz-Jensen, O. S. Jacobsen, B. Elberling, and J. Aamand, "NitrateControlled Anaerobic Oxidation of Pyrite by Thiobacillus Cultures," *Geomicrobiol. J.*, vol. 32, no. 5, pp. 412–419, 2015.

[36] K.-Y. L. Julian Bosch Guntram Jordan Kyoung-Woong Kim and Rainer U. Meckenstock, "Anaerobic, Nitrate-Dependent Oxidation of Pyrite Nanoparticles by Thiobacillus denitrificans," *Est*, pp. 1–11, 2012.

[37] M. Rimmer, D. Watkinson, and Q. Wang, "The efficiency of chloride extraction from archaeological iron objects using deoxygenated alkaline solutions," *Stud. Conserv.*, vol. 57, no. 1, pp. 29–41, 2012.

[38] E. A. Sanya, S.-A. Rezzoug, and K. Allaf, "A new method for drying waterlogged wooden artefacts: Comparison of cyclical pressure drops with conventional methods," *Chem. Eng. Res. Des.*, vol. 81, no. 9, pp. 1243–1249, 2003.

[39] K. S. Hennum-simmonds, "A Study of Alternatives to Freeze-Drying A Study of Alternatives to Freeze-Drying," 2020.

[40] X. Cao, M. Zhang, A. S. Mujumdar, Q. Zhong, and Z. Wang, "Effects of ultrasonic pretreatments on quality, energy consumption and sterilization of barley grass in freeze drying," *Ultrason. Sonochem.*, vol. 40, pp. 333–340, 2018.

[41] M. Fejfer, J. Majka, and M. Zborowska, "Dimensional Stability of Waterlogged Scots Pine Wood Treated with PEG and Dried Using an Alternative Approach," *Forests*, vol. 11, no. 12, p. 1254, 2020.

[42] J. Soni, N. Sahiba, A. Sethiya, and S. Agarwal, "Polyethylene glycol: A promising approach for sustainable organic synthesis," *J. Mol. Liq.*, vol. 315, p. 113766, 2020.

Acknowledgments

First, I would like to acknowledge my supervisor, Prof. ***Edith Joseph***. Hiring me for this PhD allows me realizing two of my wishes: to continue and earn experiences in the field of conservation-restoration as to work and have an experience in a foreign country.

With this PhD thesis, I had the opportunity to work on a new material, wood, and learn more about its conservation and preservation and the issues it encounters. You gave me the opportunity to discover or getting better with several characterization methods, quite useful in our field of research. You also permit to go on lot of conferences, all around Europe and meeting many people working on the wood, but also with specific analytical method or on different fields. Thanks for introducing me to chemometrics, that I did not know before starting in your group. I really enjoyed learning all these techniques and having fun with R. I wish to thank you also for the autonomy you gave me in the lab, how I plan my experiments, what I want to try or do. I would like to thank you for giving us the opportunity to write publications about our research and results. I thank you for the lab meeting you instituted every week so we can discuss about the life in the lab, our problems, help each other. Thank a lot also for all the group bonding such as sailing trip, restaurants for many occasions, escape game and so on! It united our group and helped us/me to have a great time in the office and the labs.

A general acknowledgment to all my colleague in the LATHEMA team: ***Lidia***, ***Sarah***, ***Luana***, ***Arianna***, ***Silvia***, ***Naïma*** but also to all the apprentices that came to learn and work with us: ***Bastian***, ***Jeremy***, and ***Dragan***. I wish you all the best!

Then, I would like to thank ***Magdalena Albelda-Berenguer***, my colleague but mostly my friend, for all the good time together. You are such an extraordinary person ***Magda***. I could not dream of a better colleague to do this PhD research. I will always remember our discussions (gossips) in the office, the laughter in the labs, the TP session with our strange students, the parties we made. But also, the time out, next to the lake for barbeque, shopping or just chilling. I hope (but I know) that we will remain friends for long time even if I go back to France and you to Spain. And to celebrate together this important page of our lives, I truly hope we will do our trip to Iceland 😉

I would like to thank Dr ***Marie Gaschard-Stephanelli*** (yes, you finish the PhD before so now, the title is mandatory) for her kindness and friendship. Thanks a lot for all the breakfasts in the morning before work, thanks for all the help you gave me during this PhD, thanks for always being there and nice when I needed it. You are a wonderful person. See you soon in Paris with Fagiolino!

An enormous thanks to ***Yassine*** for his kindness, humor and all the laughs we had during these four years. You are an amazing friend. Thank you to ***Giau***, our little Uni mascot. I will miss you, but I hope we meet again in Vietnam. Thanks to ***Célia***, for your craziness, your friendship, all the Halloween parties and succeeding making me enjoying sport. Thanks to all the other persons that were present for this PhD: ***João***, ***Chrysanthi***, ***Manuel***, ***Cristina***, ***Francesco***, ***Désirée***, ***Rocío***, ***Siva***, ***Aurélien***, ***Santi***, ***Sirine*** and ***Vidya***.

Then, I would like to thank all the persons enrolled in this project, in Switzerland or Europe. From the University of Neuchâtel, I first thanks Prof. ***Stephan von Reuss*** for his help during this thesis but also for accepting being part of the jury. Then I wish to thank ***Isidro*** and ***André***, from the Atelier mécanique, for all the help they provide, especially cutting my little wood cube samples and ***Armelle Vallat***, for the ICP-OES analyses. I would like to acknowledge ***Radu Alexandru Slobodeanu*** for his assistance regarding chemometric approach. Thanks to our collaborators in Switzerland: ***Pierre Brodard*** and ***Samuel Roth*** from HES-SO Fribourg; ***Emilie Cornet*** from the HE ARC Neuchâtel; ***Katahrina Schmid-Ott*** and ***Tiziana Lombardo*** for their help regarding Raman analysis at the Swiss National Museum; and ***Friederike Moll-Dau*** for her help concerning wood conservation. In France, I would like to acknowledge Dr ***Elodie Guilminot*** and ***Charlène Pelé*** (Arc'Antique, Nantes) for their help in the project and the discussions we shared. Also, thank you to ***Elodie*** for being part of my thesis jury. Then, my acknowledgments go to Dr ***Céline Rémazeilles*** (La Rochelle)for being available to answer any questions for the project. Finally, from Italy, I would like to acknowledge ***Nicola Macchioni*** who advices me during the preparation of the wood mock-ups preparation and analyses.

After, I wish to say thank you to my family. My ***parents***, for their support and motivation speeches. My ***sisters***, for always being present for me and cheering me up. My ***grandma***, who helped me to find my internships in laboratories engaged in cultural materials conservation which led to this PhD. My ***uncle*** and ***aunt***, leaving close to me during these four years and helping me to adapt to this new life. My ***cousins***, for their enthusiasm and kindness every time we met. My ***family-in-law***, for their welcoming in their life. ***All my friends*** in France that I cannot wait to see again and celebrate this thesis in Brittany.

Finally, I wish to thank my partner, ***Youn U***, that encouraged me during these years, accepted my choice to move abroad and comforted me when I doubted. Also thank you to ***Praseodyme***, my baby cat, who helped during these hard periods of Covid-19.

Figures Index

Tables Index

List of Publications and Disseminations

Publications :

1. **M. Monachon***, M. Albelda-Berenguer*, T. Lombardo, E. Cornet, F. Moll-Dau, J. Schramm, K. Schmidt-Ott, and E. Joseph, "Evaluation of an alternative bio-treatment for the preservation of waterlogged wood", *Eur. Phys. J.-Plus*, 2020. Submitted. *Both first authors have the same contribution.
2. E. Joseph, S. James, M. Albelda Berenguer, M. Albini, L. Comensoli, E. Cornet, E. Domon Beuret, W. Kooli, L. Brambilla, L. Mathys, **M. Monachon** and, J. Schröter, "Ground-breaking approaches for a green and sustainable metal conservation". *In preprints of ICOM-CC 18th triennial conference, Transcending Boundaries: Integrated Approaches to Conservation. Bridgland, J., managing ed. International Council of Museums Committee for Conservation (ICOM-CC): Beijing, China,* 2020 (postponed to 17-21 May 2021).
3. E. Joseph, M. Albelda-Berenguer, E. Cornet, L. Cuvillier, S. James, L. Mathys, **M. Monachon**, A. Passaretti and, S. Russo, "Innovative approaches towards a green and sustainable metal conservation". *Chimia*, 74, 611, 2020.
4. **M. Monachon**, M. Albelda-Berenguer, T. Lombardo, E. Cornet, F. Moll-Dau, J. Schramm, K. Schmidt-Ott, and E. Joseph, "Evaluation of Bio-Based Extraction Methods by Spectroscopic Methods". *Minerals*, vol. 10, no. 2, pp. 1–17, 2020, doi: 10.3390/min10020203.
5. **M. Monachon**, M. Albelda-Berenguer, C. Pelé, E. Cornet, E. Guilminot, C. Rémazeilles, and E. Joseph, "Characterization of model samples simulating degradation processes induced by iron and sulfur species on waterlogged wood". *Microchem. J.*, vol. 155, p. 104756, 2020, doi: 10.1016/j.microc.2020.104756.
6. L. Comensoli, W. Kooli, **M. Monachon**, M. Albini, P. Junier and, E. Joseph, "The Potential of Microorganisms for the Conservation- Restoration of Iron Artworks," *In 9th ICOM-CC Metals working group Conference Proceedings. Neuchâtel, Switzerland, 2nd-6th September* 2019
7. W. M. Kooli, T. Junier, M. Shakya, **M. Monachon**, K. D. Davenport, K. Vaideeswaran, A. Vernudachi, I. Marozau, T. Monrouzeau, C. D. Gleasner, K. McMurry, R. Lienhard, L. Rufener, J.-L. Perret, O. Sereda, P. S. Chain, E. Joseph and P. Junier, "Remedial treatment of corroded iron objects by environmental Aeromonas isolates," Appl. Environ. Microbiol., vol. 85, no. 3, pp. e02042-18, 2019, doi: 10.1128/AEM.02042-18.
8. P. Letardi, M. Albini, **M. Monachon** and, E. Jospeh, "Assessing protective treatment performance on outdoor sculptures to be or not to be a representative model sample?," ," *In 9th ICOM-CC Metals working group Conference Proceedings. Neuchâtel, Switzerland, 2nd-6th September* 2019
9. **M. Monachon***, M. Albelda-Berenguer* and, E. Joseph. "Bio-based treatment for the extraction of problematic iron sulfides from waterlogged archaeological wood". *In 14th ICOM-CC Wet Organic Archaeological Materials (WOAM) Conference Proceedings. Portsmouth, United Kingdom, 20th-24th May* 2019; accepted. *Both first authors have the same contribution.

10. **M. Monachon**, M. Albelda Berenguer and, E. Joseph. "Biological oxidation of iron sulphides". In *Advances in Applied Microbiology*, , G. M. Gadd and S. B. T.-A. in A. M. Sariaslani, Eds. Academic Press, vol. 107, pp. 1–27, 2019, doi: 10.1016/bs.aambs.2018.12.002. 1 citation
11. M. Albelda-Berenguer, **M. Monachon** and, E. Joseph. "Roles and applications of siderophores". In *Advances in Applied Microbiology*, G. M. Gadd, and S. B. T.-A. in A. M. Sariaslani, Eds. Academic Press, vol. 106, pp. 193–225, 2019, doi: 10.1016/bs.aambs.2018.12.001. 6 citations
12. . M. Albelda Berenguer, **M. Monachon**, C. Jacquet, P. Junier, C. Rémazeilles, E. J. Schofield, and E. Joseph, "Biological oxidation of sulfur compounds in artificially 279 degraded wood". *Int. Biodeterior. Biodegradation*, vol. 141: pp. 62-70, 2018, doi: 10.1016/j.ibiod.2018.06.009.

Conferences and meetings attended :

1. **M. Monachon**, M. Albelda-Berenguer, E. Jospeh, E. Cornet, F. MollDau, T. Lombardo, J. Schramm, K. Schmidt-Ott. Raman spectroscopy: a tool to evaluate waterlogged wood preservation. *8th Swiss Raman user meeting, Muttenz, Switzerland, November 5*, 2019. (oreal presentation)
2. M. Albelda-Berenguer, **M. Monachon**, E. Joseph. Biotechnology to the rescue of waterlogged archaeological wood. *Green conservation of cultural heritage 2019. Porto, Portugal, October 10-12,* 2019. (oral presentation)
3. **M. Monachon**, M. Albelda-Berenguer, E. Joseph. Assessment of an iron extraction green method on waterlogged wood model samples by chemometrics. *Green conservation of cultural heritage 2019. Porto, Portugal, October 10-12,* 2019. (poster)
4. **M. Monachon**, M. Albelda-Berenguer, E. Joseph. Modelling archaeological wood degradation and validation by chemometrics. *Swiss Chemical Society Fall meeting, University of Zurich, Switzerland, September 6,* 2019. (poster)
5. **M. Monachon**, M. Albelda-Berenguer, E. Joseph. A l'abordage! Les bactéries à la rescousse des épaves. *Semaine de la durabilité à Neuchâtel* 2019. (oral presentation)
6. **M. Monachon**, M. Albelda-Berenguer, E. Joseph. Bio-based treatment for the extraction of problematic iron sulfides from waterlogged archaeological wood. *14th ICOM-CC Wet Organic Archaeological Materials (WOAM) Conference Proceedings. Portmouth, United Kingdom, May 20-24,* 2019. (oral presentation)
7. **M. Monachon**, M. Albelda-Berenguer, E. Joseph. Working on site: Advantages and Limitations of a designed accessory for IS5 FTIR spectrometer. *Thermo Scientific User Meeting, Heidelberg, Germany, September 20-21,* 2018. (oral presentation)
8. **M. Monachon**, M. Albelda-Berenguer, C. Pelè, E. Guilminot, E. Joseph. Preparation of artificial waterlogged wood samples contaminated with iron sulfides. *Swiss Chemical Society Fall meeting, EPFL Lausanne, Switzerland, September 7,* 2018. (poster)
9. **M. Monachon**, M. Albelda-Berenguer, E. Joseph. Artificial impregnation for modelling waterlogged wood contaminated with iron sulfides. *3rd International Conference on Innovation in Art Research and Technology, Parma, Italy, March 26-29,* 2018 (poster)

10. **M. Monachon**, M. Albelda-Berenguer, E. Joseph. Artificial iron sulfides formation on fresh wood for the preservation of waterlogged wood. *6th Swiss Raman user meeting, Muttenz, Switzerland, November 3*, 2017. (oreal presentation)
11. **M. Monachon**. Study of chemical mechanisms involved in the bacterial oxidation of sulfur species for the preservation of waterlogged wood. *First Year Graduate Student Symposium, University of Bern, Switzerland, September 4-5*, 2017 (oral presentation)
12. M. Albelda-Berenguer, **M. Monachon**, C. Jacquet, P. Junier, C. Rémazeilles, E. J. Schofield, E. Joseph. Microbiological extraction of sulfur compounds from simulated waterlogged wood. *TECHNART2017, Bilbao, Spain, May 2-6*, 2017. (poster)

Curriculum Vitae

Personal Information

Name Mathilde Monachon
Address Rue de l'Ecluse 9
CH-2000 Neuchâtel
Telephone +41 78 697 86 20: +33 6 58 84 52 15
E-mail mathilde.monachon@unine.ch; mathilde.monachon@gmail.com
Nationality French

Experience

2016-2020 ***Research assistant – PhD thesis***
University of Neuchâtel, Neuchâtel, Switzerland

- Chemical degradation and contamination of fresh wood to mimic waterlogged archaeological wood
- Chemometric approach to evaluate bio-based extraction treatment for waterlogged archaeological wood
- Characterization methods: colorimetry, light microscopy, SEM-EDS, Raman spectroscopy, ATR-FTIR spectroscopy

Supervisor: Prof. Edith Joseph

2016 ***Master thesis***
Arc'Antique, Nantes, France

- Study of dichlorination of composites archaeological iron objects by electrolysis in neutral or slightly alkaline solutions
- Characterization methods: Raman spectroscopy, SEM-EDS

Supervisor: Dr. Elodie Guilminot

2015 ***Master thesis***
TU Delft, Delft, the Netherlands

- Preliminaries study of adhesives used for the restoration of paintings
- Mechanical tests between wood and canvas materials to develop an optimal adhesive formulation
- Characterization methods: T-test, superficial surface tension, plasma induction

Supervisor: Dr. Hans Poulis

2014 ***Bachelor thesis***
University of Rennes1, Rennes, France

- Cationic substitution of LaTiON perovskites family and their effects
- Synthesis with Pecchini method
- Characterization methods: DRX, UV-visible, nitridation

Supervisor: Dr. François Cheviré

Education

2016-2020 ***PhD student***
Laboratory for Technologies of Heritage Materials, Institute of Chemistry, University of Neuchâtel, Switzerland

2014-2016 ***Master of Science Degree***
Materials and Inorganic Chemistry, University of Rennes 1, France

2011-2014 ***Bachelor Degree***
General Chemistry, University of Rennes 1, France

Technical skills

Analytical expertise

- Scanning Electron Microscopy (SEM)
- Energy Dispersive X-Ray Spectroscopy (EDS)
- Infrared Spectroscopy (FTIR)
- Raman Spectroscopy
- Colorimetry

Computer skills

- Microsoft package
- RStudio

Language skills

French Native speaker
English Work language
Spanish Oral comprehension and base in speaking
Dutch Self-taught, base in speaking, reading, and talking